BioMed Research International

Environmental Biotechnology: Current Advances, New Knowledge Gaps, and Emerging Issues

Guest Editors: Abd El-Latif Hesham, T. Komang Ralebitso-Senior, Yu Zhang, and Qing X. Li

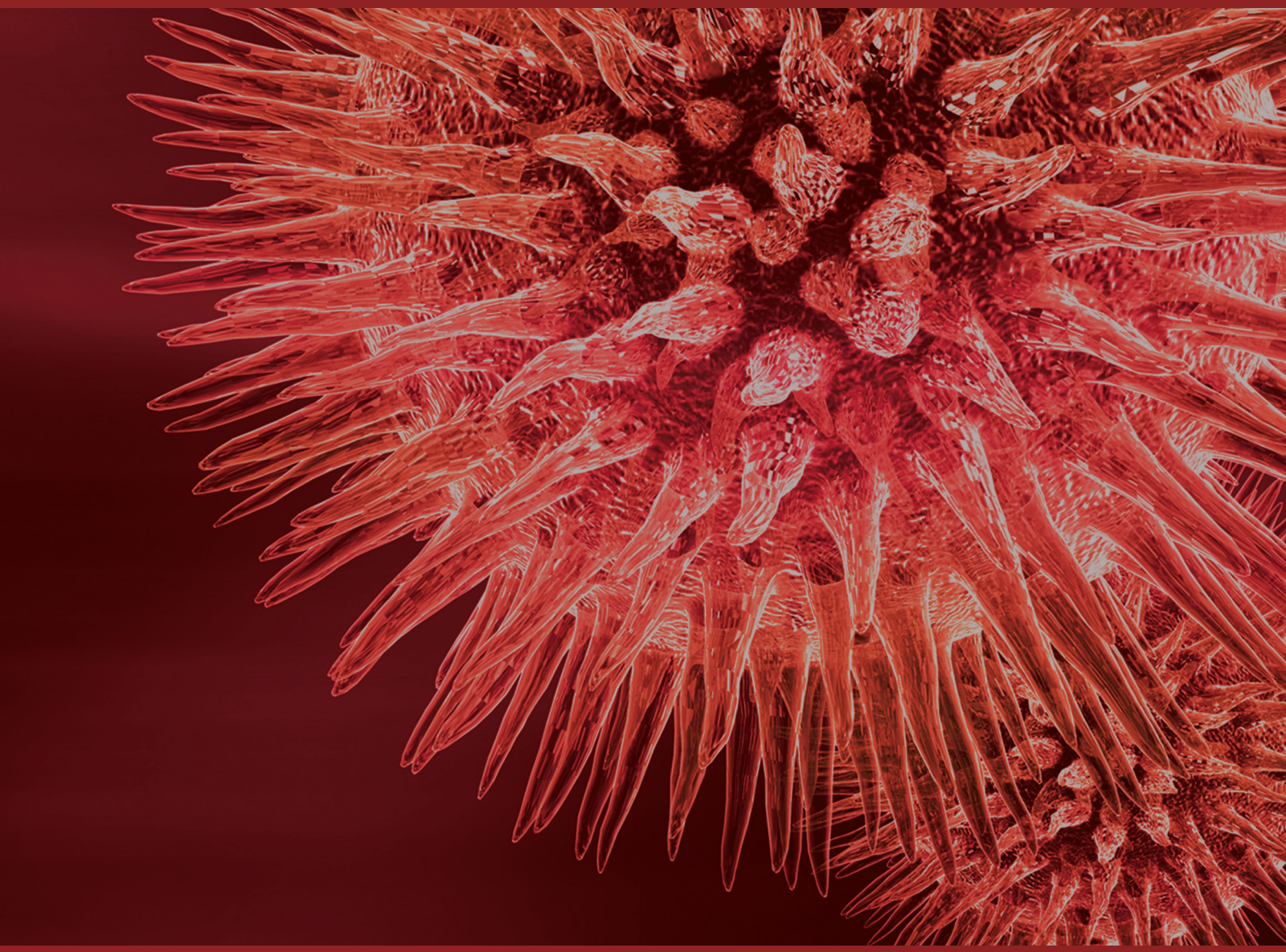

Environmental Biotechnology: Current Advances, New Knowledge Gaps, and Emerging Issues

BioMed Research International

Environmental Biotechnology: Current Advances, New Knowledge Gaps, and Emerging Issues

Guest Editors: Abd El-Latif Hesham,
T. Komang Ralebitso-Senior, Yu Zhang, and Qing X. Li

Contents

Hindawi Publishing Corporation
BioMed Research International
Volume 2015, Article ID 814529, 2 pages
http://dx.doi.org/10.1155/2015/814529

Editorial

Environmental Biotechnology: Current Advances, New Knowledge Gaps, and Emerging Issues

Abd El-Latif Hesham,[1] T. Komang Ralebitso-Senior,[2] Yu Zhang,[3] and Qing X. Li[4]

[1]*Genetics Department, Faculty of Agriculture, Assiut University, Assiut 71526, Egypt*
[2]*School of Science and Engineering, Teesside University, Borough Road, Middlesbrough, Tees Valley TS1 3BA, UK*
[3]*Research Centre for Eco-Environmental Sciences, Chinese Academy of Sciences, P.O. Box 2871, Beijing 100085, China*
[4]*Department of Molecular Biosciences and Bioengineering, University of Hawaii at Manoa, Honolulu, HI 96822, USA*

Correspondence should be addressed to Abd El-Latif Hesham; hesham_egypt5@aun.edu.eg

Received 19 November 2015; Accepted 19 November 2015

The term "environmental biotechnology" encapsulates a wide and dynamic spectrum of topics including bioremediation, biofiltration, wastewater treatment, biodegradation, waste management, and biofuel production. All these disciplines are underpinned by complex interacting microbial communities; hence exciting research has been undertaken and increasingly driven by cutting-edge ecogenomic techniques. However, understanding of microbial diversity, population, and structure for sustainable environmental management remains largely a "black box." Thus exciting findings identified new knowledge gaps and, inevitably, engendered novel research questions with inventive methodologies.

This special issue is focused on original research and review articles that (i) present a critical and succinct appreciation of the environmental biotechnology state of the art, (ii) identify emerging areas of research, (iii) illustrate the applications of innovative molecular techniques, and (iv) suggest updates of established protocols.

P. Munguia-Fragozo and his colleagues have systematically reviewed the omic technologies for microbial community analysis. They discuss the potential applications of current "omics" such as denaturing gradient gel electrophoresis, microscopy using fluorescence *in situ* hybridization, and/or cloning rRNA gene fragments and bioinformatic tools to characterize the microbial community of aquaponic systems. Also they mentioned that metatranscriptomics, proteomics, and metabolomics can provide information of functional analyses in microbial communities at different levels of gene expression, protein translation, and, more recently, the metabolite network, respectively. They indicated essential roles of "omic" approaches such as metagenomics and metatranscriptomics on future studies of microbial diversity in aquaponic biosystems.

C. Varrone et al. reported their research on the selection and adaptation of mixed microbial cultures (MMCs), able to ferment crude glycerol generated from animal fat-based biodiesel and produce building-blocks and green chemicals. Various adaptation strategies have been investigated for the enrichment of suitable and stable MMCs, trying to overcome inhibition problems and enhance substrate degradation efficiency, as well as production of soluble fermentation products. Repeated transfers in small batches and fed-batch conditions were applied. They demonstrated that next generation sequencing represented a useful tool to monitor the changes in microbial composition of MMCs, highlighting the development of a glycerol consuming community (with numerous strains belonging to the genera *Clostridium*, *Klebsiella*, and *Escherichia*), thus confirming the effectiveness of the enrichment strategy.

L. Kiseleva et al. have focused their work on the isolation and partial characterization of an electrogenic bacterium *Thalassospira* sp. strain HJ from a magnetic particle-enriched portion of a marine tidal sediment. They described the first report of electrogenic behavior within the genus *Thalassospira*. They recommended that a more extensive study would be needed to determine whether the proportion of

electrogenic bacteria obtained from this magnetic particle enrichment procedure exceeds that found in the environment. With their diurnal patterns of flooding and diversity of mineral components, tidal sediments should be rich environments to bioprospect for electrogenic bacteria.

Development of an *in situ* microfluidic biosensor for the detection of phenol, based on laccase from *Trametes pubescens* with flow-injection and amperometry as the transducer method, is reported by J. C. Gonzalez-Rivera and J. F. Osma in their study of "Fabrication of an Amperometric Flow-Injection Microfluidic Biosensor Based on Laccase for *In Situ* Determination of Phenolic Compounds." The microfluidic biosensor showed better analytic characteristics than previous biosensors, such as the lower limit of detection and increased sensitivity. Moreover, the optimum operational conditions of temperature, pH, injection flow rate, and redox potential were established. Thus the microfluidic device can be applied directly to *in situ* operation while its fabrication procedure can be introduced for industrial applications.

Lead biosorption by *Klebsiella* sp. 3S1 isolated from a wastewater treatment plant was investigated by A. J. Muñoz et al. through a Rotatable Central Composite Experimental Design. According to their results, the biosorption pathway can be described by a two-step process, one rapid, almost instantaneous, and another slower, both contributing significantly to the overall biosorption. The model that fits the experimental results best was pseudo-second order. The mechanism study revealed that lead ions were bioaccumulated into the cytoplasm and adsorbed on the cell surface. Also, the bacterium *Klebsiella* sp. 3S1 had a good potential in the bioremoval of lead in an inexpensive and effective process.

The objective of a study done by M. E. Silva et al. was to assess antagonism of metabolites produced by nematophagous fungi and their effectiveness on *Haemonchus contortus* infective larvae (L3). Their findings showed the existence of fungal antagonism on the production of reproductive structures between species with potential use for control of gastrointestinal nematodes of domestic animals. The authors recommended that biotic application of nematophagous fungi, specifically for environmental control of gastrointestinal nematodes, must be investigated thoroughly in order to evaluate success of the parasite control program before implementation *in situ*. Another study reported by M. E. da Silva et al. aimed at evaluating the predatory activity of *Duddingtonia flagrans* and *Clonostachys rosea* and their combined impacts on infective larvae (L3) of *H. contortus* in grass microplots that were maintained in a protected environment. Since the efficiency was 74.5%, it was suggested that the tested association (*Clonostachys* + *Duddingtonia*) could be explored further in future studies of biological control. According to the researchers, this was the first report of *C. rosea* and *D. flagrans* association for the control of *H. contortus* in environmental conditions.

The risks of contracting staphylococci food poisoning from the consumption of improperly manufactured salami and the possibility of these food matrices being reservoirs for antibiotic resistance were evaluated by R. S. C. Nunes et al. Nineteen distinct coagulase-negative staphylococci (CNS) strains were found in commercial and artisanal salami. The CNS strains were identified by sequencing of a 16S rDNA region and the phylogenic relationships between the enriched species were established. The presence of multiple genes encoding the classical and newly described *se/sel* and *tstH1* toxins in the CNS genomes was investigated. The risk of food poisoning was then assessed by evaluating the ability of the CNS strains in transcribing and expressing the classical and newly described enterotoxins *in vitro* by using real-time PCR and enzyme-linked immunosorbent assays. The resistance of the isolated strains to antimicrobial agents of therapeutic importance in staphylococci infections was also evaluated.

Finally, J. H. Kwon et al. described the optimization of planetary mill pretreatment and saccharification processes for improving biosugar production from *Pinus rigida* wood waste. They demonstrated that milling can be used to obtain high levels of glucose bioconversion from woody biomass for biorefinery purposes.

All of these papers show how biotechnology and molecular tools can have a significant benefit in a wide range of environmental biotechnology research. It is hoped that readers will relate to the highlighted knowledge gaps and use these to identify new or related ones. All these should, inevitably, engender novel research questions to be addressed subsequently with inventive methodologies.

Acknowledgments

The editors would like to thank the authors who submitted their research articles and to acknowledge all reviewers for their contribution to this special issue. The Lead Guest Editor thanks all Guest Editors for spending their precious time in handling the papers.

Abd El-Latif Hesham
T. Komang Ralebitso-Senior
Yu Zhang
Qing X. Li

Hindawi Publishing Corporation
BioMed Research International
Volume 2015, Article ID 483548, 17 pages
http://dx.doi.org/10.1155/2015/483548

Research Article

Safety Evaluation of the Coagulase-Negative Staphylococci Microbiota of Salami: Superantigenic Toxin Production and Antimicrobial Resistance

Raquel Soares Casaes Nunes, Eduardo Mere Del Aguila, and Vânia Margaret Flosi Paschoalin

Instituto de Química, Universidade Federal do Rio de Janeiro, Avenida Athos da Silveira Ramos 149, Sala 545, Cidade Universitária, 21949-909 Rio de Janeiro, RJ, Brazil

Correspondence should be addressed to Vânia Margaret Flosi Paschoalin; paschv@iq.ufrj.br

Received 26 May 2015; Accepted 20 October 2015

Academic Editor: Rosaria Scudiero

The risks of contracting staphylococci food poisoning by the consumption of improperly manufactured salami and the possibility of this food being reservoirs for antibiotic resistance were evaluated. Nineteen coagulase-negative staphylococci (CNS) strains were found in commercial and artisanal salami. The species in commercial salami were *S. saprophyticus*, *S. sciuri*, *S. xylosus*, and *S. carnosus*. Artisanal salami showed *S. succinus*, *S. epidermidis*, and *S. hominis* but no *S. carnosus*. Phylogenetic analyses grouped the strains into three major staphylococcal species groups, comprised of 4 refined clusters with similarities superior to 90%. Fifteen strains harbored multiple enterotoxin genes, with high incidence of *seb*/*sec* and *sea*, 57% and 50%, respectively, intermediate incidence of *sed*/*seh*/*selm* and *sei*/*seln*/*tst*-H, 33% and 27%, correspondingly, and low incidence of *see*/*selj*/*selo* and *seg*, of respectively 13% and 1%. Real time RT-PCR and enzyme-linked-immunosorbent assays confirmed the enterotoxigenicity of the strains, which expressed and produced enterotoxins *in vitro*. The CNS strains showed multiresistance to several antimicrobials of therapeutic importance in both human and veterinarian medicine, such as β-lactams, vancomycin, and linezolid. The effective control of undue staphylococci in fermented meat products should be adopted to prevent or limit the risk of food poisoning and the spread of antimicrobial-resistant strains.

In memoriam of Professor Joab Trajano Silva, Ph.D.

1. Introduction

Staphylococcal food poisoning is an illness caused by the ingestion of contaminated food containing enterotoxins produced by bacteria belonging to this genus. Enterotoxins that exhibit superantigenic activities are heat stable proteins and may not be destroyed even during cooking conditions.

In Brazil, according to data from the Ministério da Saúde (Ministry of Health), staphylococcal poisoning is the second most common foodborne disease, ranking only after outbreaks involving *Salmonella* spp. [1]. *Staphylococcus* classified as coagulase-positive are considered potential food enterotoxin-producing strains [1], although, recently, the enterotoxigenic potential of coagulase-negative staphylococci (CNS) species in food poisoning has also been recognized [2].

Initially, enterotoxin SEs family members were divided into five serological types (*sea* through *see*) based on their antigenicity [3, 4]. In recent years, however, newly described types of SEs—SEG, SEH, SEI, SElJ, SElK, SElL, SElM, SElN, SElO, SElP, SElQ, SElR, and SElU—with amino acid sequences similar to the classical SEs, were discovered. These newly described enterotoxins are designated as SE or SE-like (SEl), according to their emetic properties displayed in a primate model following oral administration [5].

The toxic shock syndrome toxin-1 (TSST-1) is also a member of the SE-related toxin family and has the ability to stimulate large populations of T cells containing a particular Vβ element in their T-cell receptors (TCR). Like other superantigenic toxins, it bypasses normal antigen presentation by binding to class II major histocompatibility complex molecules on antigen-presenting cells and to specific variable regions on the beta-chain of the T-cell antigen receptor. Through this interaction, a massive proliferation of T cells at orders of magnitude above antigen-specific activation occurs, resulting in a massive cytokine release that is believed to be responsible for the most severe features of TSST [6].

Enterotoxin (SE) genes are encoded in mobile genetic elements, such as plasmids, prophages, and *Staphylococcus* pathogenic islands (SaPIs) [7].

Salami is a kind of dry sausage obtained by the microbial fermentation of raw pork meat, using Staphylococcus *starter cultures* as technological accessories to ferment the product and give it its organoleptic characteristics. In Brazil, Italian type salami, similar to salami produced in Southern Europe, is avidly consumed, with a production trade of 13.093 tons between 2000 and 2014 [8].

S. xylosus, *S. equorum*, and *S. carnosus* are part of the starter culture microbiota that participate in the reactions required for creating the flavor and aroma during the maturing period of fermented meat production [9]. In addition, other species, such as *S. epidermidis*, *S. pasteuri*, *S. sciuri*, and *S. succinus*, may also occasionally be present in meaningful amounts [10].

However, even the combination of physical and chemical barriers cannot always guarantee the stability and microbial safety of starter cultures. Contamination of salami fermentation starter culture microbiota by pathogenic coagulase-negative staphylococci (CNS) strains is perhaps the most harmful factor in the production of cured meat products, since these pathogens are able to produce heat-stable enterotoxins with superantigenic activities in food matrices [11, 12].

Staphylococci species are not usually identified at the species level by routine laboratory testing and commercial kits, since phenotypic discrimination cannot reliably identify these species due to the variable expression of some phenotypic traits [13]. For this purpose, molecular techniques, including nucleotide sequencing within the *16S rDNA*, *hsp60*, *tuf*, *sodA*, and *rpoB* genes, have been successfully used to identify *Staphylococcus* species [14].

Depending on the conditions, some species of coagulase-negative staphylococci can present health risks, since they have shown resistance to several antibiotics of therapeutic importance, such as β-lactams [15].

The aim of the present study was to identify the members of the CNS microbiota from salami. We sampled the salami marketed in Brazil, comparing the CNS microbiota in salami produced by industrial companies and in artisanal salami manufactured by small producers. The CNS strains were identified by sequencing of a 16S rDNA region and the phylogenic relationships between the observed species were established. The presence of multiple genes encoding the classical and newly described *se*/*sel* and *tstH1* toxins in the CNS genomes was investigated. The risk of food poisoning was assessed by evaluating the ability of the CNS strains in transcribing and expressing the classical and newly described enterotoxins *in vitro* by using real time RT-PCR and enzyme-linked immunosorbent assay (ELISA). The resistance of the isolated strains to antimicrobial agents of therapeutic importance in staphylococci infections was also evaluated.

2. Materials and Methods

2.1. Isolation of Bacterial Strains. Six samples of distinct brands of salami, 03 from the meat industry and 03 from small artisanal producers, were collected in the municipality of Rio de Janeiro, Brazil. Twenty-five grams of salami was added to 225 mL of 0.1% peptone water. The suspensions were transferred to homogenizer bags (Interscience, Saint Nom, France) and coupled to a Stomacher@ 400 circulator (Seward, Worthing, West Sussex, UK) at 260 rpm for 1 min. The suspensions were serial-diluted from 10^{-6} to 10^{0} and 100 μL of each dilution was transferred onto 20 μL of Baird-Parker agar containing egg yolk tellurite emulsion (BPAþ RPF, bioMerieux, France). Eighty presumptive coagulase-negative staphylococci colonies were tested by Gram-staining, catalase, coagulase, and thermostable DNAse activities according to Bergey's Manual of Systematic Bacteriology. Sixty presumptive CNS strains were stored at −80°C in tryptone soy agar (TSA, Franklin Lakes, New Jersey, USA) plus 45% v/v glycerol.

2.2. DNA Preparation. The strains were cultured aerobically overnight in 10 mL Brain Heart Infusion broth (BD BBL, Le Pont de Claix, France) at 37°C for 24 h. The suggestive CNS colonies were adjusted to 10^{6} UFC/mL in a spectrophotometer and harvested by centrifugation at 5,700 × g for 1 min. The cell pellet was used for DNA extraction using the DNeasy blood and tissue kit (Qiagen, Dusseldorf, Germany), following the manufacturer's instructions. Genomic DNA was quantified using the Qubit fluorometer (Invitrogen, Grand Island, New York, USA) and Qubit assay kits.

2.3. PCR Tests

2.3.1. Primer Sequences and Target Genes. Primer sets flanking the *sea*, *seb*, *sec*, *sed*, *see*, *seg*, *seh*, *sei*, *selk*, *selm*, *seln*, *selo*, *selq*, *selr*, *selu*, and *tstH1* sequences are listed in Table 1.

2.3.2. Uniplex-, Duplex-, and Multiplex-PCR Tests. Uniplex-PCR tests targeting the *tstH1* sequence and duplex-PCR targeting the *sea/seb* and *sec/sed* sequences were performed. PCR mixtures contained 25 μL of 20 mM $MgCl_2$, 10x PCR buffer (Invitrogen, Grand Island, New York, USA), 100 mM dNTP mix (Fermentas Thermo Scientific, Vilnius, Lithuania), 0.2 mM of each primer (Table 1), 0.5 U Taq DNA polymerase (Invitrogen, Grand Island, New York, USA), and 100 ng of DNA templates. Uniplex- and duplex-PCR assays were performed under the following conditions: 94°C for 5 min followed by 35 cycles of 94°C for 2 min, 53°C for 2 min, and 72°C for 1 min for extension, ending with a final extension at 72°C after 7 min [16], with modifications in the annealing temperature, using a thermal cycler (MyCycler, Bio-Rad,

Table 1: Primer set for V3 16S rDNA sequencing and PCR/real time RT-PCR tests targeting the classical and newly described staphylococcal enterotoxin genes.

	Primers set and sequences (5′-3′)	Gene	Amplicon (bp)	References
SEA_f	TTGGAAACGGTTAAAACGAA	*sea*	120	[17]
SEA_r	GAACCTTCCCATCAAAAACA			
SEB_f	TCGCATCAAACTGACAAACG	*seb*	478	[17]
SEB_r	GCAGGTACTCTATAAGTGCC			
SEC_f	GACATAAAAGCTAGGAATTT	*sec*	257	[17]
SEC_r	AAATCGGATTAACATTATCC			
SED_f	CTAGTTTGGTAATATCTCCT	*sed*	317	[17]
SED_r	TAATGCTATATCTTATAGGG			
SEE_f	TAGATAAAGTTAAAACAAGC	*see*	170	[17]
SEE_r	TAACTTACCGTGGACCCTTC			
SEG_f	TGCTATCGACACACTACAACC	*seg*	704	[18]
SEG_r	CCAGATTCAAATGCAGAACC			
SEH_f	CGAAAGCAGAAGATTTACACG	*seh*	495	[18]
SEH_r	GACCTTTACTTATTTCGCTGTC			
SEI_f	GACAACAAAACTGTCGAAACTG	*sei*	630	[18]
SEI_r	CCATATTCTTTGCCTTTACCAG			
$SElJ_f$	CAGCGATAGCAAAAATGAAACA	*selj*	426	[19]
$SElJ_r$	TCTAGCGGAACAACAGTTCTGA			
$SElM_f$	CCAATTGAAGACCACCAAAG	*selm*	517	[20]
$SElM_r$	CTTGTCCTGTTCCAGTATCA			
$SElN_f$	ATTGTTCTACATAGCTGCAA	*seln*	682	[20]
$SElN_r$	TTGAAAAAACTCTGCTCCCA			
$SElO_f$	AGTCAAGTGTAGACCCTATT	*selo*	534	[20]
$SElO_r$	TATGCTCCGAATGAGAATGA			
$SElK_f$	ATGAATCTTATGATTTAATTTCAGAATCAA	*selk*	545	[21]
$SElK_r$	ATTTATATCGTTTCTTTATAAGAAATATCG			
$SElQ_f$	GGAAAATACACTTTATATTCACAGTTTCA	*selq*	539	[21]
$SElQ_r$	ATTTATTCAGTTTTCTCATATGAAATCTC			
$SElR_f$	AATGGCTCTAAAATTGATGG	*selr*	363	[22]
$SElR_r$	TCTTGTACCGTAACCGTTTT			
$SElU_f$	AATGGCTCTAAAATTGATGG	*selu*	215	[22]
$SElU_r$	ATTTGATTTCCATCATGCTC			
TSST-1_f	ATGGCAGCATCAGCTTGATA	*tstH1*	350	[17]
TSST-1_r	TTTCCAATAACCACCCGTTT			
16S $rDNA_f$	ATA AGA CTG GGA TAA CTT CGG G	*16SrDNA*	500	[23]
16S $rDNA_r$	CTT TGA GTT TCA ACC TTG CGG TCG			

f: forward; r: reverse.

Hercules, CA, USA). The amplified fragments were visualized on 1.0% agarose gels (Sigma) stained with GelRed (dilution 1 : 1000) (BioAmerica, Tel Aviv, Israel) and documented on a transilluminator (MiniLumi Imaging Bio-Systems, BioAmerica, Tel Aviv, Israel).

2.3.3. Multiplex-PCR Tests. Multiplex-PCR assays were performed by the simultaneous amplification of the *see*, *seg*, *seh*, *sei*, *selj*, *selm*, *seln*, *selo*, *selk*, *selq*, *selr*, and *selu* sequences using the primer sets listed in Table 1. Each reaction contained 50 μL of a mix containing 0.5 U Taq DNA polymerase, 10x PCR buffer, 100 mM dNTP, 0.2 μM of each primer, and 100 ng of DNA template. DNA amplification of *see*, *seg*, *seh*, and *sei* was carried out as follows: 95°C for 5 min, 35 cycles of 95°C for 30 s, 53°C for 90s and 72°C for 90 s, and a final extension at 72°C for 10 min. The DNA amplifications of the *selj, selm, seln,* and *selo* group and the *selk, selq, selr,* and *selu* group were carried out in the same conditions [3]. PCR products were visualized by electrophoresis on 1.2% agarose gels (Uniscience do Brasil, São Paulo, Brazil) in 1x TAE (Tris-boric acid-EDTA) buffer stained by 0.5 $\mu g\,mL^{-1}$ of GelRed (BioAmerica, Tel Aviv, Israel) and documented on a transilluminator (MiniLumi Imaging Bio-Systems, BioAmerica, Tel Aviv, Israel).

DNA templates from the following reference strains were used: *S. aureus* ATCC 29231 (*sea*), *S. aureus* ATCC 14458 (*seb, tstH, selk, selq, selr,* and *selu*); *S. aureus* ATCC 19095 (*sec, seg, seh,* and *sei*), *S. aureus* ATCC 13563 (*sed*), *S. aureus* ATCC 27664 (*see*), and *S. aureus* ATCC 27154 (*selj, selm, seln,* and *selo*) and *S. xylosus* ATCC 29971.

2.4. Enterotoxin Expression Assays. The observed strains were cultured aerobically overnight in 10 mL Brain Heart Infusion Broth (BD BBL, Le Pont de Claix, France) at 37°C for 72 h. Bacteria supernatants were collected by centrifugation at 4,000 ×g for 10 min and used for the detection of *sea, seb, sec, sed*, and *see* by an ELISA assay using a commercial detection kit (RIDASCREEN SET A, B, C, D, E Art. number R4101, R-Biopharm AG, Germany). The assay was performed according to the manufacturer's recommendation and as described elsewhere [16]. The mean lower limit of detection of the assay was 0.25 ng mL^{-1}. The threshold is defined as the average OD of two negative controls plus 0.15, a constant established by the kit. Samples containing SEs showed absorbance values equal to or greater than the threshold value. All experiments were performed in duplicate.

2.5. Real Time RT-PCR Assays. Total RNA was extracted by using the QIAGEN RiboPure Bacteria kit (Life Technologies, Carlsbad, California, USA) following the manufacturer's instructions and quantified using the Qubit fluorometer (Invitrogen, Grand Island, New York, USA) and Qubit assay kits. The cDNA synthesis was performed by using the High Capacity cDNA Reverse Transcription Kit (Applied Biosystems, California, USA) and the ABI PRISM 7500 Fast RT-PCR system (Applied Biosystems, California, USA). Samples were plated in triplicate in 96-well plates as follows: 12 μL of the SYBR Green PCR Master Mix; 1 μL of primer mix (*sea, seb, sec, sed,* and *see*); and 4.5 μL of the cDNA ultrapure water in each well. Amplification was performed under the following conditions: 95°C for 15 min, 40 cycles at 95°C for 15 s, 54°C for 30s, and 72°C for 30 s. The dissociation curve was performed at 95°C for 15 sec, 54°C for 30 sec, and 95°C for 15 sec. CT means, the standard deviations, and the cDNA semiquantification were calculated using the GraphPad Prism 5 software package. Calibration curves based on five points were constructed in triplicate corresponding to serial dilutions (1, 1 : 10, 1 : 100, 1 : 1000, and 1 : 10000) from 100 ng of a DNA template stock solution.

2.6. 16S rDNA Sequencing. Amplification of the V5 region of 16S rDNA fragment was performed using 50 ng of DNA templates from the 65 strains found in the salami samples. PCR was performed under the following conditions: 95°C for 10 min, followed by 30 cycles at 95°C for 30 s, 60°C for 30 s and 72°C for 45 s, and a final extension at 72°C for 10 min. PCR products were purified using the PCR DNA Purification Kit (Applied Biosystems, California, USA) and sequenced using 20 ng purified DNA and 13 μL of primer sets in a final volume of 20 μL. After amplification, products were purified according to the protocol of the BigDye Terminator Purification X Kit (Applied Biosystems, California, USA) and sequenced on a 3130 sequencer Genetic Analyzer (Applied Biosystems, California, USA). The sequences were compared to the 16S rDNA gene sequences of *Staphylococcus* species available at the GenBank database (http://www.ncbi.nlm.nih.gov/Genbank/index.html). Multiple sequence alignments were performed using Clustal W (Kyoto University, Bioinformatics Center; http://www.genome.jp/tools/clustalw/).

2.7. Sequencing of Enterotoxin PCR Products. PCR products were purified using the PCR DNA Purification Kit (Applied Biosystems, California, USA) and sequenced using 10 ng of purified DNA and 3.2 pmoles of each primer set in a final volume of 20 μL. After amplification in the same conditions as the PCR step (Section 2.3.3), products were purified according to the BigDye Terminator Purification X Kit protocol (Applied Biosystems, California, USA) and sequenced on a 3130 sequencer Genetic Analyzer (Applied Biosystems, California, USA). The sequences were compared to *Staphylococcus aureus* and *Staphylococcus pasteuri* gene sequences available at the GenBank database (http://www.ncbi.nlm.nih.gov/Genbank/index.html). Multiple sequence alignments were performed using Clustal W (Kyoto University, Bioinformatics Center; http://www.genome.jp/tools/clustalw/).

2.8. Phylogenetic Analyses. Phylogenetic relationships between the CNS strains were performed by sequence alignments using the Clustal X 2.0 software package [24]. The phylogenetic trees were constructed using the software Mega 6.0 and UPGMA methods [25].

2.9. Antibiotic Susceptibility Tests. An inoculum of each strain equivalent to a 0.5 McFarland scale was swabbed onto a Mueller-Hinton agar plate (BD BBL Franklin Lakes, New Jersey, USA) and the antibiotic disc was then placed on the plate followed by overnight incubation at 37°C. The inhibition zone was interpreted according to the Clinical Laboratory Standard (CLSI) Guidelines, formerly known as the National Committee for Clinical Laboratory Standards. The tested antibiotics were penicillin G (10 U), oxacillin (1 μg), neomycin (30 μg), sulfamethoprim (5 μg), clindamycin (2 μg), gentamicin (10 μg), cefoxitin (30 μg), rifampicin (5 μg), erythromycin (15 μg), tetracycline (30 μg), vancomycin (30 μg), ciprofloxacin (5 μg), sulfazothrim (23 μg), cefepime (30 μg), linezolid (30 μg), and chloramphenicol (30 μg).

2.10. Minimal Inhibitory Concentration (MIC) Determinations. The MICs of vancomycin, linezolid, methicillin, and ampicillin were determined by the macrodilution broth method based on CLSI recommendations, using in-house-prepared panels [26]. Antibiotic concentrations of 0.03, 0.06, 0.125, 0.25, 0.5, 1.0, and 2.0 mg mL^{-1} were tested. One mL of broth was transferred to the tubes and 100 μL of the bacteria suspension was adjusted to 10^6 CFU/mL in saline 0.85% according to a 0.5 McFarland scale and transferred to tubes containing 1 mL of each antimicrobial. Strains were grown in Mueller-Hinton broth (BD BBL Franklin Lakes, New Jersey, USA) and the MIC was estimated as the lowest

antibiotic concentration that inhibits visible growth after 24 h [26].

3. Results and Discussion

3.1. Isolation and Identification of Coagulase-Negative Strains from Salami. Sixty-five presumable coagulase-negative staphylococci microorganisms from salami were isolated by colony morphology, coagulase slide test, subsequent tube test, and biochemical tests. The sequencing of the V5 region of the 16S rDNA fragment of the strains was discriminative enough to differentiate the *Staphylococcus* isolated from salami at the subspecies level, with the exception of 1 strain, identified up to the *Staphylococcus* spp. genus.

Nineteen distinct strains were identified as CNS in salami with 08 of 19 (42%) identified as *S. saprophyticus*, the predominant species, followed by 05 strains of *S. xylosus* (26%), 02 strains of *S. carnosus* (11%), and 01 strain of each of the following species: *S. succinus*, *S. sciuri*, *S. epidermidis*, and *S. hominis* (5% each) (Table 2).

The 08 *S. saprophyticus* strains were identified as KJ699151.1, AB697717.1, JX490122.1, KJ004623.1, and HQ699510.1, EU430992.1, HF937252.1, and KJ949606.1, with the latter two and *S. sciuri* JX966436.1 being homologous (96–98%) to strains from the environment. Five *S. xylosus* strains, CP007208.1, KF198080.1, CP008724.1, AM882700.1, and KC456590.1, and a single *S. succinus* strain, KC329824.1, were identified. The last three *S. xylosus* strains and the *S. succinus* strain are homologous (97-98%) to strains found in fermented meat or meat starter cultures. *S. xylosus* CP007208.1 showed homology (98%) to potential opportunistic pathogenic strains from mammal species.

The *S. carnosus* strains identified were KJ862002.1 and NR116434.1, and the latter, as well as the single *S. hominis* JX519988.1 (96-97%) identified, were homologous (97%) to species from human microbiota.

S. carnosus and *S. xylosus* are commonly used as commercial starter cultures for sausage manufacturing [26], but *S. succinus* has also been observed in dry fermented sausages and its use as a *starter* culture has been already proposed [27].

The diversity of CNS microbiota found in the samples analyzed in the present study could be related to the origin of the salami. The microbiota from the artisanal salami showed greater biodiversity when compared to the commercial salami. In commercial salami, *S. saprophyticus* was the predominant species, but *S. xylosus and S. carnosus*, also observed in commercial salami, are commonly isolated from starter cultures [26]. The predominance of *S. saprophyticus* followed by *S. xylosus* has also been reported in salami from South Italy [28], similar to Belgian sausages, where *S. saprophyticus* was the most frequently detected species [29].

S. carnosus was not observed in artisanal salami, but *S. succinus*, *S. epidermidis,* and *S. hominis* were detected.

The biodiversity of the CNS staphylococci species found in microbiota depends on the kind of meat-fermented product, but CNS strains such as *S. saprophyticus*, *S. auricularis*, *S. xylosus*, *S. capitis*, *S. hominis*, *S. carnosus*, *S. haemolyticus*, *S. warneri*, *S. equorum*, *S. cohnii*, *S. capitis*, and *S. intermedius* have been described in Napoli-type salami, Sremska sausages, dry sausages, raw meat, and naturally fermented meat [30–33].

During the last decades *S. epidermidis* and *S. saprophyticus* have been described as emerging pathogens [34]. *S. saprophyticus* is considered a frequent contaminant of fermented sausages and raw meats and has been isolated from rectal swabs of cattle carcasses and pigs. In humans, the main reservoir of *S. saprophyticus* is the gastrointestinal tract [35]. *S. saprophyticus* and *S. epidermidis* can be opportunistic pathogens, isolated from the human urinary tract, and the presence of these species in food should be taken into account concerning possible contamination of the starter inoculum and/or improvements in the salami manufacturing process [13].

Other CNS species observed in the present study are mainly associated with ordinary food contaminants, with *S. epidermidis* and *S. hominis* being the dominant species in human skin and occasionally isolated from the skin of domestic animals [36].

3.2. Phylogenetic Relationships of the CNS Identified in Salami. CNS strains can be grouped into four species groups: *saprophyticus*, *simulans*, *epidermidis*, and *haemolyticus.* Frequently, the *saprophyticus* species group includes *S. xylosus* and *S. saprophyticus*, while the *simulans* species group is comprised of *S. carnosus* and *S. piscifermentans*; the *epidermidis* species group is composed of *S. epidermidis, S. capitis, S. caprae,* and *S. saccharolyticus* and the *haemolyticus* species group encompasses *S. haemolyticus, S. hominis,* and *S. devriesei* [37, 38]. In the present study, the main cluster grouped several *S. saprophyticus* strains, namely, KJ699151.1, AB697517.1, KJ949606.1, JX490122.1, and KJ004623.1, four *S. xylosus* strains CP008724.1, CP007208.1. AM882700.1, and KC456590.1, and the *S. succinus* KC329824.1 strain (Figure 1). These strains are homologous to those from fermented meat microbiota.

The subclusters of those clusters showed mismatches of species belonging to the four species groups. The first subcluster grouped *S. epidermidis* HF088211.1, *S. saprophyticus* HQ699510.1, and *S. carnosus* NR116434.1 and the second subcluster grouped *S. hominis* JX519988.1 and *the S. saprophyticus* EU430992.1, all of them originally isolated from animals and human beings. The third subcluster includes species previously isolated from the marine environment, such as *S. xylosus* KF198080.1, while *S. carnosus* KJ862002.1 is utilized as a probiotic organism in foods. The fourth cluster grouped the *S. sciuri* JX966436.1 and *S. saprophyticus* HF937252.1 strains, which are homologous to species found in soil.

The CNS strains clustered into groups near the bottom of the phylogenetic tree are mostly strains found in artisanal salami, whereas the species at the top of the tree are mainly CNS strains found in commercial salami (Figure 1).

The close similarities between the *S. saprophyticus* AB697517.1 and KJ949606.1 strains, the *S. succinus* KC329824.1, *S. xylosus* AM882700.1, KC456590.1, and CP008724.1 strains, the *S. saprophyticus* KJ004623.1 and KJ699151.1 strains, and *S. xylosus* CP007208.1 are supported by a bootstrap value of 100%. The interspecies similarities were over 90%, which demonstrates close phylogenies

Table 2: Genotypic and phenotypic characterization of CNS strains from salami.

Salami origin	Strains identification and characterization			
	Staphylococcus species	Genotypic		Phenotypic
	GenBank accession number and similarity (%)	Presence of enterotoxin genes	mRNA detection	Enterotoxin production (ng mL^{-1})
Commercial	*Staphylococcus* spp. KF135445.1 (96)	*sea*, *seb*	—	—
	S. carnosus KJ862002.1 (96)	*sea*, *seb*, *sed*, *seh*, *sei*,and *selj*	—	1.2 ± 0.1
	S. carnosus NR116434.1 (98)	*seb*, *sec*, *sed*, and *see*	*see*	0.3
	S. saprophyticus AB697717.1 (98)	*seh*, *sei*, and *selm*	*sei*, *selm*	0.3
	S. saprophyticus EU430992.1 (99)	*sea*, *seb*, *selm*, *seln*, *selo*,and *tstH1*	*seb*, *selm*, and *selo*	1.3 ± 0.1
	S. saprophyticus HQ699510.1 (97)	—	—	—
	S. saprophyticus JX490122.1 (99)	*sea*, *seh*	*seh*	0.5 ± 0.1
	S. saprophyticus KJ004623.1 (96)	*sec*	—	0.4
	S. saprophyticus KJ949606.1 (98)	*sea*, *seb*, *sec*,and *seh*	*sea*, *seb*, and *seh*	—
	S. sciuri JX966436.1 (98)	*sed*, *sei*	*sei*	1.0 ± 0.1
	S. xylosus AM882700.1 (97)	—	—	—
	S. xylosus CP007208.1 (99)	—	—	—
	S. xylosus CP008724.1 (98)	*sea*, *tstH1*	*sea*	1.4
	S. xylosus KC456590.1 (98)	—	—	—
Artisanal	*S. epidermidis* KF600589.1 (97)	*sec*, *sed*, *see*, *seg*, *seh*,and *sei*	*see*, *sei*	0.7 ± 0.1
	S. hominis JX519988.1 (97)	*sea*, *seb*, *sec*, *sed*, *selj*, *selm*, *seln*, and *selo*	*seln*, *selo*	0.9 ± 0.1
	S. saprophyticus HF937252.1 (97)	*seb*	*seb*	0.5
	S. saprophyticus subsp. *bovis* KJ699151.1 (98)	*sec*, *selm*, *seln*,and *tstH1*	*seln*	0.9 ± 0.1
	S. succinus KC329824.1 (99)	*sea*, *seb*, *sec*, *selj*,and *seln*	*seb*, *sec*	1.3
	S. xylosus KF198080.1 (97)	*sec*, *selm*,and *tstH1*	—	0.5 ± 0.1

The presence of enterotoxin genes *sea*, *seb*, *sec*, *sed*, *see*, *seg*, *seh*, *sei*, *selj*, *selk*, *selm*, *seln*, *selo*, *selq*, *selr*, *selu*, and *tstH1* was tested by PCR using the specific set of primers.

sea-see enterotoxin production was evaluated by immune-sorbent assays (ELISA) using the detection kit RIDASCREEN SET A, B, C, D, E. Values are displayed as the means ± SD of assays performed in duplicate.

mRNA transcripts for all enterotoxin genes were evaluated by real time RT-PCR tests.

CT values are displayed as means ± SD of RT-PCR tests performed in duplicate: *sea*—*S. xylosus* CP008724.1 30 ± 0.4; *seb*—*S. xylosus* CP008724.1 33 ± 2.0; *S. saprophyticus* JX 490122.1 30.2 ± 0.4; *S. saprophyticus* subsp. *bovis* KJ699151.1 32 ± 0.1; *S. xylosus* KF198080.1 36 ± 1.0; and *S. hominis* JX519988.1 34 ± 1.0; *sec*—*S. saprophyticus* subsp. *bovis* KJ699151.1 31 ± 1.1; *see*—*S. saprophyticus* subsp. *bovis* KJ699151.1 30.6 ± 0.5; *S. succinus* KC329824.1 28.5 ± 0.1; and *S. saprophyticus* HF937252.1 32 ± 0.4; *seh*—*S. xylosus* CP008724.1 31 ± 1.0; *S. saprophyticus* JX966436.1 33.2 ± 0.6; *sei*—*S. saprophyticus* AB697717.1 30 ± 1.0; *S. saprophyticus* JX966436.1 30.6 ± 1.0; *seln*—*S. hominis* JX519988.1 30.3 ± 1.0; *S. saprophyticus* EU430992.1 31 ± 0.3; and *selo*—*S. hominis* JX519988.1 32 ± 1.0.

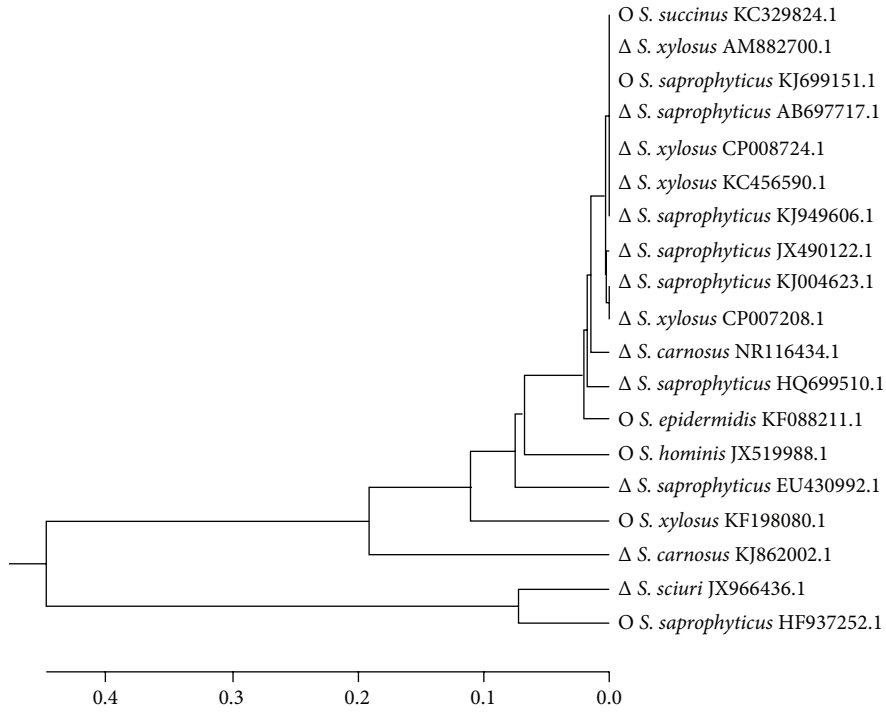

Figure 1: Phylogenetic tree generated from the multiple alignments of the 16S rDNA sequences of CNS strains found in salami using the ClustalX 2.0 software. The phylogenetic tree was constructed by using the Mega 6.0 software and the unweighted pair group method (UPGMA). Bootstrap values ranged from 0.0 to 0.4. Strains found in commercial (Δ) or artisanal salami (O).

between these CNS strains. Suzuki et al., 2012, demonstrated a bootstrap value higher than 90% for interspecies similarities between *S. saprophyticus, S. epidermidis, S. hominis,* and *S. carnosus*.

3.3. Genotypic and Phenotypic Characterization of CNS Strains. Twelve distinct combinations of staphylococcal enterotoxins genes were found in the 15 CNS strains, comprising SEs A–E, G–J, and also the enterotoxin-like toxins (SElL) K–R and U (Table 2).

Fifteen strains (79%) carried at least one gene encoding enterotoxins in their genomes (Figure 2). The *seb* and *sec* genes were the most predominant, harbored by 57% of the strains, followed by *sea,* carried by 50%, whereas the *sed/seh/selm* genes showed intermediate incidence harbored by 33% of the strains, while *sei/seln* and *tsH1* were found in 27% of strains. Finally, *see, selj,* and *selo* showed low incidence (13%) and *seg* was carried by only 1% of strains (Table 2).

The relationships between superantigenic toxin genotypes and toxin gene-encoding mobile genetic elements in CNS strains were evaluated. Distinct combinations of *SaPI* and plasmids or plasmids and genes of *egc* operon enterotoxins were found in the CNS strains obtained from salami.

Four strains presented only the classical enterotoxin genes, namely, *S. saprophyticus* KJ004623.1 and HF937252.1, *S. xylosus* CP008724.1, and *S. carnosus* NR116434.1. Another strain, *S. saprophyticus* AB697717.1, presented only the newly described enterotoxins *seh, sei,* and *selm* and, finally, 10 strains presented a combination of classical and newly described enterotoxin genes in their genomes, with at least one of each enterotoxin type (Table 2).

Previous studies have shown that *sea* is the most common toxin associated with *Staphylococcus* food poisoning, followed by *sed* and *see*, with SEH and SEI being considered as playing only a minor role [39]. Among the 15 enterotoxigenic strains found in salami, 73% of them harbored at least the *sea* gene or combinations of these 05 genes. Strains *S. carnosus* KJ862002.1, found in commercial salami, and *S. epidermidis* KF600589.1, found in artisanal salami, carry 04 of these genes. The *sea* and *seb* enterotoxin genes are known to occupy the same locus on the chromosome, which may explain why these enterotoxins are commonly found together in food poisoning outbreaks [36]. The combination of *sea* and *seb* genes was found in 05 strains: *S. saprophyticus* EU430992.1, *S. carnosus* KJ862002.1, *S. hominis* JX519988.1, *S. saprophyticus* KJ949606.1, and *S. succinus* KC329824.1. A single strain, *S. carnosus* KJ862002.1, showed the combination of *sea* and *sei* genes.

Additionally, some CNS are able to produce TSST-1 alone or in combination with other enterotoxins. Herein, 04 of the 19 strains (21%), *S. saprophyticus* EU430992.1, *S. saprophyticus* subsp. *bovis* KJ699151.1, and *S. xylosus* CP008724.1 and KF198080.1, were shown to harbor the *tstH1* combined with *se* and/or *sel* enterotoxin genes (Table 2).

The staphylococci enterotoxins genes *seg* and *sei* [40] are part of a chromosomal operon gene cluster (*egc*), comprising five genes designated as *selo*, *selm*, *sei*, *seln,* and *seg*. Two of the CNS strains determined in the present study, *S. saprophyticus* EU430992.1 and *S. hominis* JX519988.1, were

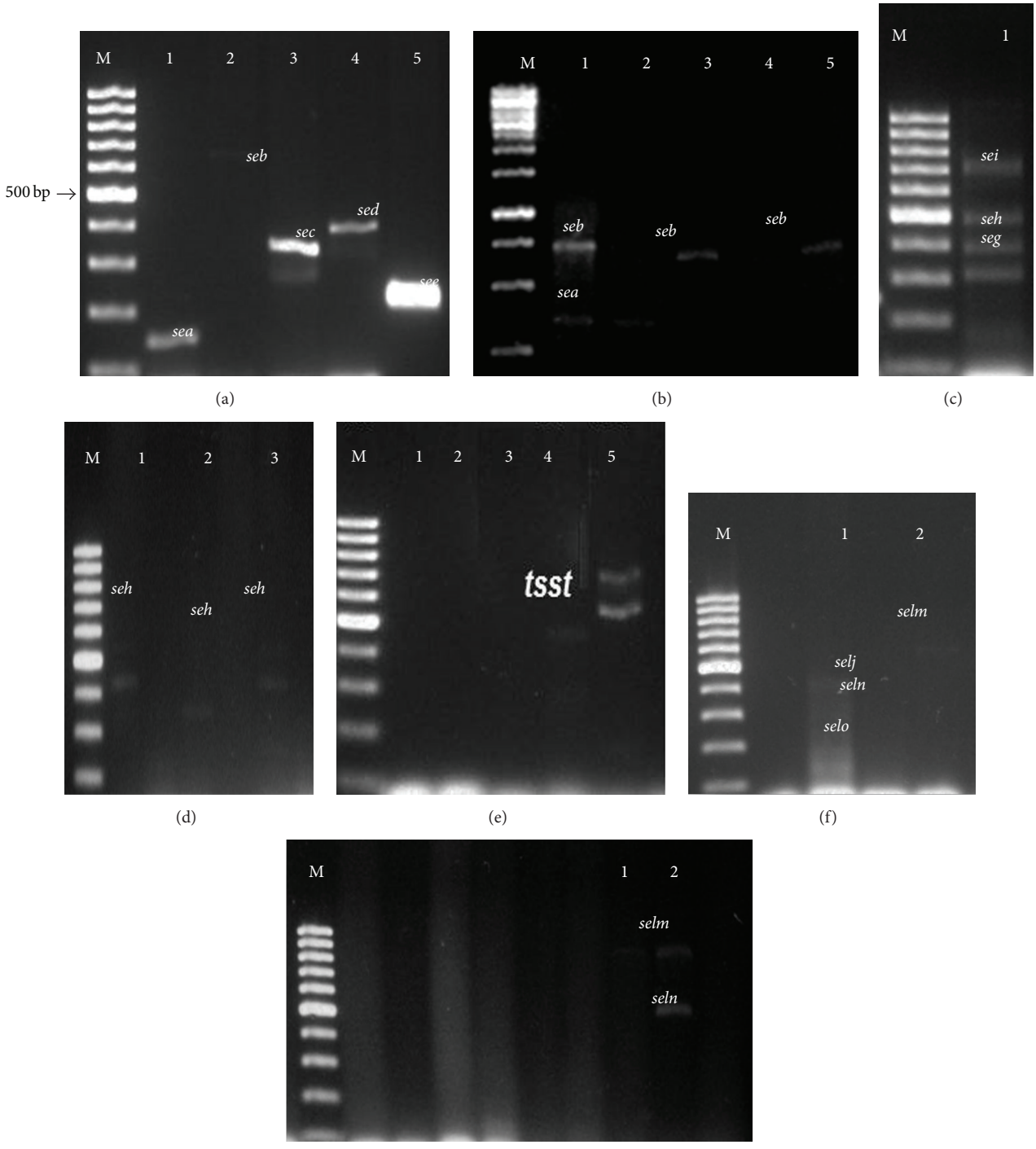

Figure 2: Uniplex, duplex, and multiplex PCR screening for the detection of enterotoxin genes in CNS strains from salami. (a) Lane M, 100 bp DNA ladder plus (Fermentas, Foster City, CA, USA); lane 1, *S. aureus* ATCC 29231 harboring *sea* gene; lane 2, *S. aureus* NCTC 10654 harboring *seb* gene; lane 3, *S. aureus* ATCC19095 harboring the *sec* gene; lane 4, *S. aureus* ATCC 13563 harboring the *sed* gene; and lane 5, *S. aureus* ATCC 27664 harboring the *see* gene. (b) Lane M 100 bp DNA ladder plus; lane 1, *Staphylococcus* spp.; lane 2, *S. carnosus* NR116434; lane 3, *S. carnosus* KJ862002; lane 4, *S. carnosus* KJ862002; and lane 5, *S. carnosus* KJ862002.1. (c) Lane M, 100 bp DNA ladder plus; lane 1, *S. aureus* ATCC 19095 harboring *seg*, *seh*, and *sei* genes. (d) Lane M, 100 bp DNA ladder plus; lane 1, *S. saprophyticus* AB697717.1; lane 2, *S. epidermidis* KF 600589.1; and lane 3, *S. sciuri* JX966436.1. (e) Lane M, 100 bp DNA ladder plus; lane 1, *S. xylosus* KF198080.1; lane 2, *S. saprophyticus* KJ699151.1. (f) Lane M, 100 bp DNA ladder plus; lane 1, *S. aureus* ATCC 27154 harboring *selj*, *slem*, *seln*, and *selo* genes. (g) Lane M, 100 bp DNA ladder plus; lane 1, *S. xylosus* KF198080.1; and lane 2, *S. saprophyticus* subsp. *bovis* KJ699151.1.

shown to carry the *selm, seln,* and *selo* genes and the *selm* and *seln* sequences were detected in the genome of a single strain, *S. saprophyticus* subsp. *bovis* KJ699151.1. *S. epidermidis* KF600589.1 showed a combination of *seg* and *sei* genes and 03 strains harbored a single gene, *sei or selm or seln*, perhaps due to the high degree of genetic polymorphism in the chromosomal assembly [41]. Indrawattana et al., 2013, detected the *seg-sei-selm-seln-selo* of the highly prevalent *egc* locus was 26.1% in contrast to this study where 13% CNS presents the combination of *selm, seln,* and *selo* genes [42].

The CNS strains clustered into groups near the bottom of the phylogenetic tree carried the classical enterotoxin genes, while the species at the top of the tree showed high diversity among the enterotoxin genes, combining the classical and the newly described genes in their genomes (Figure 1).

To assess the risk of staphylococcal food poisoning, the ability of the identified strains in harboring the *se* and *sel* genes and in expressing and producing enterotoxins *in vitro* was evaluated. The mRNA for each enterotoxin gene was evaluated by real time RT-PCR assays and enterotoxin content was estimated by a sandwich enzyme immunoassay for the combined detection of *Staphylococcus* enterotoxins (SET) A, B, C, D, and E.

The fifteen enterotoxigenic CNS strains were able to express the classical enterotoxins SEA, *seb*, *sec*, *sed*, and *see*, in concentrations ranging from 0.3 ng mL^{-1} to 1.4 ng mL^{-1}, as assessed by the *in vitro* assays (Table 2). The *S. saprophyticus* AB697717.1, KJ699151.1, JX490122.1, KJ004623.1, and HF937252.1 strains, *S. xylosus* KF198080.1, and *S. carnosus* NR116434.1 produced low amount of enterotoxins, lower than 0.5 ng mL^{-1}. *S. epidermidis* KF600589.1, *S. saprophyticus bovis* KJ699151.1, and *S. hominis* JX519988.1 produced intermediate amount of enterotoxins, ranging from 0.7 to 0.90 ng mL^{-1}, while *S. sciuri* JX966436.1, *S. saprophyticus* EU430992.1, *S. carnosus* KJ862002.1, *S. xylosus* CP008724.1, and *S. succinus* KC329824.1 produced enterotoxins in concentrations ≥1.0 ng mL^{-1}.

Although the sandwich enzyme immunoassay is considered the most sensitive method to detect *sea–see* enterotoxins, able to detect 0.125 ng mL^{-1}, differences in the specificity and sensitivity of the assays for the detection of staphylococcal enterotoxins from foods are expected [43]. A single strain, *Staphylococcus* spp. KF135445.1, which harbors both the *sea* and *seb* genes, was unable to produce *sea–see* enterotoxins.

The mRNA levels evaluated by the real time RT-PCR assays for enterotoxins were detected in 12 of 15 strains (86%) (Table 2). Transcripts for the classical enterotoxins genes were detected when *S. saprophyticus* HF937252.1, *S. carnosus* NR116434.1, *S. xylosus* CP008724.1, and *S. succinus* KC329824.1 were assayed. Transcripts for newly described enterotoxins were observed in *S. saprophyticus* JX490122.1 and AB697717.1, *S. sciuri* JX966436.1, *S. saprophyticus* subsp. *bovis* KJ699151.1, and *S. hominis* JX519988.1. Transcripts from both the classical and newly described enterotoxins were detected in *S. saprophyticus* EU430992.1 and KJ949606.1 and *S. epidermidis* KF600589.1.

No mRNA transcripts were obtained for *S. saprophyticus* KJ0046232.1 and *S. carnosus* KJ862002.1, although enterotoxin production was detected by the enzyme-linked immunosorbent tests (Table 2).

The 04 strains that carry *tstH1* in their genome, *S. saprophyticus* EU430992.1 and KJ699151.1, and *S. xylosus* CP008724.1 and KF98080.1 were not able to produce mRNA for TSST-1 in the assay conditions.

The production of classical enterotoxins *in vitro* (immunologic test) matched the results shown by real time RT-PCR assays for the following strains: *S. saprophyticus* JX490122.1, *S. sciuri* JX966436.1, *S. saprophyticus* EU430992.1, *S. saprophyticus* HF937252.1, *S. saprophyticus* subsp. *bovis* KJ699151.1, *S. hominis* JX519988.1, *S. epidermidis* KF600589.1, and *S. succinus* KC329824.1.

Ten strains, namely, *S. saprophyticus* AB697717.1, *S. saprophyticus* EU430992.1, *S. saprophyticus* HF937252.1, *S. saprophyticus* KJ699151.1, *S. saprophyticus* KJ949606.1, *S. succinus KC329824.1*, *S. hominis* JX519988.1, *S. xylosus* KF198080.1 and *S. xylosus* CP008724.1, and *S. epidermidis* KF600589.1 expressed mRNA for multiple *se* and/or *sel* genes. There is a differential transcription among these genes, where the most frequent among the classical ones were *seb* and *see/sea*, transcribed by 04 and 02 strains, respectively, and the most frequent among the newly described genes were *sei* and *seh/seln/selo,* transcribed by 03 and 02 strains, respectively.

No mRNA for the *sec* gene was detected, although *S. saprophyticus* AB697717.1 was able to produce the enterotoxin *in vitro*, as detected by the ELISA assays.

3.4. Enterotoxin Gene Homologies between Salami CNS and CPS Strains. The nucleotide sequencing of six enterotoxin genes—two of them, *sec* and *see,* encoding classical enterotoxins—and four of them, encoding the newly described genes, *seg, seh, selm,* and *seln* from CNS strains, was compared to the enterotoxin genes from *S. aureus* or *S. pasteuri*, two coagulase-positive staphylococci strains (Figure 3). The homology between the CNS and CPS enterotoxin genes varied from 65% to 98%. The homology of *sec, seg, seh, selm,* and *seln* between CNS from salami and *S. aureus* was 98%, 60%, 98%, 65%, and 70%, respectively. The homology between *see* from CNS found in salami and in *S. pasteuri* was 98%.

Although further studies should be performed, it seems that the sequences encoding enterotoxins can be conserved among coagulase-negative and coagulase-positive staphylococci, as shown in the phylogenetic analysis of the 06 enterotoxin genes (Figure 4).

3.5. Antimicrobial Multiresistance of CNS Strains (MRCNS). Another safety hazard associated with CNS strains besides the ability of producing enterotoxins in food matrices is the antimicrobial resistance to antimicrobial agents commonly used to treat staphylococci infections. The antimicrobial resistance carried by CNS strains from food matrices can be spread to the population by the consumption of an apparently safe food.

Among the 19 CNS strains identified in salami, 14 showed multiresistance to antimicrobial agents. Three strains showed the highest MAR indices, 0.93 and 0.80; 07 strains presented

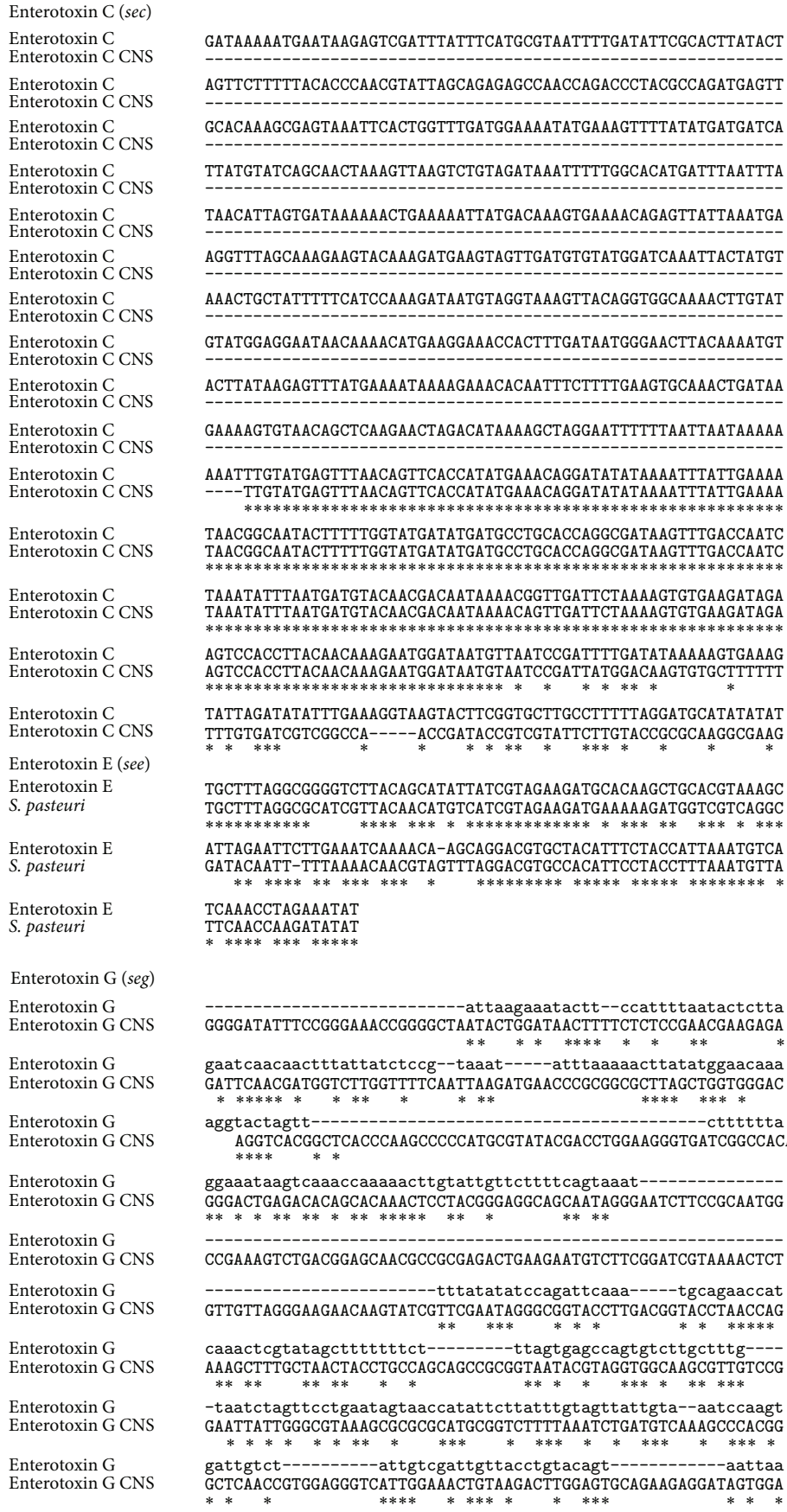

Figure 3: Continued.

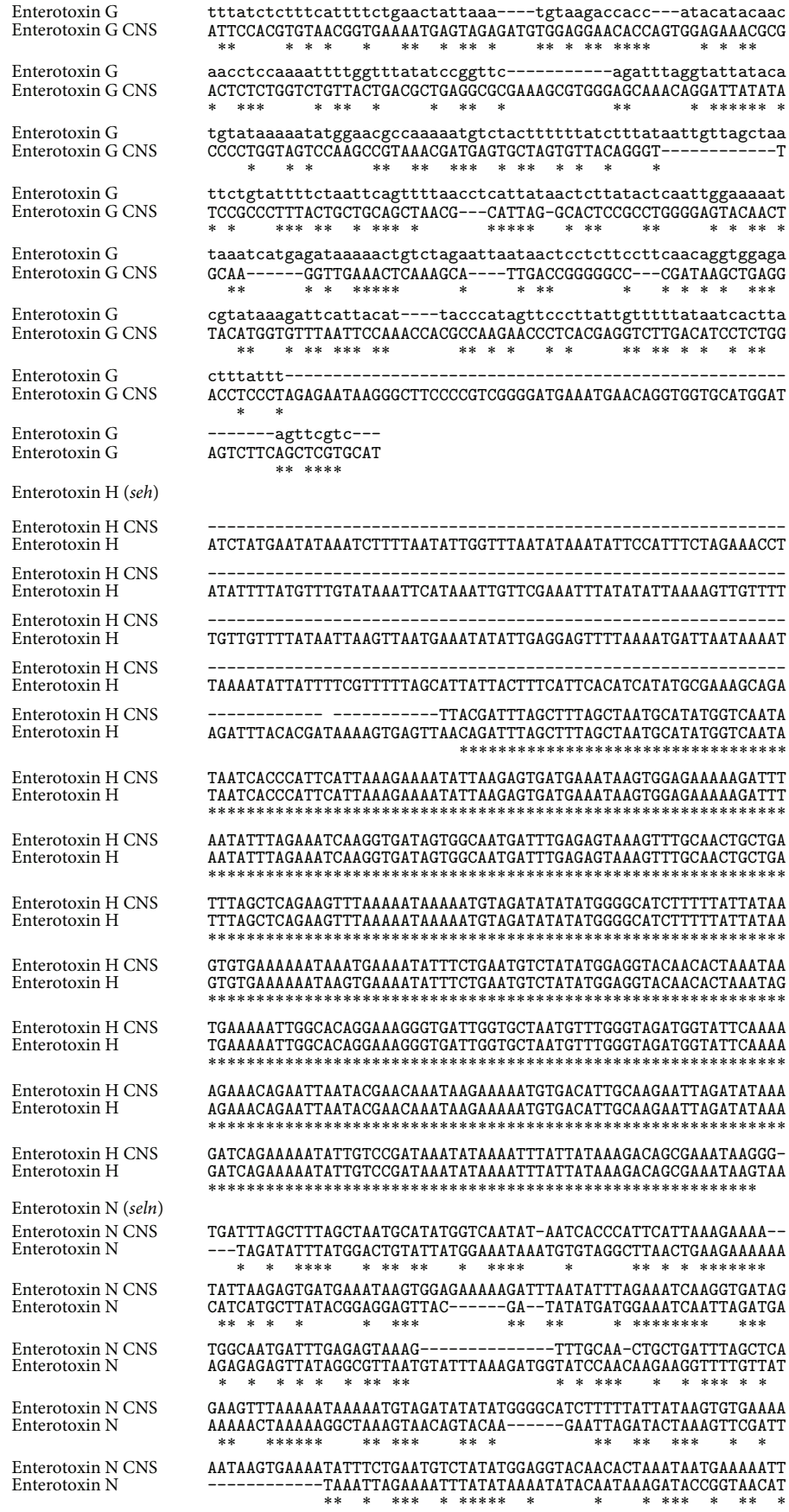

Figure 3: Continued.

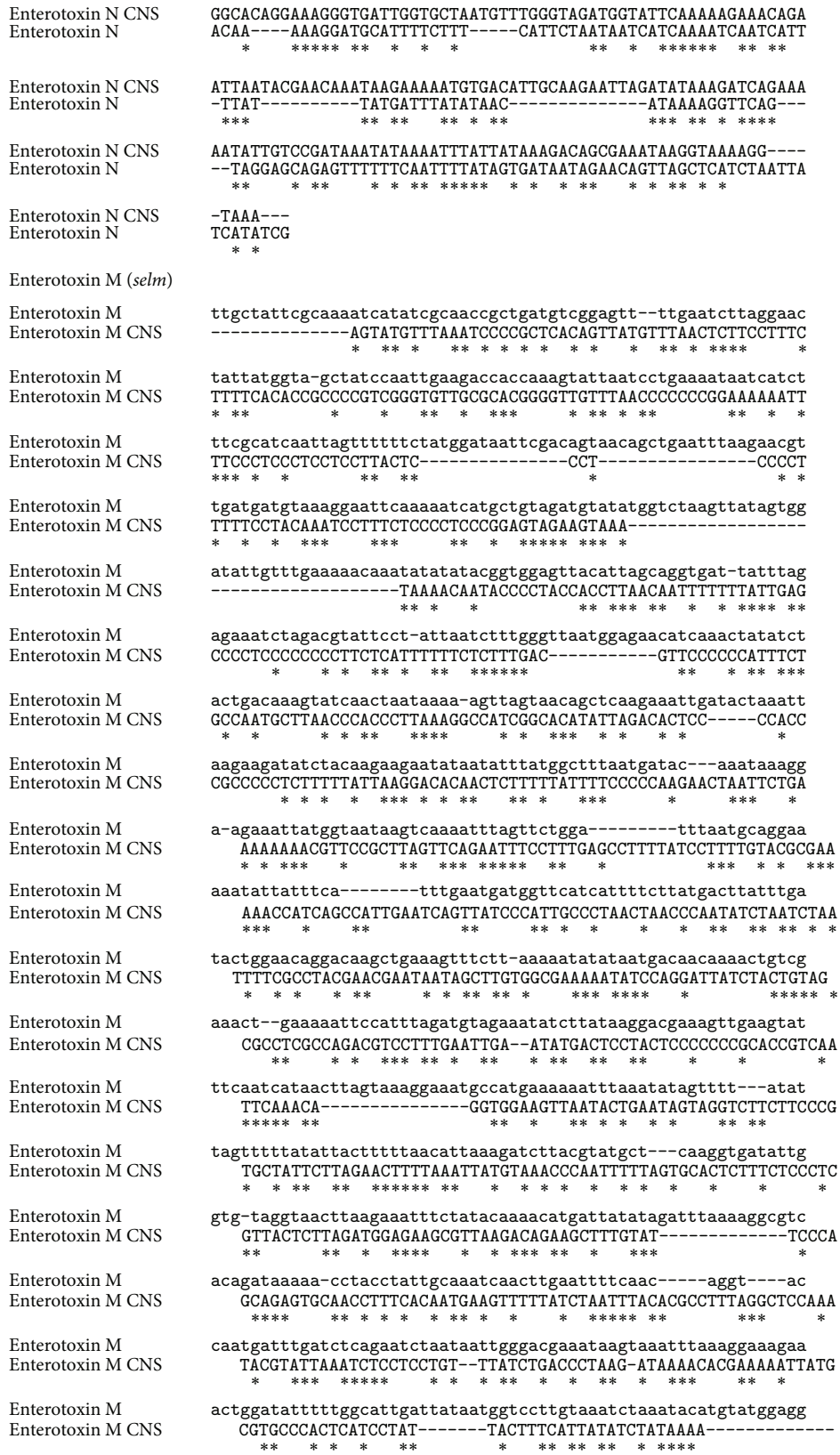

Figure 3: Alignment of the enterotoxin gene sequences found in coagulase-negative staphylococci (CNS) and in coagulase-positive staphylococci (CPS).

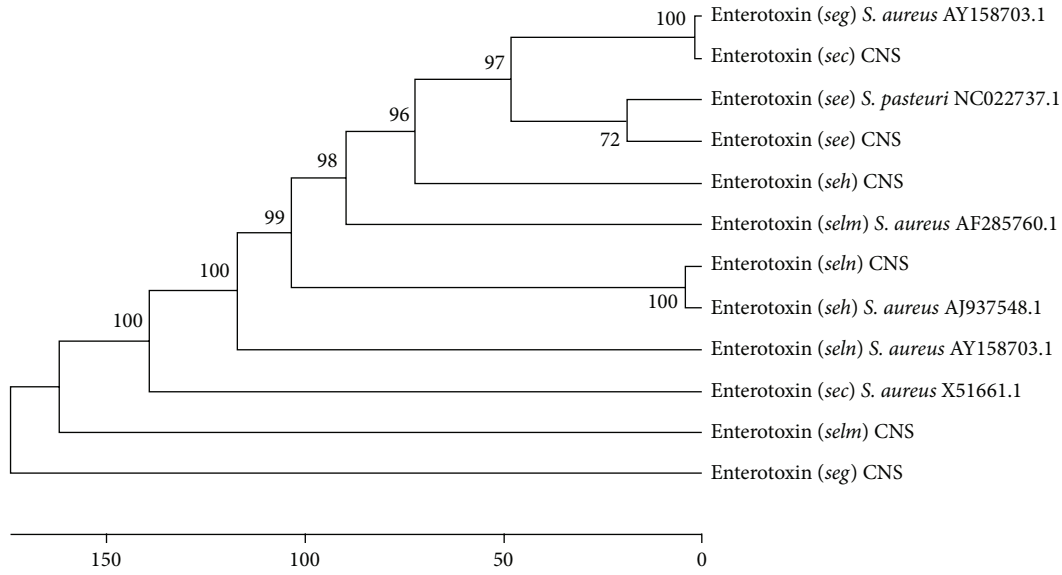

Figure 4: Phylogenetic tree generated from the multiple alignments of the enterotoxin sequences of CNS and CPS strains using the ClustalX 2.0 software package. The phylogenetic tree was constructed using the Mega 6.0 software and the unweighted pair group method (UPGMA).

MAR indices varying from 0.66 to 0.46, and the remaining 04 strains showed MAR indices ≤0.26 (Table 3).

The 14 MRCNS strains were resistant to β-lactams (oxacillin, penicillin, and/or cefoxitin) and to vancomycin, corresponding to 73% of the total CNS strains identified, while 09 strains (64%) showed resistance to tetracycline and gentamicin, 08 strains (57%) were resistant to neomycin, erythromycin, and chloramphenicol, 07 strains (50%) were resistant to sulfamethoprim, 05 strains (36%) were resistant to linezolid, 03 strains (21%) were resistant to rifampicin, 02 strains (14%) were resistant to ciprofloxacin and cefepime, and 01 strain (7%) was resistant to clindamycin (Table 3).

The multiresistance of CNS strains demonstrated herein is consistent with previous studies on coagulase-negative and coagulase-positive staphylococci that have found several resistant and multiresistant *Staphylococcus aureus* strains in raw milk, meat, and fermented meat products [43].

Surprisingly, the resistance to chloramphenicol is very similar to that estimated for MRCNS strains isolated from human clinical samples. Indeed, there is no direct correlation between the researched features and the origin of the staphylococci strains, since different virulence factors are widespread, such as antibiotic resistance [44], reinforcing the fact that the ability of food matrices strains to produce SE and SE*l* and their multiresistance character must be considered when evaluating the safety hazards of food poisoning.

S. epidermidis KF600589.1 and *S. hominis* JX519988.1 showed the highest MAR indexes (0.93 and 0.80, resp.). These strains found in artisanal salami are homologous to strains isolated from human skin microbiota and should be carefully considered among the potential pathogenic staphylococci found in food from animal origins, which can be caused by contamination by poor hygienic conditions during salami manufacturing.

Depending on the conditions, some species of coagulase-negative staphylococci can present health risks, since they have shown resistance to antibiotics of therapeutic importance, such as beta lactams [15]. However, multiresistant strains like *S. carnosus* KJ1862002.1 and *S. xylosus* CP007208.1 and CP008724.1 were intentionally introduced in the food matrix, since they are part of the culture starter used in Italian-salami manufacturing. As previously discussed, food can be a reservoir of multiresistant microorganisms that can spread by the consumption of an apparently safe food. Due to the intensive and indiscriminate use of antibiotics for human and veterinarian therapeutic purposes, multiresistant staphylococci strains are being selected and reproduced in food matrices [45].

The cefoxitin and oxacillin disk diffusion tests are recommended for determining the resistance and susceptibility breakpoint for MRSA surveillance cultures [46]. In this study, there was a good correlation between the disc test zone diameters for oxacillin and cefoxitin (Table 3). The MICs for ampicillin and methicillin/oxacillin/cefoxitin for all susceptible CNS strains were determined by the diffusion disc test, using 0.03 to 2 mg mL^{-1} of each antimicrobial agent.

S. saprophyticus HF937252.1 showed an MIC of 0.03 mg mL^{-1} for methicillin, strain *S. carnosus* KJ862002.1, *S. xylosus strains* CP008724.1 and CP007208.1, S. *saprophyticus* JX490122.1, *S. hominis* JX519988.1, and *S. succinus* KC329824.1 were resistant to 0.06 mg mL^{-1} and two strains, *S. saprophyticus* KJ699151.1 and *S. saprophyticus* KJ004623.1, showed an MIC of 0.5 mg mL^{-1} (Table 4). Two of the methicillin-resistant strains, *S. saprophyticus* KJ004623.1 and *S. xylosus* CP007208.1, harbor no enterotoxin gene.

Five strains, *S. saprophyticus* JX490122.1, *S. carnosus* KJ862002.1, *S. xylosus* CP008724.1, *S. xylosus* KF198080.1, and *S. saprophyticus* KJ004623.1, showed an MIC for ampicillin

Table 3: Multiple resistance to antimicrobial as found in CNS strains from salami.

Salami origin	CNS strains	Antimicrobial agent resistance	Multiple antimicrobial resistance (MAR) index*
Commercial	*Staphylococcus* spp. KF135445.1	CIP, CLO, CPM, GEN, NEO, OXA, PEN, SXT, TET, and VAN	0.66
Commercial	*S. carnosus* KJ862002.1	CIP, GEN, LZD, NEO, OXA, SXT, and TET	0.46
Commercial	*S. saprophyticus* AB697717.1	CFO, CLO, ERI, PEN, OXA, TET, and VAN	0.46
Commercial	*S. saprophyticus* EU430992.1	CFO, CLO, ERI, GEN, LZD, NEO, OXA, PEN, SXT, TET, and VAN	0.80
Commercial	*S. saprophyticus* JX490122.1	CFO, CLO, ERI, GEN, NEO, PEN, OXA, SXT, TET, and VAN	0.66
Commercial	*S. saprophyticus* KJ004623.1	CFO, OXA, and PEN	0.20
Commercial	*S. sciuri* JX966436.1	CFO, CLO, GEN, NEO, OXA, PEN, and TET	0.46
Commercial	*S. xylosus* CP007208.1	OXA, LZD, PEN, and VAN	0.26
Commercial	*S. xylosus* CP008724.1	CFO, CLO, ERI, GEN, NEO, OXA, PEN, TET, and VAN	0.60
Artisanal	*S. epidermidis* KF600589.1	CFO, CLI, CLO, CPM, ERI, GEN, LZD, NEO, OXA, PEN, RIF, SXT, and TET	0.93
Artisanal	*S. hominis* JX519988.1	CIP, CPM, CPO, ERI, GEN, LZD, NEO, OXA, PEN, RIF, SXT, and VAN	0.80
Artisanal	*S. saprophyticus* HF937252.1	CFO, OXA, PEN, and SXT	0.26
Artisanal	*S. saprophyticus* KJ699151.1	OXA, PEN, and VAN	0.20
Artisanal	*S. succinus* KC329824.1	CFO, CLO, ERI, GEN, OXA, PEN, RIF, SXT, TET, and VAN	0.66
Artisanal	*S. xylosus* KF198080.1	CFO, CLO, ERI, GEN, NEO, OXA, PEN, TET, and VAN	0.60

*The MAR index of an isolate is defined as a/b, where a represents the number of antimicrobials to which the isolate was resistant and b represents the number of antimicrobials to which the isolate was subjected.
S. aureus strains ATCC WB81 (*sea*), ATCC 13563 (*sed*), and ATCC 27664 (*see*) showing a MAR index of 0.5 and *S. aureus strains* ATCC14458 (*seb*) and ATCCWB72 (*sec*) and *S. xylosus* ATCC 29971 showing a MAR index of 0.3 were used as reference strains.
CPM: cefepime, CFO: cefoxitin, CLO: chloramphenicol, CIP: ciprofloxacin, CLI: clindamycin, ERI: erythromycin, GEN: gentamycin, NEO: neomycin, LZD: linezolid, RIF; rifampicin, TET: tetracycline, OXA; oxacillin, PEN: penicillin, SXT: sulfamethoprim, and VAN: vancomycin.

Table 4: Minimal inhibitory concentration (MIC) of compounds used in antimicrobial therapy against staphylococci infections.

Salami origin	GenBank accession number and similarity (%)	MIC mg mL^{-1}			
		Methicillin	Ampicillin	Vancomycin	Linezolid
Commercial	*S. carnosus* KJ862002.1	0.06	0.03	—	—
	S. xylosus CP008724.1	0.06	0.03	0.06	—
	S. saprophyticus JX490122.1	0.06	0.03	0.5	—
	S. saprophyticus AB697717.1	—	—	0.5	—
	S. saprophyticus EU430992.1	—	—	0.25	0.125
	S. succinus KC329824.1	0.06	0.25	0.03	—
Artisanal	*S. hominis.* JX519988.1	0.06	0.5	—	—
	S. saprophyticus HF937252.1	0.03	—	—	—
	S. xylosus KF198080.1		0.03	0.5	—
	S. saprophyticus KJ699151.1	0.5	0.25	0.03	—
	S. saprophyticus KJ004623.1	0.5	0.03	0.03	—
	S. xylosus CP007208.1	0.06	—	—	0.25

Strains *S. epidermidis* KF600589.1 and *Staphylococcus* spp. KF135445.1 were not susceptible to the antimicrobial concentrations tested in the present study.

of 0.03 mg mL^{-1}, two strains, *S. succinus* KC329824.1 and *S. saprophyticus* KJ699151.1, showed an MIC of 0.25 mg mL^{-1}, and *S. hominis* JX519988.1 showed an MIC of 0.5 mg mL^{-1} (Table 4). *S. saprophyticus* KJ004623.1 also showed an MIC of 0.03 mg mL^{-1} but does not harbor enterotoxin genes. It is important to note that most of the CNS strains that showed resistance to ampicillin were also resistant to methicillin, as highlighted by the MIC tests.

Five strains, *S. saprophyticus* HF937252.1, *S. saprophyticus* KJ699151.1, *S. saprophyticus* JX490122.1, *S. saprophyticus* KJ004623.1, and *S. succinus* KC329824.1, showed an MIC for vancomycin of 0.03 mg mL^{-1}, one strain, *S. xylosus* CP008724.1, showed an MIC of 0.06 mg mL^{-1}, one strain, *S. saprophyticus* EU430992.1, showed an MIC of 0.25 mg mL^{-1}, and two strains, *S. xylosus* KF198080.1 and *S. saprophyticus* AB697717.1, showed an MIC of 0.5 mg mL^{-1} (Table 4).

Additionally, five CNS strains, *S. xylosus* CP008724.1, *S. saprophyticus* JX 490122.1, *S. succinus* KC329824.1, *S. saprophyticus* KJ699151.1, and *S. saprophyticus* KJ004623.1, showed resistance to methicillin, as demonstrated by the MIC determinations (Table 4).

Previous studies have demonstrated that linezolid is active against Gram-positive bacteria, including methicillin-resistant staphylococci [47]. In the present study, 05 strains showed linezolid resistance in the disc diffusion test, but it was impossible to establish MIC values for *S. epidermidis* KF600589.1, *Staphylococcus hominis* JX519988.1, and *Staphylococcus carnosus* KJ862002.1. The remaining strains *S. saprophyticus* EU430992.1 and *S. xylosus* CP007208.1 presented an MIC for linezolid of 0.125 mg mL^{-1} and 0.25 mg mL^{-1}, respectively.

The MIC of 0.03 mg mL^{-1} for penicillin is in accordance with the previous values estimated for resistant *S. aureus* strains found in several food matrices, such as meat, dairy products, and ready-to-eat food [48].

There is still a lack of information on the antimicrobial resistance of staphylococci strains from food matrices, although they are the most worrisome vehicles of dissemination of antibiotic-resistant pathogens [49].

The high resistance found for salami staphylococci strains can be ascribed to their inappropriate use as growth promoters of antimicrobial agents like oxacillin, vancomycin, chloramphenicol, neomycin, and erythromycin, which are commonly used in veterinary medicine to treat infections [50]. Antimicrobial therapy of infections staphylococci is based on results of susceptibility tests *in vitro* [51]. Methicillin-resistant coagulase-negative *Staphylococcus* spp. found in ready-to-eat products such as meats, fish, and dairy products also offer risks and, although they are not classical food poisoning bacteria, their presence in food offers significant risks to public health due to the possible spread of antibiotic resistance [52].

The standardization of salami quality should include diagnostic methods to screen and quantify the presence of classical and newly described enterotoxins directly in the food matrices as a routine procedure to be conducted by the meat product industry in Brazil.

The safety of salami consumption could also be enhanced by the inclusion of a microbial barrier such as the inclusion of probiotic strains producing natural antibiotics or competitive flora or even the addition of natural bioagents against spoilage or pathogenic microorganisms.

Conflict of Interests

The authors declare that there is no conflict of interests regarding the publication of this paper.

Acknowledgments

The authors acknowledge the financial support from Fundação Carlos Chagas Filho de Amparo à Pesquisa do Estado do Rio de Janeiro (FAPERJ, Rio de Janeiro, Brazil), Conselho Nacional de Desenvolvimento Científico e Tecnológico (CNPq, Brasília, Brazil), and Coordenação de Aperfeiçoamento de Pessoal de Nível Superior (CAPES, Brasília, Brazil).

References

[1] ICMSF: International Comission on Microbiological Specifications for Foods, *Microorganisms in Foods. Their Significance and Methods of Enumerations*, University of Toronto Press, Toronto, Canada, 3rd edition, 1983.

[2] J. F. Veras, L. S. Carmo, L. C. Tong et al., "A study of the enterotoxigenicity of coagulase-negative and coagulase-positive staphylococcal isolates from food poisoning outbreaks in Minas Gerais, Brazil," *International Journal of Infectious Diseases*, vol. 12, no. 4, pp. 410–415, 2008.

[3] K. Omoe, D.-L. Hu, H. Takahashi-Omoe, A. Nakane, and K. Shinagawa, "Comprehensive analysis of classical and newly described staphylococcal superantigenic toxin genes in *Staphylococcus aureus* isolates," *FEMS Microbiology Letters*, vol. 246, no. 2, pp. 191–198, 2005.

[4] J. Kadariya, T. C. Smith, and D. Thapaliya, "*Staphylococcus aureus* and staphylococcal food-borne disease: an ongoing challenge in public health," *BioMed Research International*, vol. 2014, Article ID 827965, 9 pages, 2014.

[5] K. Omoe, D.-L. Hu, H. K. Ono et al., "Emetic potentials of newly identified staphylococcal enterotoxin-like toxins," *Infection and Immunity*, vol. 81, no. 10, pp. 3627–3631, 2013.

[6] J. K. McCormick, J. M. Yarwood, and P. M. Schlievert, "Toxic shock syndrome and bacterial superantigens: an update," *Annual Review of Microbiology*, vol. 55, pp. 77–104, 2001.

[7] T. Baba, F. Takeuchi, M. Kuroda et al., "Genome and virulence determinants of high virulence community-acquired MRSA," *The Lancet*, vol. 359, no. 9320, pp. 1819–1827, 2002.

[8] Associação Brasileira de Indústria Produtora e Exportadora da Carne Suínas (ABIPECS), "Statistics slaughter ranking 2000–2014," 2014, http://abpa-br.com.br/setores/suinocultura/publicacoes/relatorios-anuais.

[9] N. Zdolec, M. Hadžiosmanović, L. Kozačinski et al., "Microbial and physicochemical succession in fermented sausages produced with bacteriocinogenic culture of *Lactobacillus sakei* and semi-purified bacteriocin mesenterocin Y," *Meat Science*, vol. 80, no. 2, pp. 480–487, 2008.

[10] F. Ravyts, L. D. Vuyst, and F. Leroy, "Bacterial diversity and functionalities in food fermentations," *Engineering in Life Sciences*, vol. 12, no. 4, pp. 356–367, 2012.

[11] T. Ohlsson and N. Bengtsson, *The Hurdle Concept: Minimal Processing Technologies in the Food Industry*, Woodhead Publishing, 2002.

[12] S. Bernardi, B. B. Golineli, and C. J. Contreras-Castillo, "Revisão: aspectos da aplicação de culturas starter na produção de embutidos cárneos fermentados," *Brazilian Journal of Food Technology*, vol. 13, no. 2, pp. 133–140, 2010.

[13] F. Irlinger, "Safety assessment of dairy microorganisms: coagulase-negative *staphylococci*," *International Journal of Food Microbiology*, vol. 126, no. 3, pp. 302–310, 2008.

[14] B. Ghebremedhin, F. Layer, W. König, and B. König, "Genetic classification and distinguishing of *Staphylococcus* species based on different partial gap, 16S rRNA, hsp60, rpoB, sodA, and tuf gene sequences," *Journal of Clinical Microbiology*, vol. 46, no. 3, pp. 1019–1025, 2008.

[15] I. Babić, K. Markov, D. Kovačević et al., "Identification and characterization of potential autochthonous starter cultures from a Croatian 'brand' product 'slavonski kulen'," *Meat Science*, vol. 88, no. 3, pp. 517–524, 2011.

[16] M. Mehrotra, G. Wang, and W. M. Johnson, "Multiplex PCR for the detection of genes for *Staphylococcus aureus* enterotoxins, exfoliative toxins, toxic shock syndrome toxin, and methicillin resistance," *Journal of Clinical Microbiology*, vol. 38, no. 3, pp. 1032–1041, 2000.

[17] W. M. Johnson, S. D. Tyler, E. P. Ewan, F. E. Ashton, D. R. Pollard, and K. R. Rozee, "Detection of genes for enterotoxins, exfoliative toxins, and toxic shock syndrome toxin 1 in *Staphylococcus aureus* by the polymerase chain reaction," *Journal of Clinical Microbiology*, vol. 29, no. 3, pp. 426–430, 1991.

[18] J. Mclauchlin, G. L. Narayanan, V. Mithani, and G. O'Neill, "The detection of enterotoxins and toxic shock syndrome toxin genes in *Staphylococcus aureus* by polymerase chain reaction," *Journal of Food Protection*, vol. 63, no. 4, pp. 479–488, 2000.

[19] J. P. Rosec and O. Gigaud, "Staphylococcal enterotoxin genes of classical and new types detected by PCR in France," *International Journal of Food Microbiology*, vol. 77, no. 1-2, pp. 61–70, 2002.

[20] K. Omoe, D.-L. Hu, H. Takahashi-Omoe, A. Nakane, and K. Shinagawa, "Identification and characterization of a new staphylococcal enterotoxin-related putative toxin encoded by two kinds of plasmids," *Infection and Immunity*, vol. 71, no. 10, pp. 6088–6094, 2003.

[21] N. Sergeev, D. Volokhov, V. Chizhikov, and A. Rasooly, "Simultaneous analysis of multiple *staphylococcal* enterotoxin genes by an oligonucleotide microarray assay," *Journal of Clinical Microbiology*, vol. 42, no. 5, pp. 2134–2143, 2004.

[22] S. Holtfreter, D. Grumann, M. Schmudde et al., "Clonal distribution of superantigen genes in clinical *Staphylococcus aureus* isolates," *Journal of Clinical Microbiology*, vol. 45, no. 8, pp. 2669–2680, 2007.

[23] W. J. Mason, J. S. Blevins, K. Beenken, N. Wibowo, N. Ojha, and M. S. Smeltzer, "Multiplex PCR protocol for the diagnosis of staphylococcal infection," *Journal of Clinical Microbiology*, vol. 39, no. 9, pp. 3332–3338, 2001.

[24] E. Rahimi and H. G. Safai, "Detection of classical enterotoxins of *Staphylococcus aureus* strains isolated from bovine subclinical mastitis in Isfahan, Iran," *Veterinary Microbiology*, vol. 141, no. 3-4, pp. 393–394, 2010.

[25] M. A. Larkin, G. Blackshields, N. P. Brown et al., "Clustal W and Clustal X version 2.0," *Bioinformatics*, vol. 23, no. 21, pp. 2947–2948, 2007.

[26] P. H. A. Sneath and R. R. Sokal, *Unweighted Pair Group Method with Arithmetic Mean. Numerical Taxonomy*, W. H. Freeman, San Francisco, Calif, USA, 1973.

[27] NCCLS, "Performance standards for antimicrobial susceptibility testing; 14th informational supplement," Tech. Rep. M 100-S14, NCCLS, 2004.

[28] S. Corbiere Morot-Bizot, S. Leroy, and R. Talon, "Monitoring of staphylococcal starters in two French processing plants manufacturing dry fermented sausages," *Journal of Applied Microbiology*, vol. 102, no. 1, pp. 238–244, 2007.

[29] R. Talon, S. Leroy, I. Lebert et al., "Safety improvement and preservation of typical sensory qualities of traditional dry fermented sausages using autochthonous starter cultures," *International Journal of Food Microbiology*, vol. 126, no. 1-2, pp. 227–234, 2008.

[30] G. Mauriello, A. Casaburi, G. Blaiotta, and F. Villani, "Isolation and technological properties of coagulase negative staphylococci from fermented sausages of Southern Italy," *Meat Science*, vol. 67, no. 1, pp. 149–158, 2004.

[31] M. Janssens, N. Myter, L. De Vuyst, and F. Leroy, "Species diversity and metabolic impact of the microbiota are low in spontaneously acidified Belgian sausages with an added starter culture of *Staphylococcus carnosus*," *Food Microbiology*, vol. 29, no. 2, pp. 167–177, 2012.

[32] G. Blaiotta, D. Ercolini, G. Mauriello, G. Salzano, and F. Villani, "Rapid and reliable identification of *Staphylococcus equorum* by a species-specific PCR assay targeting the *sodA* gene," *Systematic and Applied Microbiology*, vol. 27, no. 6, pp. 696–702, 2004.

[33] L. Kozačinski, E. Drosinos, F. Čaklovica, L. Cocolin, J. Gasparik-Reichardt, and S. Vesković, "Investigation of microbial association of traditionally fermented sausages," *Food Technology and Biotechnology*, vol. 46, no. 1, pp. 93–106, 2008.

[34] S. Leroy, P. Giammarinaro, J.-P. Chacornac, I. Lebert, and R. Talon, "Biodiversity of indigenous staphylococci of naturally fermented dry sausages and manufacturing environments of small-scale processing units," *Food Microbiology*, vol. 27, no. 2, pp. 294–301, 2010.

[35] E. Coton, M.-H. Desmonts, S. Leroy et al., "Biodiversity of Coagulase-Negative *Staphylococci* in French cheeses, dry fermented sausages, processing environments and clinical samples," *International Journal of Food Microbiology*, vol. 137, no. 2-3, pp. 221–229, 2010.

[36] S. Hosseinzadeh and H. D. Saei, "Staphylococcal species associated with bovine mastitis in the North West of Iran: emerging of coagulase-negative staphylococci," *International Journal of Veterinary Science and Medicine*, vol. 2, no. 1, pp. 27–34, 2014.

[37] A. Piette and G. Verschraegen, "Role of coagulase-negative staphylococci in human disease," *Veterinary Microbiology*, vol. 134, no. 1-2, pp. 45–54, 2009.

[38] T. M. Moura, F. S. Campos, P. A. D'Azevedo et al., "Prevalence of enterotoxin-encoding genes and antimicrobial resistance in coagulase-negative and coagulase-positive *Staphylococcus* isolates from black pudding in Southern Brazil," *Revista da Sociedade Brasileira de Medicina Tropical*, vol. 45, no. 5, pp. 579–585, 2012.

[39] H. I. Suzuki, T. Lefébure, P. P. Bitar, and M. J. Stanhope, "Comparative genomic analysis of the genus *Staphylococcus* including *Staphylococcus aureus* and its newly described sister

species *Staphylococcus simiae*," *BMC Genomics*, vol. 13, article 38, 2012.

[40] R. P. Lamers, G. Muthukrishnan, T. A. Castoe, S. Tafur, A. M. Cole, and C. L. Parkinson, "Phylogenetic relationships among *Staphylococcus* species and refinement of cluster groups based on multilocus data," *BMC Evolutionary Biology*, vol. 12, article 171, 2012.

[41] I. V. Pinchuk, E. J. Beswick, and V. E. Reyes, "Staphylococcal enterotoxins," *Toxins*, vol. 2, no. 8, pp. 2177–2197, 2010.

[42] S. R. Monday and G. A. Bohach, "Genes encoding staphylococcal enterotoxins G and I are linked and separated by DNA related to other staphylococcal enterotoxins," *Journal of Natural Toxins*, vol. 10, no. 1, pp. 1–8, 2001.

[43] D. Y. Thomas, S. Jarraud, B. Lemercier et al., "Staphylococcal enterotoxin-like toxins U2 and V, two new staphylococcal superantigens arising from recombination within the enterotoxin gene cluster," *Infection and Immunity*, vol. 74, pp. 4724–4734, 2006.

[44] N. Indrawattana, O. Sungkhachat, N. Sookrung et al., "*Staphylococcus aureus* clinical isolates: antibiotic susceptibility, molecular characteristics, and ability to form biofilm," *BioMed Research International*, vol. 2013, Article ID 314654, 11 pages, 2013.

[45] V. Pereira, C. Lopes, A. Castro, J. Silva, P. Gibbs, and P. Teixeira, "Characterization for enterotoxin production, virulence factors, and antibiotic susceptibility of *Staphylococcus aureus* isolates from various foods in Portugal," *Food Microbiology*, vol. 26, no. 3, pp. 278–282, 2009.

[46] I. Anacarso, C. Condò, C. Sabia, and et al, "Antimicrobial resistance and other related virulence factors in *staphylococcus spp* isolated from food, environmental and humans in Italy," *Universal Journal Microbiology Research*, vol. 1, no. 1, pp. 1–9, 2013.

[47] B. Martín, M. Garriga, M. Hugas, S. Bover-Cid, M. T. Veciana-Nogués, and T. Aymerich, "Molecular, technological and safety characterization of Gram-positive catalase-positive cocci from slightly fermented sausages," *International Journal of Food Microbiology*, vol. 107, no. 2, pp. 148–158, 2006.

[48] N. M. Broekema, T. Van Tam, T. A. Monson, S. A. Marshall, and D. M. Warshauer, "Comparison of cefoxitin and oxacillin disk diffusion methods for detection of *mec*A-mediated resistance in *Staphylococcus aureus* in a large-scale study," *Journal of Clinical Microbiology*, vol. 47, no. 1, pp. 217–219, 2009.

[49] E. Cercenado, F. García-Garrote, and E. Bouza, "*In vitro* activity of linezolid against multiply resistant Gram-positive clinical isolates," *Journal of Antimicrobial Chemotherapy*, vol. 47, no. 1, pp. 77–81, 2001.

[50] A. Aydin, K. Muratoglu, M. Sudagidan, K. Bostan, B. Okuklu, and S. Harsa, "Prevalence and antibiotic resistance of foodborne *Staphylococcus aureus* isolates in Turkey," *Foodborne Pathogens and Disease*, vol. 8, no. 1, pp. 63–69, 2011.

[51] D. Sergelidis, A. Abrahim, T. Papadopoulos et al., "Isolation of methicillin-resistant *Staphylococcus* spp. from ready-to-eat fish products," *Letters in Applied Microbiology*, vol. 59, no. 5, pp. 500–506, 2014.

[52] I. Phillips, M. Casewell, T. Cox et al., "Does the use of antibiotics in food animals pose a risk to human health? A critical review of published data," *Journal of Antimicrobial Chemotherapy*, vol. 53, no. 1, pp. 28–52, 2004.

Hindawi Publishing Corporation
BioMed Research International
Volume 2015, Article ID 267538, 5 pages
http://dx.doi.org/10.1155/2015/267538

Research Article

Improved Sugar Production by Optimizing Planetary Mill Pretreatment and Enzyme Hydrolysis Process

Jeong Heo Kwon,[1,2] Siseon Lee,[3] Jae-Won Lee,[4] Youn-Woo Hong,[1] Jeong Ho Chang,[1] Daekyung Sung,[1] Sung Hyun Kim,[1] Byoung-In Sang,[2] Robert J. Mitchell,[3] and Jin Hyung Lee[1]

[1]*Korea Institute of Ceramic Engineering and Technology (KICET), 101 Soho-ro, Jinju-si, Gyeongsangnam-do 52851, Republic of Korea*
[2]*Department of Chemical Engineer, Hanyang University, Seoul 04763, Republic of Korea*
[3]*School of Nano-Bioscience and Chemical Engineering, Ulsan National Institute of Science and Technology, Ulsan 44919, Republic of Korea*
[4]*Department of Forest Products and Technology, Chonnam National University, Gwangju 61186, Republic of Korea*

Correspondence should be addressed to Robert J. Mitchell; esgott@unist.ac.kr and Jin Hyung Lee; leejinh1@kicet.re.kr

Received 19 May 2015; Revised 30 July 2015; Accepted 9 August 2015

Academic Editor: Yu Zhang

This paper describes an optimization of planetary mill pretreatment and saccharification processes for improving biosugar production. Pitch pine (*Pinus rigida*) wood sawdust waste was used as biomass feedstock and the process parameters optimized in this study were the buffering media, the milling time, the enzyme quantity, and the incubation time. Glucose yields were improved when acetate buffer was used rather than citrate buffer. Initially, with each process variable tests, the optimal values were 100 minutes of milling, an enzyme concentration of 16 FPU/g-biomass, and a 12-hour enzymatic hydrolysis. Typically, interactions between these experimental conditions and their effects on glucose production were next investigated using RSM. Glucose yields from the *Pinus rigida* waste exceeded 80% with several of the conditions tested, demonstrating that milling can be used to obtain high levels of glucose bioconversion from woody biomass for biorefinery purposes.

1. Introduction

Biofuel production is one of major emerging issues in environmental biotechnologies. Producing biofuels from biomass involve a series of processes: producing sugar from biomass through saccharification and biofuels from the sugar through fermentation in order of precedence. However, pretreatment of biomass, typically lignocellulosic, is a currently essential process to obtain high conversion of biomass prior to saccharification and fermentation because of the recalcitrance of biomass. Lignocellulosic biomass consists of cellulose, hemicelluloses, and lignin. Cellulose and hemicelluloses can be hydrolyzed to glucose and xylose, respectively, and subsequently converted to biofuels such as ethanol or butanol through fermentation. The purpose of pretreatment is to make the cellulose within the biomass more readily available for hydrolysis.

Previous study showed the potential of using planetary milling to pretreat biomass for downstream fermentation [1]. This method neither uses chemicals nor produces saccharification and fermentation inhibitors such as phenolics and furans, both of which are known to elicit stress responses within bacteria [2, 3]. Moreover, pretreatment with planetary milling does not involve high temperatures or pressures, making it more user friendly than many other pretreatment processes.

For an improved sugar production using planetary milling, several factors should be taken into consideration, including the milling time, the amount of enzyme added, and the time given for hydrolysis, as well as the type

Table 1: Absolute compositional percentage of each component within the native pitch pine (*Pinus rigida*).

Cellulose Glucan (%)	Hemicellulose				Lignin		Acetyl (%)	Ash (%)
	Xylan (%)	Arabinan (%)	Galactan (%)	Mannan (%)	Acid-insoluble (%)	Acid-soluble (%)		
41.54 ± 0.27	5.75 ± 0.66	2.66 ± 0.08	2.2 ± 0.02	9.52 ± 0.02	32.35 ± 0.11	0.78 ± 0.04	0.83 ± 0.04	0.37 ± 0.02

of buffer used during milling. Hence, we investigated the optimal conditions of pretreatment and enzymatic hydrolysis processes. Glucose yield is a result of combinational interaction between several experimental variables. Therefore, we investigated interactional effects of variable parameters during pretreatment and enzyme hydrolysis in this study, not only single parameter effects. We employed a softwood, pitch pine (*Pinus rigida*), as the feedstock for pretreatment and glucose production. Softwoods are dominant in the northern hemisphere but they have high lignin content and recalcitrant nature to enzymatic hydrolysis [4, 5], making them a model feedstock for this study.

2. Materials and Methods

2.1. Materials. The sawdust wood waste of pitch pine (*Pinus rigida*) after forestry manufacturing process was obtained from Suncheon Forestry Cooperative, Republic Korea. Compositional analysis of the sawdust wood waste was measured according to National Renewable Energy Laboratory protocols [6].

2.2. Planetary Mill Pretreatment. The planetary mill of sawdust wood waste of pitch pine (*Pinus rigida*) was carried out using a Pulverisette 5 (Fritsch, Germany) in zirconia jar container with 3 mm diameter zirconia balls. The jar was loaded with 7.2 g of biomass and 180 mL of 50 mM sodium acetate (pH 4.8) or 100 mM sodium citrate (pH 4.8). Planetary milling was performed at room temperature by changing the conditions of experimental factors such as milling time and types of buffer solution. The jar was rotated at a velocity of 300 rpm.

2.3. Enzymatic Hydrolysis. The buffer solutions used in planetary milling were suitable for cellulase activity. Hence, enzymatic hydrolysis process was continually carried out after the planetary milling without washing or exchanging buffer. A cellulase cocktail (Worthington Biochemical Co., USA) was added into the buffer containing milled biomass. Enzymatic hydrolysis was performed at 50°C in a shaking incubator (JEIO TECH, Rep Korea) at 200 rpm. The glucose yield was calculated using the following equation:

$$\text{Glucose yield (\%)} = \frac{\text{Glucose produced by enzyme hydrolysis}}{\text{Glucan in sawdust wood waste} \times 1.11} \times 100 \quad (1)$$

which was used in a previous study [7].

2.4. Characterization of the Samples. For investigating the morphology, pretreated pitch pine samples were incubated in dry oven. The samples were coated with Pt on a Cressington Scientific Instruments 108 Auto Sputter Coater (Cranberry Tep., USA). A scanning electron microscope (JSM-6700F, JEOL, Japan) was used to obtain microscopic images.

X-ray diffraction (Rigaku D/max-RB powder diffractometer, Japan) with Cu $\kappa\alpha$ radiation (λ = 1.542 Å) was used for investigating the crystallinity of the samples. Samples were scanned at rate of 2°/min.

The quantities of glucose produced were measured by test strips (Glucose Test Method, Merck, Germany). The color changes were analyzed using a Reflectometer (RQflex plus 10, Merck, Germany). Test strips (Glucose Test Method, Merck, Germany) were sufficiently immersed into test solutions and placed in strip adapter to measure colorimetric changes. Finally, the software installed in the Reflectometer calculated the quantities of glucose contained in the sample by using colorimetric change.

2.5. Data Analysis. All experiments were performed in triplicate for error analysis. Minitab 14 (Minitab Inc., USA) was used for 3D surface plots.

3. Results and Discussion

Table 1 presents the composition of pitch pine sawdust used in this study. We used this softwood as a feed stock material to clearly investigate the effect of various conditions during pretreatment and saccharification since it is regarded as a high lignin-containing biomass having a strong structure [4, 5]. When compared with the previously reported composition for untreated *Pinus rigida* [8], some slight variations were seen. For example, the lignin content was somewhat higher in our samples, 33.13% as compared with 29%, while the hemicellulose portion was lower, that is, 20.13% versus 23.7%. The cellulose content of *P. rigida*, however, was similar in both studies with values slightly higher than 40%. The pitch pine sawdust waste used in study had a crystallinity index of 52.5% (Table 2). As this is higher than rice straw, which had a crystallinity index of 48% in our previous study [1], it suggests that the cellulose within *P. rigida* is more recalcitrant to treatment and hydrolysis than that of rice straw. Consequently, effects of the experimental conditions during pretreatment or saccharification can be more distinctly investigated with this biomass sample to improve glucose yield.

Acetate and citrate buffers are commonly employed during the saccharification of plant-based cellulose using enzymes to produce glucose [1, 8, 9]. To minimize the number of procedural steps required and their impact on glucose yields, including the loss of biomass, we chose to evaluate these two buffers and their effects within planetary milling processes. Pretreatment of plant biomass by planetary milling

Table 2: Comparison of the pitch pine sawdust waste crystallinity after 20 minutes of planetary milling in an acetate or citrate solution.

	Untreated	Acetate	Citrate
Crystallinity index (%)	52.5 ± 0.9	31.7 ± 0.3	36.5 ± 5.1
Relative crystallinity index[1]	1.00 ± 0.02	0.60 ± 0.01	0.70 ± 0.10

[1]Relative crystallinity index: crystallinity index after planetary milling/crystallinity index of untreated sample.

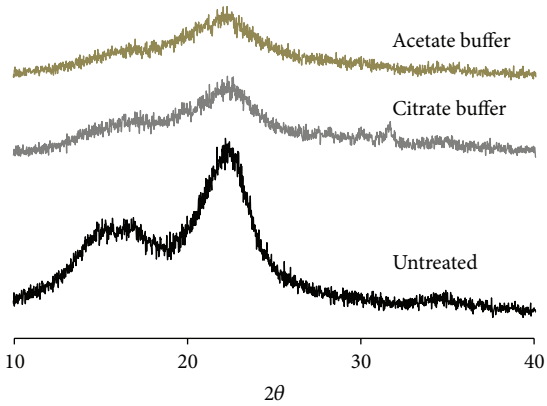

Figure 1: XRD patterns obtained for untreated pitch pine sawdust waste without planetary milling and for the milled samples using either an acetate or citrate buffer.

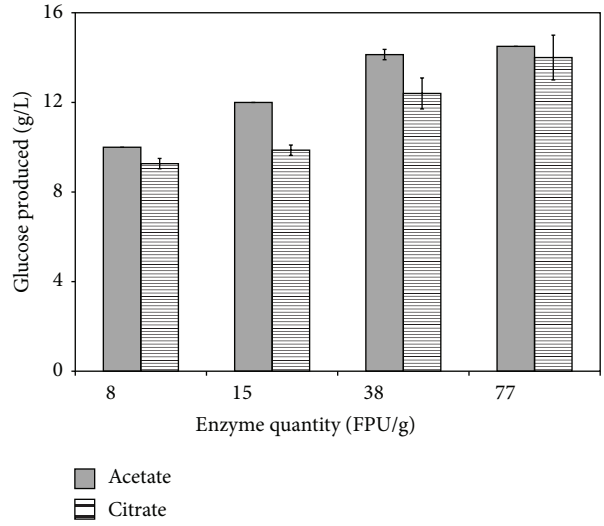

Figure 2: Comparison of the glucose yields obtained from the acetate and citrate buffers. Glucose was produced under the following conditions: 6 hr milling and 24 hr incubation. The quantities of the enzymes used are listed and were 8, 15, 38, and 77 FPU/g, respectively.

was shown previously to reduce the crystallinity of the sample [1]. Figure 1 shows the X-ray diffraction (XRD) patterns for the untreated pitch pine sample and after planetary milling in either sodium citrate or sodium acetate solution. There are two important peaks on XRD spectrums of lignocellulosic biomass: the peak at 18.7°, which represents only amorphous cellulose, and that at 22.5°, which corresponds to both crystalline and amorphous cellulose. As shown in Figure 1, the intensities of the 22.5° peaks were drastically reduced in the pretreated samples after only 20 minutes of milling when either the acetate or citrate buffer was used. According to "crystallinity index," which is a ratio of crystalline cellulose to amorphous cellulose content and is defined as $(I_{2\theta=22.5^\circ} - I_{2\theta=18.7^\circ})/(I_{2\theta=22.5^\circ}) \times 100$, planetary milling was very effective in reducing the crystallinity of the *P. rigida* cellulose. The crystallinity index of the untreated pitch pine sawdust was 52.5% but was reduced to 36.5 and 31.7% only after 20 minutes of planetary milling when citrate or acetate buffers were used, respectively (Table 2). This represents a reduction of 30% and 40% for the two buffers, respectively, indicating that acetate buffer leads to a greater level of decrystallization. This finding was further supported by the glucose yields that resulted after enzymatic treatment of the milled biomass within the respective buffers (Figure 2). As shown in this figure, glucose yields improved as the concentration of each treated biomass increased but treatment of the biomass milled in the acetate buffer consistently gave better yields. Hence, we found that acetate buffer was more effective to be employed in both planetary milling pretreatment and enzymatic saccharification.

The effects of experimental conditions on the glucose yield are combinational through the interactions between experimental variables. Initially, we investigated the effects three single variable parameters, that is, milling time, enzyme quantity, and reaction time, had on the glucose yields and found optimal values at 100 minutes, 16 FPU/g-biomass, and 12 hours, respectively (see Supplementary Material available online at http://dx.doi.org/10.1155/2015/267538). To investigate interactional effects of variable parameters, a combinatorial chart was prepared using the conditions listed above as base values along with higher and lower parameter values for analysis (Table 3). When the enzyme reaction time was set for 24 hours, it is clear that the enzyme quantity is a more dominant factor controlling the glucose yields than the milling time (Figure 3(a)). Moreover, the improvement in the glucose yields as greater amounts of enzyme were added was consistent, regardless of the milling time. This is clearly presented in Table 3 where the percent yields under these conditions increased by 35.2% to 37% for the 2-hour and 4-hour milling times, respectively, when the enzyme concentrations were increased from 5 FPU/g-biomass to 16 FPU/g-biomass. Likewise, the use of 27 FPU/g-biomass with a 24-hour reaction time led to average increase in glucose yields of 43.8% when compared to the same experiments performed with 5 FPU/g-biomass. This consistent improvement in the glucose yields suggests that the cellulose is readily available for hydrolysis by the enzymes and that the bottleneck limiting the yields lies more with the enzyme availability. Another factor that should be considered, when trying to explain why the greater addition of enzyme leads to better yields, is the accessibility of cellulose during the saccharification process. During this process, cellulase tends to irreversibly bind to the hydrophobic surface of biomass and loses it activity [10]. Also

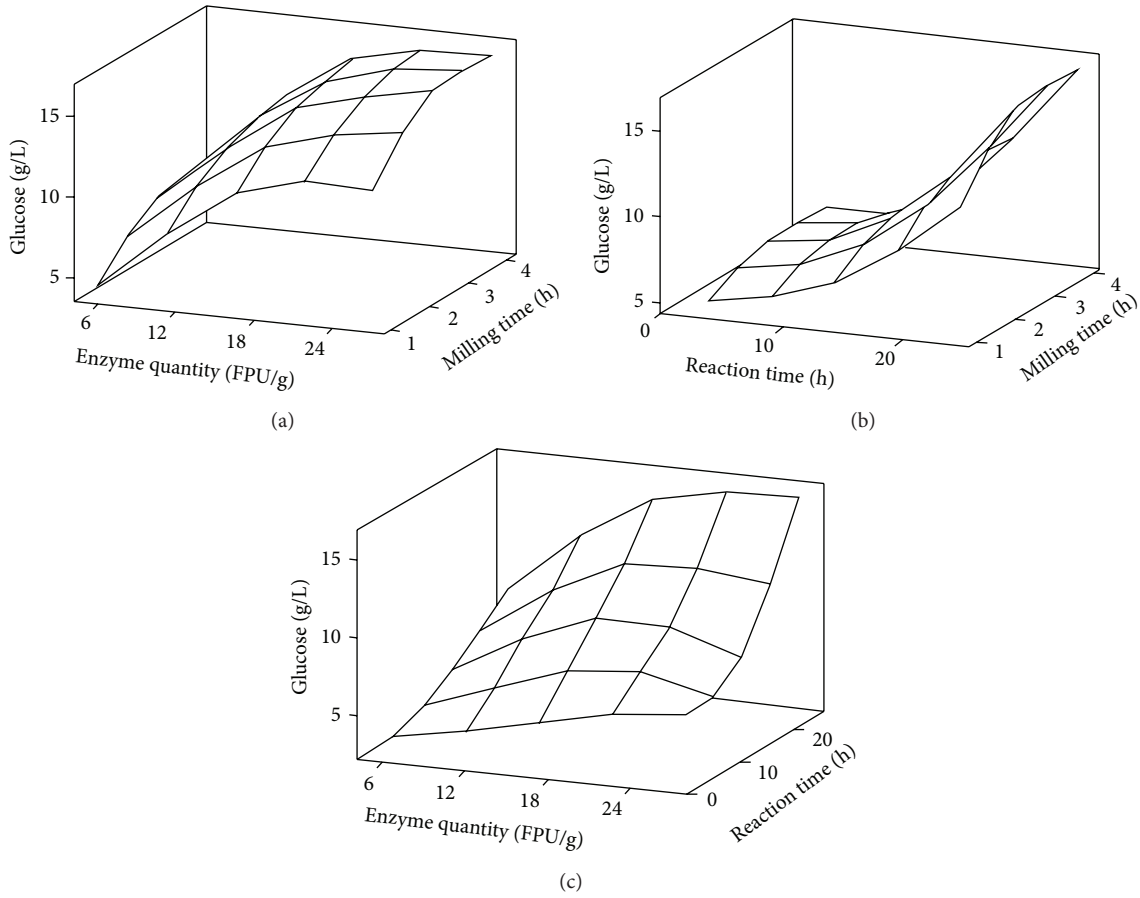

Figure 3: Combined impacts of the parameters on the resulting glucose concentrations. In each case, one of the variables was locked and the other two were varied. The plots show the relationship between and effects of the (a) milling time and enzyme quantity, (b) milling time and enzyme reaction time, and (c) enzyme reaction time and enzyme quantity. The standard values for the locked parameters were milling for 4 hours, 27 FPU/g-biomass, and an enzymatic hydrolysis time of 24 hours.

cellulase could be buried within the fibrillar architecture of the cellulose microfibrils [11]. Both of these processes work to reduce the effective activity of the enzymes but can be overcome by larger enzyme additions.

Performing similar experiments but with the cellulase enzyme concentration locked at 27 FPU/g-biomass, we once more found that the milling time did not influence the glucose yields as much as the hydrolytic treatment times, since longer reaction times give significantly better glucose yields. Interestingly, the yields did not increase linearly but rather in an exponential fashion with longer treatments (Figure 3(b)). As shown in Table 3, a comparison between the different reaction times used found that12 hours improved the yields on average by about 1.23-fold over a 3-hour treatment while the yields after a 24-hour treatment were 2-fold higher than the 12-hour treatment. This enhanced productivity over time was initially thought to be due to the early stage hydrolysis of the cellulose by the enzymes as this would improve access to the cellulose. However, as shown in Figure 3(c), this trend was only seen when a high concentration of enzyme was used.

It is clear from this figure that both of these parameters are influential, as noted above, but the reaction time had a greater effect on the glucose yield. The loss in yield with higher enzyme additions is also a fortuitous finding as the cost of the enzyme used is one of the major contributors to biofuel production costs. One recent study stated that the costs incurred by the use of these enzymes have been significantly underestimated by a large number of groups and their studies [12]. As such, the finding that less enzyme gives more glucose is encouraging, even though this study shows that with longer reaction times this benefit is lost. Table 3 shows that three of the parameter groupings lead to glucose yields that exceed 80% of the expected maximum yield. All three required a 24-hour enzymatic treatment time but varied with respect to the milling time and the enzyme concentration. While an enzyme addition of 27 FPU/g-biomass is used within two of these, the percent yield with 16 FPU/g-biomass is comparable, implying that longer milling times can partially off-set the costs associated with the enzymes. One additional cost-related benefit offered by planetary milling is that this process does not involve any washing steps. Hence, we can obtain a 100% recovery of the biomass solids and sugars, which is very useful to the biorefinery industry [13, 14].

Table 3: Experimental parameters used in the response surface methodology and their effects on the glucose yield. The parameter values that led to greater than yield that exceeded 80% are shown in bold.

Enzyme quantity (FPU/g-biomass)	Enzyme reaction time (hr)	Milling time (hr)	Glucose yield (%)
5	3	1	12.7 ± 1.2
5	3	2	14.3 ± 0.2
5	3	4	16.4 ± 0.6
5	12	1	16.8 ± 0.5
5	12	2	20.2 ± 3.0
5	12	4	25.7 ± 0.8
5	24	1	23.5 ± 0.8
5	24	2	36.7 ± 3.2
5	24	4	44.7 ± 1.4
16	3	1	22.1 ± 0.8
16	3	2	26.2 ± 0.3
16	3	4	26.9 ± 0.3
16	12	1	36.3 ± 1.4
16	12	2	40.0 ± 2.4
16	12	4	48.3 ± 0.5
16	24	1	59.6 ± 1.1
16	24	2	71.9 ± 7.2
16	**24**	**4**	**81.7 ± 4.1**
27	3	1	27.5 ± 1.3
27	3	2	33.8 ± 2.4
27	3	4	35.4 ± 1.9
27	12	1	35.4 ± 2.7
27	12	2	42.5 ± 1.4
27	12	4	40.5 ± 9.2
27	24	1	66.2 ± 4.7
27	**24**	**2**	**82.8 ± 0.6**
27	**24**	**4**	**87.5 ± 1.2**

4. Conclusions

We have investigated the improvement way of glucose yield by optimizing the planetary milling pretreatment and enzymatic saccharification processes for *P. rigida* waste. Although milling effectively reduced the cellulose crystallinity in both acetate and citrate buffers, the results with acetate were slightly better and this presumably contributed to the higher glucose yields resulting with this buffer. By evaluating combinatorial parameter effects with RSM, we obtained glucose yields that surpassed 80% from *P. rigida* waste. Moreover, we demonstrated that the costs associated with the cellulase enzymes can potentially be mitigated by increasing the milling or enzymatic hydrolysis times.

Conflict of Interests

The authors declare that there is no conflict of interests regarding the publication of this paper.

Acknowledgments

This work was supported by a grant from Korea Institute of Ceramic Engineering and Technology (KICET) and by a grant from the National Research Foundation of Korea (NRF-2009-C1AAA001-2009-0093499). The authors gratefully acknowledge the financial support.

References

[1] H. J. Kim, S. Lee, J. Kim, R. J. Mitchell, and J. H. Lee, "Environmentally friendly pretreatment of plant biomass by planetary and attrition milling," *Bioresource Technology*, vol. 144, pp. 50–56, 2013.

[2] R. J. Mitchell, S. Lee, and B. I. Sang, "Toxicogenomic analysis of lignin-hydrolysates: overcoming hurdles to renewable energy," *Journal of Biotechnology*, vol. 150, supplement, p. S20, 2010.

[3] A. K. Monnappa, J. H. Lee, and R. J. Mitchell, "Detection of furfural and 5-hydroxymethylfurfural with a *yhcN::luxCDABE* bioreporter strain," *International Journal of Hydrogen Energy*, vol. 38, no. 35, pp. 15738–15743, 2013.

[4] M. Galbe and G. Zacchi, "A review of the production of ethanol from softwood," *Applied Microbiology and Biotechnology*, vol. 59, no. 6, pp. 618–628, 2002.

[5] Y. Sun and J. Y. Cheng, "Hydrolysis of lignocellulosic materials for ethanol production: a review," *Bioresource Technology*, vol. 83, no. 1, pp. 1–11, 2002.

[6] A. Sluiter, B. Hames, R. Ruiz, J. S. Sluiter, D. Templeton, and D. Crocker, "Determination of structural carbohydrates and lignin in biomass," Laboratory Analytical Procedure TP-510-42618, National Renewable Energy Laboratory, Golden, Colo, USA, 2010.

[7] H. Wang, G. Gurau, and R. D. Rogers, "Ionic liquid processing of cellulose," *Chemical Society Reviews*, vol. 41, no. 4, pp. 1519–1537, 2012.

[8] Y. C. Park and J. S. Kim, "Comparison of various alkaline pretreatment methods of lignocellulosic biomass," *Energy*, vol. 47, no. 1, pp. 31–35, 2012.

[9] A. Hideno, H. Inoue, K. Tsukahara et al., "Wet disk milling pretreatment without sulfuric acid for enzymatic hydrolysis of rice straw," *Bioresource Technology*, vol. 100, no. 10, pp. 2706–2711, 2009.

[10] A. Berlin, N. Gilkes, A. Kurabi et al., "Weak lignin-binding enzymes: a novel approach to improve activity of cellulases for hydrolysis of lignocellulosics," *Applied Biochemistry and Biotechnology*, vol. 121, no. 1–3, pp. 163–170, 2005.

[11] V. Arantes and J. N. Saddler, "Access to cellulose limits the efficiency of enzymatic hydrolysis: the role of amorphogenesis," *Biotechnology for Biofuels*, vol. 3, article 4, 2010.

[12] D. Klein-Marcuschamer, P. Oleskowicz-Popiel, B. A. Simmons, and H. W. Blanch, "The challenge of enzyme cost in the production of lignocellulosic biofuels," *Biotechnology and Bioengineering*, vol. 109, no. 4, pp. 1083–1087, 2012.

[13] B. Hahn-Hägerdal, M. Galbe, M. F. Gorwa-Grauslund, G. Lidén, and G. Zacchi, "Bio-ethanol—the fuel of tomorrow from the residues of today," *Trends in Biotechnology*, vol. 24, no. 12, pp. 549–556, 2006.

[14] J. P. W. Scharlemann and W. F. Laurance, "Environmental science. How green are biofuels?" *Science*, vol. 319, no. 5859, pp. 43–44, 2008.

Hindawi Publishing Corporation
BioMed Research International
Volume 2015, Article ID 845261, 9 pages
http://dx.doi.org/10.1155/2015/845261

Research Article

Fabrication of an Amperometric Flow-Injection Microfluidic Biosensor Based on Laccase for In Situ Determination of Phenolic Compounds

Juan C. Gonzalez-Rivera and Johann F. Osma

CMUA, Department of Electrical and Electronics Engineering, University of Los Andes, Cra 1 E No. 19 A-40, Bogota, Colombia

Correspondence should be addressed to Johann F. Osma; jf.osma43@uniandes.edu.co

Received 18 February 2015; Revised 30 April 2015; Accepted 1 May 2015

Academic Editor: Jinsong Ren

We aim to develop an in situ microfluidic biosensor based on laccase from *Trametes pubescens* with flow-injection and amperometry as the transducer method. The enzyme was directly immobilized by potential step chronoamperometry, and the immobilization was studied using cyclic voltammetry and electrochemical impedance spectroscopy. The electrode response by amperometry was probed using ABTS and syringaldazine. A shift of interfacial electron transfer resistance and the electron transfer rate constant from 18.1 kΩ to 3.9 MΩ and 4.6×10^{-2} cm s^{-1} to 2.1×10^{-4} cm s^{-1}, respectively, evidenced that laccase was immobilized on the electrode by the proposed method. We established the optimum operating conditions of temperature (55°C), pH (4.5), injection flow rate (200 μL min^{-1}), and applied potential (0.4 V). Finally, the microfluidic biosensor showed better lower limit of detection (0.149 μM) and sensitivity (0.2341 nA μM^{-1}) for ABTS than previous laccase-based biosensors and the in situ operation capacity.

1. Introduction

Phenols are employed in several industries in the manufacture of plastics and plasticizers, resins, explosives, drugs, detergents, paper, fungicides, preservatives, dyes, and lubricants [1, 2]. Most phenolic compounds are toxic, noxious, and mutagenic and have carcinogenic activity [2] that accumulate in the environment and are found in food, potable water, sediments, and soil.

Currently, many organizations have established procedures using colorimetry, gas chromatography, liquid chromatography, capillary electrophoresis, and their variations [3]. Even though these methods attain accurate results for a wide range of phenolic compounds, conventional approaches are time-consuming and cost-intensive and require large volumes of organic solvents. Consequently, a market demand exists for a reliable, portable, simple, and cost-effective detection method of phenolic compounds.

Both enzymatic-based biosensors and microfluidic biosensors have attracted increasing among the different configurations of biosensors [4–8]. Microfluidic biosensors combine the advantages of fluidic microsystems, such as low cost, short analysis time, less consumption of sample and reagents, and portability, with the advantages of biosensors such as selectivity, moderate operational potentials, high sensitivity, specificity, and easiness to be miniaturized and integrated [3, 6, 9, 10]. Therefore they have potential in environmental safety, food, and clinic analysis.

The immobilization method is a key parameter for the design and fabrication of microfluidic biosensors [11]. The bioreceptor and the sensor elements can be coupled together with several methods, such as physical adsorption, entrapment, cross-linking, and covalent bonding [12, 13]. However, enzyme degradation and surface inaccessibility arise with the enzyme immobilization inside a microchannel. Thus, we propose the direct electrochemical immobilization of laccase after the sensor sealing since this technique enables an easier immobilization than traditional techniques.

Amperometry is the most common transducer technique in biosensors because it offers detection in real time [14, 15]. When this technique is coupled with convective mass transport, the resulting technique—hydrodynamic

amperometry—offers additional assets such as increased current and sensitivity, quicker steady state, and smaller random contribution from natural convection [16]. Besides, the amount of analyte can be regulated directly by adjusting the flow rate of the flow injection system.

We aim to develop an amperometric flow-injection microfluidic biosensor based on laccase from *Trametes pubescens*. We studied the electrochemical immobilization of laccase by cyclic voltammetry and electrochemical impedance spectroscopy. The microfluidic biosensor electric response was evaluated with ABTS and syringaldazine, both well-known laccase substrates. The characterization of the biosensor included temperature, pH, flow injection, and applied potential effects on the signal response.

2. Materials and Methods

2.1. Reagents and Instrumentation. Glass slides of 76.2 mm in length and 25.4 mm in width were purchased at a local store. ABTS (2,2-azino-bis(3-ethylbenzothiazoline-6) sulphonic acid), syringaldazine, anhydrous ethanol, potassium ferricyanide, and potassium ferrocyanide were purchased from Sigma-Aldrich (USA). The developer (Microposit MF319) and positive photoresist (Microposit SC 1827) were purchased from Shipley (USA). Gold wire (Au, 99.99%) and chromium pieces (Cr, 99.95%) were purchased from Kurt J. Lesker (USA). PRS-100 positive photoresist stripper, dipotassium phosphate, sulfuric acid 97.8%, and hydrochloric acid 37.2% were purchased from J. T. Baker (USA). Potassium phosphate monobasic was purchased from AppliChem, (Germany); and nitric acid and hydrofluoric acid 40% were purchased from Panreac (Spain). PDMS was prepared according to product information from a Sylgard 184 silicone elastomer kit (Dow Corning, USA). All other chemicals used were of analytical degree.

Gold and chrome were deposited on microscopic slides using an Edwards Auto 306 thermal evaporation system at vacuum. The electrode pattern was transferred by an optical lithography maskless exposure system (model SF-100, Intelligent Micro Patterning, USA). The electrochemical procedures were measured using an Autolab Potensiostat/Galvanostat PGSTAT128N (Metrohm, USA) computer-controlled. Data were acquired and analyzed by the software Nova version 1.9. All assays were performed in a Faraday cage at room temperature.

2.2. Laccase Production. T. pubescens (CBS 696.94) was cultured on malt extract agar (MEA) plates during 10 days at 30°C. Cultures were carried out in 1000 mL shake flasks with 50 mL of basal medium and 15 g sterilized dry coffee husk [17]. Culture medium was inoculated with three 13 mm plugs from active fungus cultured in MEA. In brief, laccase was produced in 1 l shake flask with 50 mL of basal medium and 15 g sterilized coffee husk. Cultured medium was inoculated and incubated during 21 days at 30°C under static condition. The enzymatic crude extract was removed by filtration through 10 μm filter paper (Boeco, Germany) and then centrifuged at 4°C and 4500 rpm for 15 min. Finally, the crude extract was filtered through 0.22 μm Millex filter unit (Millipore, USA).

2.3. Free Laccase Activity Assay and Protein Measurement. The activity of free laccase was determined spectrophotometrically by measuring the absorbance change for 10 min using ABTS (ε_{420} = 36 mM^{-1} cm^{-1}) as a substrate at room temperature. To perform the assay, 950 μL of 0.5 mM of ABTS in acetate buffer (0.1 M, pH 5.0) was mixed with 50 μL of laccase crude extract. The enzyme activity was expressed as units per liter (U l^{-1}), where U was defined as the amount of enzyme required to oxidized 1 μmol ABTS per minute. Protein concentration was determined by Lowry assay [18].

2.4. Microfluidic Biosensor Fabrication. The device is composed of an upper glass slide with a fluidic microsystem and a lower glass slide with an integrated three-electrode arrangement made of gold (Figure 1(a)). Both pieces were fabricated through separate steps and assembled forward electrode modification with laccase. An in-channel configuration for the microfluidic biosensor was selected because it is the most preferred choice of amperometric microchip sensors [19]. The final device has a length of 35 mm and a width of 25 mm.

2.4.1. Fabrication of the Gold Electrodes. The arrangement of gold electrodes was fabricated using first a chrome and latter a gold thin film deposition on glass slides by physical vapor deposition using a thermal evaporator Edwards E306 (Moorfield, UK) at 2.8 A with the metals on a tungsten slide at a vacuum pressure of 4×10^{-5} mbar and an evaporation rate of 0.3 nm/min [20]. The chrome/gold deposition presented an overall thickness of 50 nm. The working electrode (WE) and reference electrode (RE) were fabricated with a diameter of 200 and 300 μm, respectively. The counter electrode (CE) was fabricated with a transverse diameter of 1 mm and a conjugate diameter of 500 μm.

Before the deposition of the gold layer, a chrome intermediate layer of 5 nm was evaporated to enhance the adhesion between the glass and gold. The electrode pattern was transferred over the metallic film by using mask-free optical lithography equipment with a resolution of 5 μm. Positive photoresist was spin-coated onto the gold film at 3600 rpm for 60 s. Then, the photoresist was baked during 60 s at 115°C and patterned for 16 s. Finally, the soluble photoresist was removed submerging the substrate in the developer for 120 s with constant agitation.

The exposed gold areas were etched using aqua regia (HCl + HNO_3 3 : 1 v/v) for 5 s, and then the chrome was removed submerging the substrate for 30 s in HF 40% v/v. The residual baked photoresist was removed using stripper for 60 s leaving the three electrodes created on top of the glass slide (Figure 1(b) bottom).

2.4.2. Fabrication of the Fluidic Microsystem. Copper foil tape was stuck on a glass slide, and the fluidic microsystem mask was transferred to the substrate by mask-free technology optical lithography, as was described for the electrode fabrication. Next, the copper pattern—obtained after the development—was exposed to $FeCl_3$ 52% (w/v) with the aim to remove the unprotected copper and fabricate a physical mask for glass etching. Then, this slide with the pasted mask

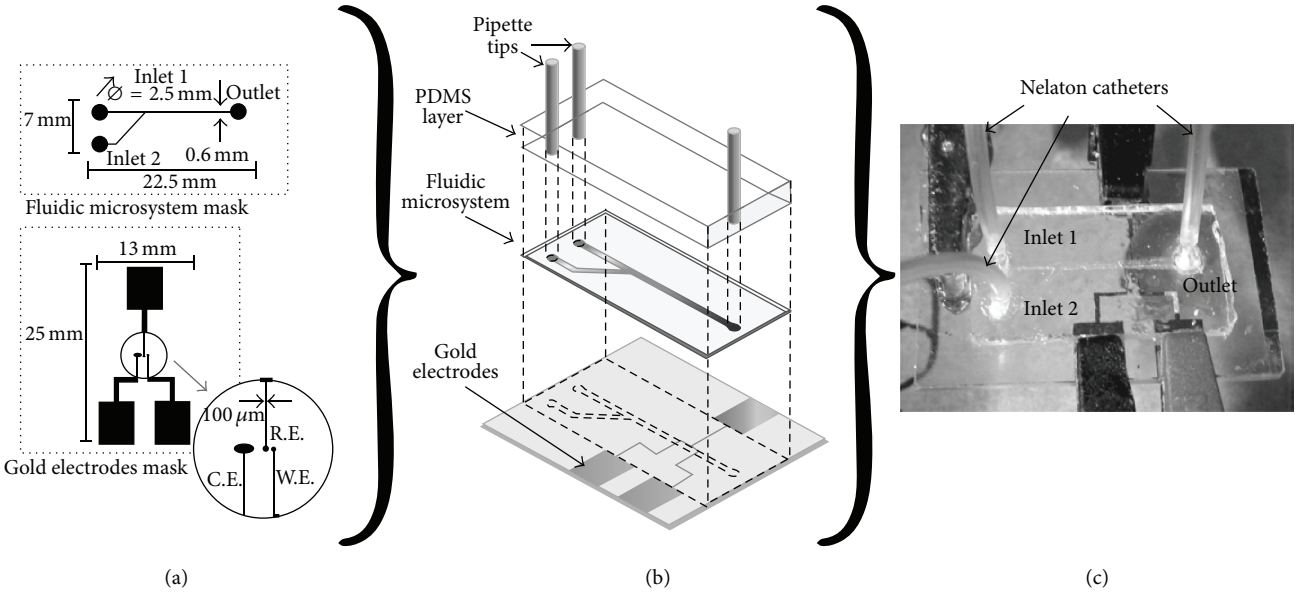

Figure 1: Masks and dimensions of the microfluidic biosensor (a); dismantled schematic diagram (b); and experimental set-up (c).

was submerged into an HF 40% solution for 4 min for glass etching. Therefore, a microchannel of 600 μm of width and 250 μm of depth was obtained in the glass slide. Finally, the copper mask was removed with $FeCl_3$ 52% (w/v) leaving the glass fluidic microsystem clean of any sacrificial layers (Figure 1(b) middle).

The fluidic microsystem inlets and outlet were perforated in the glass fluidic microsystems using a commercial moto-tool (Figure 1(b) top). The holes were drilled—immersed in water—at 17,000 rpm using a diamond coated tip.

2.4.3. Microfluidic Sensor Assembly. The fluidic microsystem and electrodes slides were assembled using UV curable epoxy. Previous to coating the fluidic microsystem slide with a glue layer, the microchannel was protected by filling it with positive photoresist to prevent channel clogging. After sealing both slides (Figure 1(b) bottom and middle) with UV curable epoxy, stripper was used to remove the positive photoresist from the microchannels.

Micropipette tips (0.2–10 μL) were cut and used as connections between reservoirs and tubes. These tips were coupled in the inlets and outlet reservoirs of the fluidic microsystem using a layer of PDMS with a thickness of 2 mm (Figure 1(c)). The connectors were joined to Nelaton catheters that were coupled to the syringes.

2.4.4. Laccase Immobilization. Laccase with an enzymatic activity of 2.13 U mg^{-1} of protein was selectively deposited on the working electrode inside the sealed fluidic microsystem by potential step chronoamperometry. To attain this process, a stream of crude extract of laccase (with a protein concentration of 0.178 mg mL^{-1}) in 0.1 M phosphate buffer (pH 7.0) purged with high purity nitrogen was driven into the fluidic microsystem. Initial potential was set at the open-circuit potential. After 10 s of initial holding, laccase was immobilized by applying 1.2 V between the counter electrode and the working electrode for 3 min.

Prior to use, the electrodes were electrochemically cleaned using a 0.1 M H_2SO_4 solution by successive cycling between −0.2 and 1.5 V at 500 mV s^{-1} until reproducible voltammograms were achieved (Figure 2(b)).

After laccase immobilization, 25 μM ABTS in acetate buffer 0.1 M (pH 5.0.) was introduced in the sealed fluidic microsystems to test possible undesirable adsorption of laccase on the glass surface. No undesired laccase adsorption was detected through high magnification optical (> ×1000) after several hours of ABTS exposure.

2.5. Electrochemical Study of Laccase Immobilization. Cyclic voltammetry (CV) and electrochemical impedance spectroscopy (EIS) were performed in 0.1 M phosphate buffer (pH 7.0) containing 1 mM $Fe(CN)_6^{3-/4-}$, due to the reasonably fast electron transfer. Voltammograms were scanned at 100 mV s^{-1} between −0.2 and 0.6 V. The frequency scan range for the EIS was from 0.1 Hz to 100 kHz and a sinusoidal potential modulation of ±5 mV was superimposed on the DC potential of 0.2 V. Before each experiment, fresh solution was purged for 10 min using high purity nitrogen. We selected the Randles circuit to fit the experimental data obtained by EIS; this circuit is comprised by a solution resistance (R_s), a charge transfer resistance (R_{ct}), a Warburg impedance (W), and a double layer capacitance (C_{dl}). The diameter of the semicircle corresponds to the interfacial electron transfer resistance (R_{ct}).

2.6. Characterization of the Microfluidic Biosensor Experimental Conditions. Temperature and pH effect on the immobilized laccase activity were studied by CV using ABTS as a substrate. Acetate buffer 0.1 M (pH 5.0) with ABTS 25 μM was injected into the fluidic microsystem, and five voltammograms were scanned at 100 mV s^{-1} between −0.2

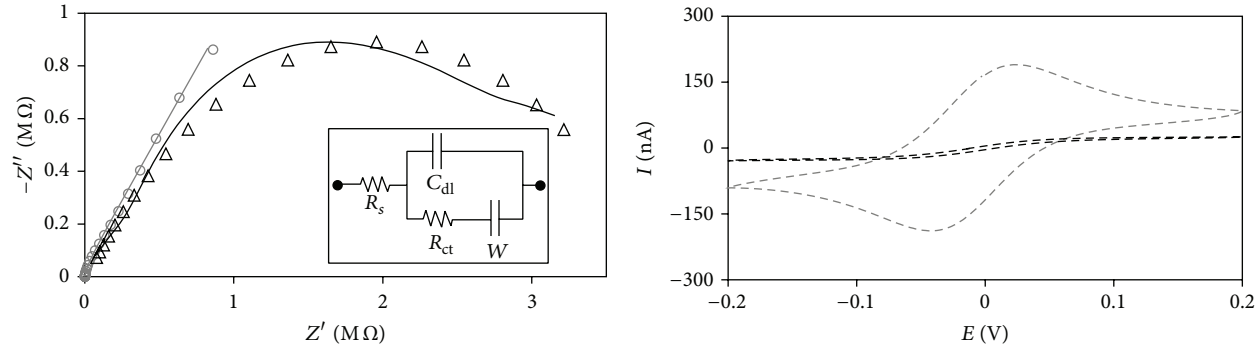

Figure 2: Nyquist plots (a) and cyclic voltammograms (b) at bare electrode (gray) and laccase modified Au electrode sealed in the fluidic microsystem (black). Continuous lines represent results from data fitting. Inset is the equivalent circuit. Solution: 1 mM $K_4[Fe(CN)_6]$ + $K_3[Fe(CN)_6]$ + 0.1 M phosphate buffer (pH. 7.0). For EIS, a sinusoidal potential modulation of ±5 mV was superimposed on the DC potential of 0.2 V versus $Ag/AgCl/KCl_{3M}$. Applied frequency was from 10^6 to 0.1 Hz. For CV the scan rate was 100 mV s^{-1}.

and 1 V. For each experiment the anodic peak height of the second voltammogram was plotted against the independent variable. Temperature effect was evaluated in the range from 20°C to 75°C at pH 5.0. Similarly, the buffer pH was varied from 4.0 to 7.5 at room temperature.

Injection flow rate effect on the immobilized laccase activity was evaluated by amperometry using acetate buffer 0.1 M (pH 5.0) as the running solution. The amperometry experiments with flow injection were conducted using the following procedure. The fluidic microsystem was treated with the running solution for 5 min. This solution was delivered into the fluidic microsystem using a syringe pump at a fixed flow rate. Then, ABTS 25 μM in acetate buffer 0.1 M (pH 5.0.) was injected into the fluidic microsystem—through the inlet 2—using another syringe pump at the same rate of the running solution. The injection flow rate effect was evaluated at 100, 120, 140, 160, 180, 240, and 320 μL min^{-1} applying 0.4 V. The current signal obtained was plotted against the independent variable. Each experiment was performed by triplicate. Data was plotted as relative current, which was defined regarding the maximum value of each experiment.

2.7. ABTS and Syringaldazine Detection Determination. ABTS and syringaldazine detection experiments were measured by amperometry with flow injection. The injection flow rate, buffer pH, and potential applied were chosen based on the results of the characterization of the experimental conditions. ABTS probes were performed with 0.1 M acetate buffer as the running buffer, and syringaldazine probes with 0.1 M acetate buffer-ethanol mixture prepared in a proportion 1 : 1 (v/v). Probes were made injecting continuously running buffer and the analyte was injected periodically each 120 s for 20 s increasing its concentration periodically. Experiments were conducted in triplicate and at room temperature unless specified.

We calculated the Michaelis-Menten parameters from the Lineweaver-Burk equation:

$$\frac{1}{I} = \frac{K_M^{\text{app}}}{I_{\max}[S]} + \frac{1}{I_{\max}}, \quad (1)$$

where I is the current response, K_M^{app} is the apparent Michaelis-Menten constant and $I_{\max}$ is the maximum current measured under saturated substrate condition.

2.8. Stability of the Microfluidic Biosensor. The stability test followed the previous procedure for ABTS detection by amperometry with flow injection. Measurements were made each 24 h for 10 days (in triplicate at room temperature) using 0.1 M acetate buffer as the running buffer and 50 μM ABTS in acetate buffer 0.1 M (pH 5.0) as the analyte solution for detection under the same conditions as for ABTS detection determination. The microfluidic biosensor was stored at 4°C after the measurements.

3. Results and Discussion

3.1. Laccase Immobilization. We determined the immobilization of laccase studying the electrochemical behavior of the working electrode. Previous the immobilization, the Nyquist profile shows a small semicircular profile at high frequencies, followed by a linear profile at low frequencies (Figure 2(a)). After the immobilization, the electrode only shows a semicircular profile within the frequency range evaluated. The estimated values of the interfacial electron transfer resistance (R_{ct}) from the Randles model were 18.1 kΩ and 3.9 MΩ for the bare electrode and laccase-modified electrode, respectively.

We calculated the electron transfer rate constant (k^0, an indicator of the kinetic facility of the redox system) by EIS [21]. The following equations were applied for the 1-electron, first order reaction of the $Fe(CN)_6^{3-/4-}$ couple, assuming that $C_{\text{ox}} = C_{\text{red}} = C$, in order to determine k^0 [22]:

$$R_{\text{ct}} = \frac{RT}{Fi_0}$$
$$i_0 = FAk^0C, \quad (2)$$

where R is the gas constant, T is the temperature, F is the Faraday constant, and A is the area of gold electrode. The k^0

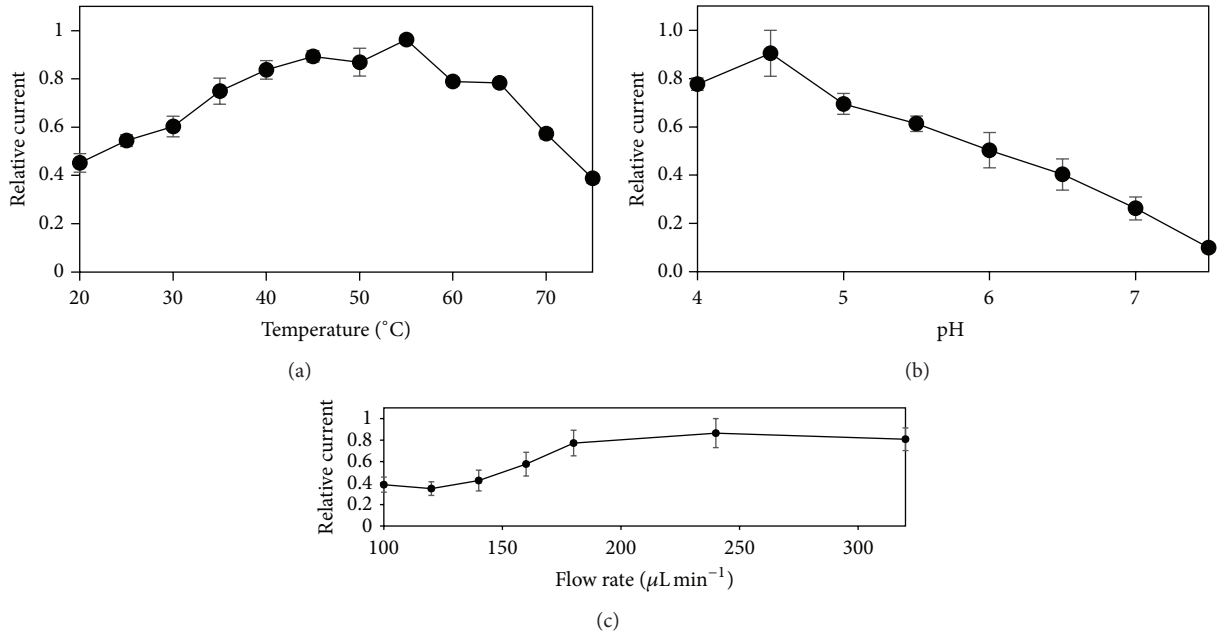

Figure 3: Effect of temperature (a), pH (b), and injection flow rate (c) on the current response of the microfluidic biosensor. Error bars describe the standard deviation of the three replicates. Solution: acetate buffer 0.1 M (pH 5.0.) as the running solution and ABTS 25 μM in acetate buffer 0.1 M (pH 5.0.) as the analyte.

measured were 4.6×10^{-2} cm s^{-1} and 2.1×10^{-4} cm s^{-1} for the bare and laccase-modified electrode, respectively.

Figure 2(b) shows the CV profiles obtained from the reaction of $Fe(CN)_6^{3-/4-}$ at the electrode interface before and after the immobilization of laccase. $Fe(CN)_6^{3-/4-}$ was used due to the reasonably fast electron transfer; however, by means of the modification of the charge transfer resistance and the electron transfer rate constant, the electrochemical immobilization of laccase on the electrode surface was evidenced. Previous the immobilization, the anodic and cathodic peak heights were 181.1 and 170.4 nA, respectively, and the peak separation was 54 mV. After the immobilization, the anodic and cathodic peak heights were 13.0 and 12.7 nA respectively, while the peak separation was 117 mV.

We induced the electrolysis of water applying a potential between the working and counter electrode in a buffer (pH 7.0) containing laccase. A decrease of the local pH in the vicinity of the working electrode produced the neutralization of laccase net charge (pI 2.6 for laccase from *Trametes pubescens* [23]). This process caused the precipitation of the enzyme on the surface of the working electrode [24, 25].

We found that laccase was immobilized on the electrode sealed inside the fluidic microsystem by this electrochemical technique without exposing laccase to denaturing conditions. The change of the Nyquist profiles showed that the $Fe(CN)_6^{3-/4-}$ reaction was initially limited by the mass transfer of the active specie from the bulk solution to the electrode interface, but the reaction shifted to kinetic-limited after the immobilization [16]. This change is evidenced by the decrease of two orders of magnitude of k^0 and the increase of R_{ct}. This behavior means that the $Fe(CN)_6^{3-/4-}$ reaction was harder to accomplish due to the presence of a layer of laccase on the surface of the working electrode, which decreased the active area of the electrode. After the immobilization, we also observed a decrease of an order of magnitude in the current response and an increase of 54% in the potential separation of the peaks by CV. These observations proved that the reaction—initially reversible—became irreversible with the functionalization of the electrode. These observations proved the hypothesis that laccase was immobilized by the electrochemical technique performed in this work.

3.2. Characterization of Experimental Conditions of the Microfluidic Biosensor. Figure 3 shows the resulting relative current from the ABTS oxidation by the working electrode modified with laccase when we evaluated the effect of temperature, pH, injection flow rate, and potential applied on the current response. The temperature profile achieved a maximum around 55°C, while the pH profile showed a maximum around 4.5 (Figures 3(a) and 3(b)). We found previously using free laccase from *Trametes pubescens* and ABTS as a substrate that the temperature profile behaved like a bell-shape with a maximum around 55°C, and the pH profile decreased as the pH increased, with a maximum in a range from 2 to 3 [26]. These profiles behaved similarly compared to the profiles from the present work, which may indicate that the electrochemical immobilization proceeded without modify the structure of the enzyme.

The maximum current was achieved at a temperature higher than previous laccase-based biosensors using nanomaterial composites and polymers [27–29] and similar to laccase immobilized on magnetic chitosan microparticles (55°C) [30]. Also, the behavior of pH profile is consistent with previous biosensors characterizations [31, 32].

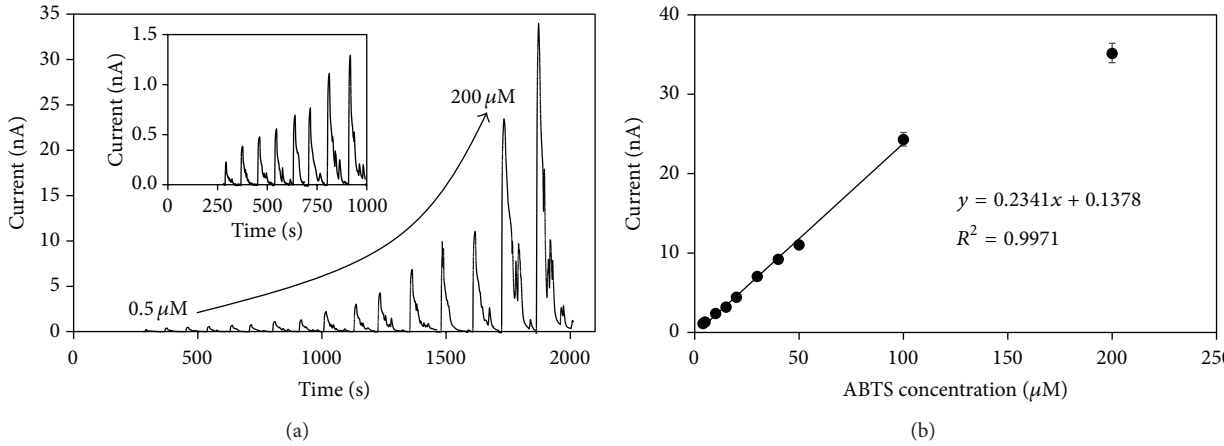

Figure 4: Current-time response curve with background signal subtracted (a) and calibration curve (b) of the microfluidic biosensor. Increasing concentrations of ABTS (from 0.5 μm to 200 μM) in 0.1 M acetate buffer (pH 4.5) were injected at 200 μL min^{-1}. Potential applied of 0.4 V at room temperature. Error bars describe the standard deviation of the three replicates.

Figure 3(c) shows that the current increases with the flow rate from 100 to 180 μL min^{-1}, and after the turning point around 180 μL min^{-1} the current became constant. Before the turning point, heterogeneous mass transfer kinetic is higher than the rates of mass transfer; therefore the reaction is kinetic controlled. After the turning point, the convective contribution to mass transfer became larger to increase the mass transfer rates turning to a mass-transfer controlled reaction. Based on these results, we selected a temperature of 55°C, a buffer pH of 4.5, an injection flow rate of 200 μL min^{-1}, and a potential applied of 0.4 V as the optimal conditions for phenolic determination.

3.3. Detection of ABTS. Figure 4 shows the current response achieved at different concentrations of ABTS. We achieved a linear relationship within 0.5 and 100 μM with a relative standard deviation (RSD) lower than 5%. The ABTS sensitivity and the detection limit (signal-to-noise ratio (S/N) = 3) calculated were 0.2341 nA μM^{-1} (741 nA μM^{-1} cm^{-2}) and 0.149 μM, respectively. The apparent Michaelis-Menten constant (K_M^{app}) and the maximum current ($I_{\max}$) were 386.5 μM and 105 nA, respectively. The sampling rate of the microfluidic biosensor calculated was 24 to 60 samples per min.

The substrate sensitivity was improved compared with the laccase electrode covalently immobilized on platinum and platinum oxide (75 nA μM^{-1}) [31, 33] and laccase on glassy carbon electrodes (358.3 ± 18.8 nA μM^{-1} cm^{-2}) [34]. The detection limit was also lower than those reported in previous results for amperometric laccase biosensors on platinum (0.2 μM) and platinum oxide (0.5 μM) [31, 33], as well as the laccase biosensor based on a matrix of carbon nanotubes-chitosan composite (0.23 μM) [32].

Figure 5 shows the stability of the microfluidic biosensor. This test showed a linear decrease with a coefficient of determination (R^2) of 0.9924, and a half-life time of 10 days. The relative standard deviation was lower than 10%.

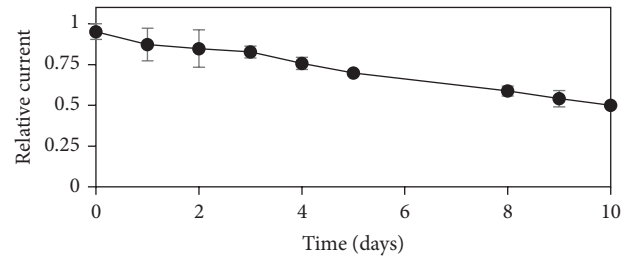

Figure 5: Stability of the microfluidic biosensor. Measurements made each 24 h for 10 days using 0.1 M acetate buffer as the running buffer and 50 μM ABTS in acetate buffer 0.1 M (pH 5.0.) as the analyte solution for detection. Error bars describe the standard deviation of the three replicates.

3.4. Detection of Syringaldazine. Figure 6 shows the current response achieved at different concentrations of syringaldazine; we achieved a linear relationship within 10 and 200 μM with a relative standard deviation (RSD) lower than 10%. The syringaldazine sensitivity and the lowest detectable concentration were 0.0012 nA μM^{-1} and 10 μM, respectively. The apparent Michaelis-Menten constant (K_M^{app}) and the maximum current ($I_{\max}$) were 540 μM and 0.9 nA, respectively. Also, the microfluidic biosensor is capable of measure 60 syringaldazine samples per min.

We found that the sensitivity and the repeatability for syringaldazine decreased compared with ABTS values. This biosensor has a ABTS limit of detection comparable to the biosensor of laccase covalently immobilized on a composite of silver nanoparticles, carboxylated multiwalled carbon nanotubes and polyaniline on a gold surface [35], a laccase biosensor based on platinum nanoparticles dispersed in 1-butyl-3-methylimidazolium hexafluorophosphate [36], and a laccase based biosensor immobilized on magnetic core-shell nanoparticles, but lower for the detection of syringaldazine [37]. Apparently ethanol, which has a lower polarity than

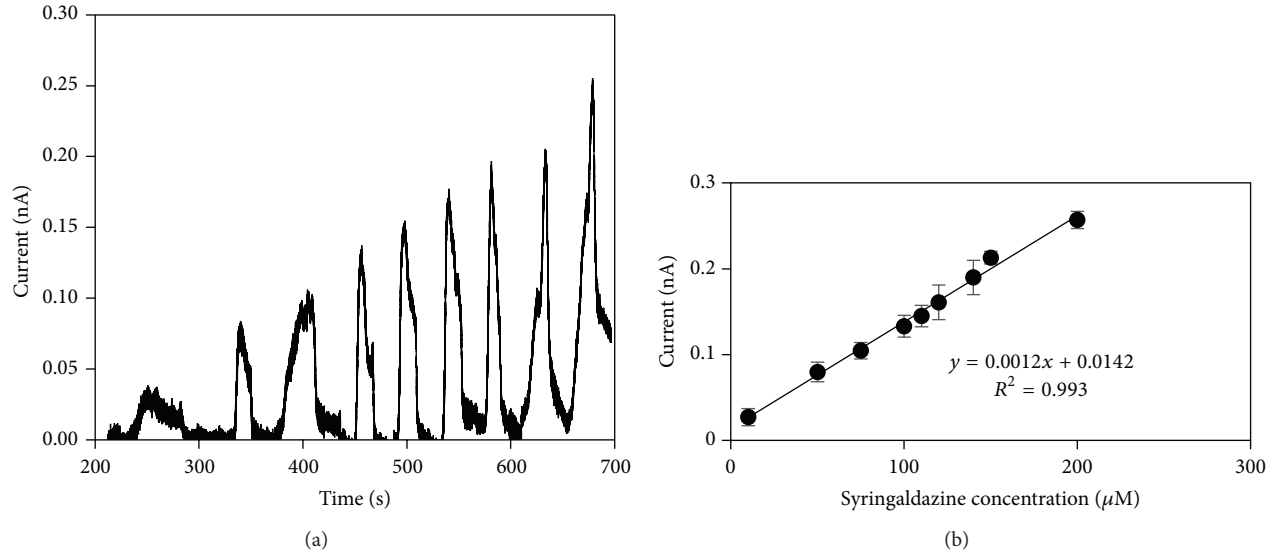

Figure 6: Current-time response curve with background signal subtracted (a) and calibration curve (b) of the microfluidic biosensor. Increasing concentrations of syringaldazine (from 10 μm to 200 μM) in 0.1 M acetate buffer (pH 4.5) : ethanol 1 : 1 (v/v) solution were injected at 200 μL min^{-1}. Potential applied of 0.4 V at room temperature. Error bars describe the standard deviation of the three replicates.

water (relative permittivity: $\varepsilon_{r\mathrm{H2O}} = 78.5$; $\varepsilon_{r\mathrm{C2H6O}} = 24.5$ at 25°C), affected the performance of the biosensor; as polarity promotes the dissociation of dissolved electrolytes and hydration of the ions, the ion mobility was much harder [38]. However, this should not be a problem in real sample since ethanol has a high volatility, and phenolic compounds can be found in aqueous solutions.

4. Conclusions

The complete process of fabrication, assembling, and enzymatic immobilization of a microfluidics biosensor for the detection of phenol is described. This microfluidics system can be functionalized after the microfabrication process takes place and the microdevice is sealed and operates in both stationary and continuous flow conditions. The material of the substrate and the confinement of the electrodes allow this microdevice to be operated in situ without any risk of deterioration or contamination of the sample. In addition, a small volume is needed to detect phenol in aqueous solutions thanks to the microchannel structure. The microfluidic biosensor showed better analytic characteristics than previous biosensors, such as the lower limit of detection and sensitivity. Moreover, the optimum operational conditions of temperature, pH, injection flow rate, and potential were established and can be directly applied to in situ operation as well as its fabrication procedure introduced for industrial applications.

Abbreviation

ABTS: 2,2-Azino-bis(3-ethylbenzothiazoline-6) sulphonic acid
ASTM: International Association of Testing Materials
CE: Counter electrode
CV: Cyclic voltammetry
EIS: Electrochemical impedance spectroscopy
EPA: Environmental Protection Agency
ISO: International Organization for Standardization
RE: Reference electrode
RSD: Relative standard deviation
WE: Working electrode.

Conflict of Interests

The authors declare that there is no conflict of interests regarding the publication of this paper.

Acknowledgments

This project was possible thanks to the collaboration of the Department of Electrical and Electronics Engineering, the Department of Mechanical Engineering, the Department of Chemical Engineering, and the personnel of the Clean Room of Universidad de los Andes.

References

[1] V. Glezer, "Environmental effects of substituted phenols," in *The Chemistry of Phenols*, Z. Rappoport, Ed., pp. 1347–1368, John Wiley & Sons, West Sussex, UK, 2003.

[2] J. Michałowicz and W. Duda, "Phenols: sources and toxicity," *Polish Journal of Environmental Studies*, vol. 16, no. 3, pp. 347–362, 2007.

[3] F. Karim and A. N. M. Fakhruddin, "Recent advances in the development of biosensor for phenol: a review," *Reviews in Environmental Science and Biotechnology*, vol. 11, no. 3, pp. 261–274, 2012.

[4] K. Morimoto, S. Upadhyay, T. Higashiyama et al., "Electrochemical microsystem with porous matrix packed-beds for enzyme analysis," *Sensors and Actuators B: Chemical*, vol. 124, no. 2, pp. 477–485, 2007.

[5] P.-C. Nien, M.-C. Huang, F.-Y. Chang, and K.-C. Ho, "Integrating an enzyme-entrapped conducting polymer electrode and a prereactor in a microfluidic system for sensing glucose," *Electroanalysis*, vol. 20, no. 6, pp. 635–642, 2008.

[6] Y. Wang, Q. He, Y. Dong, and H. Chen, "In-channel modification of biosensor electrodes integrated on a polycarbonate microfluidic chip for micro flow-injection amperometric determination of glucose," *Sensors and Actuators, B: Chemical*, vol. 145, no. 1, pp. 553–560, 2010.

[7] K. F. Lei and P. H. M. Leung, "Microelectrode array biosensor for the detection of *Legionella pneumophila*," *Microelectronic Engineering*, vol. 91, pp. 174–177, 2012.

[8] X. Li, F. Zhang, J. Shi et al., "Microfluidic devices with disposable enzyme electrode for electrochemical monitoring of glucose concentrations," *Electrophoresis*, vol. 32, no. 22, pp. 3201–3206, 2011.

[9] L. Zhang, P. Qu, J. Sheng, J. Lei, and H. Ju, "Open tubular microreactor with enzyme functionalized microfluidic channel for amperometric detection of glucose," *Chinese Journal of Chemistry*, vol. 30, no. 9, pp. 2145–2150, 2012.

[10] S. Borgmann, A. Schulte, S. Neugebauer, and W. Schuhmann, "Amperometric biosensors," in *Advances in Electrochemical Science and Engineering*, R. C. Alkire, D. M. Kolb, and J. Lipkowski, Eds., pp. 1–83, Wiley-VCH, 2011.

[11] J. Sheng, L. Zhang, J. Lei, and H. Ju, "Fabrication of tunable microreactor with enzyme modified magnetic nanoparticles for microfluidic electrochemical detection of glucose," *Analytica Chimica Acta*, vol. 709, pp. 41–46, 2012.

[12] S. F. D'Souza, "Immobilization and stabilization of biomaterials for biosensor applications," *Applied Biochemistry and Biotechnology*, vol. 96, no. 1–3, pp. 225–238, 2001.

[13] A. Sassolas, L. J. Blum, and B. D. Leca-Bouvier, "Immobilization strategies to develop enzymatic biosensors," *Biotechnology Advances*, vol. 30, no. 3, pp. 489–511, 2012.

[14] C. Karuwan, A. Wisitsoraat, T. Maturos et al., "Flow injection based microfluidic device with carbon nanotube electrode for rapid salbutamol detection," *Talanta*, vol. 79, no. 4, pp. 995–1000, 2009.

[15] K.-W. Lin, Y.-K. Huang, H.-L. Su, and Y.-Z. Hsieh, "In-channel simplified decoupler with renewable electrochemical detection for microchip capillary electrophoresis," *Analytica Chimica Acta*, vol. 619, no. 1, pp. 115–121, 2008.

[16] A. J. Bard and L. R. Faulkner, "Techniques based on concepts of impedance," in *Electrochemical Methods: Fundamentals and Applications*, pp. 368–416, John Wiley & Sons, New York, NY, USA, 2001.

[17] I. J. Gaitan, S. C. Medina, J. C. González et al., "Evaluation of toxicity and degradation of a chlorophenol mixture by the laccase produced by *Trametes pubescens*," *Bioresource Technology*, vol. 102, no. 3, pp. 3632–3635, 2011.

[18] J. H. Waterborg, "The Lowry method for protein quantitation," in *The Protein Protocols Handbook*, J. M. Walker, Ed., pp. 7–10, Humana Press, Totowa, NJ, USA, 2009.

[19] M. H. Ghanim and M. Z. Abdullah, "Integrating amperometric detection with electrophoresis microchip devices for biochemical assays: recent developments," *Talanta*, vol. 85, no. 1, pp. 28–34, 2011.

[20] L. F. Urrego, D. I. Lopez, K. A. Ramirez, C. Ramirez, and J. F. Osma, "Biomicrosystem design and fabrication for the human papilloma virus 16 detection," *Sensors and Actuators B: Chemical*, vol. 207, pp. 97–104, 2015.

[21] E. Sabatani and I. Rubinstein, "Organized self-assembling monolayers on electrodes. 2. Monolayer-based ultramicroelectrodes for the study of very rapid electrode kinetics," *Journal of Physical Chemistry*, vol. 91, no. 27, pp. 6663–6669, 1987.

[22] E. Sabatani, I. Rubinstein, R. Maoz, and J. Sagiv, "Organized self-assembling monolayers on electrodes: part I. Octadecyl derivatives on gold," *Journal of Electroanalytical Chemistry*, vol. 219, no. 1-2, pp. 365–371, 1987.

[23] C. Galhaup, S. Goller, C. K. Peterbauer, J. Strauss, and D. Haltrich, "Characterization of the major laccase isoenzyme from Trametes pubescens and regulation of its synthesis by metal ions," *Microbiology*, vol. 148, no. 7, pp. 2159–2169, 2002.

[24] B. Patil, S. Fujikawa, T. Okajima, and T. Ohsaka, "Enzymatic direct electron transfer at ascorbate oxidase-modified gold electrode prepared by one-step galvanostatic method," *International Journal of Electrochemical Science*, vol. 7, no. 6, pp. 5012–5019, 2012.

[25] N. Matsumoto, X. Chen, and G. S. Wilson, "Fundamental studies of glucose oxidase deposition on a Pt electrode," *Analytical Chemistry*, vol. 74, no. 2, pp. 362–367, 2002.

[26] J. C. Gonzalez, S. C. Medina, A. Rodriguez, J. F. Osma, C. J. Alméciga-Díaz, and O. F. Sánchez, "Production of Trametes pubescens laccase under submerged and semi-solid culture conditions on agro-industrial wastes," *PLoS ONE*, vol. 8, no. 9, Article ID e73721, 2013.

[27] S. Chawla, R. Rawal, S. Sharma, and C. S. Pundir, "An amperometric biosensor based on laccase immobilized onto nickel nanoparticles/carboxylated multiwalled carbon nanotubes/polyaniline modified gold electrode for determination of phenolic content in fruit juices," *Biochemical Engineering Journal*, vol. 68, pp. 76–84, 2012.

[28] M. E. Çorman, N. Öztürk, N. Bereli, S. Akgöl, and A. Denizli, "Preparation of nanoparticles which contains histidine for immobilization of Trametes versicolor laccase," *Journal of Molecular Catalysis B: Enzymatic*, vol. 63, no. 1-2, pp. 102–107, 2010.

[29] S. Chawla, R. Rawal, Shabnam, R. C. Kuhad, and C. S. Pundir, "An amperometric polyphenol biosensor based on laccase immobilized on epoxy resin membrane," *Analytical Methods*, vol. 3, no. 3, pp. 709–714, 2011.

[30] D.-S. Jiang, S.-Y. Long, J. Huang, H.-Y. Xiao, and J.-Y. Zhou, "Immobilization of *Pycnoporus sanguineus* laccase on magnetic chitosan microspheres," *Biochemical Engineering Journal*, vol. 25, no. 1, pp. 15–23, 2005.

[31] D. Quan, Y. Kim, and W. Shin, "Characterization of an amperometric laccase electrode covalently immobilized on platinum surface," *Journal of Electroanalytical Chemistry*, vol. 561, no. 1, pp. 181–189, 2004.

[32] Y. Liu, X. Qu, H. Guo, H. Chen, B. Liu, and S. Dong, "Facile preparation of amperometric laccase biosensor with multifunction based on the matrix of carbon nanotubes-chitosan composite," *Biosensors and Bioelectronics*, vol. 21, no. 12, pp. 2195–2201, 2006.

[33] D. Quan, Y. Kim, K. B. Yoon, and W. Shin, "Assembly of laccase over platinum oxide surface and application as an amperometric biosensor," *Bulletin of the Korean Chemical Society*, vol. 23, no. 3, pp. 385–390, 2002.

[34] R. Fogel and J. L. Limson, "Electrochemically predicting phenolic substrates' suitability for detection by amperometric laccase biosensors," *Electroanalysis*, vol. 25, no. 5, pp. 1237–1246, 2013.

[35] R. Rawal, S. Chawla, and C. S. Pundir, "Polyphenol biosensor based on laccase immobilized onto silver nanoparticles/multiwalled carbon nanotube/polyaniline gold electrode," *Analytical Biochemistry*, vol. 419, no. 2, pp. 196–204, 2011.

[36] D. Brondani, C. W. Scheeren, J. Dupont, and I. C. Vieira, "Biosensor based on platinum nanoparticles dispersed in ionic liquid and laccase for determination of adrenaline," *Sensors and Actuators B: Chemical*, vol. 140, no. 1, pp. 252–259, 2009.

[37] Y. Zhang, G.-M. Zeng, L. Tang, D.-L. Huang, X.-Y. Jiang, and Y.-N. Chen, "A hydroquinone biosensor using modified core-shell magnetic nanoparticles supported on carbon paste electrode," *Biosensors & Bioelectronics*, vol. 22, no. 9-10, pp. 2121–2126, 2007.

[38] V. S. Bagotsky, "Nonaqueous electrolytes," in *Fundamentals of Electrochemistry*, pp. 128–137, Wiley-Interscience, Hoboken, NJ, USA, 2006.

Hindawi Publishing Corporation
BioMed Research International
Volume 2015, Article ID 932934, 14 pages
http://dx.doi.org/10.1155/2015/932934

Research Article

Comparison of Different Strategies for Selection/Adaptation of Mixed Microbial Cultures Able to Ferment Crude Glycerol Derived from Second-Generation Biodiesel

C. Varrone,[1,2] T. M. B. Heggeset,[3] S. B. Le,[3] T. Haugen,[3] S. Markussen,[3] I. V. Skiadas,[1,2] and H. N. Gavala[1,2]

[1]*Department of Chemistry and Biosciences, Aalborg University, 2350 Copenhagen, Denmark*
[2]*Department of Chemical and Biochemical Engineering, Technical University of Denmark, 2800 Lyngby, Denmark*
[3]*Biotechnology and Nanomedicine, SINTEF Materials and Chemistry, 7465 Trondheim, Norway*

Correspondence should be addressed to C. Varrone; cristiano.varrone@gmail.com

Received 29 May 2015; Accepted 12 July 2015

Academic Editor: Abd El-Latif Hesham

Objective of this study was the selection and adaptation of mixed microbial cultures (MMCs), able to ferment crude glycerol generated from animal fat-based biodiesel and produce building-blocks and green chemicals. Various adaptation strategies have been investigated for the enrichment of suitable and stable MMC, trying to overcome inhibition problems and enhance substrate degradation efficiency, as well as generation of soluble fermentation products. Repeated transfers in small batches and fed-batch conditions have been applied, comparing the use of different inoculum, growth media, and Kinetic Control. The adaptation of activated sludge inoculum was performed successfully and continued unhindered for several months. The best results showed a substrate degradation efficiency of almost 100% (about 10 g/L glycerol in 21 h) and different dominant metabolic products were obtained, depending on the selection strategy (mainly 1,3-propanediol, ethanol, or butyrate). On the other hand, anaerobic sludge exhibited inactivation after a few transfers. To circumvent this problem, fed-batch mode was used as an alternative adaptation strategy, which led to effective substrate degradation and high 1,3-propanediol and butyrate production. Changes in microbial composition were monitored by means of Next Generation Sequencing, revealing a dominance of glycerol consuming species, such as *Clostridium*, *Klebsiella*, and *Escherichia*.

1. Introduction

The exponential growth of biodiesel production in the last decade has led to a concomitant increase in crude glycerol [1, 2]. Hence, new uses of crude glycerol are required in order to overcome the problem of glycerol glut. Methods for glycerol utilization or disposal include combustion, composting, anaerobic digestion, animal feed, and thermochemical or biological conversion to value-added products [3]. New methods for the valorization of glycerol involve the bioconversion into biofuels and green chemicals, which might provide several advantages, compared to some of the above-mentioned methods. Environmental biotechnologies are thus going to provide a significant contribution to tackle the challenge of a more efficient use of by-products and waste streams. In this frame, a so-called "ecobiotechnological approach" has been recently proposed as an interesting tool for a more effective exploitation of wastes and wastewaters [4].

As stated by Johnson and colleagues [5], ecobiotechnology aims at applying "processes based on open mixed cultures and ecological selection principles (rather than genetic or metabolic engineering), thus combining the methodology of environmental biotechnology with the goals of industrial biotechnology." Some recent studies have started to apply such principles also to the valorization of crude glycerol, showing interesting results, in terms of conversion efficiencies and decreased substrate and operating costs (no substrate pretreatment, no sterilization, etc.) mainly due to lower energy consumption [2, 4, 6, 7]. Glycerol fermentation can

lead to the production of several useful metabolites, such as alcohols (i.e., ethanol and butanol), 1,3-propanediol (1,3 PD), 2,3-butanediol (2,3 BD), hydrogen, polyhydroxyalkanoates (PHA), and volatile fatty acids (VFAs) [8–13]. The latter represent important bulk chemicals and preferred substrates for many bioprocesses [14]. Interestingly, they are also known to be preferred substrates for enhanced polyhydroxyalkanoates (PHA) production [15] and in principle they might be used for a 2-stage process for the bioconversion of glycerol into VFAs, followed by PHA production.

Thus, in recent years, the glycerol glut problem has led to several studies on the conversion of crude glycerol. However, valorization of crude glycerol derived from second-generation (2G) biodiesel has been scarcely investigated and, to our knowledge, bioconversion of crude glycerol from the processing of animal fat derived biodiesel has been reported only by Sarma and colleagues [16] so far. On the other hand, production of 2G biodiesel is expected to increase in the near future, due to incentives. Europe, for instance, has proposed subsidies for the production of biofuels produced from waste feedstocks (i.e., "multiple accounting mechanism," Renewable Energy Directive 2009/28/EC), thus leading to an enhanced production of crude glycerol derived from 2G biodiesel.

Nevertheless, the use of such a substrate, containing high amounts of contaminants such as soaps and long chain fatty acids (LCFA), salts, ashes, and methanol, can strongly interfere with, or even inhibit, the microbial growth and conversion efficiency, especially in the case of pure strains [17, 18]. In fact, crude glycerol derived from complex waste materials, such as meat processing and restaurant waste, is considered to have even more impurities (very high amount of sulfur and LCFA, very low pH, etc.) than the crude glycerol derived from pure substrates [16]. For this reason, most studies working with pure strains focus on the use of purified glycerol. This allows for higher substrate conversion efficiency but significantly increases processing costs [19]. A very important step to reduce costs related to the conversion of glycerol would therefore be to use crude glycerol directly, without previous pretreatment. This might be achieved by using selected mixed microbial cultures (MMCs). Since sterile cultivation enables an easy way of controlling microbial growth and product formation, most industrial biotechnological processes today are based on a single microbial strain. Nonetheless, there are many cases where the utilization of mixed cultures and/or cocultures appears to be advantageous over a single microorganism [20].

The ability of the selected MMC to create synergistic effects can help degrading complex substrates with different grades of impurities, also in nonsterile conditions. MMC can thus utilize a wide variety of complex substrates, rich in nutrients, but also potentially inhibiting effluents. This is particularly advantageous if industrial waste feedstock, containing compounds of undefined composition, are used [21]. In fact, unlike monocultures, MMCs show a complementary metabolism and are able to utilize different carbon sources. For this reason, they are considered by several authors to be of special interest in the fermentative processes [5, 22, 23], representing a promising alternative approach [5], in some cases even showing better performances than pure strains [24]. Therefore, a new promising direction in environmental biotechnology is to apply the principles of ecobiotechnology and adaptive laboratory evolution to develop a mixed microbial population, selected to achieve a higher production yield and which would have unique metabolic capacities [25], at lower operational costs [6, 26].

Table 1: Crude glycerol characteristics.

Content	Typical values
Raw glycerine	75%
Fat	10%
Methanol	<1%
Sulphur	1-2%
Moisture	10%
Ash	5%
Density	1.2–1.3 Kg/L
pH	1.5

The objective of this study is the selection and adaptation of MMC, able to ferment crude glycerol generated from animal fat derived biodiesel and produce building-blocks and green chemicals. Various adaptation strategies have been investigated for the enrichment of suitable and stable MMCs, trying to overcome inhibition problems and enhance substrate degradation efficiency, as well as production of soluble fermentation products.

2. Material and Methods

2.1. Choice of Crude Glycerol. Unless differently stated, non-pretreated crude glycerol provided by Daka Biodiesel (Denmark), obtained from the transesterification of butchery waste (based on animal fat categories 1 and 2 according to the EU regulation number 1069/2009 and 142/2011), was used. The main characteristics of this type of crude glycerol are reported in Table 1.

2.2. Experimental Plan. The enrichment and selection were performed in small batches through repeated transfers of different inocula, in order to compare their performances. Each experiment was performed in triplicate. Activated sludge and anaerobic sludge were used as inoculum source. The latter underwent heat-shock treatment and the fermentation performance was compared to the nonpretreated sludge. Heat-shock allows selecting for spore forming bacteria (typically Gram-positive bacteria, such as Clostridia, which are abundant in anaerobic sludge and are well-known in dark fermentation processes), while getting rid of methanogens. Activated sludge instead is mainly made of enterobacteria, typically nonspore forming bacteria, which would be inhibited by the heat-shock. Enterobacteria are considered to be an important component in dark fermentation processes and the heat shock would lead to a reduction of additional fermentation pathways [27]. Moreover the activated sludge is not anaerobic and does not favor the growth of methanogens,

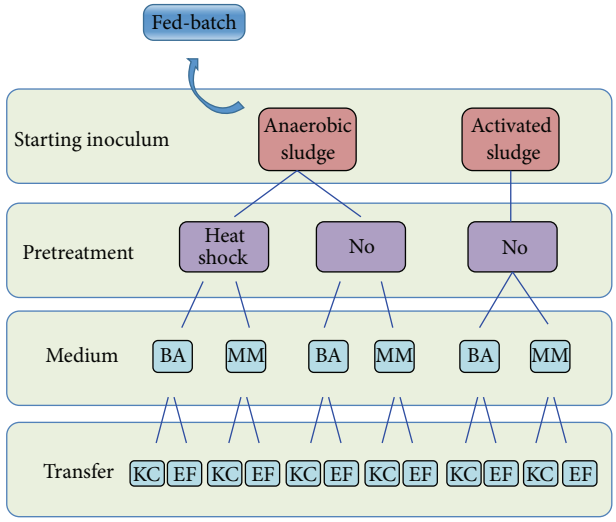

FIGURE 1: Transfer scheme for the selection and enrichment in batch conditions. KC = Kinetic Control; EF = End of Fermentation; MM = Minimal Medium; BA = BA medium.

and thus the heat-shock treatment would not be necessary or beneficial.

Two different growth media were used for the enrichment, containing 10 g/L glycerol: a medium rich in trace metals, vitamins, and growth factors (BA) and a Minimal Medium (MM), which does not include yeast extract, tryptone, vitamin, or mineral solutions.

Transfers. 10% inoculum was used in 125 mL vials of 40 mL working volume. The experiments were performed to compare the efficiency of two enrichment strategies: (a) Kinetic Control (KC) and (b) non-Kinetic Control, in which the inoculum was transferred only at the End of Fermentation (EF).

Kinetic Control. Transfers occurred during the (late) exponential growth phase, in rapid successions (after 21 h fermentation).

End of Fermentation. The transfers occurred after 72 h, when no more fermentation gases were produced. A scheme of the experimental inoculum transfers is presented in Figure 1. In addition, fed-batch experiments (400 mL working volume in 1 L serum bottle) and enrichment on hexane-pretreated crude glycerol were also performed, using anaerobic sludge as starting inoculum.

Liquid and gas samples were collected on a regular basis.

2.2.1. Microorganisms Storage and Activation. MMCs obtained during the exponential growth phase were stored in the freezer at −18°C and periodically refreshed. Prior to use, the frozen mixed culture was transferred to the refrigerator at 4°C, for 2 hours and then for an additional hour at room temperature, before being inoculated. Activation was performed in the same conditions as the respective enrichment and 10% v/v inoculum was transferred into fresh medium after 21 hours (in case of Kinetic Control experiments) or 72 hours (in case of End of Fermentation experiments).

2.2.2. Batch Experiments. 125 mL serum vials were used for batch experimentation, to enrich the (activated or anaerobic) sludge through repeated transfers into fresh medium, according to the transfer scheme shown in Figure 1. 36 mL growth medium (either MM or BA medium), containing around 10 g/L glycerol, was flushed for 5 minutes with a mixture of 80% N_2 and 20% CO_2, in order to obtain anaerobic conditions, prior to inoculation, and incubated at 37°C, using an orbital shaker at 150 rpm. Gas and liquid samples were collected before transferring 10% v/v of fermentation broth (representing the new inoculum) into fresh medium. All transfer steps were performed in triplicate.

2.2.3. Hexane Pretreatment of Crude Glycerol. Enrichment of (heat-shock treated) anaerobic sludge was also performed (in the same batch conditions described in Section 2.2.2) using hexane-pretreated crude glycerol. The extraction step was applied in order to reduce the concentration of lipids and (long chain) fatty acids present in the crude glycerol (coming from fat derived biodiesel) and evaluate its potential inhibitory effect on the microbial growth. Hexane pretreatment was performed as described by Anand and Saxena [28] and the batch transfers were performed with Kinetic Control (every 21 h).

2.2.4. Fed-Batch Experiments. Repeated fed-batch culture was used for the enrichment of heat-shock treated anaerobic sludge, in a 1 L serum vial with 300 mL work solution, containing 90% anaerobic sludge and 10% BA medium, with around 10 g/L (nonpretreated) glycerol. The serum vial was flushed for 15 minutes with a mixture of 80% N_2 and 20% CO_2, in order to obtain anaerobic conditions, and incubated at 37°C and 150 rpm. Every day, an aliquot of around 30 mL was collected and substituted with an equivalent amount of fresh BA medium, containing 10 g/L glycerol. Gas and liquid samples were collected prior to this operation.

2.3. Media Composition

2.3.1. Minimal Medium. Minimal Medium (MM) is a very simple growth medium, containing, per litre of distilled water: 10 g glycerol, 3.4 g $K_2HPO_4{\cdot}3H_2O$, 1.3 g KH_2PO_4, 2 g $(NH_4)_2SO_4$, 0.2 g $MgSO_4{\cdot}7H_2O$, 20 mg $CaCl_2{\cdot}2H_2O$, and 5 mg $FeSO_4{\cdot}7H_2O$ [29].

For cultivation, 36 mL of medium was dispensed into 125 mL serum bottles and sealed with butyl rubber stoppers. Subsequently the medium was flushed with a mixture of nitrogen and CO_2 (80 : 20 v/v) for 5 minutes and inoculated with 4 mL inoculum (10% v/v inoculum), before being incubated at 37°C with continuous stirring (150 rpm). Initial pH was 7.

2.3.2. Rich Medium. A complete synthetic medium for anaerobes (referred to as BA medium [30]), which contains salts, vitamins, and trace elements beside pH buffers

and reducing agents was also used. The medium was prepared from the following stock solutions (containing, per litre of distilled water): (A) 100 g NH_4Cl, 10 g NaCl, 10 g $MgCl_2 \cdot 6H_2O$, and 5 g $CaCl_2 \cdot 2H_2O$; (B) 200 g $K_2HPO_4 \cdot 3H_2O$; (C) trace metal and selenite solution: 2 g $FeCl_2 \cdot 4H_2O$, 0.05 g H_3BO_3, 0.05 g $ZnCl_2$, 0.038 g $CuCl_2 \cdot 2H_2O$, 0.05 g $MnCl_2 \cdot 4H_2O$, 0.05 g $(NH_4)_6Mo_7O_{24} \cdot 4H_2O$, 0.05 g $AlCl_3$, 0.05 g $CoCl_2 \cdot 6H_2O$, 0.092 g $NiCl_2 \cdot 6H_2O$, 0.5 g ethylenediaminetetraacetate, 1 mL concentrated HCl, and 0.1 g $Na_2SeO_3 \cdot 5H_2O$; (D) 52 g $NaHCO_3$; and (E) vitamin mixture according to Wolin et al. [31].

974 mL of redistilled water was added to the following stock solutions: A, 10 mL; B, 2 mL; C, 1 mL; D, 50 mL; and E, 1 mL [30].

2.4. Inocula. Activated sludge was collected from the wastewater treatment plant of Daka Biodiesel, Denmark, as it was anticipated that it should be already enriched in microbes able to use glycerol and lipid substances as carbon source.

Anaerobic sludge was obtained from the Lundtofte Wastewater Treatment plant (Denmark) and supplemented with the effluent of a lab-scale anaerobic digester (50/50 v/v), treating swine manure.

The heat-shock pretreatment was obtained by heating the anaerobic sludge mixture for 15 minutes at 90°C, while flushing with the N_2-CO_2 mixture.

2.5. Analytical Methods. Detection and quantification of glycerol, ethanol, 1,3-propanediol, and lactic acid were obtained with a HPLC equipped with a refractive index and Aminex HPX-87H column (BioRad) at 60°C. A solution of 4 mM H_2SO_4 was used as an eluent at a flow rate of 0.6 mL/min.

Samples for HPLC analysis were centrifuged at 10,000 rpm for 10 min, filtered through a 0.45 μm membrane filter, and finally acidified with a 10% w/w solution of H_2SO_4.

For the quantification of volatile fatty acids (VFAs), filtered samples were acidified with H_3PO_4 (30 μL of 17% H_3PO_4 was added in 1 mL of sample) and analyzed on a gas chromatograph (PerkinElmer, Clarus 400), equipped with a flame ionization detector and a capillary column (Agilent HP-FFAP, 30 m long, 0.53 mm inner diameter). The oven was programmed to start with 105°C (for 3 minutes), followed by a ramp that reaches 130°C at a rate of 8°C/min and subsequently 230°C (held for 3 min) at a rate of 45°C/min. Nitrogen was used as the carrier gas at 13 mL/min; the injector temperature was set at 240°C and the detector at 230°C.

The total volume of gas production was measured using a water displacement system [32].

Hydrogen content in the produced gas was measured with a gas chromatograph (SRI GC model 310) equipped with a thermal conductivity detector and a packed column (Porapak-Q, length 6 ft and inner diameter 2.1 mm). The volume of H_2 produced in sealed vials during glycerol fermentation tests was calculated by the mass balance equation [33].

Multivariate data analysis was performed using Unscrambler X 10.1 software (by Camo). A Principal Component Analysis (PCA) [34] was chosen as a tool to explore the big data matrix obtained from the main fermentation parameters monitored during the enrichments.

2.6. Next Generation Sequencing. DNA was extracted from the pellets of 5 mL crude samples using the PowerSoil DNA Isolation Kit (MoBio) according to the standard procedure. Sequencing amplicon libraries were generated by PCR following the "16S Metagenomic Sequencing Library Preparation, Preparing 16S Ribosomal RNA Gene Amplicons for the Illumina MiSeq System" protocol (Illumina part number 15044223 rev. B). Internal parts of the 16S ribosomal RNA (rRNA) gene, covering variable regions V3 and V4, were PCR-amplified with the KAPA HiFi HotStart ReadyMix (KAPA Biosystems) and the primers 5′-TCGTCGGCAGCGTCAGATGTGTATAAGAGACAGCCTACGGGNGGCWGCAG-3′ and 5′-GTCTCGTGGGCTCGGAGATGTGTATAAGAGACAGGACTACHVGGGTATCTAATCC-3′ and purified with the Agencourt AMPure XP kit (Beckman Coulter Genomics). The Nextera XT Index Kit was used to add sequencing adapters and multiplexing indices. Pooled DNA libraries were sequenced on a MiSeq sequencer (Illumina) using the MiSeq Reagent Kit v3 in the 2·300 bp paired-end mode.

Sequencing reads were demultiplexed, trimmed, and OTU-classified using the Metagenomics Workflow of the MiSeq Reporter Software v.2.3 (Illumina). This workflow uses an Illumina proprietary classification algorithm and an Illumina-curated version of the Greengenes 13.5 (May 2013) taxonomy database, which covers 3 kingdoms, 33 phyla, 74 classes, 148 orders, 321 families, 1086 genera, and 6466 species.

Due to the relatively high number of unclassified reads found at the species level, comparisons between samples are presented at the genus level, while comparisons at the species, family, order, class, and phylum level are available as supplementary information (in Supplementary Material available online at http://dx.doi.org/10.1155/2015/932934). Sequencing reads have been deposited to the sequence read archive of NCBI under the Bioprojects PRJNA285034 (http://www.ncbi.nlm.nih.gov/bioproject/285034) and PRJNA284929 (http://www.ncbi.nlm.nih.gov/bioproject/284929).

3. Results and Discussion

3.1. Enrichment in Batch Conditions

3.1.1. Activated Sludge. Based on the experimental scheme (Figure 1), 12 different selection conditions were tested in triplicate. The enrichment using activated sludge showed good results in terms of substrate degradation, and it continued unhindered for several transfers, with no evident inhibition (due to the use of crude glycerol). This actually indicated the possibility to increase the substrate concentration in future studies. The best results obtained, in terms of substrate degradation efficiency (practically reaching 100%) and biogas production, were observed with MM-KC. This experimental condition led to the highest ethanol production, converting

about 10 g/L glycerol in 21 h (maximum yield = 4.6 g/g), with a concomitant 1,3 PD yield of approximately 3 g/g. After 16 transfers, however, the distribution of the main metabolites changed, with 1,3 PD becoming the dominant one, and showing an increase in butyrate during the last transfers.

MM-EF also showed a high substrate degradation efficiency and (with exception of transfers 5–7) the main metabolites were represented by 1,3 PD and butyrate. This condition performed the best butyrate production, with a maximum yield of 3.3 g/g (from 8.5 g/L glycerol in 72 h fermentation), together with 1,3 PD yield of 4.7 g/g.

The use of BA medium (experiments 3 and 4) seemed not to favor solventogenesis pathway (almost no ethanol production was observed), while 1,3 PD was still by far the main metabolite (with an average production of 3.67 ± 0.56 g/L and 3.99 ± 0.74 g/L for KC and EF, resp.), followed by butyrate and acetate. Also in this case, the End of Fermentation seemed to favor butyrate production, with a yield reaching up to 2.99 g/g (from 7.7 g/L glycerol in 72 h fermentation) in BA-EF.

Hydrogen % in the biogas was rather modest in all experiments, reaching in most cases around 20%.

The distribution of main metabolites and substrate degradation (%) observed during the enrichment process with activated sludge are shown in Figures 2(a) and 2(b).

Principal Component Analysis, based on the complete data matrix of 240 samples with 11 variables, showed clear differences between the tested enrichment strategies (Figure 3), with EF closer related to butyrate (especially MM-EF) and BA-KC closer related to acetate. In general, the first Principal Component (PC) showed an increase of ethanol and hydrogen, moving towards the right, while the second PC showed an increase of butyrate production moving upwards. The first PC roughly separated EF and KC (with the exception of MM-EF), while the second PC separated MM from BA.

Furthermore, a comparison of the correlation loadings obtained with the data of the four enrichment conditions (MM-KC, MM-EF, BA-KC, and BA-EF) separately, showed that, only in the case of BA, butyric acid was related to H_2 production (Figure 4), as would be expected from a direct glycerol conversion into butyrate. In fact, glycerol conversion to butyric acid has a theoretically yield of 2 mol/mol [35].

Interestingly, in the case of MM, butyrate production was negatively correlated with lactic and acetic acid, and also with hydrogen in MM-EF, while it was positively correlated with hydrogen production when using BA medium, thus implying a secondary fermentation (*sensu* Agler et al. [21]) (a butyrate production which does not come directly from glycerol conversion).

There might be several possible pathways, leading to butyrate production through the conversion of lactate and acetate [36], besides the above-mentioned conversion of glycerol. Some examples are provided in

$$\text{Lactate} + 0.4\,\text{Acetate} + 0.7H^+ \longrightarrow 0.7\,\text{Butyrate} + 0.6H_2 + CO_2 + 0.4H_2O \quad (1)$$
$$\Delta G = -183.9$$

$$\text{Lactate} + \text{Acetate} + H^+ \longrightarrow \text{Butyrate} + 0.8H_2 + 1.4CO_2 + 0.6H_2O \quad (2)$$
$$\Delta G = -59.4$$

$$2\text{Lactate} + H^+ \longrightarrow \text{Butyrate} + 2H_2 + 2CO_2 \quad (3)$$
$$\Delta G = -64.1$$

It is also worth noting that Zhu and Yang [37] observed a metabolic shift from butyrate formation to lactate and acetate at pH < 6.3, associated with decreased activities of phosphotransbutyrylase and NAD-independent lactate dehydrogenase, and increased activities of phosphotransacetylase and lactate dehydrogenase. Our batch experiments were operated without pH control, starting at pH 7 and typically ending at around 4.8, due to glycerol acidification. Therefore it is likely that such a metabolic shift was also involved in our fermentation tests.

3.1.2. Anaerobic Sludge. Differently from activated sludge, the enrichment of anaerobic sludge in batch conditions showed a clear inhibition, regardless of the selection strategy (BA and MM growth medium, EF or KC transfers). The inhibition was presumably related to the high concentration of LCFA and the negative interaction with the cell membranes of Gram-positive anaerobic bacteria of the anaerobic sludge, rather than product inhibition. In fact, even after centrifuging the inoculum, washing away the supernatant and resuspending the pellet into fresh medium (thus washing away extracellular soluble metabolites), no recovery of the fermentation was achieved. Addition of specific elements such as yeast extract or vitamin and mineral solution did not have any effect either.

The distribution of main metabolites and fraction of H_2 (in the headspace) detected during the enrichment process with anaerobic sludge are shown in Figure 5. The use of MM (without nutrient supplements) led to inactivation after only 1 transfer, while BA reached 6-7 transfers before being inhibited (Figure 5(a)). Nonpretreated sludge (Figure 5(b)) showed a high production of propionic acid, while, with heat-shock treated sludge (Figure 5(c)), butyric acid was the dominant metabolite. The latter condition was chosen for an alternative selection strategy, using fed-batch conditions.

3.1.3. Hexane-Pretreated Glycerol Tests. As mentioned above, heat-shock treated (HS) inoculum was chosen for further experimentation. The possible inhibiting effect of LCFA and "lipidic compounds" was evaluated in the following test. The hypothesis was that the animal fat derived crude glycerol would contain inhibiting amounts of LCFA, which might negatively interfere with the membrane of Gram-positive bacteria of the anaerobic sludge. Activated sludge was not included in this test, since it did not show any inhibition.

Nonextracted crude glycerol showed an organic carbon content, expressed as chemical oxygen demand (COD), of 1309 ± 32 g COD/L, while the extracted crude glycerol was 1172 ± 12 g COD/L, thus suggesting that approximately 137 g COD/L of "lipidic compounds" was removed (which would

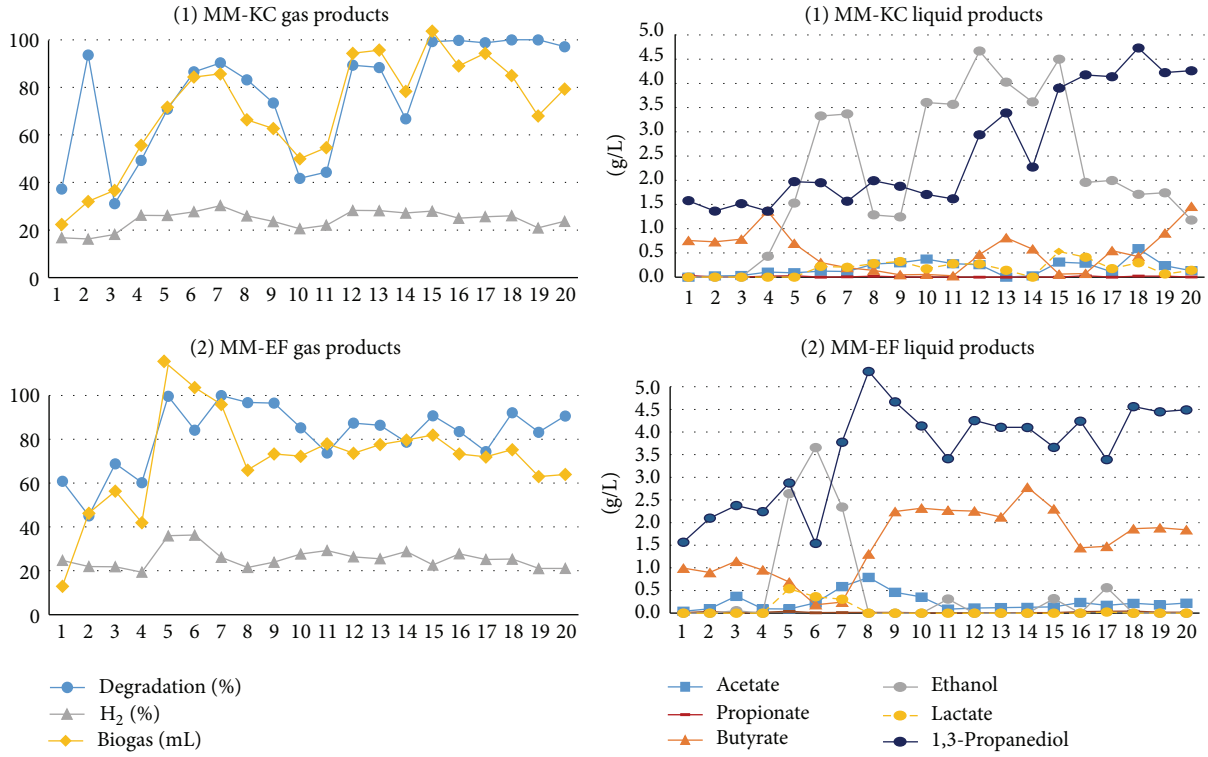

(a)

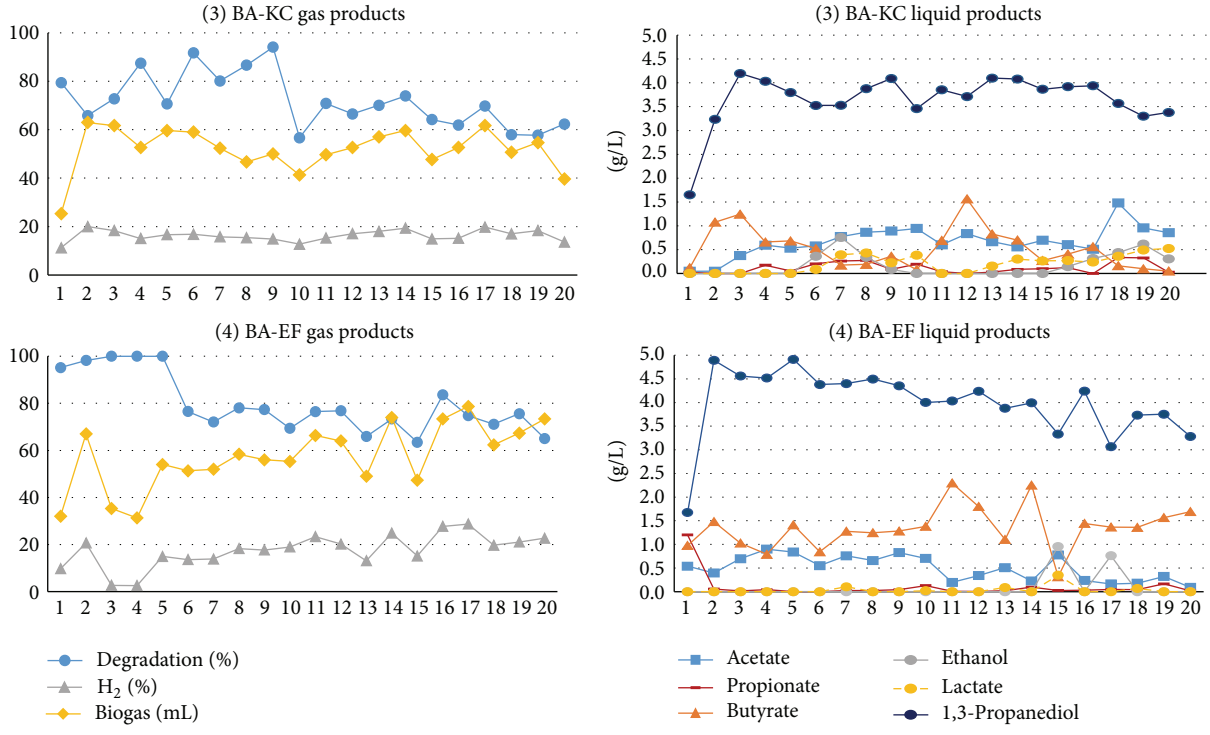

(b)

Figure 2: Fermentation products monitored during the enrichment of activated sludge in batch conditions, through repeated transfers using MM (a) and BA (b) medium. (1) MM-KC = Minimal Medium with Kinetic Control (21 h); (2) MM-EF = Minimal Medium with End of Fermentation (72 h); (3) BA-KC = Basal Medium with Kinetic Control (21 h); (4) BA-EF = Basal Medium with End of Fermentation (72 h).

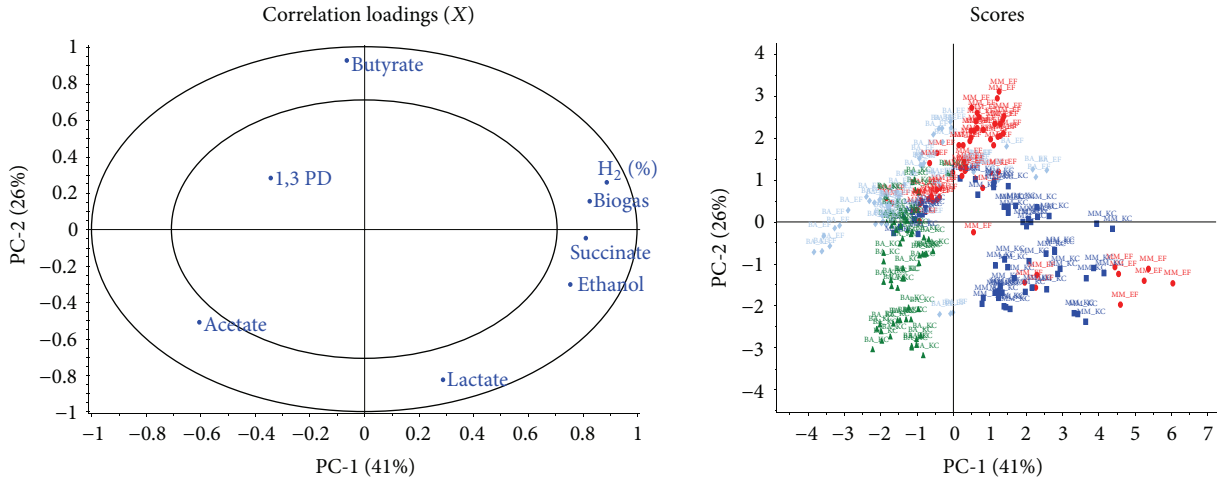

Figure 3: Principal Component Analysis showing the distribution of the main fermentation parameters (correlation loading plot) and the distribution of the samples (score plot) during the experiments with activated sludge: MM-EF (in red), MM-KC (in blue), BA-EF (in grey), and BA-KC (in green). The first two components explain together about 67% of the total variability.

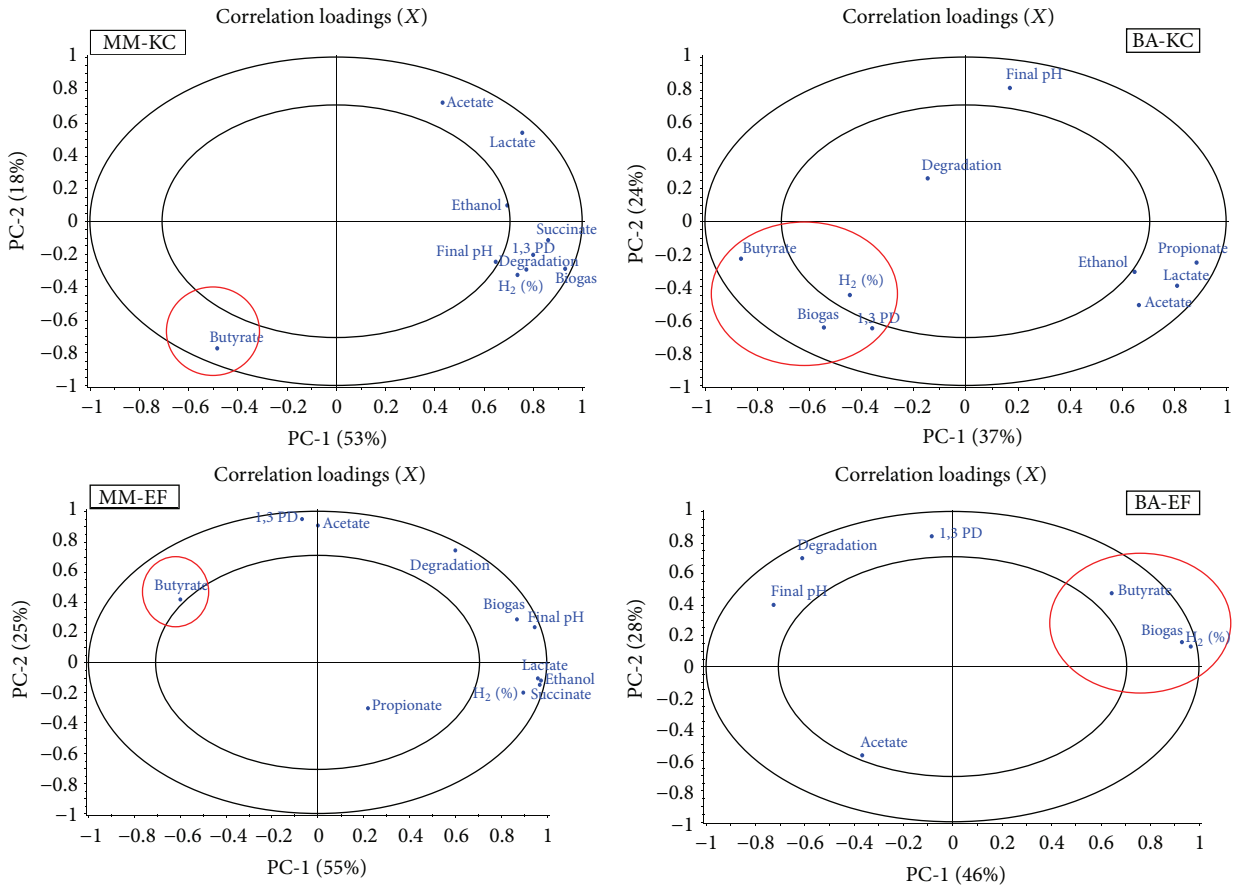

Figure 4: Principal Component Analysis showing the distribution of the main fermentation parameters (correlation loading plot) of the four experimental conditions (namely, MM-EF, MM-KC, BA-EF, and BA-KC) separately, during the experiments with activated sludge. The first two components explain together more than 60% of the total variability, in all cases.

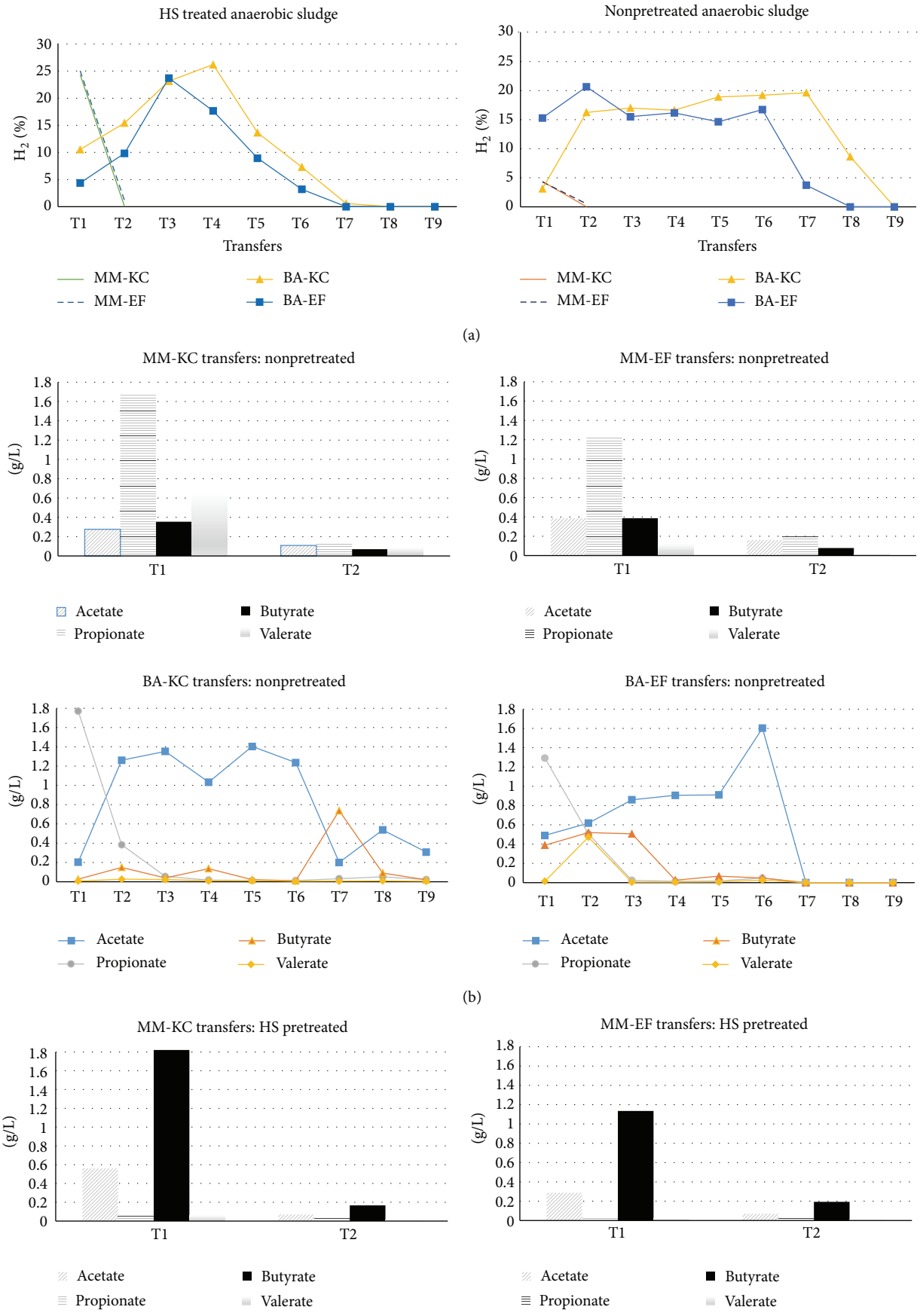

Figure 5: Continued.

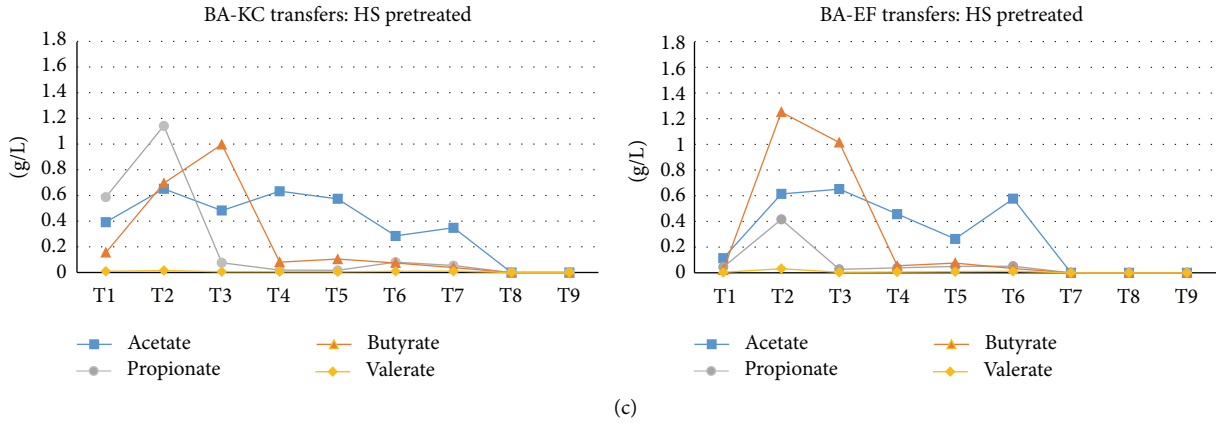

(c)

Figure 5: Results of batch transfers, during the enrichment of anaerobic sludge, showing H2% (a) in the headspace, soluble metabolites from nonpretreated anaerobic sludge (b), and soluble metabolites from heat-shock treated anaerobic sludge (c). MM-KC = Minimal Medium with Kinetic Control (21 h); MM-EF = Minimal Medium with End of Fermentation (72 h); BA-KC = Basal Medium with Kinetic Control (21 h); BA-EF = Basal Medium with End of Fermentation (72 h).

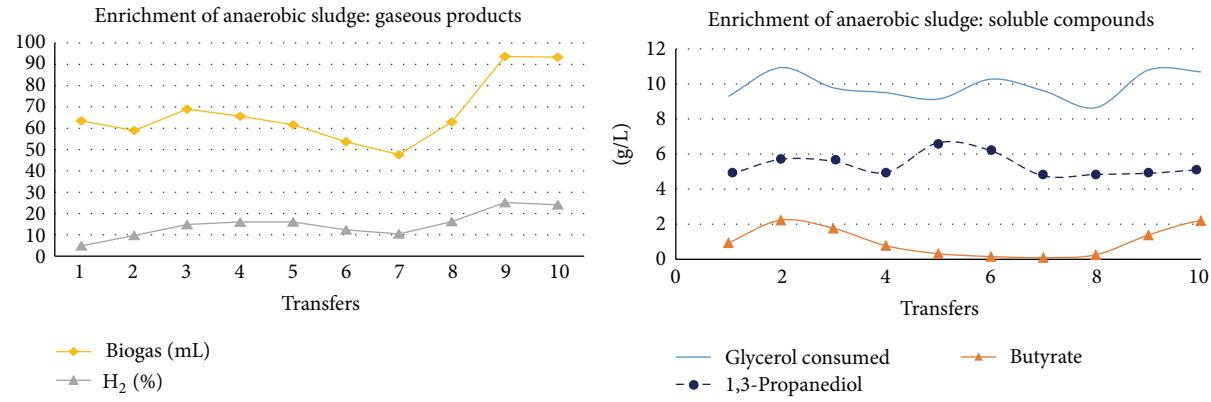

(a) (b)

Figure 6: Results from the batch transfers of anaerobic sludge, using hexane-treated crude glycerol, showing gas products (a) and glycerol consumption, together with the main soluble metabolites (b).

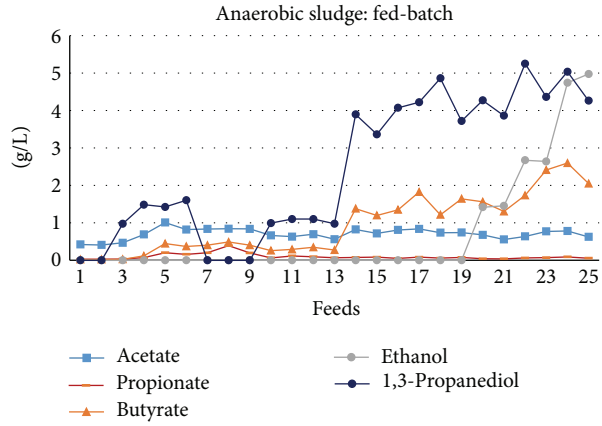

Figure 7: Distribution of main soluble metabolites observed during the fed-batch enrichment process with heat-shock treated anaerobic sludge.

approximately correspond to 34.7 g/L of oleic acid, a typical LCFA known for its inhibiting effect).

As can be seen in Figure 6, repeated transfers in batch conditions with the hexane-treated crude glycerol led to high substrate degradation efficiency and the MMC was never inactivated, showing glycerol fermentation performances comparable with those obtained with activated sludge. This implied that, indeed, the inactivation of anaerobic sludge depended on the high LCFA content of the 2G crude glycerol.

However, since the aim of this study was the selection of MMC that can grow on nonpretreated crude glycerol, the possibility to achieve enrichment and adaptation tests of anaerobic sludge using fed-batch conditions was investigated.

3.2. Enrichment in Fed-Batch Conditions. As can be seen in Figure 7, the fed-batch operations allowed effective overcoming of crude glycerol inhibition with anaerobic sludge, leading to a good substrate conversion into mainly 1,3 PD, ethanol, and butyrate (after about 14 feedings). However, the reactor started to develop a community of sulfate reducing bacteria (SRB) that inhibited fermentation after roughly 7 feedings. For this reason, the sludge underwent a second heat-shock treatment (at 10 feedings) to allow further glycerol fermentation. Nonetheless, H_2S production occurred again after 21 feedings. Probably, continuous mode fermentation with short hydraulic retention time (HRT) would thus represent a suitable approach for successful adaptation/enrichment of anaerobic sludge to untreated crude glycerol (possibly helping to rinse out slower growing SRB). For this reason, ongoing work is now focusing on identification of the operating parameters for maintaining a stable MMC in continuous mode and statistical optimization of key parameters for green chemicals production. Since activated sludge was successfully enriched in batch conditions, there was no need to perform fed-batch tests with this inoculum.

3.3. Molecular Characterization of the MMC during the Enrichment Process. The development of the MMC was monitored by sequencing amplicons of the V3 and V4 variable regions of the 16S rRNA gene. Operational taxonomic units (OTUs) were then assigned from each sequencing read and used as a measure of the microbial diversity of each sample. The copy number of the 16S rRNA gene varies from 1 to 15, depending on the species, and the OTUs are therefore only providing an estimate of the true microbial diversity. The copy number is varying but is relatively high in the taxa Firmicutes and Gammaproteobacteria, with a mean of 5.8 ± 2.8 copies, while it is lower for Bacteroidetes (3.5 ± 1.5), Betaproteobacteria (3.3 ± 1.6), Actinobacteria (3.1 ± 1.7), and Spirochaetes (2.4 ± 1.0) [38]. Overall, the Firmicutes and Gammaproteobacteria are overestimated in the analysis and the cell-count may for some genera be ~5–10-fold lower than the OTU count.

3.3.1. Activated Sludge Experiments. In all these samples there was a dominance of bacteria belonging to the phylum Firmicutes, in particular from the classes Clostridia and Bacilli and of the class Gammaproteobacteria (Figures S1–S6).

MM-KC. The enrichment was characterized by a strong decrease of the genera *Clostridium* and *Lactobacillus*, both Firmicutes, and an increase of *Klebsiella* and *Escherichia*, both Gammaproteobacteria (Table 2; Figure S2). In particular, the joint increase of the latter two probably favored an enhanced ethanol production (T10 and T13), while the dominance of *Klebsiella* alone (T18) was associated with a metabolic shift towards 1,3 PD (see Figure 2(a)). These results are in good agreement with previous observations with enriched activated sludge, selected with Kinetic Control [39].

MM-EF. The distribution of the main genera observed during these tests showed a sequence of dominance shifts, going from *Escherichia* to *Klebsiella*, and finally to *Clostridium* and *Escherichia*. The ethanol peak observed in T6 is associated with the dominance of *Escherichia* (around 55%), while the subsequent increase of *Klebsiella* (reaching almost 70%) shifted towards 1,3 PD production (T8: 5.2 g/L 1,3 PD and no ethanol production). Moreover, the stability of the community from T8 to T15 is also reflected in the distribution of the main metabolites (see Figure 2(a)). The higher butyric acid production observed after T7 might be related to the increase of the genus *Clostridium*, which includes several butyric acid producing species.

BA-KC. Interestingly, a clear increase in biodiversity could be observed during the enrichment of BA-KC, with an initial dominance of *Clostridium* (86%) and a sharp decrease over time, leading to less than 8%. This decrease is associated with a concomitant increase of other genera, such as *Escherichia* (reaching 34%), *Lactobacillus* (13%), and a number of unclassified genera (approximately 14% in total, primarily from the classes Gammaproteobacteria and Clostridia; Figure S5), followed by *Serratia* and *Klebsiella* (10%). Higher butyric acid was observed in T1 and T12 in the presence of at least 70% of *Clostridium*, while an increased acetic acid production was observed in T18.

BA-EF. In general, this enrichment was characterized by a dominance of *Clostridium,* with a decrease towards the last transfers. A decrease of acetic acid, and concomitant increase in butyric acid, could be observed comparing the samples T7 and T11, which were associated with a decrease of the genus *Slackia* (typically producing acetic acid and lactic and formic acid [40]) and an increase in *Clostridium*. A very sharp decrease of butyric acid (together with an increase in acetic acid and ethanol) could be observed in T15, which was associated with a decrease in *Clostridium* and a concomitant increase of unclassified genera, primarily belonging to the phylum Proteobacteria and in particular the class Gammaproteobacteria (Figures S5 and S6).

3.3.2. Anaerobic Sludge Experiments. This subparagraph reports the results of MMC taxonomical characterization for the anaerobic sludge enriched on hexane-pretreated crude

Table 2: Metagenomic classification of the MMC at the genus level. Results of batch transfers, during the enrichment of activated sludge, expressed as fraction (%). MM-KC = Minimal Medium with Kinetic Control (21 h); MM-EF = Minimal Medium with End of Fermentation (72 h); BA-KC = Basal Medium with Kinetic Control (21 h); BA-EF = Basal Medium with End of Fermentation (72 h). T0–T20 = transfer numbers. ND = Not detected. Genera appearing at frequencies below 1% in all samples were omitted.

	MM-KC						MM-EF						BA-KC			BA-EF				
GENERA	T1	T3	T7	T10	T13	T18	T0	T6	T7	T8	T15	T20	T1	T12	T18	T0	T7	T11	T15	T20
	%	%	%	%	%	%	%	%	%	%	%	%	%	%	%	%	%	%	%	%
Clostridium	51.3	80.8	37.0	12.4	28.8	18.1	28.4	1.42	1.21	40.1	43.2	83.9	86.4	67.4	7.92	67.9	60.3	73.7	32.0	45.4
Klebsiella	0.74	0.42	47.4	28.9	19.1	65.4	28.0	0.13	66.7	0.15	0.07	0.03	0.30	9.12	9.18	0.02	0.03	0.19	6.61	0.03
Escherichia	0.54	8.46	0.60	33.5	28.7	1.05	0.99	54.2	7.05	31.0	31.6	0.05	0.74	5.16	34.4	0.05	0.11	0.84	30.9	42.8
Unclassified	6.47	2.83	8.31	8.14	11.5	8.88	13.8	18.4	10.5	13.5	10.9	1.23	2.91	6.56	14.2	18.3	3.41	5.93	5.72	4.03
Lactobacillus	29.7	0.07	0.11	0.01	0.02	0.01	0.39	3.53	0.78	0.79	4.74	14.3	6.05	4.72	13.3	0.01	16.8	14.8	21.8	4.12
Slackia	0.07	<0.01	<0.01	<0.01	0.01	<0.01	0.01	7.04	1.21	5.16	0.41	0.03	<0.01	3.61	0.55	1.05	18.1	2.61	0.21	1.01
Serratia	0.01	2.06	0.45	9.97	5.72	0.59	0.64	8.02	2.68	4.36	4.35	0.01	0.28	1.05	10.3	0.01	0.01	0.14	1.73	1.35
Enterobacter	0.01	1.58	0.93	3.86	3.72	1.39	0.66	3.67	1.78	2.27	2.50	<0.01	0.08	0.55	2.61	<0.01	<0.01	0.07	0.74	0.25
Alkaliphilus	0.29	0.01	0.02	<0.01	<0.01	0.01	3.66	0.01	<0.01	0.01	0.01	<0.01	0.14	<0.01	0.01	0.65	<0.01	0.02	ND	ND
Tolumonas	0.01	0.22	1.74	1.19	0.70	2.73	1.43	0.04	2.66	0.03	0.03	ND	0.06	0.48	0.63	<0.01	<0.01	0.01	0.01	<0.01
Negativicoccus	0.02	<0.01	0.01	<0.01	<0.01	<0.01	0.01	<0.01	0.00	<0.01	<0.01	<0.01	0.01	0.14	2.56	0.06	0.02	0.04	<0.01	ND
Blautia	0.20	0.05	0.57	0.04	0.01	0.04	0.92	0.07	0.02	0.01	0.01	<0.01	0.10	0.01	0.29	0.03	0.01	0.01	ND	ND
Ruminococcus	ND	ND	ND	<0.01	ND	ND	0.02	0.13	2.17	0.14	0.13	ND	<0.01	<0.01	<0.01	0.05	0.24	ND	ND	ND
Erwinia	<0.01	2.11	0.06	0.10	0.06	0.07	0.03	0.05	0.46	0.03	0.04	ND	<0.01	0.04	0.25	ND	<0.01	<0.01	0.05	<0.01
Methylotenera	0.91	0.05	<0.01	<0.01	ND	<0.01	0.89	ND	<0.01	ND	ND	<0.01	0.10	ND	<0.01	1.97	ND	ND	ND	ND
Geobacillus	0.14	0.02	0.05	0.03	<0.01	0.05	1.44	<0.01	0.02	<0.01	<0.01	<0.01	0.05	<0.01	0.03	0.03	<0.01	<0.01	ND	ND
Pseudomonas	0.73	0.12	0.06	0.18	0.04	0.01	1.16	0.04	0.02	0.04	0.03	0.01	0.02	0.01	0.01	0.01	<0.01	0.02	0.01	0.27
Weissella	1.08	0.02	<0.01	<0.01	<0.01	<0.01	0.55	<0.01	<0.01	<0.01	<0.01	ND	0.21	<0.01	0.01	0.41	<0.01	0.01	ND	ND

Table 3: Metagenomic classification of the MMC at the genus level, for the anaerobic sludge enriched on hexane-pretreated crude glycerol in batch tests (HT) and with the untreated crude glycerol in fed-batch, expressed as fraction (%). T0–T11 = transfer numbers. ND = Not detected. Genera appearing at frequencies below 1% in all samples were omitted.

Genera	HT		FED-BATCH
	T0	T9	T11
	%	%	%
Blautia	0.24	0.04	50.8
Clostridium	30.1	46.6	16.2
Unclassified	31.5	6.45	9.89
Klebsiella	0.01	28.8	0.02
Escherichia	0.06	10.3	<0.01
Enterococcus	0.02	0.27	6.19
Alkaliphilus	5.64	0.06	0.88
Soehngenia	<0.01	ND	3.52
Serratia	0.01	2.67	0.04
Pedobacter	2.38	0.02	0.08
Enterobacter	0.02	2.21	0.01
Propionispora	1.99	0.01	0.03
Treponema	1.42	0.01	0.03
Peptoniphilus	0.07	0.02	1.35
Flavobacterium	1.33	0.03	0.54
Sedimentibacter	0.33	<0.01	1.26

glycerol in batch tests (HT) and with the untreated crude glycerol in fed-batch (Figures S7–S12). Anaerobic sludge grown on untreated glycerol underwent quick inhibition and was thus not analyzed.

The main difference that can be observed between the batch and fed-batch conditions was the dominant presence of *Blautia* (up to 50%) in the latter (Table 3). The fed-batch community was also characterized by the genus *Clostridium,* in addition to a number of unclassified genera, primarily of the phylum Firmicutes. Dominant genera in batch conditions (HT) at T0 were *Clostridium* and unclassified genera (both around 30%), with an increase of *Clostridium* (reaching more than 45%) and *Klebsiella* (almost 30%) in T9. It is worth noting that T0 was a highly diverse sample, with multiple genera having abundances in the range of 0.1–0.9%, explaining why the total fraction only reached about 75% (see Figure S8). The unclassified genera found in T0 mainly belonged to the phyla Proteobacteria (in particular to the class Deltaproteobacteria) and Firmicutes (especially to the class Clostridia) (Figures S11 and S12).

A total of 19 genera belonging to SRB were retrieved in the different anaerobic sludge samples, even though always at a very low % (far below the cut-off set at 1%). Initial sludge (HS_T0) contained 18 different genera (mainly *Desulfovibrio* and *Desulfofrigus*), accounting for 1.19%, which decreased to 10 genera (0.0023%) in T9. This suggests that the Kinetic Control was effective in enriching faster growing (glycerol consuming) bacteria, such as *Clostridium* and *Klebsiella* species over SRB. In fed-batch conditions, instead, the absence of a Kinetic Control allowed the growth of SRB. Thus, even though a second heat-shock treatment (T11) was able to decrease SRB from initial 19 genera to 16 (accounting for 0.59%), this was probably sufficient to allow SRB to grow in the following weeks of fed-batch experimentation, as witnessed by the H_2S production observed in the fed-batch reactor (which turned black and was characterized by the typical strong H_2S smell). The most abundant genus found in T11 was *Desulfotomaculum* (mainly with the species *D. halophilum*). *Desulfotomaculum* comprises endospore forming, Gram-positive bacteria. *Desulfotomaculum* spp. are able to grow autotrophically (using H_2/CO_2) and produce sulfide and acetate. Besides H_2 as electron donor, they are able to utilize alcohols and organic acids, which were likely to accumulate in the fed-batch system. Besides sulfate reduction they may also use various other sulfur compounds [41].

4. Conclusions

The selection and adaptation of *activated sludge* inoculum through successive transfers in batch conditions were performed successfully and continued unhindered for several months. The best results showed a substrate degradation efficiency of almost 100% (about 10 g/L) and different dominant metabolic products were obtained, depending on the selection strategy (mainly 1,3 PD, ethanol, or butyrate). In particular, the strategy of Kinetic Control coupled with Minimal Medium (MM-KC) led to a maximum ethanol yield of 4.6 g/L, together with a 1,3 PD yield of around 3 g/g, with complete substrate degradation within 21 h. The End of Fermentation coupled with Minimal Medium (MM-EF) showed a degradation efficiency of around 90–95%, with a maximum butyric acid yield of 3.3 g/g (from 8.5 g/L glycerol in 72 h fermentation), together with a 1,3 PD yield of 4.7 g/g. Tests with the rich BA medium showed a general lower substrate degradation efficiency but were also characterized by a high 1,3 PD and butyric acid production. Multivariate data analysis showed clear differences between different strategies and further suggested that only in the case of BA medium the butyric acid was directly produced from glycerol. In addition, End of Fermentation enrichment seemed to favor butyric acid production. On the other hand, *anaerobic sludge* (both, heat pretreated and not) exhibited inactivation after a few transfers in batch conditions, probably due to the presence of high concentration of lipidic compounds. Fed-batch mode turned out to be a valid alternative adaptation strategy, overcoming inhibition problems related to crude glycerol composition but was also associated with H_2S production, thus implying the use of continuous mode to better select and adapt anaerobic sludge to the conversion of animal fat derived crude glycerol. After overcoming inhibition problems, main metabolites produced were comparable with those obtained with activated sludge, with a high 1,3 PD and butyric acid production.

Next Generation Sequencing represented a useful tool to monitor the changes in microbial composition of MMCs, highlighting the development of a glycerol consuming community (with numerous strains belonging to the genera

Clostridium, *Klebsiella,* and Escherichia), thus confirming the effectiveness of the enrichment strategy.

Conflict of Interests

The authors declare that there is no conflict of interests regarding the publication of this paper.

Acknowledgment

The authors wish to thank the European Commission for the financial support of this work under FP7 Grant Agreement no 613667 (acronym: GRAIL).

References

[1] M. Ayoub and A. Z. Abdullah, "Critical review on the current scenario and significance of crude glycerol resulting from biodiesel industry towards more sustainable renewable energy industry," *Renewable & Sustainable Energy Reviews*, vol. 16, no. 5, pp. 2671–2686, 2012.

[2] C. Varrone, R. Liberatore, T. Crescenzi, G. Izzo, and A. Wang, "The valorization of glycerol: economic assessment of an innovative process for the bioconversion of crude glycerol into ethanol and hydrogen," *Applied Energy*, vol. 105, pp. 349–357, 2013.

[3] N. Kolesárová, M. Hutan, I. Bodík, and V. Špalková, "Utilization of biodiesel by-products for biogas production," *Journal of Biomedicine and Biotechnology*, vol. 2011, Article ID 126798, 16 pages, 2011.

[4] I. Ntaikou, C. Valencia Peroni, C. Kourmentza et al., "Microbial bio-based plastics from olive-mill wastewater: generation and properties of polyhydroxyalkanoates from mixed cultures in a two-stage pilot scale system," *Journal of Biotechnology*, vol. 188, pp. 138–147, 2014.

[5] K. Johnson, Y. Jiang, R. Kleerebezem, G. Muyzer, and M. C. M. van Loosdrecht, "Enrichment of a mixed bacterial culture with a high polyhydroxyalkanoate storage capacity," *Biomacromolecules*, vol. 10, no. 4, pp. 670–676, 2009.

[6] P. Kumar, M. Singh, S. Mehariya, S. K. S. Patel, J.-K. Lee, and V. C. Kalia, "Ecobiotechnological approach for exploiting the abilities of *Bacillus* to produce co-polymer of polyhydroxyalkanoate," *Indian Journal of Microbiology*, vol. 54, no. 2, pp. 151–157, 2014.

[7] H. Moralejo-Gárate, R. Kleerebezem, A. Mosquera-Corral, and M. C. M. Van Loosdrecht, "Impact of oxygen limitation on glycerol-based biopolymer production by bacterial enrichments," *Water Research*, vol. 47, no. 3, pp. 1209–1217, 2013.

[8] A.-P. Zeng and H. Biebl, "Bulk chemicals from biotechnology: the case of 1,3-propanediol production and the new trends," *Advances in Biochemical Engineering/Biotechnology*, vol. 74, pp. 239–259, 2002.

[9] J. Hao, R. Lin, Z. Zheng, H. Liu, and D. Liu, "Isolation and characterization of microorganisms able to produce 1,3-propanediol under aerobic conditions," *World Journal of Microbiology and Biotechnology*, vol. 24, no. 9, pp. 1731–1740, 2008.

[10] G. P. da Silva, M. Mack, and J. Contiero, "Glycerol: a promising and abundant carbon source for industrial microbiology," *Biotechnology Advances*, vol. 27, no. 1, pp. 30–39, 2009.

[11] E. K. C. Yu and J. N. Saddler, "Biomass conversion to butanediol by simultaneous saccharification and fermentation," *Trends in Biotechnology*, vol. 3, no. 4, pp. 100–104, 1985.

[12] P. Kumar, R. Sharma, S. Ray et al., "Dark fermentative bioconversion of glycerol to hydrogen by *Bacillus thuringiensis*," *Bioresource Technology*, vol. 182, pp. 383–388, 2015.

[13] P. Kumar, S. Mehariya, S. Ray, A. Mishra, and V. C. Kalia, "Biodiesel industry waste: a potential source of bioenergy and biopolymers," *Indian Journal of Microbiology*, vol. 55, pp. 1–7, 2014.

[14] A. Zhou, J. Du, C. Varrone, Y. Wang, A. Wang, and W. Liu, "VFAs bioproduction from waste activated sludge by coupling pretreatments with *Agaricus bisporus* substrates conditioning," *Process Biochemistry*, vol. 49, no. 2, pp. 283–289, 2014.

[15] L. Marang, Y. Jiang, M. C. M. van Loosdrecht, and R. Kleerebezem, "Butyrate as preferred substrate for polyhydroxybutyrate production," *Bioresource Technology*, vol. 142, pp. 232–239, 2013.

[16] S. J. Sarma, S. K. Brar, Y. Le Bihan, G. Buelna, and C. R. Soccol, "Hydrogen production from meat processing and restaurant waste derived crude glycerol by anaerobic fermentation and utilization of the spent broth," *Journal of Chemical Technology and Biotechnology*, vol. 88, no. 12, pp. 2264–2271, 2013.

[17] Z. Chi, D. Pyle, Z. Wen, C. Frear, and S. Chen, "A laboratory study of producing docosahexaenoic acid from biodiesel-waste glycerol by microalgal fermentation," *Process Biochemistry*, vol. 42, no. 11, pp. 1537–1545, 2007.

[18] S. K. Athalye, R. A. Garcia, and Z. Wen, "Use of biodiesel-derived crude glycerol for producing eicosapentaenoic acid (EPA) by the fungus *Pythium irregulare*," *Journal of Agricultural and Food Chemistry*, vol. 57, no. 7, pp. 2739–2744, 2009.

[19] W. J. Choi, "Glycerol-based biorefinery for fuels and chemicals," *Recent Patents on Biotechnology*, vol. 2, no. 3, pp. 173–180, 2008.

[20] J. Bader, E. Mast-Gerlach, M. K. Popović, R. Bajpai, and U. Stahl, "Relevance of microbial coculture fermentations in biotechnology," *Journal of Applied Microbiology*, vol. 109, no. 2, pp. 371–387, 2010.

[21] M. T. Agler, B. A. Wrenn, S. H. Zinder, and L. T. Angenent, "Waste to bioproduct conversion with undefined mixed cultures: the carboxylate platform," *Trends in Biotechnology*, vol. 29, no. 2, pp. 70–78, 2011.

[22] P. A. Selembo, J. M. Perez, W. A. Lloyd, and B. E. Logan, "Enhanced hydrogen and 1,3-propanediol production from glycerol by fermentation using mixed cultures," *Biotechnology and Bioengineering*, vol. 104, no. 6, pp. 1098–1106, 2009.

[23] A. Gadhe, S. S. Sonawane, and M. N. Varma, "Kinetic analysis of biohydrogen production from complex dairy wastewater under optimized condition," *International Journal of Hydrogen Energy*, vol. 39, no. 3, pp. 1306–1314, 2014.

[24] I. Z. Boboescu, M. Ilie, V. D. Gherman et al., "Revealing the factors influencing a fermentative biohydrogen production process using industrial wastewater as fermentation substrate," *Biotechnology for Biofuels*, vol. 7, no. 1, article 139, 2014.

[25] B. S. Saharan, A. Grewal, and P. Kumar, "Biotechnological production of polyhydroxyalkanoates: a review on trends and latest developments," *Chinese Journal of Biology*, vol. 2014, Article ID 802984, 18 pages, 2014.

[26] J. Wang, W.-W. Li, Z.-B. Yue, and H.-Q. Yu, "Cultivation of aerobic granules for polyhydroxybutyrate production from wastewater," *Bioresource Technology*, vol. 159, pp. 442–445, 2014.

[27] A. Marone, G. Izzo, L. Mentuccia et al., "Vegetable waste as substrate and source of suitable microflora for bio-hydrogen production," *Renewable Energy*, vol. 68, pp. 6–13, 2014.

[28] P. Anand and R. K. Saxena, "A comparative study of solvent-assisted pretreatment of biodiesel derived crude glycerol on growth and 1,3-propanediol production from *Citrobacter freundii*," *New Biotechnology*, vol. 29, no. 2, pp. 199–205, 2012.

[29] F. Barbirato, C. Camarasa-Claret, J. P. Grivet, and A. Bories, "Glycerol fermentation by a new 1,3-propanediol-producing microorganism: *Enterobacter agglomerans*," *Applied Microbiology and Biotechnology*, vol. 43, no. 5, pp. 786–793, 1995.

[30] I. Angelidaki, S. P. Petersen, and B. K. Ahring, "Effects of lipids on thermophilic anaerobic digestion and reduction of lipid inhibition upon addition of bentonite," *Applied Microbiology and Biotechnology*, vol. 33, no. 4, pp. 469–472, 1990.

[31] E. A. A. Wolin, M. J. J. Wolin, and R. S. S. Wolfe, "Formation of methane by bacterial extracts," *The Journal of Biological Chemistry*, vol. 238, pp. 2332–2286, 1963.

[32] V. C. Kalia, S. R. Jain, A. Kumar, and A. P. Joshi, "Fermentation of biowaste to H_2 by *Bacillus licheniformis*," *World Journal of Microbiology and Biotechnology*, vol. 10, no. 2, pp. 224–227, 1994.

[33] B. E. Logan, S.-E. Oh, I. S. Kim, and S. Van Ginkel, "Biological hydrogen production measured in batch anaerobic respirometers," *Environmental Science and Technology*, vol. 36, no. 11, pp. 2530–2535, 2002.

[34] J. E. Jackson, *A User's Guide to Principal Components*, Wiley, 2003.

[35] B. T. Maru, M. Constanti, A. M. Stchigel, F. Medina, and J. E. Sueiras, "Biohydrogen production by dark fermentation of glycerol using *Enterobacter* and *Citrobacter* Sp," *Biotechnology Progress*, vol. 29, no. 1, pp. 31–38, 2013.

[36] A. Marone, G. Massini, C. Patriarca, A. Signorini, C. Varrone, and G. Izzo, "Hydrogen production from vegetable waste by bioaugmentation of indigenous fermentative communities," *International Journal of Hydrogen Energy*, vol. 37, no. 7, pp. 5612–5622, 2012.

[37] Y. Zhu and S.-T. Yang, "Effect of pH on metabolic pathway shift in fermentation of xylose by *Clostridium tyrobutyricum*," *Journal of Biotechnology*, vol. 110, no. 2, pp. 143–157, 2004.

[38] T. Větrovský and P. Baldrian, "The variability of the 16S rRNA gene in bacterial genomes and its consequences for bacterial community analyses," *PLoS ONE*, vol. 8, no. 2, Article ID e57923, 2013.

[39] C. Varrone, *Bioconversion of crude glycerol into hydrogen and ethanol by microbial mixed culture [Ph.D. dissertation]*, Harbin Institute of Technology, Harbin, China, 2015.

[40] F. Nagai, Y. Watanabe, and M. Morotomi, "*Slackia piriformis* sp. nov. and *Collinsella tanakaei* sp. nov., new members of the family *Coriobacteriaceae*, isolated from human faeces," *International Journal of Systematic and Evolutionary Microbiology*, vol. 60, no. 11, pp. 2639–2646, 2010.

[41] T. Aüllo, A. Ranchou-Peyruse, B. Ollivier, and M. Magot, "*Desulfotomaculum* spp. and related gram-positive sulfate-reducing bacteria in deep subsurface environments," *Frontiers in Microbiology*, vol. 4, article 362, 2013.

Hindawi Publishing Corporation
BioMed Research International
Volume 2015, Article ID 480386, 10 pages
http://dx.doi.org/10.1155/2015/480386

Review Article

Perspective for Aquaponic Systems: "*Omic*" Technologies for Microbial Community Analysis

Perla Munguia-Fragozo, Oscar Alatorre-Jacome, Enrique Rico-Garcia, Irineo Torres-Pacheco, Andres Cruz-Hernandez, Rosalia V. Ocampo-Velazquez, Juan F. Garcia-Trejo, and Ramon G. Guevara-Gonzalez

C. A. Ingeniería de Biosistemas, División de Investigación y Posgrado de la Facultad de Ingeniería, Universidad Autónoma de Querétaro, Centro Universitario, Cerro de las Campanas s/n, Colonia Las Campanas, 76010 Santiago de Querétaro, QRO, Mexico

Correspondence should be addressed to Ramon G. Guevara-Gonzalez; ramon.guevara@uaq.mx

Received 21 February 2015; Accepted 17 June 2015

Academic Editor: Abd El-Latif Hesham

Aquaponics is the combined production of aquaculture and hydroponics, connected by a water recirculation system. In this productive system, the microbial community is responsible for carrying out the nutrient dynamics between the components. The nutrimental transformations mainly consist in the transformation of chemical species from toxic compounds into available nutrients. In this particular field, the microbial research, the "*Omic*" technologies will allow a broader scope of studies about a current microbial profile inside aquaponics community, even in those species that currently are unculturable. This approach can also be useful to understand complex interactions of living components in the system. Until now, the analog studies were made to set up the microbial characterization on recirculation aquaculture systems (RAS). However, microbial community composition of aquaponics is still unknown. "*Omic*" technologies like metagenomic can help to reveal taxonomic diversity. The perspectives are also to begin the first attempts to sketch the functional diversity inside aquaponic systems and its ecological relationships. The knowledge of the emergent properties inside the microbial community, as well as the understanding of the biosynthesis pathways, can derive in future biotechnological applications. Thus, the aim of this review is to show potential applications of current "*Omic*" tools to characterize the microbial community in aquaponic systems.

1. Introduction

The continuous rise in global human population makes the expansion and intensification of our current food production systems necessary. In addition, in order to mitigate negative environmental impacts, it is also desirable to design new productive models with the capability to save energy cost, to reduce greenhouse gas emissions, to minimize waste disposals, and, even more, to recycle nutrients inside the system. From this approach, traditional food production systems have been under public eyes being questioned about its sustainability [1, 2]. One example is the case of aquaculture industry. Like other human activities, its problems concern the scientific community in many ways, but principally for its large waste discharges into environment and its accelerative growing rate [3]. However, as a result of the continuous innovations in the field, it has been possible to develop economically feasible systems capable to cultivate species at high densities, even with unfavorable climatic regime and limited water availability [3, 4]. These kinds of proposals are nowadays considered as culture models for sustainable food production systems [5].

Recirculation aquaculture systems (RAS) have been developed due to environmental restrictions in many countries with land and water limitations. RAS allows a reduction of water consumption due to waste management and nutrient recycling [3]. Historically, the concept of practical and efficient food production systems is not new. Cultures of China, Perú, and México had integrative systems which produce aquatic species and vegetables near to region of consumption [6]. In the XX century, the first attempts to create practical, efficient, and integrative fish production systems alongside

vegetables were made in the 70s with the work of Lewis and Naegel [7–9]. These systems are known with the term "aquaponics."

Aquaponics are a type of RAS in which water filtration technologies allow reuse of water for fish aquatic species production with integration of hydroponics [10]. The final byproduct of fish protein metabolism is ammonia (NH_3) [11]. Ammonia accumulates in aquaculture ponds and it can be dangerous to fish at specific temperature and pH levels (above 30°, pH > 8.5) [12]. Wastes of ammoniacal nitrogen are transformed into less harmful compounds like nitrate by biological filtration [13, 14]. Accumulation of nitrate in water is less toxic for fish, but in RAS it is common to add make-up water in order to dissolve this compound (10% of total volume per day are make-up water) [15]. In contrast, aquaponics do not require water replacement; addition of make-up water is for losses because evaporation or replacement volume is less than 2% per day [16, 17].

The water is the common media that contain enough nitrogen compounds like ammonia, nitrate, nitrite, and other dissolved nutrients like phosphorus, potassium, and some other elements [18, 19]. These nutrients are enough for vegetable consumption [20]. Then, dissolved nutrients in the media are absorbed by root plants, optimizing the use of nutrients and water, and reduce wastes for fish and environmental impact [19]. On this way, the system allows minimizing resources as land, water, and energy [15].

One challenge of these systems is maintenance of water quality for both aquatic species and plants. For maintaince of water quality RAS have been utilized for solid removal and biological filtration. For this purpose, there are two or more components before the water returns to aquaculture pond [21]. In aquaponics, both solids removal and biological filtration are in the same component. Accumulation of uneaten food, fecal matter, and organic and nitrogen compounds in biofilter provide the adequate environment for microbial development [22]. However, the need of different physicochemical conditions in water for living components makes the management of the system very complex. The recommended pH for aquaculture systems is 6.5–8.5, for hydroponics is 5.5–6.5, and for nitrification process is 8.5. The pH is a parameter that can limit the development for plants, fish, or bacteria [14, 23]. Populations of microorganisms or microbial community in biofilter of aquaponics have an essential role in aquaponic systems development [21]. Biofiltration takes advantage of bacterial metabolic process. This process, the nitrification, is carried out in two steps, ammonia oxidizing and nitrate oxidizing. Each reaction involved different species of bacteria: *Nitrosomonas* and *Nitrobacter* [10, 24].

Probably best studied group of environmental importance in this type of ecosystems are nitrifying prokaryotes including both the ammonium oxidizing and the nitrite oxidizing prokaryotes [25]. However, microbial community in aquaponic system is not characterized. Due to biological interactions in biofilter of aquaponic system, microbial communities are very interesting to analyze.

The most important revolution in microbial ecology was the use of molecular techniques and DNA sequencing in phylogenetic studies and their applications to uncultured organisms [26]. These strategies can help to understand the interaction of microbial populations with each other and their environment as a consequence of nutrient input (from fish wastes) [16]. Moreover, using these tools, the vast prokaryotic diversity must be more revealed than with traditional techniques. Metagenomic techniques combined with next generations sequencing (NGS) and bioinformatic tools have boosted microbial ecology. The use of metagenomics approaches has allowed the discovery of large array of genes [26]. This modern approach allows knowledge of the diversity of metabolic functionality in order to understand in more detail the response of community at internal and external perturbations in relation to environmental dynamics and emergent properties [27]. With these studies it is possible to evaluate the potential of aquaponic microbial community for future biotechnological uses. The aim of this review is to show potential applications of current "*Omic*" and bioinformatic tools to characterize the microbial community of aquaponic systems.

2. Microbial Community in RAS

In RAS environment, aquaponic system is very important microbial community in the same order of magnitude as fish because they are directly involved into fish activities and their effect on water quality. The system provides different microniches for the microbial populations according to a differential gradient of oxygen and nutrients. Every microniche supports development of specific microbial populations [28]. Additionally freshwater, brackish, or marine RAS presented differences on microbial diversity [24, 29]. Biofilter component presents the most abundant content of microbes [22].

Microbial populations contribute to the processing of particulate and dissolved wastes of aquatic species (ammonia excreted by fish, and carbon and nitrogen accumulated from uneaten food and fecal matter). One of the most important conversions is carried out by nitrifying bacteria; they are involved in nitrification, ammonification, nitrate reduction, and denitrification processes [16, 22, 30]. Other microbial metabolisms are involved in proteolysis and sulfate reduction [30]. The populations are distributed according to respiratory metabolism determined in strict aerobic or microaerophilic and facultative anaerobes/aerobes, according to type of growth in fixed film bacteria or suspended bacterial, and according to the component of the system [22]. In general, the most common approach for nitrogen removal from water is based on the processes of aerobic autotrophic nitrification and anaerobic heterotrophic nitrification [31].

Autotrophic and heterotrophic microorganisms are present in RAS. Autotrophic organisms use CO_2 as carbon source and inorganic nitrogen, sulphur, or iron compounds as energy source. Plants, algae, and some bacteria in aquaponic systems present this metabolism. Heterotrophic organisms use carbohydrates, amino acids, peptides, and lipids as carbon and energy source. In the system, organic matter from uneaten feeds, excreta of aquatic species, and detritus are mineralized by this type of microorganisms [22, 32].

Autotrophic nitrification removes ammonia at sufficient rate to maintain water quality at a level to prevent ammonia toxicity to the fish [33]. However, autotrophs are vulnerable to high loads of ammonium and organic matter. To overcome this latter situation, ammonia removal is in a very low level of removal, then making more components on the system for optimal ammonium removal necessary and then creating the need of additional steps in nitrogen oxidizing [34].

On the other hand, heterotrophic bacteria constitute an important factor in terms of O_2 consumption and compete with autotrophic bacteria, diseases in fish and later in human. Some populations of these bacteria are suspected of having a positive effect against pathogenic bacteria [33]. Heterotrophic microorganisms exhibit higher growth rates than autotrophs and can use organic substrates as source of carbon and energy to convert ammonium into nitrogenous gas under aerobic conditions (heterotrophic nitrification) [31, 34]. The main source of heterotrophic bacteria is within the biofilter. Bacteria of heterotrophic nitrification are probably ideal prokaryotes for coupled nitrification-denitrification in wastewater treatment and, probably, the most abundant microorganisms in aquaponic systems [25]. The dissolved organic carbon (C) accumulated is the main source of C for heterotrophic bacteria. High concentration of organic carbon affects negatively nitrate production; it means concentration of nitrite was always very low [28, 35]. Some strains of heterotrophic nitrifiers had the capability to use nitrite (NO_2) and nitrate (NO_3) as the source for nitrogen for growth and as an energy source for denitrification [36].

Ammonia Oxidizer Bacteria (AOB), like *Nitrosococcus*, *Nitrosospira*, and *Nitrosomonas* oxidized ammonia to nitrite. The general microdistribution of nitrifiers is that AOB live in dense clusters and their occurrence is reasonably well-correlated with oxygen content. These bacteria depend on availability of ammonia as their sole source of energy. On the other hand, Nitrite Oxidizer Bacteria (NOB) oxidized nitrite to nitrate by some *Nitrospira* sp. and *Nitrobacter*. These bacteria integrate more open aggregations but may also be found distributed in the biofilm systems. Another general observation is that *Nitrospira* spp., the dominant NOB in most systems, can still be detected below the oxic-anoxic interface, although in lower numbers and using small amounts of nitrite, and, in comparison with *Nitrobacter*, use oxygen more efficiently [22, 25]. The aforementioned theoretical distribution of autotrophic and heterotrophic bacteria in aquaponic systems is showed in Figure 1. The heterotrophic bacteria will be distributed near to outlet of flux water pumped from fish pond due to higher concentration of nutrients and inside the pond culture near to sediment. Autotrophic bacteria like strains of AOB-*Nitrosomonas* sp. will be in clusters in the middle of biofilter (here nutrient concentrations like ammonium and organic matter are lower) but in a portion of high O_2 concentration; meanwhile NOB-*Nitrobacter* sp. and -*Nitrospira* will be in open aggregations in a portion of the oxic-anoxic interface in the middle of biofilter.

During oxidation of NH_4^+, pH increased from 7.1 to 8.45 under high ammonium loads. Ammonia Oxidizers Bacteria (AOB) and Nitrite Oxidizers Bacteria (NOB) are inhibited by free ammonia in range from 10 to 150 mg/L and from 0.1 to 1.0 mg/L, respectively. Free ammonia is NH_3, the toxic form of ammoniacal N. High free ammonia (NH_3) might inhibit the heterotrophic nitrification activity but not the growth. Heterotrophic nitrification and cellular growth differ according to pH conditions. Highest removal of ammonium (54.7%) and oxygen demand was presented at 7.5 pH (±0.5). At lower pH values or at more alkalinity, the growth of heterotrophic bacteria of group *Acinetobacter* increased. Efficient removal of ammonium at the slightly alkaline environment may be caused by more free ammonia contained in medium, which is preferentially by ammonia monooxygenase (*amoA*) [34].

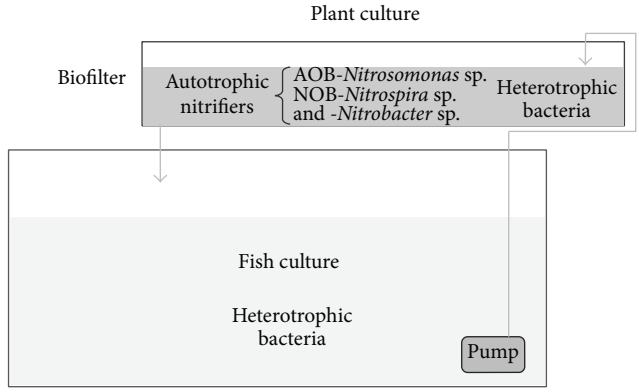

Figure 1: General distribution of microbial populations in aquaponic systems.

High ratio of C/N helps to maintain safety values of toxic ammonium inside the system, mainly by its utilization on prokaryotic cell synthesis processes. There is evidence that intracellular nitrogen concentration removed from NH_4^+-N has close values from 52% to 56%. It means that bacterial growth was preferentially proceeding at high C/N ratios [28, 34].

2.1. Microbial Diversity Characterization. In 2000 decade, some species have been characterized in diverse components of RAS and mainly on biofilters [30, 37–39]. Considering studies of microbial populations that can be cultured, most of fixed bacteria were found in biofilter. Average CFU in biological filter was $7.3 \times 10^6 \pm 7.25 \times 10^6\ g^{-1}$ of media. Bacterial density in the inlet of biofilter was in lower level than in the outlet. Concentration of bacteria on the biofilter media was $5.1 \pm 3.43 \times 10^6$ to $1.1 \times 10^8 \pm 3.41 \times 10^7$. Thus, bacterial concentration does not depend of fish stocking density [28].

Several studies have been done in order to characterize microbial communities in RAS with freshwater. These studies revealed that the main bacterial groups presented in freshwater RAS biofilter were Actinobacteria, α-proteobacteria, β-proteobacteria, γ-proteobacteria, Bacilli, Bacteroidetes, Nitrospirae, Planctomycetes, and Sphingobacteria and the genus *Nitrosomonas* (Table 1). From these bacterial groups only *Hyphomicrobium facilis*, *Rhizobium* sp., *Flavobacterium* sp., *Sphingobacterium* sp., *Comamonas* sp., *Rhodobacter* sp., *Acinetobacter* sp., *Aeromonas* sp., *Pseudomonas* sp., *Flexibacter* sp., *Pirellula staleyi*, *Nitrospira moscoviensis*, and *Nitrosomonas oligotropha* are common genera in systems with high richness and diversity.

Table 1: Microorganisms identified in RAS biofilter component related with freshwater.

Group	Microorganism	Process	References
Actinobacteria	*Microbacterium imperiale*		[30]
	Mycobacterium chitae		[30]
	Corynebacterium tuberculostearicum	Pathogen in humans	[39]
	Propionibacterium acnes		[39]
Acidobacteria	*Acidobacteria bacterium*		[39]
Bacteroidetes	*Chryseobacterium* sp.	Some strains pathogen in humans	[37]
	Flavobacteriales bacterium	Sulfate reduction	[37]
	Flavobacterium columnare	Pathogen in fish	[39]
	Flavobacterium sp.	Heterotrophic denitrification	[38, 39]
	Bacteroides plebeius	Sulfate reduction	[39]
	Myroides sp.	Pathogen in humans	[37]
	Sphingobacterium sp.	Pathogen in fish	[30, 37, 39]
	Flectobacillus	Heterotrophic bacteria	[39]
α-Proteobacteria	*Agrobacterium tumefaciens*	Pathogen in superior plants/nitrogen fixation	[30]
	Filomicrobium fusiforme		[30]
	Hyphomicrobium facilis		[30, 39]
	Hyphomicrobium denitrificans sp.	Heterotrophic denitrification	[30]
	Nitrobacter winogradskyi	Nitrite oxidation	[30, 40]
	Nordella oligomobilis		[30]
	Ochrobactrum anthropi		[30]
	Rhizobium sp.	Nitrogen fixation	[30, 37, 39]
	Rhodopseudomonas acidophila		[30]
	Rhodovulum euryhalinum	Denitrification	[30]
	Bradyrhizobium japonicum		[39]
	Woodsholea maritima		[39]
	Rhodobacter sp.	Autotrophic denitrification/nitrogen fixation	[22, 30]
β-Proteobacteria	*Aquaspirillum* sp.	Pathogen in fish	[37]
	Comamonas	Heterotrophic denitrification/pathogen in fish	[22, 37, 39]
	Azovibrio restrictus		[30]
	Thiobacillus thioparus	Ammonia oxidation	[30]
	Herbaspirillum sp.		[39]
	Ideonella dechloratans	Heterotrophic bacteria	[39]
	Rhodoferax fermentans	Autotrophic denitrification	[30]
	Nitrosomonas aestuarii	Anammox	[38]
	Nitrosomonas marina	Anammox	[16]
	Nitrosomonas oligotropha	Anammox	[38]
γ-Proteobacteria	*Gemmatimonas aurantiaca*		[39]
	Acinetobacter sp.	Heterotrophic bacteria	[37, 39]
	Aeromonas sp.	Heterotrophic denitrification/pathogen in fish and humans	[37, 39]
	Pseudomonas sp.	Heterotrophic denitrification/pathogen in fish and humans	[16, 22, 37, 39]
	Marinobacter sp.		[39]
	Vibrio sp.		[39]
	Edwardsiella sp.	Pathogen in fish	[37]
ϵ-Proteobacteria	*Arcobacter nitrofigilis*	Nitrogen fixation	[39]
Firmicutes	*Bacillus* sp.	Pathogen in fish	[37]
	Lactobacillus paraplantarum		[30]
	Lactococcus lactis		[39]
	Macrococcus brunensis		[30]
	Macrococcus lamae		[30]
	Sarcina sp.	Dissimilatory nitrate reduction to ammonium (DNRA)	[37]

Table 1: Continued.

Group	Microorganism	Process	References
Sphingobacteria	*Flexibacter* sp.		[30, 39]
	Runella slithyformis		[39]
Verrucomicrobia	*Verrucomicrobia spinosum*		[39]
Planctomycetes	*Pirellula staleyi*	Anammox	[30, 41]
	Planctomycetales sp.	Anammox	[38]
	Planctomyces maris	Anammox	[38]
	Planctomicetes sp.	Nitrite oxidation	[38]
Nitrospirae	*Nitrospira moscoviensis*	Nitrite oxidation	[30, 38, 39]

All microorganisms of this table were analysed with 16S rRNA clone library method, denaturing gradient gel electrophoresis (DGGE), and few cases with biochemical procedures.

PCR-based molecular techniques have mainly been used to describe microbial diversity using denaturing gradient gel electrophoresis (DGGE), microscopy using FISH (fluorescence *in situ* hybridization), and/or cloning 16S rRNA gene fragments [25, 30, 39, 42]. The last molecular technique is the most common for study of microbial communities in RAS with freshwater. For AOB, comparison between phylogenies based on 16S rRNA genes was done with *amoA* (gene of active subunit of monooxygenase), *nirK* (nitrite reductase gen), and *norB* (nitric oxide reductase) [25, 43].

The analysis using 16S rRNA genes as a phylogenetic marker was a revolutionary strategy for microbial ecology with cultured-independent method being developed since 90s, after the work of Lane and collaborators [44]. The 16S rRNA gene in bacteria contains highly conserved and variable interspersed regions that allow a reliable and detailed microbial classification. For this molecular technique the correct selection of primers is critical. Some pairs of primers can overestimate or underestimate species richness; it implied uncertain biological conclusions. This happened when primers selected do not anneal equally to DNA target in all members of community and the amplification was carried out on certain taxonomic group [45]. Some particular regions are recommended to obtain representational characterization in complex microbial community [45, 46].

Differences in microbial communities represent their unique and complex environments [16]. Microbial communities in aquatic system or in RAS are as complex as changes in environmental variables according to period of time [30, 39, 47]. Besides, every aquatic species in a RAS introduces its own unique microbial flora [30]. Aquaponic RAS system introduces additional living component compared to other RAS analyzed. Plants can introduce their own microbial flora to the system, thus making the study of the changes on microbial diversity very interesting. Ammonia Oxidizing Bacteria (AOB) *Nitrosomonas communis* introduced in rhizoplane of aquaponic plants has been isolated and identified [48]. Other processes of reduction/uptake of nitrogen compounds are carried out by eukaryotic microorganisms like diatoms, algae, and fungi [49]. Less well-studied is the heterotrophic nitrification carried out by fungi. These organisms have been associated with assimilatory nitrate reduction in RAS, removed ammonium, and nitrite and protein [49, 50]. These eukaryotic microorganisms have an important pathogen relationship with higher plants in humidity environments. Nowadays, there are no works reported about an analysis of bacterial or eukaryotic community in aquaponic systems. The microbial characterization on this field has been done in order to determine the presence of bacterial pathogens for human and for aquatic species [5, 51, 52].

3. Pathogens in Aquaponic Systems

Aquaponic systems have been used as sustainable agricultural systems [5, 51]. With the same volume of water for fish production can be produced edible vegetables. These systems are discussed as regards their utilization in improving sustainability through management and integration of the living components [10]. Many species of bacteria and coliforms are inherently present in aquaponic recirculating biofilter carrying out transformations of organic matter and wastes of fishes. This implies the presence of many microorganisms that can be pathogens for plants, fishes, and, mostly, human.

One of the most important considerations for this food production system is food safety. In agricultural systems, the evaluation of food safety is emerging as a critical procedure in harvesting and management operations. For this purpose, some microorganisms have been considered as safety-indicators for products and water quality in the system [5]. Some of these safety-indicators are *Escherichia coli* and *Salmonella* spp. These microorganisms are typically found in the intestines of warm-blooded animals like birds, mice, cattle, and others. They are common indicators of fecal contamination and microbial water quality. These bacteria are zoonotic enteric bacteria transient in fish gut microflora from contaminated water in open systems because of animals like birds [29]. Research on aquaponic fields has been carried out recently in order to ascertain microbial safety of its by-products [5, 51]. The microbial profile of lettuce produced under soil-free (aquaponics) *versus* in-soil has been evaluated. Comparative analysis showed significant differences between aquaponic and conventional lettuce in aerobic plate counts (APC), coliform, *E. coli*, and yeast count. Aquaponics had significantly lower concentration of coliform (no detectable *E. coli* were observed), spoilage and fecal microorganisms (lettuce from market contained 2–3.5 log CFU *E. coli*/g), and yeast counts (2-3 log CFU yeast/g for aquaponic and 5.5–5 log CFU yeast/g for conventional

and organic lettuce). The later work suggests postharvest contamination due to packaging process and transport that conventional and organic lettuce suffered from in contrast to aquaponic one, in which the postharvest process was minimum [51].

Other works evaluated microbial water quality related to food safety in aquaponic system. This report analyzed plant and fish tissue, water, and supplement aquaponic input samples (that can be a contamination vector) from 11 different farms in Hawaii for approximately one year. Methodology used for food safety determination was the traditional microbial isolation of *E. coli* O157:H7 and *Salmonella*. The results showed very low levels of *E. coli* during initial sampling period according to EPA standards for recreational use of water. Plant and fish tissue analyzed and supplement inputs were shown to have very low levels of generic *E. coli* or undetectable *E. coli* O157:H7 and *Salmonella* [5]. Aforementioned works analyzed microbial profile of only two bacteria related with pathogenicity in humans. However microbial determination was carried out with conventional methods for microbial detection. This can be likely conducted to analyze a short range of microbial pathogens, because fish and plants pathogens were not considered in the study. For a deep microbial profile the use of modern metagenomic approaches is necessary.

On the other hand, some pathogens in biofilter component in RAS have been identified by 16S RNA clone library and DGGE (Table 1). Some strains of *Bacillus* sp. (like *B. mycoides*), *Aeromonas* sp., *Acinetobacter* sp., *Pseudomonas* sp., *Edwardsiella* sp., *Comamonas* sp., and *Flavobacterium* sp. are related with pathogenicity in fish [37]. Other pathogens found in biofilters are related to fish and human pathogenicity like *Vibrio*, *Erwinia*, *Coxiella*, and *Aeromonas* [16]. Species of *Vibrio* have been isolated from freshwater, estuarine, and seawater environments, although most of them are probably saprophytic [28].

Biosafety of aquaponic RAS will depend on correct management and control of opportunist microbial proliferation in the system [22]. Metagenomic and metatranscriptomic profile can be a powerful tool for determining the diversity of pathogens and functional activity that can help to understand their relationship with other microbes and possibly its regulation in the system. Metagenomics approaches allow the meta-analysis of diversity in microorganisms of the aquaponic environment [53–56].

4. "*Omic*" Tools for Future Analysis of the System

The development of sequencing and high-throughput methods for cloning microbial genes directly from environment has opened the possibilities for ecological microbiology, mostly considering that microbes possess the highest potential of producing bioactive metabolites, enzymes, and polymers and other tools with biotechnological application. The study of larger fragments of environmental DNA of whole community is known as environmental genomics, ecogenomics, or metagenomics [57]. The genetic, enzymatic, and metabolic pool is the result of a vast interaction cell-to-cell and/or synergistic or antagonistic relationships that could make the community perform as metaorganism with emergent properties [27].

4.1. Metagenomics for Microbial Diversity Description. PCR amplification of genes has allowed the study of microbial diversity. Throughout all the research done in this field the conclusion is that majority of prokaryotic diversity still remains unknown, mainly because these cells cannot be grown under laboratory conditions [58, 59]. Several works PCR-based molecular techniques for study of microbial diversity since about three decades ago have been carried out [60]. These tools has allowed to have a look of general scene of microbial diversity in environmental samples. However, techniques derived from PCR, like 16S rRNA, hybridization, and DGGE/TGGE, among others, have their limitations and only can give some information about communities [61]. The amplification of 16S rRNA gene technique is based on amplification of hypervariable regions of the gene anchoring to conserved sequences. There are nine (9) hypervariable regions named V1–V9 that spanned between 50 and 100 bp in length depending on region. Hypervariable regions are the key for universal microbial identification. Primers have been designed to amplify 16S rRNA hypervariable regions from large number of different bacteria species [26]. Primers that targeted regions V1–V3 and V7–V9 are recommended for obtaining representational characterization in complex microbial community [46]. The information of this technique indicates the taxonomic composition of the environmental sample [62]. There are several semiquantitative assays like FISH, MAR-FISH, and CARD-FISH *in situ* that identify prokaryotic cells without cultivation by applying fluorescence *in situ* hybridization (FISH) with ribosomal RNA (rRNA) targeted oligonucleotide probes. These oligonucleotides have an extention from 15 to 25 nucleotides in length and are labelled covalently at the 50' end with a fluorescent dye. After stringent washing, specifically stained cells are detected via epifluorescence microscopy or flow cytometry [63]. Quantitative analyses of the composition and dynamics of microbial communities are an integral component of microbial ecology. These techniques in combination with 16S rRNA have allowed real progress in some cases, especially in very simple ecosystems such as endosymbionts or extreme environments. The contribution of these techniques to a better understanding of functionality of ecosystems like microbial communities in ocean environment is discussed [56, 64]. On the other hand, NGS technologies have more throughput because they have 100 times more capacity of sequencing than Sanger method. These technologies sequenced DNA molecules massively in parallel in a flow cell. The sequencing is carried out in two forms, in a continuous real time or in a stepwise iterative process. In both types of processes each clonal template or single DNA molecule is sequenced and can be quantified among the total sequences generated [26]. Moreover, these modern technologies focus on sequencing of large fragments of DNA as entire genomes or plasmids instead of gene(s) or operons. For this process is necessary to fragment the total DNA in pieces up to 700 bp, in the case

of shotgun the fragments are of 3 kb, 8 kb, and 40 kb [26, 65]. After this step further bioinformatical analysis is necessary in which these fragments are assembled in linear sequences that conform part of genome or total genome [65, 66]. The assembling overlaps the different fragments and thus rebuilds complete linear sequences of the genome, known as contigs. The build of entire genome is a little difficult but possible if the sequenced fragments cover the entire genome. The challenge of this strategy lies on computational effort that requires furthermore huge analysis and computational capacity [65, 67]. Metagenomics analysis comprises environmental single-gene surveys and random shotgun studies of all environmental genes. The former analysis focuses on metagenomic study by single targets amplified with PCR and, then, the products are sequenced. On the other hand, shotgun metagenomics is targeted in total DNA isolated from an environmental sample and then sequenced, resulting in a profile of all genes within the community. The basic definition of metagenomics is the analysis of genomic DNA from a whole community; this separates it from genomics, which is the analysis of genomic DNA from an individual organism or cell [68, 69]. Metagenomic studies combined with NGS technologies promise to be a tool that helps the evolution of microbial ecology at very fast step. Nowadays, there is a discussion on this topic because metagenomics allow microbial analysis on a low or medium complex ecosystem but in highly complex environment it has not been successful due to effort in heterogeneity assembly [26, 70].

4.2. Metatranscriptomics, Proteomics, and Metabolomics for Microbial Functionality Description. Metatranscriptomics, proteomics, and metabolomics can provide information of functional analyses in microbial community at different levels, gene expression, protein translation, and more recently the metabolite network, respectively.

Metatranscriptomic data are a set of cDNA derived from community RNA. This information can help to infer what are microorganisms doing in a precise moment, how is their reaction to the environment, and what are they saying to the neighboring cell and the community [71].

For transcriptomic approach the gene(s) is required isolated in precise time of expression. It shows that transcriptome was very different every time. The functional "*Omic*" study has two main objectives: determine differences in functionality and metabolic pool from each member of a community that produce different effects on the system and identify the variations within functional compositions of different communities [71].

The integration of metagenomic and metatranscriptomic data revealed many unassignable transcripts that make evident the gap in knowledge for gene-protein that enables the ecophysiology of microorganisms in the ecosystem [72]. The mRNA concentration has been used to approximate the concentration and activities of their corresponding proteins; however with recent technologies it has been demonstrated that concentration of transcripts helps to predict partially the protein abundance. The latter assumption suggests that there are other mechanisms of regulations influencing the level of proteins in cells [73].

On the other hand, proteomics is the analysis of proteome, the full complement of proteins expressed by an organism. The number of proteins in the proteome organism exceeds by far the number of genes [74]. Every fragment of DNA is biochemically similar to one another. However, every type of protein is very different to the others. This protein diversity represents one of the greatest challenges of "*Omic*" technologies because to define its own identity, quantity, structure, and functionality of complete complements of proteins and, moreover, to characterize how these properties change through every cellular context are very complex [75].

In contrast, metabolites are the end products of cellular regulatory processes that can be chemically transformed during metabolism and provide a functional state of cellular biochemistry. The level of these chemical entities can be regarded as the ultimate response of biological systems to genetic (posttranslational modifications) or environmental changes (epigenetic regulation). Metabolites serve as direct signatures of biochemical activity and therefore they are easy to correlate with phenotype making it a powerful tool in order to explode in different fields of science. In parallel with the terms "transcriptome" and "proteome," the set of metabolites synthesized by a biological system constitute its "metabolome" [76]. This can be defined on all levels of complexity, such as organisms, tissue, cells, or cell compartments. For this reason in a biological experiment it is necessary to be specific about the environmental conditions as exactly as possible [77].

In metabolome analysis the most functional characterizations of genes involved in a metabolism are not based upon rigid biochemical testing. Many of putative function assignments of proteins do not describe biochemical function or biological role. It can be the result of gene duplication that is responsible for many enzyme isoforms and exhibits different characteristics. In contrast with transcriptome analysis (but in common with proteome analysis) methods are not available for amplification of metabolites and, therefore, sensitivity is a major issue. Metabolite products can be labile species and by their nature are chemically very diverse. For this reason, they are present in a wide dynamic range. On the other hand, in contrast with transcript or protein identification, metabolites are not organism specific and are not sequenced-dependent; thus when how to measure the metabolite once has been identified, the analytical protocol is equally applicable to prokaryotes, fungi, plants, and animals [78].

Biotechnology development is based on a very small diversity of species like *E. coli* and recent "*Omic*" tools offer high potential for discovery and exploitation of novel species, enzymes, and process that before were inaccessible [79, 80]. However, the data generated with these technologies have a small role on biotechnological research; most of novel developments occur on heterologous expression of enzymes. Other constrains with these approaches have been detected, that is, "under- or overestimation of the complexity of microbial diversity, limited data with the source of each sample, the identification of many genes, difficulties in integrating and comparing results obtained with different technologies, mismatched expectations between researchers who sought to generate understanding of ecological patterns with those who

were excited to test the limits of new technology, and the lack of agreed upon data standards" [65, 79].

The experimental design and the adoption of minimum standards to generate an adequate number of samples that allows the significant statistical analysis are highly desirable for future "*Omic*" studies. This step can be the key for determining their patterns of cooccurrence on gene(s) with taxa that are difficult to characterize and dominant factors structuring the community across time and space [79].

There are many factors to take into account in experimental design: replicates that can consume time and cost, but it must be sufficient for biosystem description, the definition of the most significant source of variations in a given biosystem being difficult, choosing of sequencing platform (each one has differences in length of sequences needed and advantages and disadvantages), and interpretation of sequence data and metadata collection [79, 81].

The "*Omic*" technologies challenges for characterized microbial diversity are the experiment itself, the statistical analysis of results, and the biological interpretation, which is the most complex and time-consuming part.

5. Conclusions

"*Omic*" approaches as metagenomics and metatranscriptomics must be crucial in future studies of microbial diversity in aquaponic biosystems. In addition, other "*Omic*" approaches as proteomics and metabolomics, together with respective bioinformatic analysis, should increase the knowledge of the ecological role and functionality of microbial components in these study models.

Conflict of Interests

The authors declare that there is no conflict of interests regarding the publication of this paper.

Acknowledgments

The authors thank Fondo Institucional de Fomento Regional para el Desarrollo Científico, Tecnológico y de Innovación (FORDECyT) (193512) for financial support for this work. The author Perla Munguia-Fragozo thanks Consejo Nacional de Ciencia y Tecnología (CONACyT) (379944) for financial support.

References

[1] S. J. Beddington, "The future of food and farming," *International Journal of Agricultural Management*, vol. 1, no. 2, pp. 2–6, 2011.

[2] P. T. Anastas and J. B. Zimmerman, "Design through the 12 principles of green engineering," *Environmental Science and Technology*, vol. 37, no. 5, pp. 94–101, 2003.

[3] C. I. M. Martins, E. H. Eding, M. C. J. Verdegem et al., "New developments in recirculating aquaculture systems in Europe: a perspective on environmental sustainability," *Aquacultural Engineering*, vol. 43, no. 3, pp. 83–93, 2010.

[4] J. Bostock, B. McAndrew, R. Richards et al., "Aquaculture: global status and trends," *Philosophical Transactions of the Royal Society B*, vol. 365, no. 1554, pp. 2897–2912, 2010.

[5] B. K. Fox, C. S. Tamaru, J. Hollyer et al., *A Preliminary Study of Microbial Water Quality Related to Food Safety in Recirculating Aquaponic Fish and Vegetable Production Systems*, College of Tropical Agriculture and Human Resources, University of Hawaii at Manoa. Food Safety and Technology, 2012.

[6] S. Jones, "Evolution of aquaponics," *International Journal of Agricultural Management*, vol. 6, pp. 14–17, 2002.

[7] W. M. Lewis and L. W. Wehr, "A fish-rearing system incorporating cages, water circulation, and sewage removal," *The Progressive Fish-Culturist*, vol. 38, no. 2, pp. 78–81, 1976.

[8] L. C. A. Naegel, "Combined production of fish and plants in recirculating water," *Aquaculture*, vol. 10, no. 1, pp. 17–24, 1977.

[9] W. M. Lewis, J. H. Yopp, H. L. Schramm Jr., and A. M. Brandenburg, "Use of hydroponics to maintain quality of recirculated water in a fish culture system," *Transactions of the American Fisheries Society*, vol. 107, no. 1, pp. 92–99, 1978.

[10] R. V. Tyson, D. D. Treadwel, and E. H. Simonne, "Opportunities and challenges to sustainability in aquaponic systems," *HortTechnology*, vol. 21, no. 1, pp. 6–13, 2011.

[11] R. M. Durborow, D. M. Crosby, and M. W. Brunson, "Ammonia in fish ponds," *Journal of the Fisheries Research Board of Canada*, vol. 32, pp. 2379–2383, 1997.

[12] O. Alatorre-Jácome, E. Rico-García, F. García-Trejo, and G. M. Soto-Zarazúa, *Aquaculture Water Quality for Small-Scale Producers*, InTech, 2011.

[13] R. M. Durborow, D. M. Crosby, and M. W. Brunson, *Nitrite in Fish Ponds*, Southern Regional Aquaculture Center, 1997.

[14] R. V. Tyson, E. H. Simonne, J. M. White, and E. M. Lamb, "Reconciling water quality parameters impacting nitrification in aquaponics: the pH levels," *Proceedings of the Florida State Horticultural Society*, vol. 117, pp. 79–83, 2004.

[15] M. B. Timmons, J. M. Ebeling, F. W. Wheaton, S. T. Summerfelt, and J. B. Vinci, *Recirculating Aquaculture Systems*, NRAC Publication, 2nd edition, 2002.

[16] H. J. Schreier, N. Mirzoyan, and K. Saito, "Microbial diversity of biological filters in recirculating aquaculture systems," *Current Opinion in Biotechnology*, vol. 21, no. 3, pp. 318–325, 2010.

[17] J. E. Rakocy, M. P. Masser, and T. M. Losordo, "Recirculating aquaculture tank production systems: aquaponics-integrating fish and plant culture," SRAC Publication No. 454, 2006.

[18] T. M. Losordo, M. P. Michael, and J. Rakocy, "Recirculating aquaculture tank production systems. an overview of critical considerations," Publication 451, Southern Regional Aquaculture Center, 1998.

[19] S. Diver, *Aquaponics—Integration of Hydroponics with Aquaculture*, National Sustainable Agriculture Information Service, pp. 1, 2006.

[20] S. E. Yeo, F. P. Binkowski, and J. E. Morris, *Aquaculture Effluents and Waste by-Products: Characteristics, Potential Recovery, and Beneficial Reuse*, NCRAC Publications Office, North Central Regional Aquaculture Center, Iowa State University, 2004.

[21] Y. Bai, J. Zhang, Y.-F. Li, Y.-N. Gao, and Y. Li, "Biomass and microbial activity in a biofilter during backwashing," *Journal of Zhejiang University: Science B*, vol. 6, no. 5, pp. 427–432, 2005.

[22] E. Rurangwa and M. C. Verdegem, "Microorganisms in recirculating aquaculture systems and their management," *Reviews in Aquaculture*, vol. 7, no. 2, pp. 117–130, 2015.

[23] R. V. Tyson, E. H. Simonne, D. D. Treadwell, J. M. White, and A. Simonne, "Reconciling pH for ammonia biofiltration and cucumber yield in a recirculating aquaponic system with perlite biofilters," *HortScience*, vol. 43, no. 3, pp. 719–724, 2008.

[24] Y. Tal, J. E. M. Watts, S. B. Schreier, K. R. Sowers, and H. J. Schreier, "Characterization of the microbial community and nitrogen transformation processes associated with moving bed bioreactors in a closed recirculated mariculture system," *Aquaculture*, vol. 15, pp. 187–687, 2003.

[25] N. P. Revsbech, N. Risgaard-Petersen, A. Schramm, and L. P. Nielsen, "Nitrogen transformations in stratified aquatic microbial ecosystems," *Antonie van Leeuwenhoek*, vol. 90, no. 4, pp. 361–375, 2006.

[26] S. Nikolaki and G. Tsiamis, "Microbial diversity in the era of omic technologies," *BioMed Research International*, vol. 2013, Article ID 958719, 15 pages, 2013.

[27] A. Konopka, "What is microbial community ecology?" *The ISME Journal*, vol. 3, no. 11, pp. 1223–1230, 2009.

[28] N. Leonard, J. P. Blancheton, and J. P. Guiraud, "Populations of heterotrophic bacteria in an experimental recirculating aquaculture system," *Aquacultural Engineering*, vol. 22, no. 1-2, pp. 109–120, 2000.

[29] H. Sugita, K. Shibuya, H. Shimooka, and Y. Deguchi, "Antibacterial abilities of intestinal bacteria in freshwater cultured fish," *Aquaculture*, vol. 145, no. 1–4, pp. 195–203, 1996.

[30] H. Sugita, H. Nakamura, and T. Shimada, "Microbial communities associated with filter materials in recirculating aquaculture systems of freshwater fish," *Aquaculture*, vol. 243, no. 1–4, pp. 403–409, 2005.

[31] H.-S. Joo, M. Hirai, and M. Shoda, "Characteristics of ammonium removal by heterotrophic nitrification-aerobic denitrification by *Alcaligenes faecalis* no. 4," *Journal of Bioscience and Bioengineering*, vol. 100, no. 2, pp. 184–191, 2005.

[32] P. A. Del Giorgio and J. J. Cole, "Bacterial growth efficiency in natural aquatic systems," *Annual Review of Ecology and Systematics*, vol. 29, pp. 503–541, 1998.

[33] L. Michaud, J. P. Blancheton, V. Bruni, and R. Piedrahita, "Effect of particulate organic carbon on heterotrophic bacterial populations and nitrification efficiency in biological filters," *Aquacultural Engineering*, vol. 34, no. 3, pp. 224–233, 2006.

[34] Y.-X. Ren, L. Yang, and X. Liang, "The characteristics of a novel heterotrophic nitrifying and aerobic denitrifying bacterium, *Acinetobacter junii* YB," *Bioresource Technology*, vol. 171, pp. 1–9, 2014.

[35] N. Leonard, J. P. Guiraud, E. Gasset, J. P. Cailleres, and J. P. Blancheton, "Bacteria and nutrients—nitrogen and carbon—in a recirculating system for sea bass production," *Aquacultural Engineering*, vol. 26, no. 2, pp. 111–127, 2002.

[36] S. K. Padhi, S. Tripathy, R. Sen, A. S. Mahapatra, S. Mohanty, and N. K. Maiti, "Characterisation of heterotrophic nitrifying and aerobic denitrifying *Klebsiella pneumoniae* CF-S9 strain for bioremediation of wastewater," *International Biodeterioration & Biodegradation*, vol. 78, pp. 67–73, 2013.

[37] O. Schneider, M. Chabrillon-Popelka, H. Smidt et al., "HRT and nutrients affect bacterial communities grown on recirculation aquaculture system effluents," *FEMS Microbiology Ecology*, vol. 60, no. 2, pp. 207–219, 2007.

[38] S. Itoi, A. Niki, and H. Sugita, "Changes in microbial communities associated with the conditioning of filter material in recirculating aquaculture systems of the pufferfish *Takifugu rubripes*," *Aquaculture*, vol. 256, no. 1–4, pp. 287–295, 2006.

[39] S. Itoi, N. Ebihara, S. Washio, and H. Sugita, "Nitrite-oxidizing bacteria, *Nitrospira*, distribution in the outer layer of the biofilm from filter materials of a recirculating water system for the goldfish *Carassius auratus*," *Aquaculture*, vol. 264, no. 1–4, pp. 297–308, 2007.

[40] T. A. Hovanec and E. F. DeLong, "Comparative analysis of nitrifying bacteria associated with freshwater and marine aquaria," *Applied and Environmental Microbiology*, vol. 62, no. 8, pp. 2888–2896, 1996.

[41] Y. Tal, J. E. M. Watts, and H. J. Schreier, "Anaerobic ammonium-oxidizing (Anammox) bacteria and associated activity in fixed-film biofilters of a marine recirculating aquaculture system," *Applied and Environmental Microbiology*, vol. 72, no. 4, pp. 2896–2904, 2006.

[42] G. A. Kowalchuk and J. R. Stephen, "Ammonia-oxidizing bacteria: a model for molecular microbial ecology," *Annual Review of Microbiology*, vol. 55, no. 1, pp. 485–529, 2001.

[43] A. Cébron and J. Garnier, "*Nitrobacter* and *Nitrospira* genera as representatives of nitrite-oxidizing bacteria: detection, quantification and growth along the lower Seine River (France)," *Water Research*, vol. 39, no. 20, pp. 4979–4992, 2005.

[44] D. J. Lane, B. Pace, G. J. Olsen, D. A. Stahl, M. L. Sogin, and N. R. Pace, "Rapid determination of 16S ribosomal RNA sequences for phylogenetic analyses," *Proceedings of the National Academy of Sciences of the United States of America*, vol. 82, no. 20, pp. 6955–6959, 1985.

[45] N. Shah, H. Tang, T. G. Doak, and Y. Ye, "Comparing bacterial communities inferres from 16s rrna gene sequencing and shotgun metagenomics," *WSPC—Proceedings*, vol. 17, no. 6, 2010.

[46] P. S. Kumar, M. R. Brooker, S. E. Dowd, and T. Camerlengo, "Target region selection is a critical determinant of community fingerprints generated by 16s pyrosequencing," *PLoS ONE*, vol. 6, no. 6, Article ID e20956, 2011.

[47] J. A. Gilbert, J. A. Steele, J. Gregory Caporaso et al., "Defining seasonal marine microbial community dynamics," *ISME Journal*, vol. 6, no. 2, pp. 298–308, 2012.

[48] T. Tokuyama, A. Mine, K. Kamiyama et al., "Nitrosomonas communis strain YNSRA, an ammonia-oxidizing bacterium, isolated from the reed rhizoplane in an aquaponics plant," *Journal of Bioscience and Bioengineering*, vol. 98, no. 4, pp. 309–312, 2004.

[49] F. M. Yusoff, S. Banerjee, H. Khatoon, and M. Shariff, "Biological approaches in management of nitrogenous compounds in aquaculture systems," *Dynamic Biochemistry, Process Biotechnology & Molecular Biology*, vol. 5, pp. 21–31, 2011.

[50] J. van Rijn, Y. Tal, and H. J. Schreier, "Denitrification in recirculating systems: theory and applications," *Aquacultural Engineering*, vol. 34, no. 3, pp. 364–376, 2006.

[51] S. Sirsat and J. Neal, "Microbial profile of soil-free versus in-soil grown lettuce and intervention methodologies to combat pathogen surrogates and spoilage microorganisms on lettuce," *Foods*, vol. 2, no. 4, pp. 488–498, 2013.

[52] P. Martins, D. F. R. Cleary, A. C. C. Pires et al., "Molecular analysis of bacterial communities and detection of potential pathogens in a recirculating aquaculture system for *Scophthalmus maximus* and *Solea senegalensis*," *PLoS ONE*, vol. 8, no. 11, Article ID e80847, 2013.

[53] J. Tamames, J. J. Abellán, M. Pignatelli, A. Camacho, and A. Moya, "Environmental distribution of prokaryotic taxa," *BMC Microbiology*, vol. 10, article 85, 2010.

[54] E. A. Dinsdale, R. A. Edwards, D. Hall et al., "Functional metagenomic profiling of nine biomes," *Nature*, vol. 452, no. 7187, pp. 629–632, 2008.

[55] M. Breitbart, A. Hoare, A. Nitti et al., "Metagenomic and stable isotopic analyses of modern freshwater microbialites in Cuatro Ciénegas, Mexico," *Environmental Microbiology*, vol. 11, no. 1, pp. 16–34, 2009.

[56] H. Parthasarathy, E. Hill, and C. MacCallum, "Global ocean sampling collection," *PLoS Biology*, vol. 5, no. 3, article e83, 2007.

[57] F. Rodríguez-Valera, "Environmental genomics, the big picture?" *FEMS Microbiology Letters*, vol. 231, no. 2, pp. 153–158, 2004.

[58] W. B. Whitman, D. C. Coleman, and W. J. Wiebe, "Prokaryotes: The unseen majority," *Proceedings of the National Academy of Sciences of the United States of America*, vol. 95, no. 12, pp. 6578–6583, 1998.

[59] J. Handelsman, "Metagenomics: application of genomics to uncultured microorganisms," *Microbiology and Molecular Biology Reviews*, vol. 68, no. 4, pp. 669–685, 2004.

[60] P. Hugenholtz, B. M. Goebel, and N. R. Pace, "Impact of culture-independent studies on the emerging phylogenetic view of bacterial diversity," *Journal of Bacteriology*, vol. 180, no. 18, pp. 4765–4774, 1998.

[61] G. Muyzer, "DGGE/TGGE a method for identifying genes from natural ecosystems," *Current Opinion in Microbiology*, vol. 2, no. 3, pp. 317–322, 1999.

[62] P. F. Kemp and J. Y. Aller, "Bacterial diversity in aquatic and other environments: what 16S rDNA libraries can tell us," *FEMS Microbiology Ecology*, vol. 47, no. 2, pp. 161–177, 2004.

[63] M. Wagner, M. Hornt, and H. Daims, "Fluorescence in situ hybridisation for the identification and characterisation of prokaryotes," *Current Opinion in Microbiology*, vol. 6, no. 3, pp. 302–309, 2003.

[64] J. A. Gilbert and C. L. Dupont, "Microbial metagenomics: beyond the genome," *Annual Review of Marine Science*, vol. 3, pp. 347–371, 2011.

[65] G. Bonilla-Rosso, L. E. Eguiarte, and V. Souza, "Metagenómica, genómica y ecología molecular: La nueva ecología en el bicentenario de darwin," *TIP Revista Especializada en Ciencias Químico-Biológicas*, vol. 11, no. 1, pp. 41–51, 2008.

[66] A. K. Bansal, "Bioinformatics in microbial biotechnology—a mini review," *Microbial Cell Factories*, vol. 4, article 19, 2005.

[67] J. C. Venter, K. Remington, J. F. Heidelberg et al., "Environmental genome shotgun sequencing of the sargasso sea," *Science*, vol. 304, no. 5667, pp. 66–74, 2004.

[68] C. S. Riesenfeld, P. D. Schloss, and J. Handelsman, "Metagenomics: genomic analysis of microbial communities," *Annual Review of Genetics*, vol. 38, no. 1, pp. 525–552, 2004.

[69] J. Kennedy, B. Flemer, S. A. Jackson et al., "Marine metagenomics: new tools for the study and exploitation of marine microbial metabolism," *Marine Drugs*, vol. 8, no. 3, pp. 608–628, 2010.

[70] P. D. Schloss and J. Handelsman, "Biotechnological prospects from metagenomics," *Current Opinion in Biotechnology*, vol. 14, no. 3, pp. 303–310, 2003.

[71] T. Prakash and T. D. Taylor, "Functional assignment of metagenomic data: challenges and applications," *Briefings in Bioinformatics*, vol. 13, no. 6, Article ID bbs033, pp. 711–727, 2012.

[72] J. A. Gilbert and H. Margaret, "Gene expression profiling: metatranscriptomics," in *High-Throughput next Generation Sequencing*, Y. M. Kwon and S. R. Ricke, Eds., Springer, Humana Press, 2011.

[73] C. Vogel and E. M. Marcotte, "Insights into the regulation of protein abundance from proteomic and transcriptomic analyses," *Nature Reviews Genetics*, vol. 13, no. 4, pp. 227–232, 2012.

[74] B. R. Graveley, "Alternative splicing: increasing diversity in the proteomic world," *Trends in Genetics*, vol. 17, no. 2, pp. 100–107, 2001.

[75] E. Phizicky, P. I. H. Bastiaens, H. Zhu, M. Snyder, and S. Fields, "Protein analysis on a proteomic scale," *Nature*, vol. 422, no. 6928, pp. 208–215, 2003.

[76] G. J. Patti, O. Yanes, and G. Siuzdak, "Innovation: metabolomics: the apogee of the omics trilogy," *Nature Reviews Molecular Cell Biology*, vol. 13, no. 4, pp. 263–269, 2012.

[77] O. Fiehn, "Metabolomics—the link between genotypes and phenotypes," *Plant Molecular Biology*, vol. 48, no. 1-2, pp. 155–171, 2002.

[78] K. Hollywood, D. R. Brison, and R. Goodacre, "Metabolomics: current technologies and future trends," *Proteomics*, vol. 6, no. 17, pp. 4716–4723, 2006.

[79] R. Knight, J. Jansson, D. Field et al., "Unlocking the potential of metagenomics through replicated experimental design," *Nature Biotechnology*, vol. 30, no. 6, pp. 513–520, 2012.

[80] J. Xu, "Microbial ecology in the age of genomics and metagenomics: concepts, tools, and recent advances," *Molecular Ecology*, vol. 15, no. 7, pp. 1713–1731, 2006.

[81] K. G. Frey, J. E. Herrera-Galeano, C. L. Redden et al., "Comparison of three next-generation sequencing platforms for metagenomic sequencing and identification of pathogens in blood," *BMC Genomics*, vol. 15, no. 1, article 96, 2014.

Hindawi Publishing Corporation
BioMed Research International
Volume 2015, Article ID 582471, 7 pages
http://dx.doi.org/10.1155/2015/582471

Research Article

Magnet-Facilitated Selection of Electrogenic Bacteria from Marine Sediment

Larisa Kiseleva,[1] Justina Briliute,[1] Irina V. Khilyas,[1,2] David J. W. Simpson,[1] Viacheslav Fedorovich,[1] M. Cohen,[1] and Igor Goryanin[1,3]

[1] *Biological Systems Unit, Okinawa Institute of Science and Technology, 1919-1 Tancha, Onna-son, Okinawa 904-045, Japan*
[2] *Institute of Fundamental Medicine and Biology, Kazan (Volga Region) Federal University, Ulitsa, Kremlyovskaya 18, Kazan, Republic of Tatarstan 420008, Russia*
[3] *School of Informatics, University of Edinburgh, 10 Crichton Street, Edinburgh EH8 9AB, UK*

Correspondence should be addressed to Igor Goryanin; goryanin@oist.jp

Received 8 April 2015; Revised 3 July 2015; Accepted 13 July 2015

Academic Editor: Yu Zhang

Some bacteria can carry out anaerobic respiration by depositing electrons on external materials, such as electrodes, thereby creating an electrical current. Into the anode chamber of microbial fuel cells (MFCs) having abiotic air-cathodes we inoculated microorganisms cultured from a magnetic particle-enriched portion of a marine tidal sediment, reasoning that since some external electron acceptors are ferromagnetic, electrogenic bacteria should be found in their vicinity. Two MFCs, one inoculated with a mixed bacterial culture and the other with an axenic culture of a helical bacterium isolated from the magnetic particle enrichment, termed strain HJ, were operated for 65 d. Both MFCs produced power, with production from the mixed culture MFC exceeding that of strain HJ. Strain HJ was identified as a *Thalassospira* sp. by transmission electron microscopic analysis and 16S rRNA gene comparisons. An MFC inoculated with strain HJ and operated in open circuit produced 47% and 57% of the maximal power produced from MFCs inoculated with the known electrogen *Geobacter daltonii* and the magnetotactic bacterium *Desulfamplus magnetomortis*, respectively. Further investigation will be needed to determine whether bacterial populations associated with magnetic particles within marine sediments are enriched for electrogens.

1. Introduction

As a group, bacteria obtain electrons for respiratory metabolism from a vast range of sources and, likewise, deliver these electrons to an equally impressive array of acceptor molecules. A growing list of bacteria have been found to be electrogenic, that is, capable of reducing external solid electron acceptors. From a biotechnological standpoint electrogenic bacteria are of interest because they can efficiently oxidize compounds within the anaerobic environment of microbial fuel cells (MFCs) while creating an electrical current [1].

Among the electrogenic bacteria a variety of mechanisms are employed for reducing external electron acceptors [2]. Two types of "nanowires" have been identified by which cells can deliver electrons from cell membrane respiratory proteins: type IV pili, found in *Geobacter* spp., and cytochrome-containing outer membrane extensions found in *Shewanella* spp. [3, 4]. Bacteria may stably associate with a solid electron acceptor surface as attached biofilms [5] or transiently by electrokinesis, a dynamic process in which bacteria cycle between depositing electrons and swimming in the vicinity of the acceptor [6]. Some bacteria are also capable of transferring electrons to external solid electron acceptors via diffusible electron carrying shuttle molecules, some of which can be exchanged between species [7]. Other unidentified mechanisms for external electron delivery almost certainly exist. Development of means to screen for and isolate electrogens would aid in the discovery of such mechanisms.

Conductive minerals (e.g., magnetite Fe_3O_4) confer centimeter-long conductivity to anaerobic marine sediments [8], promoting the activity of electrogens in these environments, and enabling applications such as powering of remote devices and reductive dechlorination of contaminants

[9]. Magnetite can facilitate electron transfer from bacteria to external receptors [10], including transfer to nitrate-reducing bacteria [11], and under acidic conditions magnetite it can be an external electron acceptor [12]. Recently, it was demonstrated that magnetite, owing to its mixed valency, can behave as a battery, being oxidized by phototrophic bacteria in the light and reduced by electrogenic bacteria in the dark [13]. We reasoned, therefore, that electrogenic bacteria may be found in preferential association with magnetic particles of marine sediments. Here we describe the isolation and partial characterization of an electrogenic bacterium *Thalassospira* sp. strain HJ from a magnetic particle-enriched portion of a marine tidal sediment.

2. Materials and Methods

2.1. Sediment Sampling and Preparation. Sandy sediment from Kaichu-Doro Beach (26° 19′ 56.1″ N, 127° 54′ 0″ E; October, 2013) Okinawa Japan, was sampled to 25 cm depth and placed into 500 mL bottles to approximately half capacity, filling the remainder of the bottle with seawater. At the laboratory, the sample was vigorously mixed and allowed to settle with a magnet pressed against the outside of the container positioned above the height of the sediment surface before mixing. After the sediment had settled, 4 mL of liquid and adherent magnetic particles from the region closest to the magnet was sampled with a sterile Pasteur pipette. The "capillary racetrack method" was then used to enrich for magnet-associated bacteria from the sample [14]. Fluid from the capillary was inoculated into a test tube containing 10 mL culture medium (Difco Marine Broth 2216) supplemented with 50 mg L^{-1} $FeCl_3$ (Marine-Fe broth) and grown overnight at 23°C without shaking. A sample was streaked to Marine-Fe Agar, incubated for 2 d, and a resulting colony of a spiral bacterium (termed strain HJ) was subcultured into Marine-Fe broth. 50 mL subcultures of both the original capillary racetrack-derived mixed community and strain HJ were poured into separate MFCs that were topped off with ~125 mL 0.1 M sodium/potassium phosphate buffer (pH 5.9) and 1 mL 2% sodium acetate.

2.2. Operation of Sediment-Derived Culture-Inoculated Microbial Fuel Cells. Two single-chamber, air-cathode MFCs (*H*, 10 cm; *L*, 12 cm; *W*, 10 cm) were prepared to have internal working volume of 175 mL. The internal MFC chamber contained two anodes (approximately 6 × 8 cm), suspended 2-3 mm off the bottom of the chamber, composed of a layer of 0.4 mm proprietary conductive carbon cloth to which 2 mm average size activated carbon granules were bound with conducted glue to provide more surface area. The granules had been prepared from birch precursor and pretreated with a neutral red catalyst to facilitate electron transfer. The two cathodes (6 × 8 cm) were graphite plates (3 mm thick; 60% porosity) sprayed on the liquid-facing side with an aqueous 5% Fumion membrane polymer (FuMA-Tech, Bietigheim-Bissingen, Germany) while activated carbon granules (treated with iron(II) phthalocyanine) were mechanically pressed to the air-facing side using netting frame. Unit cathode

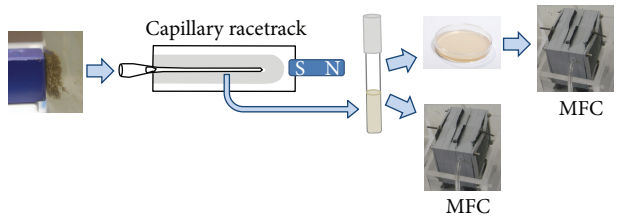

Figure 1: A flow scheme indicating the procedure for enrichment of magnetic particles from sediment and inoculation of marine broth medium and microbial fuel cells.

section (including membrane) was cleaned by immersion in concentrated HCl before module assembly for 20 min to remove any organics and was then soaked in sterile distilled water, with water changes every 1 h until the pH was neutralized. The reactor cell PVC surfaces were cleaned by washing with soap and water, drying, and then wiping down with acetone solvent. Anode and internal reactor areas were sprayed with 70% ethanol solution just prior to final assembly. The cathode extended into a bath containing an electrolyte solution maintained at pH 2 with regular additions of 1 N HCl to provide a source of protons for the abiotic reduction of oxygen to water. The MFCs were maintained on a 24 h open circuit/24 h closed circuit cycle, using an external resistance of 40 Ω. The anode and cathode electrodes were connected with a multichannel logger (Graphtec midi LOGGER GL820, Japan) for daily voltage measurements. The corresponding electric current was calculated using Ohm's law ($V = IR$). Power density was obtained according to the equation $P = IV/A$, where I is the current, V is the voltage, and A is the projected surface area of the cathode.

Once weekly, after removal of 1 mL mixed contents for chemical oxygen demand (COD) analysis, the MFCs were fed with approximately 5 mL phosphate buffer containing 1 g L^{-1} sodium acetate when COD analysis indicated substrate depletion. The extra volume of the feed was needed to replace losses due to evaporation through the cathode membrane. Upon completion of the monitoring period on the 65th day of operation, due to declining power production, the MFCs were disassembled. Anode material was sampled and bacteria were isolated from the strain HJ-inoculated MFC to confirm the presence of strain HJ.

2.3. Bacterial Isolation and Initial Characterization. DNA from strain HJ was isolated and subject to genomic sequencing [15]. Phylogenetic analyses of the 16S rRNA gene (GenBank accession number KP704219) were performed using the Phylogeny.fr platform [16]. Minimum and maximum temperatures for growth were determined by culturing on Marine Agar plates. Catalase and oxidase activities were tested and Gram staining was carried out using standard microbiological methods.

2.4. Transmission Electron Microscopy. Transmission electron microscope (TEM) imaging was performed on a JEOL JEM-1230R Electron Microscope at an accelerating voltage of

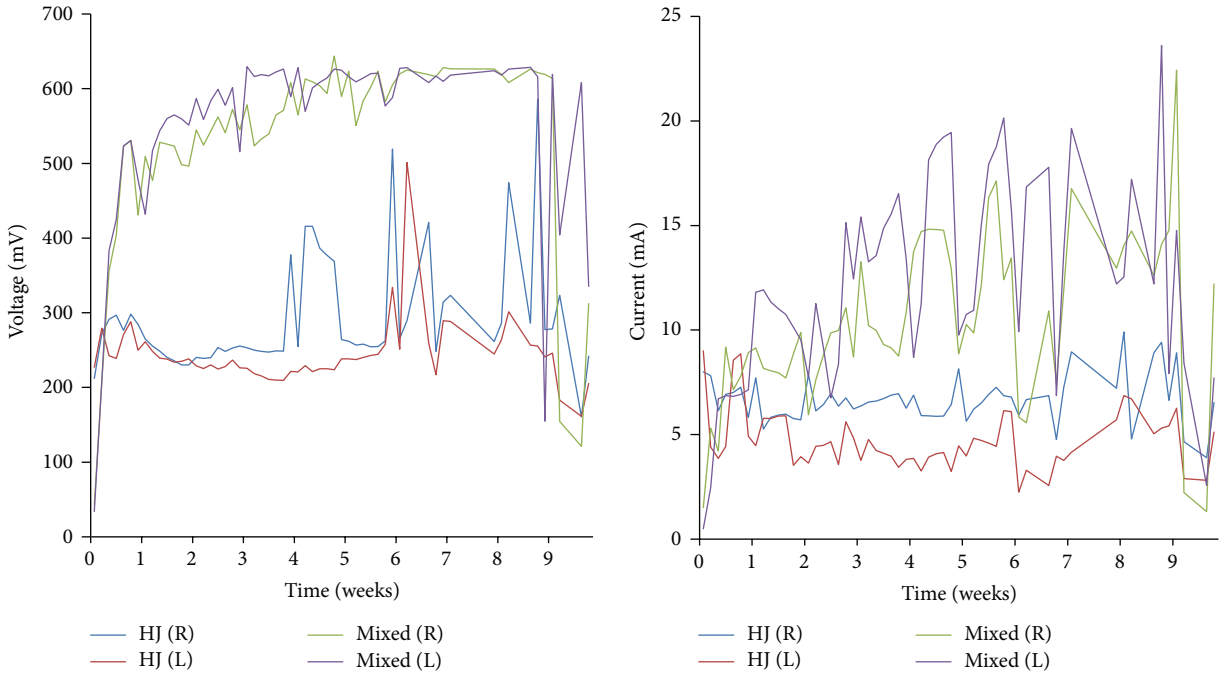

FIGURE 2: Electrical output from microbial fuel cells inoculated with cultures derived from tidal beach sediment obtained from Kaichu-Doro Beach, Okinawa, Japan. Total anode surface area, 151 cm^2 (75.5 cm^2 per anode); 175 mL volume. Plotted lines indicate activity from the mixed culture-inoculated MFC and the strain HJ-inoculated MFC; R, right, and L, left anode-cathode couple.

100 KV. Strain HJ cells were prepared from cultures grown at room temperature (23°C) in 50 mL of Marine-Fe broth to an OD_{600} of 1.0. The pelleted cells were fixed with 1% osmium tetroxide in 0.1 M cacodylate buffer (pH = 7.2) for 30 min and washed with water three times for 5 min. A drop of fixed bacterial cells was deposited onto a carbon-coated HF34 200 mesh copper grid, washed once with distilled water, and stained for 3 to 5 sec with 1% uranyl acetate.

2.5. Inoculation and Monitoring of Microbial Fuel Cells Inoculated with Axenic Bacterial Cultures. A micro-MFC array was developed from two parts of Plexiglas with three 4 cm microchambers to test for current generation by three axenic bacterial cultures. Each chamber consisted of an anode and a cathode compartment (8 mm deep) separated by a cation-exchange membrane Nafion 117 (19.6 cm^2; DuPont Co., Delaware USA). The anode and cathode electrodes (3 mm thick graphite plates; 45–50% porosity, Xinghe County Muzi Carbon Co., Ltd, China) were connected with a multichannel logger (Graphtec midi LOGGER GL820, Japan) for daily voltage measurements. 1 mm thick rubber gaskets were used for sealing between the anode and cathode compartments. A titanium screw held the electrode against the membrane and acted as electrical connector. Each micro-MFC chamber was equipped with a 2.5 ID mm polyurethane inlet tube (FESTO, Germany) on the bottom for medium and electrolyte feeding and one on the top for biogas output and replacement of exhausted electrolyte. For disinfection the plexiglas microchambers were soaked in a 10% bleach solution, rinsed with deionized water, and then exposed to UV light for 12 h. Graphite plates were washed with 100% isopropanol in an ultrasonic bath and then heated in an oven for 2 h at 200 C. Micro-MFCs were operated in the open circuit mode and current measurements were performed every 24 hours starting from time of inoculation. 50 mM iron(II) phthalocyanine, without N_2 sparging, was used as the cathode electrolyte solution.

Axenic bacterial cultures (*Thalassospira* sp. HJ, the known electrogen *Geobacter daltonii*, and the magnetotactic *Desulfamplus magnetomortis*) were pregrown with shaking at 37°C for 12 h in 5 mL of modified PBS medium containing (per liter) 4.58 g Na_2HPO_4, 2.45 g $NaH_2PO_4{\cdot}H_2O$, 0.31 g NH_4Cl, 0.13 g KCl, 5 g glucose, 5 g yeast extract, and 5 g peptone. Bacterial cells were harvested, washed with 16 mM phosphate buffer (pH 7.0), and resuspended into 50 mL fresh modified PBS medium. The initial cell concentration was adjusted to an optical density at 600 nm of 0.3 as measured by a Spectronic GENESYS 5 spectrophotometer (Milton Roy Company, Rochester, NY, USA) with filtered cell-free culture medium as reference.

The micro-MFCs were inoculated initially with 15 mL medium containing bacterial cells (exceeding the ~10 mL volume of the anode chamber since the porous graphite absorbed some liquid). Bacteria-free modified PBS medium containing 0.1% NaN_3 was used for control experiments. All experiments were set up in two technical replications and two biological replications. The axenicity of the anolytes for the strain HJ-containing MFCs was determined at the end of the experiments by plating serial dilutions to Marine Agar medium. Experiments were performed at room temperature.

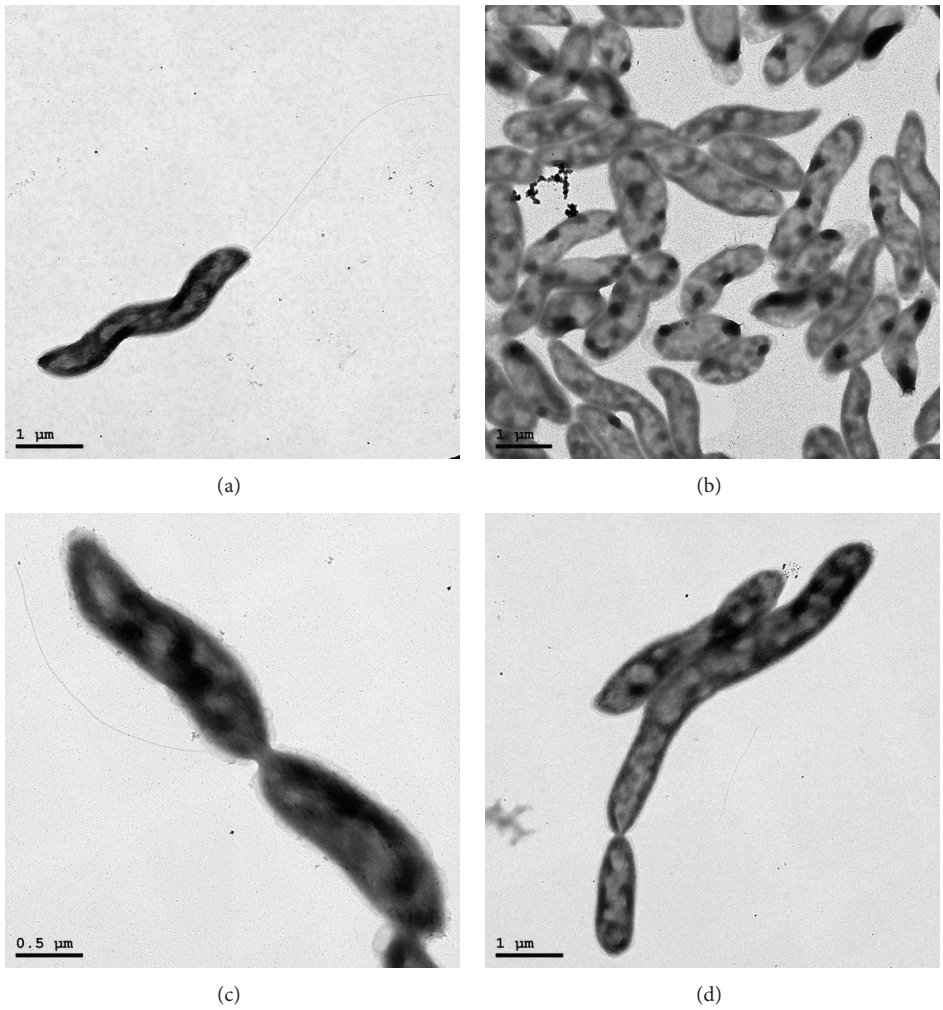

(a) (b) (c) (d)

Figure 3: Transmission electron micrographs of *Thalassospira* sp. strain HJ showing various features. (a) A single polar flagellum; (b) intracellular electron-dense regions; (c) symmetric cell division; and (d) asymmetric cell division. Representative images are shown.

3. Results and Discussion

To obtain magnetic particle-associated bacteria, some of which should be electrogenic [12], we subjected tidal beach sediment to the enrichment procedure depicted in Figure 1. One MFC was inoculated with a mixed culture derived from the magnetic particle-enriched sediment and the other with an axenic culture of a helical bacterium, strain HJ, isolated from the enriched sediment. Both MFCs were found to produce power, with the current and voltage generated from the mixed culture MFC being substantially higher (Figure 2). The comparatively low power density observed of strain HJ is typical of axenic bacterial cultures relative to that of the communities from which they are derived [5]. At the end of the experiment strain HJ was reisolated from the MFC to confirm its retention.

Strain HJ was identified by means of microscopic analysis (Figure 3) and 16S rRNA gene sequence comparisons (Figure 4) to be of the genus *Thalassospira*. TEM images show cells of 0.5–0.7 μm width and 1.5–5.7 μm length having single polar flagella typical of the genus *Thalassospira* [17], with evidence of both symmetric and asymmetric cell division (Figure 3). One or more electron-dense staining regions can be seen within most cells (Figure 3). Cells were motile, stained Gram negative, and tested positive for catalase and oxidase activity. Growth occurred on Marine Agar at temperatures ranging from 12°C to 39°C and pH values ranging from 5.5 to 10.5. The closest matching 16S rRNA gene sequence to a named species within the GenBank database was that of *Thalassospira profundimaris* strain WP0211 (1449/1453, 99.7% identity), which notably differs from strain HJ in its lack of flagella [18].

Micro-MFC chambers inoculated with axenic cultures of *Thalassospira* sp. strain HJ and, for comparison, *Geobacter daltonii* and *Desulfamplus magnetomortis* showed electrical current production immediately after inoculation but differed in the intensity and shape of the subsequent production curve (Figure 5). *Thalassospira* sp. strain HJ and *D. magnetomortis* displayed gradual increases in current after initiation whereas current production from *G. daltonii* decreased

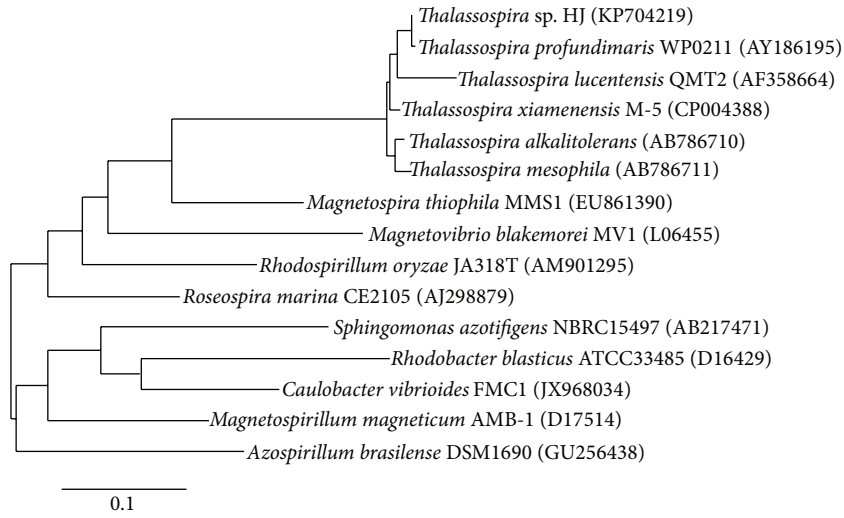

FIGURE 4: Phylogenetic tree of strain HJ and selected alphaproteobacteria based on 16S rRNA gene sequences. The tree was constructed from sequences aligned by MUSCLE using maximum-likelihood method of PhyML 3.0 [16, 21]. The scale bar reflects evolutionary distance, measured in units of substitution per nucleotide site.

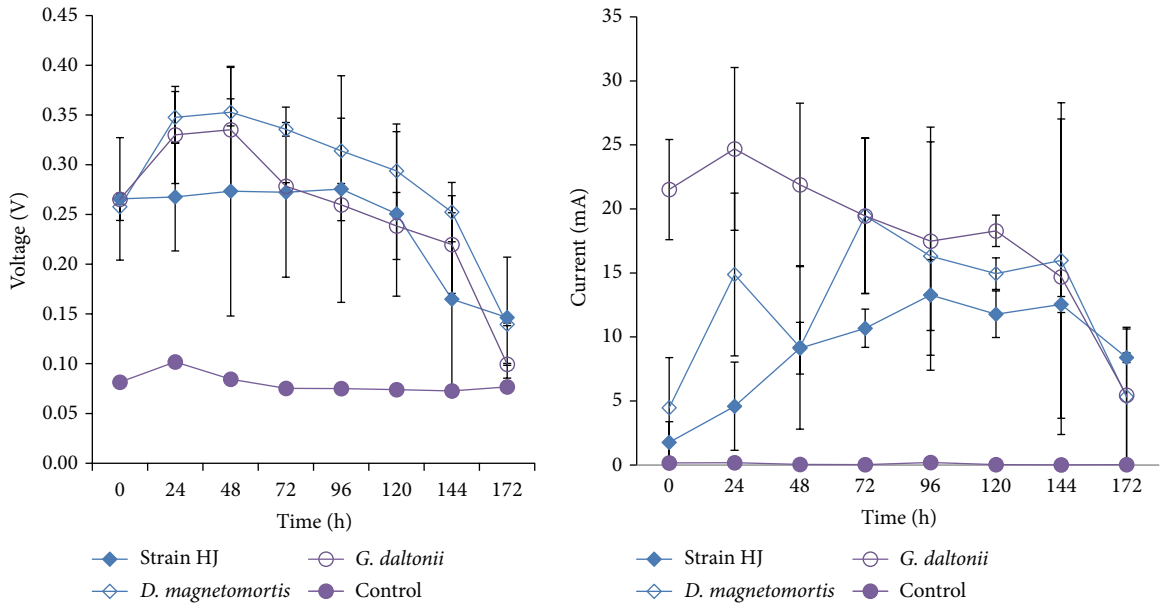

FIGURE 5: Voltage and current readings (±range; $n = 2$) from microbial fuel cells inoculated with axenic cultures of *Thalassospira* sp. strain HJ, *Geobacter daltonii*, and *Desulfamplus magnetomortis* or medium only with 1 g L^{-1} sodium azide (control). Anode surface area, 19.6 cm^2; 10 mL volume.

with time. After 172 h, the current for all axenic cultures decreased to 5–8 mA, which was attributed with C-source depletion. Voltage drop was observed after 144 h from the strain HJ-inoculated micro-MFC, whereas *G. daltonii* and *D. magnetomortis* MFCs demonstrated voltage loss after 48 h. As a control, to determine the contribution of growth medium components to current and voltage production, a micro-MFC was filled with sterile medium. Although there was no observable current generation background voltage was observed (Figure 5). The maximal single-value power readings from the micro-MFCs were of 2.6 W m^{-2} (at 96 h) for *Thalassospira* sp. strain HJ, 5.5 W m^{-2} (at 144 h) for *D. magnetomortis*, and 4.6 W m^{-2} (at 24 h) for *G. daltonii*.

Geobacter is a well-characterized genus of electrogenic bacteria and although we are not aware of prior reports of electrogenicity by the magnetotactic bacterium *D. magnetomortis* members of sulfate-reducing members of the Deltaproteobacteria, to which *D. magnetomortis* belongs, were found to display transcriptomic responses to changes in MFC electrode potential indicative of electrogenic behavior [19]. We hypothesize that magnetosomes could confer a selective benefit by enabling bacteria to hone in on ferromagnetic

external electron acceptors. A wider survey of magnetotactic bacteria for electrogenicity would be warranted.

Recently, two marine sediment-derived *Thalassospira* sp. isolates were reported to exhibit electrotrophic behavior, accepting electrons from insoluble sulfur [20] but the capacity of these strains to transfer electrons to an anode as we have found here of *Thalassospira* sp. strain HJ was not examined. Examination of the strain HJ genome does not reveal any homologs for the pili or outer membrane extension-type external electron transfer systems found in *Geobacter* or *Shewanella* species [15], and microscopic imaging of anodes from strain HJ-colonized MFCs implies that biofilm formation is not necessary for electrogenicity (data not shown). Thus, we hypothesize that external electron transfer occurs via an electron shuttle-type mechanism.

4. Conclusions

A microbial community derived from magnetic particle-enriched marine sediment displayed electrogenic behavior and yielded an electrogenic bacterium identified to be a *Thalassospira* species. This is the first report of electrogenic behavior within the genus *Thalassospira*. A more extensive study would be needed to determine whether the proportion of electrogenic bacteria obtained from this magnetic particle enrichment procedure exceeds that found in the environment. With their diurnal patterns of flooding and diversity of mineral components tidal sediments should be rich environments to bioprospect for electrogenic bacteria.

Conflict of Interests

The authors declare that there is no conflict of interests regarding the publication of this paper.

Acknowledgments

Funding was provided by the Okinawa Institute of Science and Technology. I. V. Khilyas was supported by Russian Government Program of Competitive Growth of Kazan Federal University. The authors thank M Power World, Ltd., for consultations and provision of equipment and T. Sasaki for conducting transmission electron microscopy.

References

[1] V. Gude, B. Kokabian, and V. Gadhamshetty, "Beneficial bioelectrochemical systems for energy, water, and biomass production," *Journal of Microbial & Biochemical Technology*, vol. 6, article 005, p. 2, 2013.

[2] S. A. Patil, C. Hägerhäll, and L. Gorton, "Electron transfer mechanisms between microorganisms and electrodes in bioelectrochemical systems," *Bioanalytical Reviews*, vol. 4, no. 2–4, pp. 159–192, 2012.

[3] D. R. Lovley and N. S. Malvankar, "Seeing is believing: Novel imaging techniques help clarify microbial nanowire structure and function," *Environmental Microbiology*, vol. 17, no. 7, pp. 2209–2215, 2015.

[4] S. Pirbadian, S. E. Barchinger, K. M. Leung et al., "*Shewanella oneidensis* MR-1 nanowires are outer membrane and periplasmic extensions of the extracellular electron transport components," *Proceedings of the National Academy of Sciences of the United States of America*, vol. 111, no. 35, pp. 12883–12888, 2014.

[5] B. E. Logan, "Exoelectrogenic bacteria that power microbial fuel cells," *Nature Reviews Microbiology*, vol. 7, no. 5, pp. 375–381, 2009.

[6] H. W. Harrisa, M. Y. El-Naggarb, O. Bretschgerc et al., "Electrokinesis is a microbial behavior that requires extracellular electron transport," *Proceedings of the National Academy of Sciences of the United States of America*, vol. 107, no. 1, pp. 326–331, 2010.

[7] K. Rabaey, N. Boon, M. Höfte, and W. Verstraete, "Microbial phenazine production enhances electron transfer in biofuel cells," *Environmental Science & Technology*, vol. 39, no. 9, pp. 3401–3408, 2005.

[8] N. S. Malvankar, G. M. King, and D. R. Lovley, "Centimeter-long electron transport in marine sediments via conductive minerals," *The ISME Journal*, vol. 9, no. 2, pp. 527–531, 2015.

[9] D. R. Lovley and K. P. Nevin, "A shift in the current: new applications and concepts for microbe-electrode electron exchange," *Current Opinion in Biotechnology*, vol. 22, no. 3, pp. 441–448, 2011.

[10] F. Liu, A. Rotaru, P. M. Shrestha, N. S. Malvankar, K. P. Nevin, and D. R. Lovley, "Magnetite compensates for the lack of a pilin-associated *c*-type cytochrome in extracellular electron exchange," *Environmental Microbiology*, vol. 17, no. 3, pp. 648–655, 2015.

[11] S. Kato, K. Hashimoto, and K. Watanabe, "Microbial interspecies electron transfer via electric currents through conductive minerals," *Proceedings of the National Academy of Sciences of the United States of America*, vol. 109, no. 25, pp. 10042–10046, 2012.

[12] J. E. Kostka and K. H. Nealson, "Dissolution and reduction of magnetite by bacteria," *Environmental Science & Technology*, vol. 29, no. 10, pp. 2535–2540, 1995.

[13] J. M. Byrne, N. Klueglein, C. Pearce, K. M. Rosso, E. Appel, and A. Kappler, "Redox cycling of Fe(II) and Fe(III) in magnetite by Fe-metabolizing bacteria," *Science*, vol. 347, no. 6229, pp. 1473–1476, 2015.

[14] R. S. Wolfe, R. K. Thauer, and N. Pfennig, "A 'capillary racetrack' method for isolation of magnetotactic bacteria," *FEMS Microbiology Letters*, vol. 45, no. 1, pp. 31–35, 1987.

[15] L. Kiseleva, S. K. Garushyants, J. Briliute, D. J. Simpson, M. F. Cohen, and I. Goryanin, "Genome sequence of the electrogenic petroleum-degrading *Thalassospira* sp. strain HJ," *Genome Announcements*, vol. 3, no. 3, Article ID e00483-15, 2015.

[16] A. Dereeper, V. Guignon, G. Blanc et al., "Phylogeny.fr: robust phylogenetic analysis for the non-specialist," *Nucleic Acids Research*, vol. 36, supplement 2, pp. W465–W469, 2008.

[17] J. I. Baldani, S. S. Videira, J. I. Baldani et al., "The family *Rhodospirillaceae*," in *The Prokaryotes*, E. Rosenberg, E. DeLong, S. Lory, E. Stackebrandt, and F. Thompson, Eds., pp. 533–618, Springer, Berlin, Germany, 2014.

[18] C. Liu, Y. Wu, L. Li, M. Yingfei, and Z. Shao, "*Thalassospira xiamenensis* sp. nov. and *Thalassospira profundimaris* sp. nov," *International Journal of Systematic and Evolutionary Microbiology*, vol. 57, no. 2, pp. 316–320, 2007.

[19] S. Ishii, S. Suzuki, T. M. Norden-Krichmar et al., "A novel metatranscriptomic approach to identify gene expression dynamics during extracellular electron transfer," *Nature Communications*, vol. 4, article 1601, 2013.

[20] A. R. Rowe, P. Chellamuthu, B. Lam, A. Okamoto, and K. H. Nealson, "Marine sediments microbes capable of electrode oxidation as a surrogate for lithotrophic insoluble substrate metabolism," *Frontiers in Microbiology*, vol. 5, article 784, 2015.

[21] S. Guindon, J.-F. Dufayard, V. Lefort, M. Anisimova, W. Hordijk, and O. Gascuel, "New algorithms and methods to estimate maximum-likelihood phylogenies: assessing the performance of PhyML 3.0," *Systematic Biology*, vol. 59, no. 3, pp. 307–321, 2010.

Hindawi Publishing Corporation
BioMed Research International
Volume 2015, Article ID 241582, 6 pages
http://dx.doi.org/10.1155/2015/241582

Research Article

Fungal Antagonism Assessment of Predatory Species and Producers Metabolites and Their Effectiveness on *Haemonchus contortus* Infective Larvae

Manoel Eduardo Silva,[1] Fabio Ribeiro Braga,[1,2] Pedro Mendoza de Gives,[1] Jair Millán-Orozco,[3] Miguel Angel Mercado Uriostegui,[4] Liliana Aguilar Marcelino,[4] Filippe Elias de Freitas Soares,[5] Andréia Luiza Araújo,[2] Thainá Souza Vargas,[2] Anderson Rocha Aguiar,[2] Thiago Senna,[2] Maria Gorete Rodrigues,[2] Frederico Vieira Froes,[2] and Jackson Victor de Araújo[1]

[1]*Departamento de Veterinária, Universidade Federal de Viçosa, Viçosa, MG, Brazil*
[2]*Universidade Vila Velha, Vila Velha, ES, Brazil*
[3]*Facultad de Ciencias Agropecuárias, UAEM, Avenida Universidad 1001, Col. Chamilpa, 62209 Cuernavaca, MOR, Mexico*
[4]*Instituto Nacional de Investigaciones Forestales, Agricolas y Pecuarias INIFAP/CENID, Avenida Progreso No. 5, Colonia Barrio de Santa Catarina, 04010 Delegación Coyoacán, DF, Mexico*
[5]*Departamento de Bioquímica e Biologia Molecular, Universidade Federal de Viçosa, Viçosa, MG, Brazil*

Correspondence should be addressed to Fabio Ribeiro Braga; fabioribeirobraga@hotmail.com

Received 13 April 2015; Accepted 21 July 2015

Academic Editor: Giuseppe Piccione

The objective of this study was to assess antagonism of nematophagous fungi and species producers metabolites and their effectiveness on *Haemonchus contortus* infective larvae (L_3). Assay A assesses the synergistic, additive, or antagonistic effect on the production of spores of fungal isolates of the species *Duddingtonia flagrans*, *Clonostachys rosea*, *Trichoderma esau*, and *Arthrobotrys musiformis*; Assay B evaluates in vitro the effect of intercropping of these isolates grown in 2% water-agar (2% WA) on L_3 of *H. contortus*. *D. flagrans* (Assay A) produced 5.3×10^6 spores and associated with *T. esau*, *A. musiformis*, or *C. rosea* reduced its production by 60.37, 45.28, and 49.05%, respectively. *T. esau* produced 7.9×10^7 conidia and associated with *D. flagrans*, *A. musiformis*, or *C. rosea* reduced its production by 39.24, 82.27, and 96.96%, respectively. *A. musiformis* produced 7.3×10^9 spores and associated with *D. flagrans*, *T. esau*, or *C. rosea* reduced its production by 99.98, 99.99, and 99.98%, respectively. *C. rosea* produced 7.3×10^8 conidia and associated with *D. flagrans*, *T. esau*, or *A. musiformis* reduced its production by 95.20, 96.84, and 93.56%, respectively. These results show evidence of antagonism in the production of spores between predators fungi.

1. Introduction

Brazil has a herd of 212 million head of cattle and 171 million hectares of pastures that produce approximately 96% of Brazilian beef. On the other hand, gastrointestinal nematodes are a serious problem in ruminant production; once the animals have been exposed to high parasite loads they may succumb, especially younger individuals, which are more susceptible [1, 2].

The parasite-host relationship is characterized as a balanced relationship, being controlled by the intraspecified variability of host and parasite, allied to environmental factors. Epidemiologically whole herd raised under grazing conditions has some degree of gastrointestinal nematode infection, which results in a complex series of pathological events ranging between subclinical effects, production losses, and even death of the animal [3]. In this context, nematodes, especially the genus *Haemonchus*, are responsible for large

economic losses in livestock. The conventional method for controlling such gastrointestinal parasites is to use synthetic anthelmintic drugs but they leave residues of the products in the treated animal, affect nontarget organisms, and select resistant strains of the parasites. Thus, use of nematophagous fungi, as an alternative control, has been constantly tested, with interesting results both in the field and under laboratory conditions [4].

A heterogeneous group of microfungi experts in capturing and using intestinal parasitic nematodes of domestic animals and phytonematodes as a source of nutrients are considered highly feasible and promising in environmental reduction of infective larvae [5, 6]. *Duddingtonia flagrans* and *Arthrobotrys* spp. are fungi predators and the most studied and effective in the control of parasites of animals [4, 7]. *Clonostachys* spp. and *Trichoderma* spp. are primarily used as biological controls of phytonematodes, but the diversity of the produced metabolites and adaptability to different environmental conditions give them the opportunity to be used in the biotechnology industry [7–10].

Although competition between microorganisms is very intense and severe making the introduction of new fungal species as biocontrol agents in certain environments practically impossible, it is necessary to evaluate the effect of combinations of fungi predators, opportunists, and ovicidal and metabolites producers and also abiotic factors, raising the possibility of establishment of fungi and potentiating the nematodes control [11–14]. Commercial spore production is usually performed in organic substrates or inert carriers, but several attempts to select substrates more productively and with low cost production have been carried out, especially with byproducts of agroindustry [15].

For use in biocontrol program as for survival and dissemination in environment condition of fungal spores is necessary [13] and when it comes to parasites animal control is important to select species and/or isolates capable of crossing the digestive tract and maintain the viability and predatory ability [16]. Thus, the objective of this study was to assess antagonism of nematophagous fungi and species producers metabolites and their effectiveness on L_3 of *H. contortus*.

2. Materials and Methods

2.1. Organisms. Organisms were used as fungal isolates of *D. flagrans* (strain FTHO-8) [17], *Clonostachys rosea* (strain Yucatán, CICY-CONACYT), *Arthrobotrys musiformis*, and *Trichoderma esau* maintained on agar-water 2% (AA 2%) of mycology library of the National Institute for Forestry, Agricultural and Livestock, INIFAP, and *H. contortus* infective larvae (L_3) (isolated Hueytamalco, Puebla) maintained by artificial infection in Pelibuey sheep in INIFAP facilities.

2.2. Spore Production. Two fragments of a previous crop in 2% WA of *D. flagrans*, *A. musiformis*, *C. rosea*, and *T. esau*, with approximately 4 mm^2 being transferred alone or in association with other fungi to Petri dishes of 100 × 15 mm (06 replicates) containing 20 mL of 2% WhA culture medium, were maintained at room temperature and protected from light. The initial inoculum present in each fragment isolated from *D. flagrans*, *A. musiformis*, *C. rosea*, and *T. esau* was, respectively, 1.1×10^3, 1.9×10^6, 4.2×10^4, and 7.1×10^5 conidia and/or chlamydospores. After 7 days of cultivation 5 mL of distilled water was added on the plate surface and the spores were scraped with a spatula and stored in a sterile Falcon tubes. The volume was completed to 45 mL and 10 replicates were evaluated in a Neubauer chamber. Counting averages were extrapolated to the final volume of spores produced per plate.

2.3. "In Vitro" Test. Two fragments of a previous crop in 2% WA of *D. flagrans*, *A. musiformis*, *C. rosea*, and *T. esau*, with approximately 4 mm^2 being transferred alone or associated with other fungi to Petri dishes of 600 × 15 mm (08 replicates) containing 10 mL of 2% WA culture medium, were maintained at room temperature and protected from light for 7 days. After cultivation, each Petri dish was inoculated with approximately 300 L_3 of *H. contortus* obtained by the Baermann method from coprocultures of sheep faeces artificially infected. The Petri dishes were kept at room temperature and protected from light; in the seventh day of interaction between fungal isolates and nematodes, Baermann was taken from the agar contained in Petri plates for recovery of larvae not preyed upon.

2.4. Statistical Analysis. Assay A was designed in a factorial combination of fungal isolates × association of the same isolates (4 isolates, 6 associations, and 6 replicates) and Assay B was designed in a factorial combination of fungal isolates × nematode parasites (4 isolates, 6 associations, and 8 replicates) and one control group. The average number of produced spores or recovered larvae was subjected to analysis of variance and compared by Tukey test in 1% significance level using BioEstat 5.3 software.

3. Results and Discussion

The results observed in Table 1 show that, in the culture conditions described, the *D. flagrans* alone produced 5.3 × 10^6 conidia/chlamydospores by Petri dish and when it was associated with *T. esau*, *A. musiformis*, or *C. rosea* the structure production was 2.1 × 10^6, 2.9 × 10^6, and 2.7 × 10^6, respectively, showing a reduction of 60.37, 45.28, and 49.05%, respectively, in the spores production (Table 1 and Figure 1(a)).

The production of spores of *T. esau* alone, in the same conditions described, was 7.9×10^7 conidia per plate and in association with *D. flagrans*, *A. musiformis*, or *C. rosea* was 4.8×10^7, 1.4×10^7, and 2.4×10^6 structures, reducing at 39.24, 82.27, and 96.96%, respectively (Table 1 and Figure 1(b)).

A. musiformis alone produced 7.3×10^9 conidia/chlamydospores per plate and in association with *D. flagrans*, *T. esau*, or *C. rosea* the reproductive structure production was 1.4 × 10^6, 1.7 × 10^5, and 1.4 × 10^6, respectively, being reduced at 99.98, 99.99, and 99.98%, respectively (Table 1 and Figure 1(c)).

C. rosea alone reached a production of 2.8×10^8 conidia per plate and in association with *D. flagrans*, *T. esau*, or *A.*

Table 1: Mean, standard deviation, and % of reduction of spores produced by different fungal isolates after 7 days on medium 2% wheat-agar (2% WhA).

Duddingtonia flagrans				
Isolate	*D. flagrans*	*T. esau*	*A. musiformis*	*C. rosea*
Conidia/chlamydospores	5.3×10^{6a}	2.1×10^{6b}	2.9×10^{6b}	2.7×10^{6b}
Standard deviation	$(\pm 2.1 \times 10^{6})$	$(\pm 7.1 \times 10^{5})$	$(\pm 1.5 \times 10^{6})$	$(\pm 8.7 \times 10^{5})$
% reduction	—	−60.37%	−45.28%	−49.05%
Trichoderma esau				
Isolate	*T. esau*	*D. flagrans*	*A. musiformis*	*C. rosea*
Conidia/chlamydospores	7.9×10^{7a}	4.8×10^{7ba}	1.4×10^{7bb}	2.4×10^{6bb}
Standard deviation	$(\pm 2 \times 10^{7})$	$(\pm 5.4 \times 10^{6})$	$(\pm 4.3 \times 10^{6})$	$(\pm 8.7 \times 10^{5})$
% reduction	—	−39.24%	−82.27%	−96.96%
Arthrobotrys musiformis				
Isolate	*A. musiformis*	*D. flagrans*	*T. esau*	*C. rosea*
Conidia/chlamydospores	7.3×10^{9a}	1.4×10^{6b}	1.7×10^{5b}	1.4×10^{6b}
Standard deviation	$(\pm 1.9 \times 10^{9})$	$(\pm 9.1 \times 10^{5})$	$(\pm 2.5 \times 10^{5})$	$(\pm 5.1 \times 10^{5})$
% reduction	—	−99.98%	−99.99%	−99.98%
Clonostachys rosea				
Isolate	*C. rosea*	*D. flagrans*	*T. esau*	*A. musiformis*
Conidia/chlamydospores	2.8×10^{8a}	3.5×10^{7b}	2.3×10^{7b}	4.7×10^{7b}
Standard deviation	$(\pm 3.9 \times 10^{7})$	$(\pm 2.1 \times 10^{7})$	$(\pm 9.2 \times 10^{6})$	$(\pm 2.1 \times 10^{7})$
% reduction	—	−95.20%	−96.84%	−93.56%

Different lowercase letters indicate existence of statistical difference ($p < 0.01$), Tukey test.

musiformis the spores production was 3.5×10^{7}, 2.3×10^{7}, and 4.7×10^{7}, being reduced at 95.20, 96.84, and 93.56%, respectively (Table 1 and Figure 1(d)).

The isolates, *A. musiformis* and *C. rosea* alone, showed the greatest production of reproductive structures per plate; on the other hand they also had the highest percentage of reduction in spores production when they were grown in association with other fungal isolates (Table 1).

In "*in vitro*" test the effectiveness of fungus predator *D. flagrans* was 100% against L_3 of *H. contortus* in isolated culture ($p < 0.01$); the remaining 100% of efficacy cultivated in association with *A. musiformis* or *T. esau* was not antagonized by these fungi, but in association with *C. rosea* the predatory activity was reduced to 95.65% (Table 2).

The *A. musiformis* isolate grown in isolation preyed on 91.30% of larvae ($p < 0.01$) and associated with the fungus predator *D. flagrans* or metabolites producers, *T. esau* or *C. rosea*, showed additive predatory effect of 100, 100, and 95.65%, respectively (Table 2).

The fungi metabolites producers, *T. esau* and *C. rosea*, preyed on 82.60% of larvae grown in isolation ($p < 0.01$), but when they were grown in conjunction they showed strong antagonism, preying on 60.86% of larvae, not differing statistically from the control group ($p > 0.05$). In addition, these isolates showed additive effect by the presence of predators fungi *D. flagrans* or *A. musiformis*, preying on 100 and 95.65%, respectively, of L_3 of *H. contortus* (Table 2).

3.1. Assay A: Evaluation of Spores Production. In this evaluation *D. flagrans* alone produced 5.3×10^{6} spores per Petri dish in AT 2% medium; Sagüés et al. [18] observed similar production with the addition of mesoinositol and wheat flour plus powder milk in Sabouraud Glucose Agar, SGA (5.1×10^{7} and 2×10^{8} chlamydospores, resp.), grown in a temperature of 27°C for 28 days, showing production potential of reproductive structures of *D. flagrans*. Hernández Mansilla et al. [19] obtained in biphasic system the production of 1×10^{5} chlamydospores/gram of *D. flagrans* in solid substrate (rice) after 30 days of culture at room temperature and demonstrated the efficacy of the spores on infective larvae of nematode of sheep. Boguś et al. [20] showed that the proteins of nematode are the best assailable nitrogen source for nematophagous fungi and then observed that nematodes homogenized induce the habit change from saprophyte to predator of *D. flagrans* in culture medium with a low concentration of carbon and nitrogen; these observations confirm the predatory potential of this species on infective larvae. The isolate of *D. flagrans* present a reduction of 60.37, 45.28, and 49.05% spores production when grown in association with *T. esau*, *A. musiformis*, or *C. rosea*, respectively, although Assis et al. [7] observed no difference in production of structures when that species was cultivated in association with the ovicidal fungus *Mucor circinelloides*; these observations demonstrated that isolated with different mechanisms of action may or not be antagonists in environmental conditions. In this case the antagonistic effect of metabolites producers fungi *T. esau* and *C. rosea* was more evident than that caused by predator fungus *A. musiformis* (Table 1).

The isolate of *A. musiformis* alone produced 7.3×10^{9} conidia/chlamydospores per Petri dish. When grown in association with *D. flagrans*, *T. esau*, or *C. rosea* the production of reproductive structures was, respectively, 1.4×10^{6}, 1.7

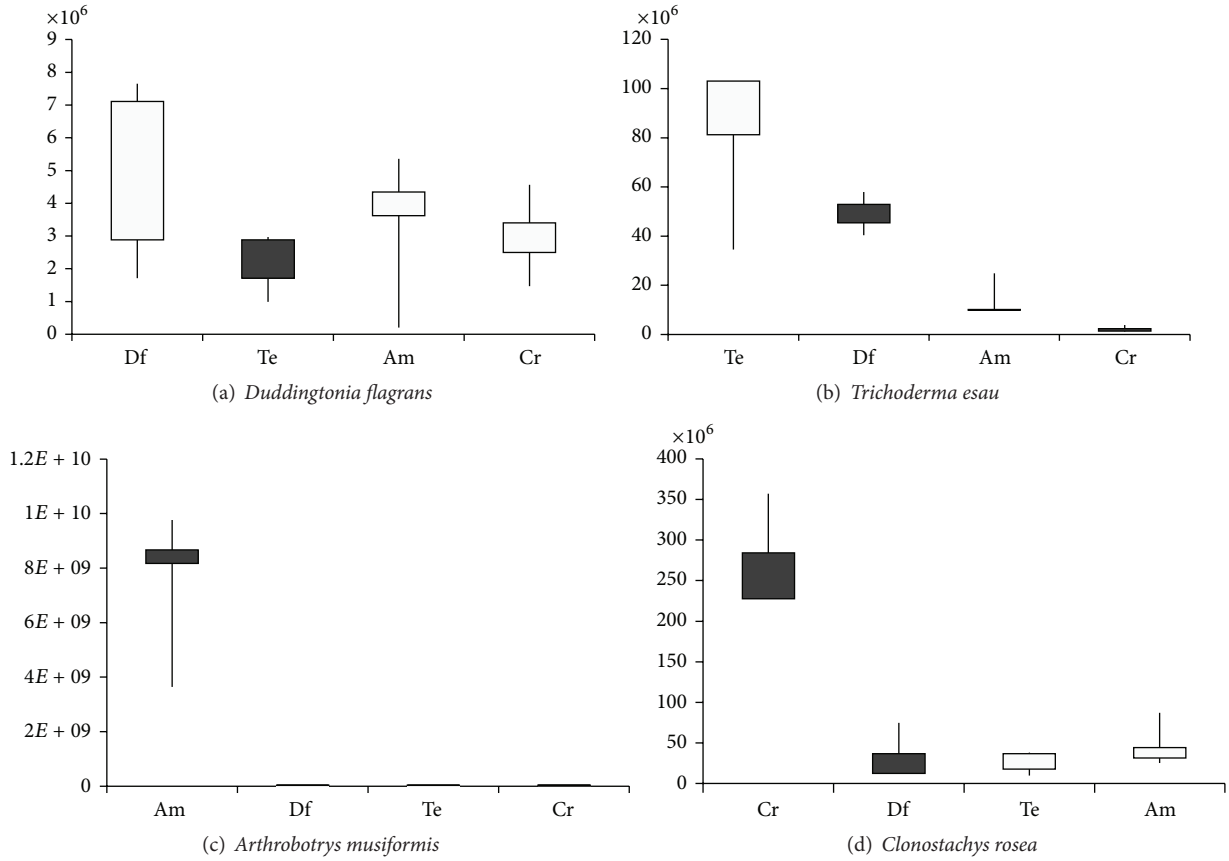

Figure 1: Mean and standard deviation of spores produced by different fungal isolates after 7 days on medium −2% wheat-agar (2% WhA).

Table 2: Mean, standard deviation, and percentage of predation of *Haemonchus contortus* infective larvae recovered from Petri dishes by Baermann method after 7 days of interaction with different fungal species grown in conjunction or alone (Df = *Duddingtonia flagrans*, Am = *Arthrobotrys musiformis*, Te = *Trichoderma esau,* and Cr = *Clonostachys rosea*).

Parameters	Control	Df × Am	Df × Te	Df × Cr	Am × Te	Am × Cr	Te × Cr	Df	Am	Te	Cr
Mean	115^{bb}	0^{a}	0^{a}	5^{aa}	0^{a}	5^{aa}	45^{ba}	0^{a}	10^{aa}	20^{aa}	20^{aa}
Deviation	±54.54	±0	±0	±13.23	±0	±13.23	±31.22	±0	±26.46	±28.28	±28.28
% predation	0%	100%	100%	95.65%	100%	95.65%	60.86%	100%	91.30%	82.60%	82.60%

Different lowercase letters indicate existence of statistical difference ($p < 0.0001$), Tukey test.

$\times 10^5$, and 1.4×10^6. This isolate shows decrease of the spores production by 99.98, 99.99, and 99.98%, respectively, demonstrating suffering greater antagonism by other fungal species (predators and/or producers of metabolites) (Table 1 and Figure 1(c)). This fact shows that this fungal species may not be a good competitor in the natural environment. Dias and Ferraz [21] observed the production of 2.58×10^6 structures per Petri dish of spores of *A. musiformis* in YPSSA. Zhao et al. [22] showed that the disruption of *AoMls* gene of enzyme in the glyoxylate cycle, virulence factor in microbial pathogens from the nematode-trapping fungus *Arthrobotrys oligospora*, led to a significant reduction in conidiation and failure to utilize fatty acids and sodium acetate for growth, and its conidia were unable to germinate on minimal medium supplemented with sodium oleate.

The production of spores of *T. esau* alone was 7.9×10^7 conidia per plate and associated with *D. flagrans*, *A. musiformis*, or *C. rosea* was 4.8×10^7, 1.4×10^7, and 2.4×10^6 structures, respectively, reducing the spores production by 39.24, 82.27, and 96.96%, respectively, with statistically significant difference ($p < 0.01$), between the production alone and in association with other fungi (Table 1 and Figure 1(b)). These results support the data previously cited in which the fungal antagonism is exacerbated by producers species metabolites. This fact is highlighted by Hernández Mansilla et al. [19] who observed the antagonism of different species of *Trichoderma* on fungi phytopathogens that attack the pineapple.

The *C. rosea* isolate grown alone produced 2.8×10^8 conidia per plate and in association with *D. flagrans*, *T.*

esau, and *A. musiformis* produced 3.5×10^7, 2.3×10^7, and 4.7×10^7 spores, respectively. The spores production of this isolate grown in association with *D. flagrans*, *T. esau*, or *A. musiformis* reduced spores production by 95.20, 96.84, and 93.56%, respectively, demonstrating suffering great antagonism from these species (Table 1 and Figure 1(d)). According to Sun et al. [23] the proportion of resistant spores of *C. rosea* 67-1 increased to 17.4 and 15.5% in potato dextrose and rice meal media, respectively, in 8 days and the percentage of chlamydospores decreased rapidly with increased pH. Viccini et al. [24] observed that using rice as a substrate after 15 days of culture in plastic bottles and bags resulted in a production of 3.4×10^9 and 1.1×10^8 spores, respectively, per gram of dry matter, confirming the high productive potential of these fungal species.

Evaluating the production of reproductive structures presented in Table 1 demonstrates that all fungal isolates tested, producers metabolites and predators, exert strong antagonism when grown in conjunction, negatively influencing the production of spores in percentages ranging from 39.24 to 99.99% ($p < 0.01$); this fact exemplifies for the largest gathering and isolation of certain species in detriment to others in various environmental conditions.

3.2. Assay B: "In Vitro" Predation Test. In relation to "*in vitro*" test in this work it was observed that predators fungi *D. flagrans* and *A. musiformis* have the highest percentage of reduction of larvae compared with metabolites producers fungi. Santos et al. [25] assessed, in coprocultures performed using cattle faeces collected on the third day after the oral administration of large concentrations (200 grams' grain/animal) of isolate *A. musiformis*, 99% reduction in the number of L_3 gastrointestinal nematodes. del Carmen Acevedo Ramírez et al. [26] isolated and identified isolates of *A. musiformis* in different regions of Mexico demonstrating their effectiveness *in vitro* against *H. contortus* infective larvae. Gutiérrez et al. [27] observed "*in vitro*" a reduction of 97% of L_3 of *H. contortus* and 75% of (L_4) histotrophic larvae by species, *A. musiformis*. Ojeda-Robertos et al. [28] observed that, after oral administration of chlamydospores of *D. flagrans* to naturally infected sheep, this isolate was able to reduce the number of larvae and eggs per gram of faeces in "*in vitro*" test confirming the predatory potential of these species on gastrointestinal helminths of veterinary and zootechnical importance.

The literature is scarce in studies that evaluate predatory activity of *T. esau* and *C. rosea* against gastrointestinal nematode infective larvae. In agricultural activities Ruano-Rosa et al. [29] observed that combinations of *T. atroviride* with strains *P. chlororaphis* and *P. pseudoalcaligenes* significantly improved the control of white root rot (WRR) caused by *R. necatrix* during the *in vitro* experiments, though a protective effect of *Trichoderma* and some bacteria has been observed in the control of WRR avocado when applied alone.

According to Baloyi et al. [9] isolate of *C. rosea* reduced nematode counts by 44% to 69.9%, in the faecal bioassay and in the water bioassay of 62.7% to 89.3% were observed. According to Ahmed et al. [30] *A. comosus* combined with *C. rosea* (AcCr) is better at controlling nematodes of sheep within a treatment which were paired and penned in individual paddocks than either Ac or Cr individually. *A. comosus* or AcCr reduced EPG and L_3 counts on grass, but *C. rosea* only reduced L_3. The daily feed of Merino sheep with 0.25, 0.5, and 1.0 g of *C. rosea* chlamydospores per kilogram BW reduced larval development (LD) time on day 70 of treatment by 33, 72, and 89%, respectively, in pastures. In the control group, LD was reduced by only 2.6% as the number of larvae per gram in faecal cultures [31].

On the other hand studies evaluating the use of fungal associations with different mechanisms of action are still emerging in the agriculture and animal sector. Tavela et al. [32] showed that the fungal isolates *Pochonia chlamydosporia*, *D. flagrans*, and *Monacrosporium thaumasium* were efficient in controlling horse cyathostomin under *in vitro* conditions, acting alone or in conjunction.

The findings in this study show the existence of fungal antagonism in the production of reproductive structures between species with potential use for control of gastrointestinal nematodes of domestic animals, especially among isolates predators and those producers of metabolites, although predatory reduction has not been observed in the effectiveness of this species. The biotic research in site for application nematophagous fungi with objective environmental control of gastrointestinal nematodes must be thoroughly investigated in order to obtain success in the parasite control program to be implemented.

Conflict of Interests

The authors declare that they have no conflict of interests.

References

[1] A. F. T. do Amarante, "Why is it important to correctly identify *Haemonchus* species?" *Revista Brasileira de Parasitologia Veterinaria*, vol. 20, no. 4, pp. 263–268, 2011.

[2] M. E. da Silva, F. R. Braga, L. A. Borges et al., "Evaluation of the effectiveness of *Duddingtonia flagrans* and *Monacrosporium thaumasium* in the biological control of gastrointestinal nematodes in female bovines bred in the semiarid region," *Veterinary Research Communications*, vol. 38, no. 2, pp. 101–106, 2014.

[3] M. B. Molento, M. Almeida, E. Guterres, J. Roman, F. Freitas, and M. Rocha, "Bezerras de corte infectadas naturalmente com parasitas gastintestinais—epidemiologia e tratamento e tratamento seletivo," *Archives of Veterinary Science*, vol. 10, pp. 45–50, 2005.

[4] F. R. Braga and J. V. de Araújo, "Nematophagous fungi for biological control of gastrointestinal nematodes in domestic animals," *Applied Microbiology and Biotechnology*, vol. 98, no. 1, pp. 71–82, 2014.

[5] A. S. Maciel, J. V. Araújo, and A. K. Campos, "Viabilidade sobre larvas infectantes de *Ancylostoma* spp dos fungos nematófagos *Arthrobotrys robusta*, *Duddingtonia flagrans* e *Monacrosporium thaumasium* após esporulação em diferentes meios de cultura," *Revista Brasileira de Parasitologia Veterinária*, vol. 15, pp. 182–187, 2006.

[6] P. Mendoza-de-Gives and F. Torres-Acosta, "Biotechnological use of fungi in the control of ruminant parasitic nematodes," in *Fungi: Types, Environmental Impact and Role in Disease*, M. S.

Arias and A. Paz-Silva, Eds., pp. 389–408, Nova Editorial, New York, NY, USA, 2012.

[7] R. C. L. Assis, F. D. Luns, J. V. Araújo et al., "Comparison between the action of nematode predatory fungi *Duddingtonia flagrans* and *Monacrosporium thaumasium* in the biological control of bovine gastrointestinal nematodiasis in tropical southeastern Brazil," *Veterinary Parasitology*, vol. 193, no. 1–3, pp. 134–140, 2013.

[8] J. Li, J. Yang, X. Huang, and K.-Q. Zhang, "Purification and characterization of an extracellular serine protease from *Clonostachys rosea* and its potential as a pathogenic factor," *Process Biochemistry*, vol. 41, no. 4, pp. 925–929, 2006.

[9] M. A. Baloyi, M. D. Laing, and K. S. Yobo, "Isolation and *in vitro* screening of *Bacillus thuringiensis* and *Clonostachys rosea* as biological control agents against sheep nematodes," *African Journal of Agricultural Research*, vol. 6, no. 22, pp. 5047–5054, 2011.

[10] B. Martínez, D. Infante, and Y. Reyes, "*Trichoderma* spp. y su función en el control de plagas en los cultivos," *Revista de Protección Vegetal*, vol. 28, no. 1, pp. 1–11, 2013.

[11] G. R. Stirling, *Biological Control of Plant Parasitic Nematodes: Progress, Problems and Prospects*, CAB International, Wallingford, UK, 1991.

[12] F. A. A. M. De leij, B. R. Kerry, and J. A. Dennehy, "The effect of fungal application rate and nematode density on the effectiveness of *Verticillium chlamydosporium* as a biological control agent for *Meloidogyne incognita*," *Nematologica*, vol. 38, no. 1–4, pp. 112–122, 1992.

[13] E. A. Lopes, S. Ferraz, P. A. Ferreira et al., "Potencial de isolados de fungos nematófagos no controle de *Meloidogyne javanica*," *Nematologia Brasileira*, vol. 31, pp. 78–84, 2007.

[14] A. Swe, J. Li, K. Q. Zhang, S. B. Pointing, R. Jeewon, and K. D. Hyde, "Nematode-trapping fungi," *Current Research in Environmental & Applied Mycology*, vol. 1, pp. 1–26, 2011.

[15] M. E. da Silva, J. V. de Araújo, F. R. Braga, F. E. D. F. Soares, and D. S. Rodrigues, "Control of infective larvae of gastrointestinal nematodes in heifers using different isolates of *Nematophagous fungi*," *Revista Brasileira de Parasitologia Veterinaria*, vol. 22, no. 1, pp. 78–83, 2012.

[16] F. R. Braga, R. O. Carvalho, A. R. Silva et al., "Predatory capability of the nematophagous fungus *Arthrobotrys robusta* preserved in silica gel on infecting larvae of *Haemonchus contortus*," *Tropical Animal Health and Production*, vol. 46, no. 3, pp. 571–574, 2014.

[17] R. D. Llerandi-Juárez and P. Mendoza-de Gives, "Resistance of chlamydospores of nematophagous fungi to the digestive processes of sheep in Mexico," *Journal of Helminthology*, vol. 72, no. 2, pp. 155–158, 1998.

[18] M. F. Sagüés, L. A. Fusé, L. E. Iglesias, F. C. Moreno, and C. A. Saumell, "Optimization of production of chlamydospores of the nematode-trapping fungus *Duddingtonia flagrans* in solid culture media," *Parasitology Research*, vol. 112, pp. 1047–1051, 2013.

[19] A. A. Hernández Mansilla, B. L. M. García, C. R. Álvarez, C. C. González, Á. C. P. González, and A. L. Mayea, "Control químico de patógenos fungosos en piña de vivero (I)," *Fitosanidad*, vol. 14, no. 1, pp. 31–37, 2010.

[20] M. I. Boguś, M. Czygier, E. Kędra, and J. Samborski, "In vitro assessment of the influence of nutrition and temperature on growing rates of five *Duddingtonia flagrans* isolates, their insecticidal properties and ability to impair *Heligmosomoides polygyrus* motility," *Experimental Parasitology*, vol. 109, no. 2, pp. 115–123, 2005.

[21] W. P. Dias and S. Ferraz, "Crescimento e esporulação de *Arthrobotrys* spp em diferentes substratos, meios de cultura, pH e níveis de temperatura," *Nematologia Brasileira*, vol. 17, pp. 168–181, 1992.

[22] X. Zhao, Y. Wang, Y. Zhao, Y. Huang, K.-Q. Zhang, and J. Yang, "Malate synthase gene AoMls in the nematode-trapping fungus *Arthrobotrys oligospora* contributes to conidiation, trap formation and pathogenicity," *Applied Microbiology and Biotechnology*, vol. 98, no. 6, pp. 2555–2563, 2014.

[23] M. H. Sun, Y. M. Chen, J. F. Liu, S. D. Li, and G. Z. Ma, "Effects of culture conditions on spore types of *Clonostachys rosea* 67-1 in submerged fermentation," *Letters in Applied Microbiology*, vol. 58, no. 4, pp. 318–324, 2014.

[24] G. Viccini, M. Mannich, D. M. F. Capalbo, R. Valdebenito-Sanhueza, and D. A. Mitchell, "Spore production in solid-state fermentation of rice by *Clonostachys rosea*, a biopesticide for gray mold of strawberries," *Process Biochemistry*, vol. 42, no. 2, pp. 275–278, 2007.

[25] C. P. Santos, T. Padilha, and C. A. Saumell, "Efficacy of *Arthrobotrys musiformis* in reducing infective larvae of trichostrongylid nematodes in fecal cultures after passage through bovine gastrointestinal tract," in *Simpósio de Controle Biológico*, vol. 5, p. 65, Anais, Embrapa-CNPSO, Foz do Iguaçu, Brazil, 1996.

[26] P. M. del Carmen Acevedo Ramírez, H. Quiroz-Romero, R. O. Valero-Coss, P. Mendoza-de-Gives, and P. J. L. Gomez, "Nematophagous fungi from Mexico with activity against the sheep nematode *Haemonchus contortus*," *Revista Ibero-Latinoamericana de Parasitología*, vol. 70, no. 1, pp. 101–108, 2011.

[27] I. C. F. Gutiérrez, P. M. Mendoza-de-Gives, E. L. Hernández, M. E. López-Arellano, R. O. Valero-Coss, and V. M. H. Velázquez, "Nematophagous fungi (Orbiliales) capturing, destroying and feeding on the histotrophic larvae of *Haemonchus contortus* (Nematoda: Trichostrongylidae)," *Revista Mexicana de Micología*, vol. 33, pp. 29–35, 2011.

[28] N. F. Ojeda-Robertos, J. F. D. J. Torres-Acosta, A. J. Aguilar-Caballero et al., "Assessing the efficacy of *Duddingtonia flagrans* chlamydospores per gram of faeces to control *Haemonchus contortus* larvae," *Veterinary Parasitology*, vol. 158, no. 4, pp. 329–335, 2008.

[29] D. Ruano-Rosa, F. M. Cazorla, N. Bonilla, R. Martín-Pérez, A. De Vicente, and C. J. López-Herrera, "Biological control of avocado white root rot with combined applications of *Trichoderma* spp. and rhizobacteria," *European Journal of Plant Pathology*, vol. 138, no. 4, pp. 751–762, 2014.

[30] M. Ahmed, M. D. Laing, and I. V. Nsahlai, "A new control strategy for nematodes of sheep using chlamydospores of a fungus, *Clonostachys rosea f. rosea*, and an ethanolic extract of a plant, *Ananas comosus*," *Biocontrol Science and Technology*, vol. 24, no. 8, pp. 860–871, 2014.

[31] M. Ahmed, M. D. Laing, and I. V. Nsahlai, "Use of *Clonostachys rosea* against sheep nematodes developing in pastures," *Biocontrol Science and Technology*, vol. 24, no. 4, pp. 389–398, 2014.

[32] A. O. Tavela, J. V. Araújo, F. R. Braga et al., "In vitro association of nematophagous fungi *Duddingtonia flagrans* (AC001), *Monacrosporium thaumasium* (NF34) and *Pochonia chlamydosporia* (VC1) to control horse cyathostomin (Nematoda: Strongylidae)," *Biocontrol Science and Technology*, vol. 22, no. 5, pp. 607–610, 2012.

Hindawi Publishing Corporation
BioMed Research International
Volume 2015, Article ID 474879, 5 pages
http://dx.doi.org/10.1155/2015/474879

Research Article

Efficacy of *Clonostachys rosea* and *Duddingtonia flagrans* in Reducing the *Haemonchus contortus* Infective Larvae

Manoel Eduardo da Silva,[1,2] Fabio Ribeiro Braga,[3] Pedro Mendoza de Gives,[4] Miguel Angel Mercado Uriostegui,[4] Manuela Reyes,[5] Filippe Elias de Freitas Soares,[6] Lorendane Millena de Carvalho,[1] Francielle Bosi Rodrigues,[6] and Jackson Victor de Araújo[1]

[1]*Departamento de Veterinária, Universidade Federal de Viçosa, 36570000 Viçosa, MG, Brazil*
[2]*URECO/EPAMIG, 35650000 Pitangui, MG, Brazil*
[3]*Universidade Vila Velha, Vila Velha, ES, Brazil*
[4]*Área de Helmintologia, CENID-Parasitologia, INIFAP, Jiutepec, MOR, Mexico*
[5]*Departamento de Microbiología Ambiental y Biotecnología, UAC, CAM, Mexico*
[6]*Programa de Pós Graduação em Ciências Farmacêuticas (PPGF-UVV), Universidade Vila Velha, 29102920 Vila Velha, ES, Brazil*

Correspondence should be addressed to Fabio Ribeiro Braga; fabioribeirobraga@hotmail.com

Received 29 January 2015; Accepted 10 April 2015

Academic Editor: José L. Campos

The biocontrol is proven effective in reducing in vitro and in situ free-living stages of major gastrointestinal helminths, allowing progress in reducing losses by parasitism, maximizing production, and productivity. This study aimed at evaluating the predatory activity of fungal isolates of *Duddingtonia flagrans* and *Clonostachys rosea* species and its association on infective larvae (L_3) of *H. contortus* in microplots formed by grasses and maintained in a protected environment. All groups were added with 10 mL of an aqueous suspension with 618 *H. contortus* L_3 approximately. Group 1 was used as control and only received the infective larvae. Groups 2 and 3 received *D. flagrans* chlamydospores and *C. rosea* conidia at doses of 5×10^6. Group 4 received the combination of 5×10^6 *D. flagrans* chlamydospores + 5×10^6 *C. rosea* conidia. *D. flagrans* and *C. rosea* showed nematicidal effectiveness reducing by 91.5 and 88.9%, respectively, the population of *H. contortus* L_3. However, when used in combination efficiency decreased to 74.5% predation of *H. contortus* L_3. These results demonstrate the need for further studies to determine the existence of additive effects, synergistic or antagonistic, between these species.

1. Introduction

Endoparasitic nematodiasis are considered as one of the main factors seriously affecting the livestock industry, since they cause an important reduction not only in the animal weight but also their main products; that is, meat and milk are also diminished [1]. Other problems derived from nematode parasitic infections are the continuous expenses in chemical treatments and eventually the death of young animals [2]. The use of chemical drugs is so far the unique method of anthelmintic control that is established around the world [3]. Unfortunately the use of drugs and other measures of control is in most of the cases not based on the adequate recommendations, that is, the general animal state, body weight, diagnosis of parasitic burden, and other important factors that should be considered to establish a successful control as quantity and quality of food, selection of gastrointestinal parasitic genetically resistant animals, and the presence of parasites resistance to chemical drugs [4].

A number of alternatives of control different than the use of chemical drugs are being proposed, although the most promising measure of control is the use of natural nematode antagonists like nematophagous fungi [5, 6]. Allied to chemical control, one of the most promising and sustainable

methods of control is biological control, which has shown a good effectiveness either in laboratory trials or in pasture experiments which is an important activity reducing the free-living stages of mayor gastrointestinal helminths. This method can be considered as a useful tool of control which reduces the economic losses caused by parasites and can promote a higher animal productivity [7, 8].

The species *Clonostachys rosea* belonging to the order Hypocreales (family: Bionectriacea) has being recorded as a parasite of other microfungi and also as a nematode parasite, apart from being a saprophyte fungus [9]. This species colonizes plants and it has attracted interest by workers as a potential biological control agent, since it produces volatile organic compounds toxic for some living organisms [10, 11].

Duddingtonia flagrans is an "old friend" of scientists who envision biological control as an alternative to the treatment of herd animals by chemical means and also in the future of prevention of high levels of contamination by nematodes in public areas and squares used by humans [3, 12]. Again it must be remembered here that the ability to pass through the gastrointestinal tract of domestic animals makes this species of fungus an eternal ally in combating nematodes present in the environment [13].

This fungal species is said to be the "most promising." Its main focus of activity culminates in the predation of infective helminth forms (in this case, nematode larvae), by means of simple adhesive hyphae.

The fungus *D. flagrans* belonging to the order Moniliales (family: Moniliaceae) is one of the most promising microorganisms for biological control of ruminant parasitic nematodes [14]. This species is harmless to plants, animals, and human being [15, 16] and it is possible to isolate it mainly from soil samples and animal faeces [17]. This microorganism possesses dual food habits, being saprobius in absence of nematodes and becoming either predatory or parasite of nematodes in the presence of them [18].

Taking into account the representation of the world livestock and its socioeconomics, it is important to evaluate, improve, and provide the use of technologies that can contribute to the development of this segment of agrobusiness. The aim of this study was to evaluate the predatory activity of fungal isolates of the species *C. rosea* and *D. flagrans* and their association on *H. contortus* infective larvae (L_3) in microplots with graminaceous forage plant.

2. Material and Methods

2.1. Fungi. The *C. rosea* Yucatan strain, belonging to the CICY collection, was used. This strain was maintained in 2% water-agar (2% WA) at the Department of Helminthology (CENID-PAVET-INIFAP-MEXICO). The *D. flagrans* fungal strain (FTHO-8) belonging to the Fungal Collection of CENID-Parasitología Veterinaria, INIFAP-Mexico, was used. This strain was originally obtained from a sheep faecal sample from a farm at Fierro del Toro Village, Huitzilac Municipality, Morelos State, Mexico [19].

2.2. Nematodes. A *H. contortus* isolate was originally obtained from a naturally infected sheep from "Las Margaritas" Experimental Sheep Farm (INIFAP) in Hueytamalco Municipality in the state of Puebla, Mexico. A *H. contortus* egg donor lamb was orally infected with an aqueous suspension containing 350 larvae/kg of body weight. Twenty days after infection the presence of *H. contortus* eggs in faecal samples was detected through the McMaster technique. Faecal cultures were prepared by mixing faeces with polystyrene particles in plastic bowls. Water was added to the faecal cultures and the mixture was homogenized to keep the cultures hydrated and oxygenated to promote better larval hatching [20]. Faecal cultures were covered with paper foil and incubated for 7 days at room temperature (25–30°C). Infective larvae were extracted from faeces using the Baermann funnel technique [21]. The larvae were washed several times in density gradients of 50% sucrose solution and rinsed and suspended in sterile water.

2.3. Assay. The pots were conformed as follows: thirty-six plastic (gardening) pots with a capacity of 100 grams (75 × 55 mm) were used. Seventy grams of soil acquired from commercial nurseries was autoclaved at 1.2 atm and 115°C for 15 minutes and added to the plastic pots. Every pot with soil was added with 0.06 grams of a commercial mixture of different genera/species grass seeds; about 70 graminaceous seeds were added to the soil surface in order to obtain a homogeneous grass growing. Six mL of top water was added to every pot every day during 18 days of the experiment using a Pasteur pipette to maintain the pots humidity.

After germination the pots were randomly divided into four (4) experimental groups with 8 replicates each. All groups were added with 10 mL average of an acqueos suspension with 618 *H. contortus* L_3 approximately. Group 1 was used as control and only received the infective larvae. Groups 2 and 3 received *D. flagrans* chlamydospores and *C. rosea* conidia at doses of 5×10^6, respectively. Group 4 received the combination of 5×10^6 *D. flagrans* chlamydospores + 5×10^6 *C. rosea* conidia.

The pots were maintained under a shading rate hedging protected screen and after 12 days of interaction between nematophagous fungi and parasitic nematodes, the whole nematode population from total soil and grass of every single pot was recovered using the Baermann Funnel method [21].

2.4. Location. The experiment was conducted in CENID-PAVET-INIFAP-MEXICO, located at 18°53′04″ N latitude and 98°51′34″ W and 1615.16 meters above sea level, in the municipality of Jiutepec, Morelos, Mexico.

2.5. Weather Data. Meteorological data including maximum and minimum temperatures, relative humidity, and rainfall during the experiment were obtained from the closest experimental weather station (National Institute for Water Technology), Jiutepec, Morelos, Mexico.

2.6. Statistical Analysis. Data were analysed using an ANOVA test and the Tukey test was used as a complementary technique for discriminating the mean different from the others. Data were analysed using the software BioEstat 5.3.

Table 1: Number and percentage of reduction of *Haemonchus contortus* L_3 recovered by the method of Baermann 12 days after interaction with fungal isolates *Clonostachys rosea* and *Duddingtonia flagrans*, and association of these microfungi.

Treatment	Control	*C. rosea*	*D. flagrans*	*D. flagrans* + *C. rosea*
H. contortus	118 (±114)[a]	13 (±19)[b]	10 (±15)[b]	30 (±19)[b]
% reduction L_3	0	88.9%	91.5%	74.5%

[*] Different small letters in rows indicate the existence of a statistical difference ($p < 0.01$).

3. Results and Discussion

The results are shown in Table 1, which shows the mean, standard deviation, and the *H. contortus* larvae reduction percentage after being recovered from pots after 12 days of interaction between nematophagous fungi and nematode larvae. The average temperature value during the experimental period was 16.1°C, ranging from 15 to 33°C; the environmental relative humidity was 71.03%, ranging from 15.2 to 108% and 7 mm of rain. These environmental conditions are considered as ideal for the development of ruminant parasitic larvae [22] and nematophagous fungi [23].

The results obtained using *D. flagrans* in reducing the nematode larvae population into animal faeces have generated the development of studies focused on the production of chlamydospores which are resistant stages of some microfungi for the control of ruminant parasitic nematodes [13]. The results of the present work are promising and an important reduction in the larval population recovered from treated pots has shown evidence that fungi produce satisfactory results with the use of 5×10^6 conidia and chlamydospores per pot; and although this is only a model of study, it gives a clear image about the potential use of this biological system of control of infective larvae on the contaminated grass.

The recovery larvae mean values have shown statistical difference among the treated groups when compared with control group ($p < 0.001$). However, no differences were found among the treated groups ($p > 0.005$) (Table 1). Such results corroborate those published of De Almeida et al. [24] that demonstrated high effectiveness of the specie *D. flagrans* against different genera of parasites affecting ruminants such as *Haemonchus, Teladorsagia,* and *Trichostrongylus*.

The nematophagous *C. rosea* fungus was able to reduce by 88.9% the number *H. contortus* L_3. *D. flagrans* was able to reduce by 91.5% the number *H. contortus* L_3. The association of the micro fungi *D. flagrans* and *C. rosea* was able to reduce 74.5% of *H. contortus* (L_3) infective larvae.

Higher in vitro reductions (94.21–99.61%) in the *H. contortus* L_3 population by different *D. flagrans* isolates were recently found by Priego-Cortes [25], although it is important to remark that this research was performed under in vitro conditions on water agar plates. In the same work the in vitro activity of *D. flagrans* isolates, FTHO-8, M3, and DFIPC, showed 99.2, 98.23, and 98.8% reductions against the root-knot nematode *Meloidogyne* sp. Such results are encouraging in searching for a fungal candidate as a potential agent of agricultural pest control.

Assis et al. [5] evaluated the predatory activity of *D. flagrans* and *M. thaumasium* in the control of nematodiasis in grazing cattle by administering fungal pellets obtaining a reduction of 47.8 and 56.67% of the number of larvae, respectively, and these results were lower than those found in our study, although conducted in animals grazing.

In the present study, the nematophagous fungus *C. rosea* reduced by 76.9% the number of *H. contortus* L_3 under environmental conditions. Similar results were recently obtained using two isolates, *C. rosea* (Yucatán strain) and *Clonostachys* sp.

One Campeche strain *C. rosea* reduced 84.2 and 59.5% *H. contortus* L_3, respectively. These fungi also showed 94.3 and 95.9% reduction on the phytonematode *Meloidogyne* sp. (J2), respectively [26].

Baloyi et al. [27] evaluated the in vitro predatory activity of *C. rosea* (in faeces and in water) against trichostrongylids larvae and they reported 69.9 and 89.3%, reductions, respectively, of the number of trichostrongylids larvae in bioassays made in sheep feces and water. On the other hand, Rodriguez-Martínez [28] evaluated in vitro predatory activity of *C. rosea* against *Rhabditis* sp., *Caenorhabditis elegans*, *Panagrellus redivivus, Butlerius* sp., and *H. contortus* and they recorded 71.9, 94.7, 92.7, 100, and 87.7%, larvae reductions, respectively. Their results have shown evidence about the potential of these species in the control of parasites of veterinary importance. These results are similar to those described in the present work performed in soil pots.

Dong et al. [10] showed that the metabolites obtained of *C. rosea* were lethal 24 hours after treatment to 50% of *C. elegans, P. redivivus,* and *B. xylophilus* larvae; in our work we obtained better results of predation for free-living nematodes same test being done in vivo. Other researches in phytopathology highlight the relevance and efficiency of the species *C. rosea* as entomopathogenic against *Cicadellidae hemiptera*, causing, respectively, 82.5 and 45% mortality in *Oncometopia tucumana* and *Tapajosa rubromaginata* at 14 days after incubation [29]. Vega et al. [30] showed that *C. rosea* and *B. bassiana* associated were able to reduce 82.5% of the insects *Hypothenemus hampei* in coffee beans and Carreño-Perez et al. [31] showed that *C. rosea* reduction 79% of diseases caused by plant pathogenic fungus *Phytophthora cactorum* isolated on apple fruits.

According to Ayers et al. [32] a group of compounds extracted from *C. candelabrum* showed 90% of efficacy against *H. contortus*. These compounds were synthesized by Rama Rao [11], the macrolide clonostachydiol derived from *C. cilindrospora* that showed 80–90% of reduction of *H. contortus* in artificially infected sheep when subcutaneously administered at a dose of 2.5 mg/kg, corroborating with 21 our results, although we have worked with environmental control.

The association of the micro fungi *D. flagrans* and *C. rosea* was able to reduce 74.5% of *H. contortus* (L_3) infective larvae. Furthermore Baloyi et al. [27] demonstrated that the combination of *B. thuringiensis* and *C. rosea* showed an additive effect in vitro causing a mortality of 76.7% of parasites nematode of sheep possibly due to the action of *C. rosea* (enzyme production) and *B. thuringiensis* (endotoxin production).

Some studies have noted the combination of nematophagous fungi under natural conditions to combat parasitic forms (eggs and/or larvae) of gastrointestinal nematode parasites. This association of fungi has been tested and the results are relevant. Tavela et al. (2013) reported that the nematophagous fungi have been used as an alternative for controlling gastrointestinal nematodes from domestic animals under natural and laboratory conditions. At that time, those authors demonstrated that the associations of *D. flagrans* and *M. thaumasium* were viable after passing through the gastrointestinal tract in horses and could be used under natural conditions. However, these authors have stated that it is unclear "whether the association of some of these species could bring some kind of advantage," from the biological point of view, since the antagonism or synergism between species must be better understood.

In the present study, the association of *Clonostachys* and *D. flagrans* was effective and can be used in new experimental designs under laboratory conditions and in the field. *C. rosea* and *D. flagrans* have shown nematicidal effectiveness when were used alone or in combination, effectively reducing the population of infective larvae (L_3) of *H. contortus* in controlled environmental conditions.

However, the authors believe that there is a need for further studies to determine the existence of additive, synergistic, or antagonistic effects between these species. It is read here that Braga et al. (2014) discuss the predatory activity of an isolate from the nematophagous fungus *Arthrobotrys robusta*, as an example of predatory activity on L_3 of *H. contortus*. At that time, the authors demonstrated a percentage reduction of 73.8% by the end of seven days. Thus, in this study, it is suggested that the tested association (*Clonostachys* + *Duddingtonia*) could be further explored in future studies of biological control, since the percentage obtained was 74.5%. This is the first report of *C. rosea* and *D. flagrans* association and is the first report to control *H. contortus* in environmental conditions.

Conflict of Interests

The authors declare that they have no conflict of interests.

Acknowledgments

The authors also would like to thank CNPq, Capes, Fapes, and Fapemig for financial support and grant concession.

References

[1] F. Pisseri, C. Benedictis, S. P. Roberti, and B. Azzarello, "Sustainable animal production, systemic prevention strategies in parasitic diseases of ruminants," *Alternative and Integrative Medicine*, vol. 2, no. 2, 2013.

[2] A. Al-Rofaai, W. A. Rahman, and M. Abdulghani, "Sensitivity of two in vitro assays for evaluating plant activity against the infective stage of *Haemonchus contortus* strains," *Parasitology Research*, vol. 112, no. 2, pp. 893–898, 2013.

[3] F. R. Braga and J. V. de Araújo, "Nematophagous fungi for biological control of gastrointestinal nematodes in domestic animals," *Applied Microbiology and Biotechnology*, vol. 98, no. 1, pp. 71–82, 2014.

[4] A. S. Cezar, J. B. Catto, and I. Bianchin, "Controle alternativo de nematódeos gastrintestinais dos ruminantes: atualidade e perspectivas," *Ciência Rural*, vol. 38, no. 7, pp. 2083–2091, 2008.

[5] R. C. L. Assis, F. D. Luns, J. V. Araújo et al., "Comparison between the action of nematode predatory fungi *Duddingtonia flagrans* and *Monacrosporium thaumasium* in the biological control of bovine gastrointestinal nematodiasis in tropical southeastern Brazil," *Veterinary Parasitology*, vol. 193, no. 1–3, pp. 134–140, 2013.

[6] P. Mendoza-de-Gives and J. F. J. Torres-Acosta, "Biotechnological use of fungi in the control of ruminant parasitic nematodes," in *Fungi: Types, Environmental Impact and Role in Disease*, V. Arias and A. Paz-Silva, Eds., Nova Science Publishers, New York, NY, USA, 2012.

[7] F. R. Braga, J. V. Araújo, F. E. F. Soares et al., "Interaction of the nematophagous fungus *Duddingtonia flagrans* on *Amblyomma cajannense* engorged females and enzymatic characterisation of its chitinase," *Biocontrol Science and Technology*, vol. 23, no. 5, pp. 584–594, 2013.

[8] V. L. R. Vilela, T. F. Feitosa, F. R. Braga et al., "Biological control of goat gastrointestinal helminthiasis by *Duddingtonia flagrans* in a semi-arid region of the northeastern Brazil," *Veterinary Parasitology*, vol. 188, no. 1-2, pp. 127–133, 2012.

[9] J. Li, J. Yang, X. Huang, and K.-Q. Zhang, "Purification and characterization of an extracellular serine protease from *Clonostachys* rosea and its potential as a pathogenic factor," *Process Biochemistry*, vol. 41, no. 4, pp. 925–929, 2006.

[10] J.-Y. Dong, H.-P. He, Y.-M. Shen, and K.-Q. Zhang, "Nematicidal epipolysulfanyldioxopiperazines from *Gliocladium roseum*," *Journal of Natural Products*, vol. 68, no. 10, pp. 1510–1513, 2005.

[11] A. V. Rama Rao, V. S. Murthy, and G. V. M. Sharma, "Studies directed towards the synthesis of clonostachydiol. Part I," *Tetrahedron Letters*, vol. 36, no. 1, pp. 139–142, 1995.

[12] M. Faedo, M. Larsen, and S. Thamsborg, "Effect of different times of administration of the nematophagous fungus *Duddingtonia flagrans* on the transmission of ovine parasitic nematodes on pasture—a plot study," *Veterinary Parasitology*, vol. 94, no. 1-2, pp. 55–65, 2000.

[13] A. Paz-Silva, I. Francisco, R. O. Valero-Coss et al., "Ability of the fungus *Duddingtonia flagrans* to adapt to the cyathostomin egg-output by spreading chlamydospores," *Veterinary Parasitology*, vol. 179, no. 1–3, pp. 277–282, 2011.

[14] N. F. Ojeda-Robertos, J. F. J. Torres-Acosta, A. J. Ayala-Burgos, C. A. Sandoval-Castro, R. O. Valero-Coss, and P. Mendoza-de-Gives, "Digestibility of *Duddingtonia flagrans* chlamydospores in ruminants: In vitro and in vivo studies," *BMC Veterinary Research*, vol. 5, article 46, 2009.

[15] J. K. Chamuah, P. Perumal, and A. Mech, "Epidemiology and control measures of helminth parasites in small ruminants," *International Journal of Bio-Resource and Stress Management*, vol. 4, pp. 278–287, 2013.

[16] E. Jagla, E. Jodkowska, and M. Popiolek, "Alternative methods for the control of gastrointestinal parasites in horses with a special focus on nematode predatory fungi: a review," *Annals of Animal Science*, vol. 13, no. 2, pp. 217–227, 2013.

[17] M. Larsen, "Biological control of nematode parasites in sheep," *Journal of Animal Science*, vol. 84, pp. E133–E139, 2006.

[18] G. L. Barron, *The Nematode-Destroying Fungi*, Topics in Mycology no. 1, Canadian Biological Publications, Ontario, Canada, 1977.

[19] R. D. Llerandi-Juárez and P. Mendoza-de Gives, "Resistance of chlamydospores of nematophagous fungi to the digestive processes of sheep in Mexico," *Journal of Helminthology*, vol. 72, no. 2, pp. 155–158, 1998.

[20] E. Liébano-Hernández, "Identificación morfométrica de larvas infectantes de nematodos gastrointestinales y pulmonares en rumiantes domésticos de México," in *Diagnóstico y control de los nematodos gastrointestinales de los rumiantes en México*, V. M. V. Prats, Ed., pp. 27–34, 2nd edition, 2004.

[21] A. Chaney, *Identification of Internal Parasites of Sheep and Goats*, Honors College, 2012.

[22] E. Liébano-Hernández, "Ecología de larvas de nematodos gastrointestinales de bovinos, ovinos y caprinos," in *Epidemiología de Enfermidades Parasitarias em Animales Domésticos*, E. Q. Romero, J. A. F. Castillo, F. I. Velarde, and M. E. L. Arellano, Eds., Version Electronic, 1st edition, 2011.

[23] O. D. Dhingra and J. B. Sinclair, *Basic Plant Pathology Methods*, CRC Press, 1995.

[24] G. L. De Almeida, J. M. Santurio, J. O. J. Filho et al., "Predatory activity of the fungus Duddingtonia flagrans in equine strongyle infective larvae on natural pasture in the Southern Region of Brazil," *Parasitology Research*, vol. 110, no. 2, pp. 657–662, 2012.

[25] I. Priego-Cortes, *Aislamiento y caracterización morfológica y molecular del hongo nematófago Duddingtonia flagrans y evaluación de su actividad biológica in vitro en contra de nematodos de importancia para la industria agrícola y pecuaria [Tesis de Licenciatura]*, Universidad Politécnica del Estado de Morelos, 2013.

[26] S. Rojas-Jiménez, *Evaluación de la actividad nematicida in vitro del hongo Clonostachys spp en contra de Haemonchus contortus (L3) y Meloidogyne sp. (J2) [Tesis de Licenciatura]*, Universidad Politécnica del Estado de Morelos, 2013.

[27] M. A. Baloyi, M. D. Laing, and K. S. Yobo, "Isolation and in vitro screening of *Bacillus thuringiensis* and *Clonostachys rosea* as biological control agents against sheep nematodes," *African Journal of Agricultural Research*, vol. 6, no. 22, pp. 5047–5054, 2011.

[28] R. Rodriguez-Martínez, *Evaluación de la actividad letal in vitro del hongo nematófago Clonostachys rosea contra cinco nematodos diferentes [Tesis de Licenciatura]*, Facultad de Medicina Veterinaria y Zootecnia, Universidad del Estado de México, 2011.

[29] A. V. Toledo, E. Virla, R. A. Humber, S. L. Paradell, and C. C. L. Lastra, "First record of *Clonostachys rosea* (Ascomycota: Hypocreales) as an entomopathogenic fungus of *Oncometopia tucumana* and *Sonesimia grossa* (Hemiptera: Cicadellidae) in Argentina," *Journal of Invertebrate Pathology*, vol. 92, no. 1, pp. 7–10, 2006.

[30] F. E. Vega, F. Posada, M. Catherine Aime, M. Pava-Ripoll, F. Infante, and S. A. Rehner, "Entomopathogenic fungal endophytes," *Biological Control*, vol. 46, no. 1, pp. 72–82, 2008.

[31] A. J. Carreño Perez, J. O. Blanco Valbuena, and B. Villegas Estrada, "Selección de hongos biocontroladores de *Phytophthora cactorum*, agente causal de la pudrición radical y de corona en manzano," *Agronomia*, vol. 14, pp. 89–96, 2006.

[32] S. Ayers, D. L. Zink, K. Mohn et al., "Anthelmintic constituents of *Clonostachys candelabrum*," *Journal of Antibiotics*, vol. 63, no. 3, pp. 119–122, 2010.

Hindawi Publishing Corporation
BioMed Research International
Volume 2015, Article ID 719060, 12 pages
http://dx.doi.org/10.1155/2015/719060

Research Article

Biosorption of Pb(II) Ions by *Klebsiella* sp. 3S1 Isolated from a Wastewater Treatment Plant: Kinetics and Mechanisms Studies

Antonio Jesús Muñoz, Francisco Espínola, Manuel Moya, and Encarnación Ruiz

Department of Chemical, Environmental and Materials Engineering, University of Jaén, 23071 Jaén, Spain

Correspondence should be addressed to Encarnación Ruiz; eruiz@ujaen.es

Received 14 May 2015; Accepted 29 July 2015

Academic Editor: T. Komang Ralebitso-Senior

Lead biosorption by *Klebsiella* sp. 3S1 isolated from a wastewater treatment plant was investigated through a Rotatable Central Composite Experimental Design. The optimisation study indicated the following optimal values of operating variables: 0.4 g/L of biosorbent dosage, pH 5, and 34°C. According to the results of the kinetic studies, the biosorption process can be described by a two-step process, one rapid, almost instantaneous, and one slower, both contributing significantly to the overall biosorption; the model that best fits the experimental results was pseudo-second order. The equilibrium studies showed a maximum lead uptake value of 140.19 mg/g according to the Langmuir model. The mechanism study revealed that lead ions were bioaccumulated into the cytoplasm and adsorbed on the cell surface. The bacterium *Klebsiella* sp. 3S1 has a good potential in the bioremoval of lead in an inexpensive and effective process.

1. Introduction

Biotechnology has a great potential to remove heavy metals using the ability of different bacteria and other microorganisms to capture metal ions, mainly through biosorption. This ability has a high potential for the development of effective and economic processes for heavy metal bioremoval, especially for dilute solutions (<100 mg/L) [1]. Low cost is the most important advantage of biosorption over conventional treatments because biosorbents are usually inexpensive and abundant materials, and biosorption also often offers the advantages of metal recuperation and biomass regeneration [2]. The main mechanisms involved can be cell-surface binding, intracellular bioaccumulation, and extracellular precipitation [3]. The binding of metal on the cell surface can occur with living microorganism or death biomass. Nevertheless, metal bioaccumulation takes place only in living cells.

Microorganisms and other biomass types have the advantage of having components as lipopolysaccharides, proteins, and phospholipids which have many functional groups. These groups confer a negative charge and thus offer the possibility of adding metal cations. This ability is present in all types of biomass, dead or alive. In the case of living microorganisms, other active cellular mechanisms are involved: synthesis of specific enzymes, action of cytoplasmic or membrane proteins, and so forth [4, 5].

In order to improve biosorption effectiveness, the identification of additional microbial strains with high metal uptake capacity and specificity is a key aspect. In this way, the isolation of autochthonous microorganisms from contaminated sites is an interesting option to obtain metal-resistant strains [6–8].

Lead is known for its high environmental impact and toxicity [9]. This metal, along with mercury and cadmium, is considered one of "the big three" heavy metals present in contaminated effluents [2]. The European Directive 2008/105/EC includes lead and its compounds in the list of priority substances in environmental quality standards, establishing a concentration of lead of 0.0072 mg/L as the maximum permissible in the case of surface water.

In this work, the biosorption characteristics of *Klebsiella* sp. 3S1 were investigated. This strain is a bacterium selected from a group of microorganisms isolated from wastewater treatment plants that showed high resistance to several heavy metals, namely, Pb, Zn, and Ag [10]. Kinetic studies were conducted to determine the optimal working time. A Rotatable Central Composite Design (RCCD) with six central points was employed to optimise the operational conditions: sorbent dosage, pH, and temperature. The interactions between the experimental factors were evaluated by Response Surface Methodology (RSM). This technique has proved its effectiveness in optimising the variables that influence the adsorption process and reducing both time and cost [11–13]. Finally, equilibrium studies were performed. Additionally, potential mechanisms of biosorption were studied by FTIR, SEM, and TEM techniques.

2. Materials and Methods

2.1. Preparation of Klebsiella sp. 3S1. Ten strains were selected and identified by molecular techniques in a previous study from wastewater treatment plants [10]. After preliminary biosorption tests, the bacterial strain *Klebsiella* sp. 3S1 was selected for kinetic and equilibrium studies. This isolate showed 98% homology with that of standard *Klebsiella* species based on its 16S-rDNA gene sequence (1476 bp) and was named *Klebsiella* sp. 3S1 (GenBank accession number HE975030).

For the biosorption experiments, the biomass was prepared by incubating the strain in tryptic soy broth (TSB, 30 g/L) medium at 30°C with stirring, after centrifugation at 6000 rpm and washing twice with electrolyte solution. The cells of *Klebsiella* sp. 3S1 used in kinetic studies and the adsorption isotherm were harvested by centrifugation from exponential phase cultures. Then, the cells were resuspended in the lead solution.

2.2. FTIR Spectroscopy. The infrared spectra of the biomass samples before and after metal uptake were recorded using a VERTEX 70 (Bruker Corporation) Fourier transform infrared spectrometer operating in the range of 4000–400 cm^{-1}. Measurements were performed with lyophilised samples. The samples were measured using Attenuated Total Reflection (ATR). FTIR characterisation was performed to identify characteristic chemical functional groups of the bacterium *Klebsiella* sp. that might be involved in the metal uptake procedure.

2.3. FE-SEM-EDX Analysis. Field emission scanning electron microscopy (MERLIN of Carl Zeiss) coupled with energy dispersive X-ray spectroscopy was carried out to characterise the *Klebsiella* sp. 3S1 surface before and after Pb(II) ion uptake. Samples were fixed with a 2.5% glutaraldehyde solution in PBS (pH 7.4), dehydrated with increasing solutions of acetone (50, 70, 90, and 100%), and, finally, dried by critical point drying and metalized with carbon.

2.4. HR-TEM-EDX Analysis. High-resolution transmission electron microscopy and energy dispersive X-ray analysis (Philips CM-20) were used to determine the location of the metal within the cell. The samples were fixed, dehydrated, and dried as in the previous case; these were then treated with resin and were finally polymerised.

2.5. Batch Biosorption. The test solutions of Pb(II) were prepared using $Pb(NO_3)_2$ and 0.1 M NaCl as an electrolyte. The initial pH was controlled with 0.1 M NaOH or 0.1 M HNO_3.

The preliminary biosorption tests were performed in Erlenmeyer flasks with the ten strains (Section 2.1). The biosorbents were suspended in 50 mL of Pb(II) solution (25 mg/L) to reach different cell concentrations. The cell/metal suspension was gently agitated (200 rpm) at 30°C in an orbital shaker (CERTOMAT IS, Sartorius). To prevent precipitation of the metal, the lead solution was adjusted to pH 5.0. After 24 h, the metal solution was filtered (pore size 0.22 μm). Finally, the sample was acidified with HNO_3 and analysed by absorption atomic spectrometry (AAS) using an AANALYST 800 (Perkin Elmer) to know the final metal concentration. The tests for each strain were performed in triplicate.

Isothermal and kinetic studies were conducted as described above. Two kinetics experiments were performed, with two different concentrations of biomass and metal: Experiment number 1: 50 mg/L of Pb(II) and 0.11 g/L of dry biomass and Experiment number 2: 25 mg/L of Pb(II) and 0.28 g/L of dry biomass. The adsorbent was separated from the solution by centrifugation at predetermined time intervals (5–3600 min), with two flasks at each time point. Then, the residual lead concentration was analysed by AAS. The biosorption isotherm was obtained for a constant biomass concentration (0.52 g/L) and different concentrations of metal at 25°C.

In all cases, the amount of metal ions biosorbed per unit mass of dry biosorbent (lead biosorption capacity) was determined according to the following equation:

$$q = \frac{\left(C_i - C_f\right)V}{m}, \tag{1}$$

where q is the biosorption capacity (mg metal/g of the dry biosorbent); C_i and C_f are the initial and final metal concentrations, respectively; V is the liquid volume (0.05 L); and m is the amount of the biosorbent sample on a dry basis (g).

2.6. Experimental Design and Statistical Analysis. A Rotatable Central Composite Design (RCCD) with six central points was performed to evaluate the relationship between obtained results and experimental factors as well as optimise the working conditions. Biosorbent dosage (B), pH, and temperature (T) were chosen as independent variables, and the equilibrium biosorption capacity (q_e) was chosen as the dependent output response variable. The lead concentration used in all cases was 100 mg/L.

According to the RCCD, the total number of experimental combinations is $2^k + 2k + n_0$, where k is the number of independent variables and n_0 is the number of repetitions of the experiments at the centre point. The independent variables (factors), experimental range, and levels for lead

Table 1: Experimental design and response.

Run order	Factor			Response
	B: biosorbent dosage (mg/mL)	pH	T: temperature (°C)	q_e: biosorption capacity (mg/g)
12	0.55	5.50	25	104.02
6	0.80	4.30	34	118.51
13	0.55	4.75	10	80.97
11	0.55	4.00	25	87.42
1	0.30	4.30	16	67.27
15	0.55	4.75	25	105.02
18	0.55	4.75	25	105.75
4	0.80	5.20	16	86.16
10	1.00	4.75	25	94.99
19	0.55	4.75	25	108.65
5	0.30	4.30	34	127.21
9	0.10	4.75	25	122.13
3	0.30	5.20	16	76.36
7	0.30	5.20	34	138.52
16	0.55	4.75	25	105.31
2	0.80	4.30	16	79.17
20	0.55	4.75	25	106.18
8	0.80	5.20	34	119.79
14	0.55	4.75	40	163.53
17	0.55	4.75	25	106.18

removal are given in Table 1. The experimental design incorporated 20 experimental points, including six replicates at the central point.

The overall quadratic equation for biosorption capacity was

$$q_e = \beta_0 + \beta_1 B + \beta_2 \mathrm{pH} + \beta_3 T + \beta_{11} B^2 + \beta_{22} \mathrm{pH}^2 + \beta_{33} T^2 + \beta_{12} B\mathrm{pH} + \beta_{13} BT + \beta_{23} \mathrm{pH}T, \quad (2)$$

where q_e is equilibrium biosorption capacity (mg metal/g of the dry biosorbent); B is the biosorbent dosage; T is the temperature (°C); β_0 is the interception coefficient; β_1, β_2, and β_3 are the linear terms; β_{11}, β_{22}, and β_{33} are the quadratic terms; and β_{12}, β_{13}, and β_{23} are the interaction terms.

The response data were analysed by parameters obtained from the analysis of variance (ANOVA) using Design-Expert program, 8.0.7.1 version. The statistical significance was fixed at 5% probability level (p value = 0.05).

2.7. Modelling of Uptake Kinetics. To know the biosorption mechanisms and speed of the process, it is important to study the mass transfer and chemical reactions. To do this, the experimental data have been adjusted to several kinetic models. In most cases, it is assumed that adsorption is controlled by chemical reaction and not by diffusion, which contributes to the mechanical agitation. However, we have tested three kinetic models of chemical reaction control and one of intraparticle diffusion. The kinetic models tested are shown in Table 2. To adjust the experimental data to the kinetic models, we used the IBM SPSS Statistics software, 19 version (SPSS Inc. and IBM Company).

Table 2: Kinetic models tested.

Model	Equation
Pseudo-first order or Lagergren [14]	$\frac{dq}{dt} = k_1 (q_e - q)$
Pseudo-second order [15]	$\frac{dq}{dt} = k_2 (q_e - q)^2$
Elovich [16]	$\frac{dq}{dt} = ae^{-bq}$
Intraparticle diffusion or Weber and Morris [14]	$q = k\sqrt{t}$

q: biosorption capacity (mg/g) at time t, according to (1).
q_e: biosorption capacity (mg/g) at equilibrium.
k_1: pseudo-first-order kinetic rate constant (min^{-1}).
k_2: pseudo-second-order kinetic rate constant ($\mathrm{g{\cdot}mg^{-1}{\cdot}min^{-1}}$).
a: Elovich constant ($\mathrm{mg{\cdot}g^{-1}{\cdot}min^{-1}}$).
b: Elovich constant ($\mathrm{g{\cdot}mg^{-1}}$).
k: intraparticle diffusion rate constant in the bacterium ($\mathrm{mg{\cdot}g^{-1}{\cdot}min^{-1/2}}$).

2.8. Modelling of the Biosorption Isotherm. Several adsorption isotherms have been tested to fit experimental data. The most widely used among them are the Langmuir and Freundlich models; other well-known models are the Sips and Redlich-Peterson equations (Table 3). Adsorption isotherms originally used for gas phase adsorption can be readily adapted to correlate adsorption equilibrium in heavy metals biosorption. The Langmuir model establishes a relationship between the amount of gas adsorbed on a surface and the pressure of gas and assumes monolayer coverage of the adsorbate over a homogeneous adsorbent surface. The Freundlich model is an empirical equation, which assumes that as the adsorbate concentration in solution increases it also increases on

Table 3: Isotherm models used to represent the biosorption equilibrium.

Model	Equation
Langmuir [17]	$q_e = \frac{q_m b C_e}{1 + bC_e}$
Freundlich [18]	$q_e = K_F C_e^{1/n}$
Sips [19]	$q_e = \frac{K_s C_e^{1/n}}{1 + a_s C_e^{1/n}}$
Redlich-Peterson [20]	$q_e = \frac{K_{RP} C_e}{1 + a_{RP} C_e^{\beta}}$

q_e: biosorption capacity (mg/g) at equilibrium.
q_m: maximum biosorption capacity (mg/g).
b: Langmuir biosorption equilibrium constant (L/mg).
C_e: equilibrium concentrations of metal (mg/L).
K_F: characteristic constant related to the biosorption capacity.
n: characteristic constant related to the biosorption intensity.
K_s and a_s: Sips isotherm parameters.
K_{RP}, a_{RP}, and β: Redlich-Peterson parameters; and β varies between 0 and 1.

the adsorbent surface. This model can be applied to nonideal sorption on heterogeneous surfaces as well as to multilayer sorption. The Sips model is also called the Langmuir-Freundlich isotherm; this isotherm model incorporates features of both the Langmuir and Freundlich isotherms and may be used to represent adsorption equilibrium over a wide concentration range. The Redlich-Peterson model is another empirical equation that can represent adsorption equilibrium over a wide concentration range. When $\beta = 1$, it effectively reduces to a Langmuir isotherm, and when $\beta = 0$, it obeys Henry's law. To adjust the experimental data to kinetic models, IBM SPSS Statistics software described above was employed.

3. Results and Discussion

3.1. Preliminary Biosorption Tests. Ten strains isolated from wastewater treatment plants showed resistance to lead in our previous study [10]. Preliminary biosorption tests were performed on these strains to select the most appropriate one. Table 4 shows the results obtained, which range from 45 to 104 mg/g for fungi, 22 to 38 mg/g for yeast, and 78 to 90 mg/g for bacteria. The best results are obtained with the fungus *Trichosporon* sp. 1L1 and the bacterium *Klebsiella* sp. 3S1.

To choose the most suitable strain for heavy metals biosorption, other aspects of interest should be taken into account. It is very interesting to support microbial biomass in low cost inert solids. Therefore, microorganisms with greater ability to form biofilms are always the most appropriate [31]. This was the reason why that *Klebsiella* sp. 3S1 was chosen.

3.2. FTIR Spectroscopic Study. FTIR analysis was performed to identify the main functional groups and to study their evolution during biosorption process. This technique has proved

Table 4: Lead biosorption capacity from preliminary tests.

Isolates	q (mg/g)
Fungi	
Galactomyces geotrichum 5L2	66.00
Penicillium sp. 8L2	44.74
Pseudallescheria boydii 3S3	85.17
Trichosporon sp. 1L1	104.53
Yeasts	
Trichosporon sp. 4L2	22.29
Trichosporon sp. 4S3	35.72
Rhodotorula mucilaginosa 1S1	23.95
Rhodotorula mucilaginosa 2S4	37.59
Bacteria	
Klebsiella sp. 3S1	90.48
Enterobacter sp. 2E2	78.10

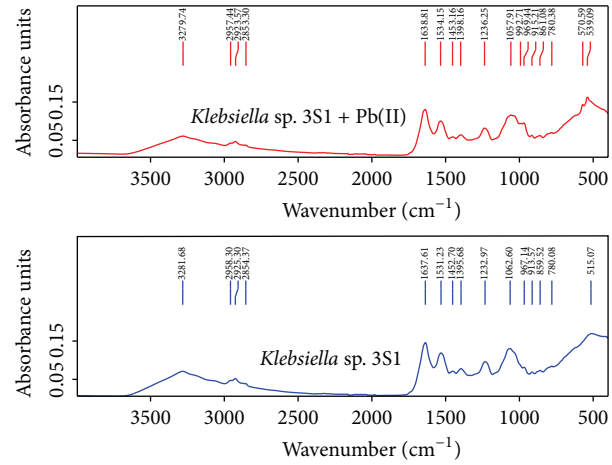

Figure 1: FTIR spectra of *Klebsiella* sp. 3S1 before and after Pb(II) biosorption.

effective in obtaining structural information on metal-microbe bonds [32]. The results for *Klebsiella* sp. 3S1 showed the presence of the following functional groups: amino, carbonyl, carboxylic, hydroxyl, and phosphate. Table 5 shows band assignments and the typical functional groups present in this bacterium before and after Pb(II) uptake [33–35]. The IR spectra of metal-free and metal-loaded biomass showed differences in the functional groups (Figure 1). After contact with the metal solution, the spectra obtained show a shift of the frequency band and the appearance of new peaks [36]; furthermore, a decrease in band intensity was observed. These changes indicate that the functional groups are involved in the process of adsorption. Moreover, it is important to note the appearance of a peak at 1038 cm^{-1}; this peak occurs after contact with the metal solution, and this shift is typical of the complexation of phosphate or carboxyl

Table 5: IR absorption bands: changes and possible assignment.

FTIR peak	Original biomass wavenumbers (cm^{-1})	Pb(II) loaded biomass wavenumbers (cm^{-1})	Displacement (cm^{-1})	Functional groups	Assignment
1	3282	3280	2	–OH, –NH	Stretching vibrations of amino and hydroxyl groups
2	2958	2957	1	$–CH_3$	$–CH_3$ asymmetric stretching
3	2925	2924	1	$–CH_2$	$–CH_2$ asymmetric stretching vibrations
4	2875	2875	0	$–CH_3$	$–CH_3$ symmetric stretching vibrations
5	2854	2853	1	$–CH_2$	$–CH_3$ asymmetric stretching vibrations
6	1638	1639	1	–CO, C–N	C=O and C–N stretching in amide I group
7	1531	1534	3	–CN, –NH	C–N stretching in amide II group and N–H bending
8	1453	1453	0	$–CH_2$, –CO	$–CH_2$ bending, symmetric C=O
9	1396	1398	2	$–COO^-$	$–COO^-$ symmetric stretching of carboxyl groups
10	1233	1236	3	$–PO_2^-$, –CO	P=O asymmetric stretching of phosphate groups, deformation vibration of C=O carboxylic acids
11	1063	1058	5	$–PO_2^-$, –OH	P=O symmetric stretching of phosphate groups, –OH of polysaccharides
12		1038	1038	–CO, PO_2^-	C–O stretching of alcoholic groups, symmetric stretching of phosphate groups
13		993	993	–C–O, $–CH_2$	C–O–C, C–O–P, and $–CH_2$ stretching vibrations of polysaccharides
14	967	969	2		N-containing bioligands
15	914	915	1		N-containing bioligands
16	860	861	1		S=O stretching
17	796	796	0		N-containing bioligands
18	780	780	0		N-containing bioligands
19		571	571		N-containing bioligands
20	515	539	24		N-containing bioligands

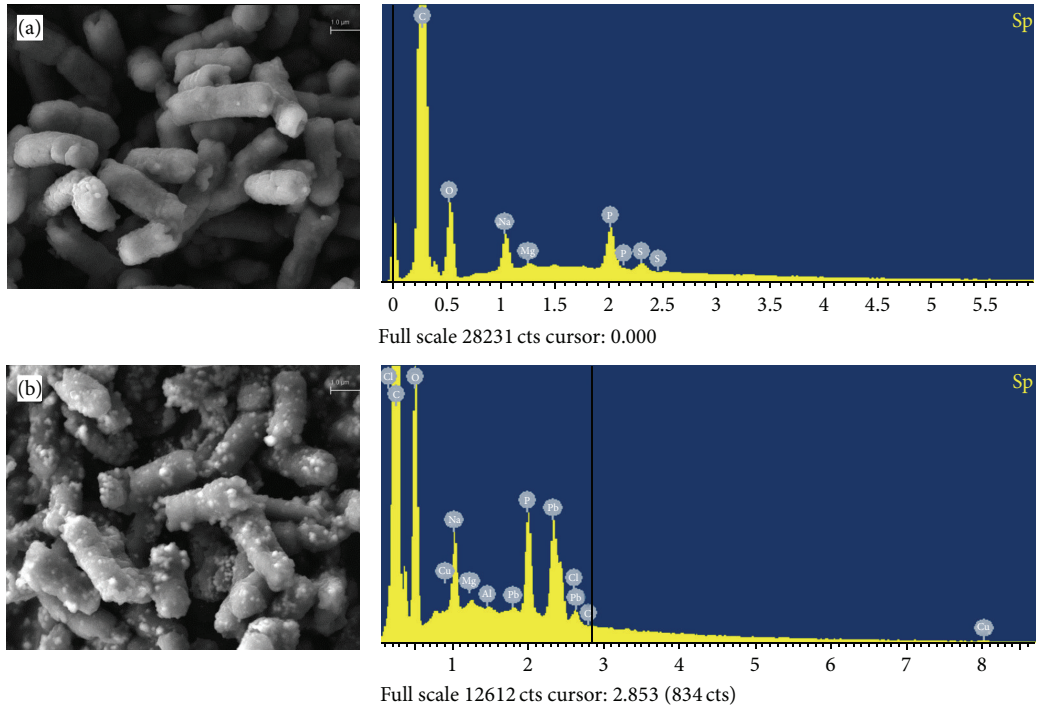

Figure 2: SEM-EDX analysis of *Klebsiella* sp. 3S1 before (a) and after Pb(II) biosorption (b).

groups by coordination with metal ions [37, 38]. Finally, two new peaks were observed in the region with low wave numbers (under 800 cm^{-1}); these peaks (571 and 539 cm^{-1}) could be attributed to the interaction between the metal ions and N-containing bioligands [39, 40].

3.3. Chemical and SEM Analysis. Figure 2 shows micrographs and EDX spectra obtained after and before the biosorption process. These micrographs show changes in the cell morphology of *Klebsiella* sp. 3S1; there is also a large presence of bright particles on the surface of the bacteria treated with lead. EDX analysis supported this observation, confirming that the metal remained adsorbed by the entire cell surface. Other authors have obtained similar results with different microorganisms [39, 41].

3.4. Chemical and TEM Analysis. The location of the metal within the cell was evaluated using HR-TEM-EDX technique. The micrographs obtained together with the corresponding EDX microanalysis (Figure 3) show that the metal is largely fixed at the cell surface. However, in some cases, lead accumulation also appears within the cytoplasm, which could indicate the presence of a bioaccumulation mechanism; some authors have identified this capacity in different microorganisms [42]. Perdrial et al. [43] localised lead accumulations associated with polyphosphate bodies in bacteria isolated from the environment.

3.5. Uptake Kinetics. Sorption kinetics is important because it describes the solute uptake, which also controls the residence time of the metal ions at the solid-solution interface. Figure 4 shows the results of two biosorption experiments. The observed values are the average of two replicates. From the figure, it can be observed that the biosorption occurs in two phases: first a very fast initial rate within the first 5 min and then a slow attainment of equilibrium within 1 to 2 days, both of which contribute to the total metal biosorption. This finding suggests that adsorption of lead may occur by two mechanisms: cell-surface binding and intracellular accumulation. To contemplate both mechanisms, we used different boundary conditions. Ho et al. [44] considered an imaginary negative time when the rate of sorption is infinity, in the same case.

Kinetic behavior during adsorption has been studied by numerous models [45]. They have attempted to quantitatively describe the process. However, they present limitations that can be solved with theoretical assumptions and specific experimental conditions. The models that best fit our experimental data were pseudo-first and second order. To fit models to data, we used linear and nonlinear regression (always getting the best results from nonlinear regressions) and used different boundary conditions; namely, $q = q_i$ at $t = 0$ and $q = q$ at $t = t$, where q_i corresponds to a quick, practically instantaneous biosorption at the beginning of the experiment. The use of the latter boundary conditions is

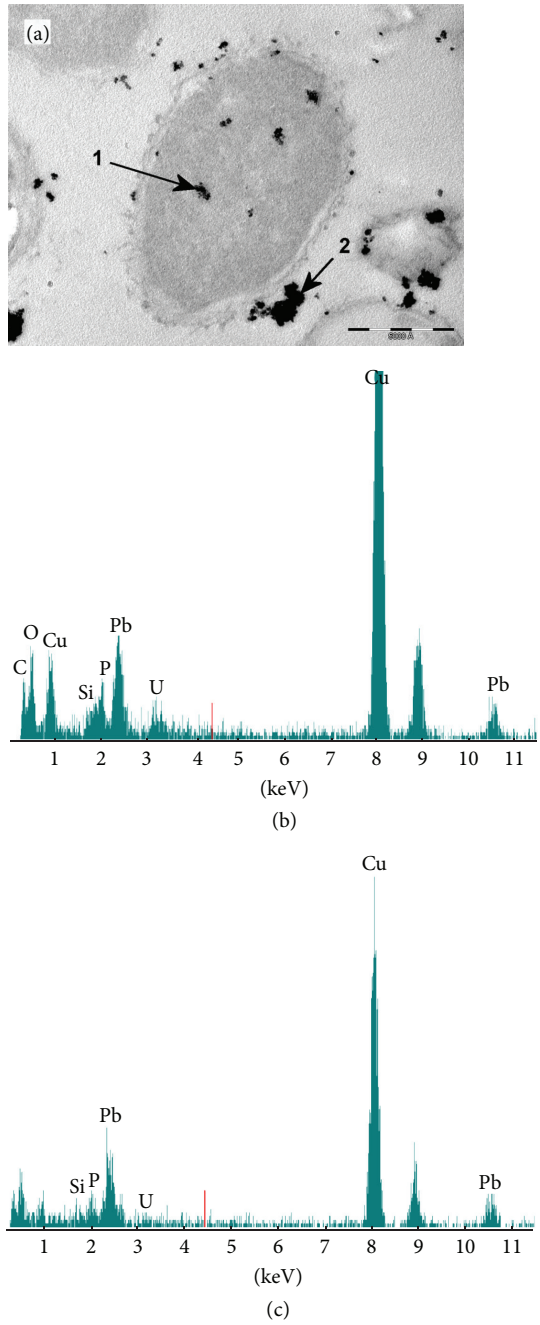

Figure 3: Transmission electron micrographs of a thin section of *Klebsiella* sp. 3S1 and the location of fixed lead (a). Energy dispersive X-ray spectra of the intracellular accumulation of lead (b) acquired from the region indicated by arrow 1 in (a) and the surface biosorption (c) acquired from the region indicated by arrow 1 in (a).

a major difference from what is found in the literature, as the typical boundary condition is $q = 0$ at $t = 0$.

Table 6 shows the values of the parameters that best fit the models provided. The higher correlation coefficients confirm that pseudo-second-order kinetics is the most suitable to represent the biosorption data. This fact also supports the assumption of the model, namely, that adsorption is due to chemisorption. Our results are similar to those obtained by other authors with different microorganisms [14, 21]. Figure 4 also shows the curves corresponding to the model that best fits the experimental results so that the experimental data can easily be compared with the model predictions.

3.6. Response Surface Modelling and Optimum Biosorption Conditions. A Rotatable Central Composite Design was performed. Table 1 shows the values of the operating variables, that is, biosorbent dosage (B), pH and temperature (T), and the biosorption capacity (q_e) response. The results were fit to

Table 6: Integrated equations, boundary conditions, and kinetic parameters of the biosorption by *Klebsiella* sp. 3S1.

		Exp. number 1	Exp. number 2
Pseudo-first order			
$q = 0$ at $t = 0$ and $q = q$ at $t = t$ $q = q_e\left(1 - e^{-k_1 t}\right)$	q_e	103.2	78.15
	k_1	0.00775	0.00607
	r^2	0.437	0.627
	$\sum (q - q_{\text{cal}})^2$	5826	2781
$q = q_i$ at $t = 0$ and $q = q$ at $t = t$ $q = q_e\left(1 - e^{-k_1 t}\right) + q_i e^{-k_1 t}$	q_e	115.7	85.43
	q_i	49.43	30.21
	k_1	0.0013	0.0018
	r^2	0.992	0.983
	$\sum (q - q_{\text{cal}})^2$	81.65	124.5
Pseudo-second order			
$q = 0$ at $t = 0$ and $q = q$ at $t = t$ $q = \dfrac{t}{1/k_2 q_e^2 + t/q_e}$	q_e	107.5	82.64
	k_2	$1.53E-04$	$1.40E-04$
	r^2	0.629	0.774
	$\sum (q - q_{\text{cal}})^2$	3836	1686
$q = q_i$ at $t = 0$ and $q = q$ at $t = t$ $q = q_e - \dfrac{q_e - q_i}{1 + k_2 t\,(q_e - q_i)}$	q_e	130.9	96.56
	q_i	47.57	28.84
	k_2	$1.75E-05$	$3.00E-05$
	r^2	0.996	0.974
	$\sum (q - q_{\text{cal}})^2$	45.26	197.4
Elovich			
$q = 0$ at $t = 0$ and $q = q$ at $t = t$ $q = \dfrac{1}{b}\ln(1 + abt)$	a	26.55	7.176
	b	0.07855	0.08845
	r^2	0.922	0.923
	$\sum (q - q_{\text{cal}})^2$	811.1	570.1
$q = q_i$ at $t = 0$ and $q = q$ at $t = t$ $q = \dfrac{1}{b}\ln\left(abt + e^{bq_i}\right)$	a	1.832	1.516
	b	0.04807	0.06404
	q_i	45.76	26.39
	r^2	0.992	0.962
	$\sum (q - q_{\text{cal}})^2$	78.03	286.7
Intraparticle diffusion			
$q = k\sqrt{t}$	k	2.488	1.971
	r^2	—	0.241
	$\sum (q - q_{\text{cal}})^2$	11718	5652
$q = q_i + k\sqrt{t}$	k	1.305	1.146
	q_i	48.84	31.50
	r^2	0.957	0.903
	$\sum (q - q_{\text{cal}})^2$	439.8	719.0

Exp. number 1: 50 mg/L of Pb(II) and 0.11 g/L of dry biomass. Exp. number 2: 25 mg/L of Pb(II) and 0.28 g/L of dry biomass. r^2 is the correlation coefficient, and $\sum (q - q_{\text{cal}})^2$ is the sum of the errors squared.

Table 7: ANOVA for the response surface reduced quadratic model.

Source	Sum of squares	DF	Mean square	F-value	p value
Model	9588.53	8	1198.57	437.66	<0.0001
B: biosorbent dosage	4.10	1	4.10	1.50	0.2520
pH	234.13	1	234.13	85.49	<0.0001
T: temperature	8164.13	1	8164.13	2981.14	<0.0001
BpH	18.39	1	18.39	6.72	0.0291
BT	301.72	1	301.72	110.17	<0.0001
B^2	161.57	1	161.57	59.00	<0.0001
pH^2	164.17	1	164.17	59.95	<0.0001
T^2	387.29	1	387.29	141.42	<0.0001
Residual	24.65	9	2.74		
Lack of fit	16.26	4	4.06	2.42	0.1790
Pure error	8.39	5	1.68		
Cor total	9613.18	17			
CV %	1.58				
R-Squared	0.9974				
Adj. R-Squared	0.9952				
Pred. R-Squared	0.9837				

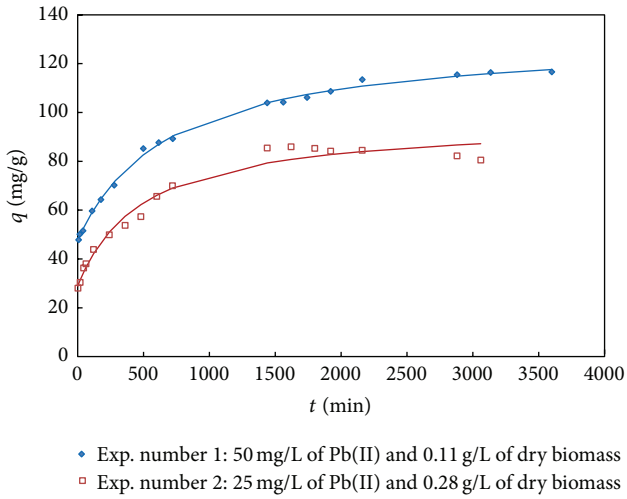

Figure 4: Experimental data and curves corresponding to the model that best fits the experimental results, pseudo-second order with boundary conditions: $q = q_i$ at $t = 0$ and $q = q$ at $t = t$.

a quadratic equation for biosorption capacity, (2), by using the Design-Expert statistical package. The final equation in terms of actual factors is shown below:

$$q_e = -483.84 + 245.13B + 193.33\text{pH} + 0.65726T - 105.22B^2 - 18.598\text{pH}^2 + 0.071415T^2 - 13.477B\text{pH} - 2.7294BT. \quad (3)$$

Analysis of variance (ANOVA) was performed to determine the influence of the significant factors involved in the biosorption capacity. Table 7 shows the variability of the factors and their interactions. The effect of a factor can be defined as the response variation produced by a change in the factor level, where only terms found to be statistically significant were included. In this case, seven effects showed p values below 0.05. This indicates that they are significantly different from zero with a 95% confidence level and one required to support hierarchy.

The model is significant (F-value = 437.66) and the lack of fit is not significant (F-value = 2.42). Therefore, it can be stated that the model can predict biosorption capacity as an equation of the three studied factors. The R-Squared suggests that the model explains 99.74% of the variability in the response.

The perturbation plots were obtained to study the effects of several factors. These plots showed that temperature has the greatest influence on Pb(II) removal efficiency, and the biosorbent dosage exerts less influence. This is shown in Figure 5, with the response surface corresponding to pH 4.75. Moreover, this figure also shows that q_e increases with biosorbent dosage for low values of temperature, whereas if the temperature values are high, the biosorbent dosage influence is negative; this is justified by the interaction between the biosorbent dosage and temperature.

The empirical model given as (3) was also optimised: the maximum q_e, 139.96 mg/g, was mathematically located at 34°C, pH 5.05, and biosorbent dosage 0.40 mg/mL. However, the adjusted model also allows different operational conditions, for example, a temperature of 25°C, which is closer to room temperature (Figure 6).

3.7. Biosorption Equilibrium. Equilibrium data were obtained experimentally using different initial concentrations of Pb(II) between 50 and 320 mg/L and a constant biomass concentration (0.52 g/L), at 25°C and pH 5 (Figure 7). These are

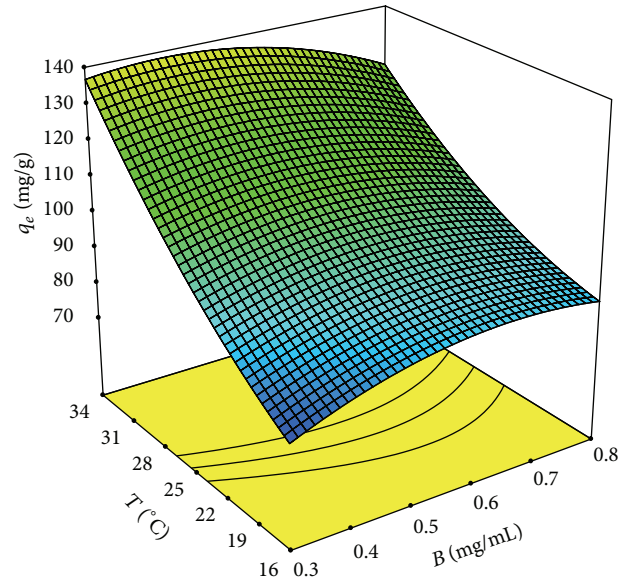

Figure 5: Response surface plot for biosorption of Pb(II) by *Klebsiella* sp. 3S1 showing the interactive effect of temperature (T) and biosorbent dosage (B) (pH, 4.75, and initial lead concentration, 100 mg/L).

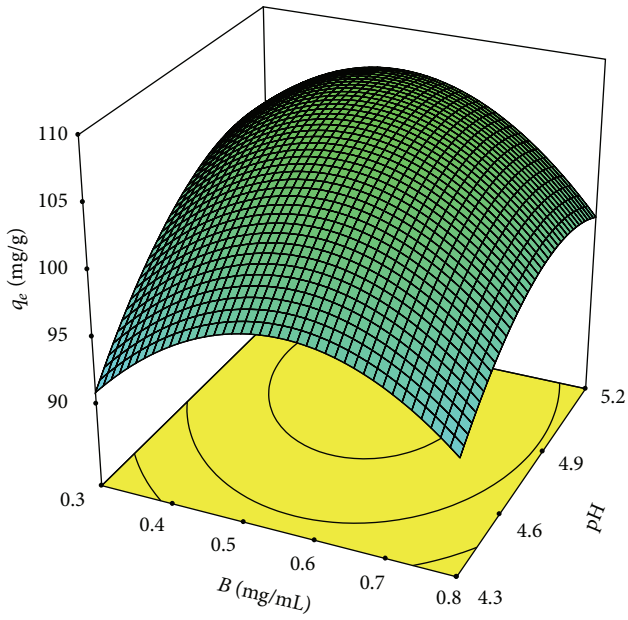

Figure 6: Response surface plot for biosorption of Pb(II) by *Klebsiella* sp. 3S1 showing the interactive effect of biosorbent dosage (B) and pH (temperature, 25°C, and initial lead concentration, 100 mg/L).

the optimum conditions according to the obtained model, (3), given a temperature of 25°C, which was chosen because it is more like environmental conditions.

Four isotherm equations have been examined in the present study. All parameters were adjusted by nonlinear regression. Table 8 shows the results obtained. The biosorption isotherms for Pb(II) ion uptake by *Klebsiella* sp. 3S1 were found to be appropriate for all predictions. Only the correlation coefficient of the Langmuir curve was lower. This fact suggests that heterogeneous surface conditions predominate, but monolayer biosorption may coexist. Accordingly, the biosorption process on the bacteria is complex, involving several mechanisms.

The maximum biosorption capacity (q_m) was obtained with the Langmuir model (140.18 mg/g), which is comparable to other types of biomass studied (Table 9). A direct comparison between different biosorbents is difficult because of

Table 8: Biosorption equilibrium parameters of the isotherm models by *Klebsiella* sp. 3S1.

Langmuir	q_m	140.19
	b	0.075353
	r^2	0.9395
	$\sum (q - q_{cal})^2$	60.955
Freundlich	K_F	65.266
	n	7.4312
	r^2	0.9901
	$\sum (q - q_{cal})^2$	15.920
Sips	K_s	66.223
	a_s	0.019748
	n	7.1713
	r^2	0.9901
	$\sum (q - q_{cal})^2$	15.915
Redlich-Peterson	K_{RP}	20850.6
	a_{RP}	319.3393
	β	0.86949
	r^2	0.9901
	$\sum (q - q_{cal})^2$	15.923

r^2 is the correlation coefficient.
$\sum (q - q_{cal})^2$ is the sum of the errors squared.

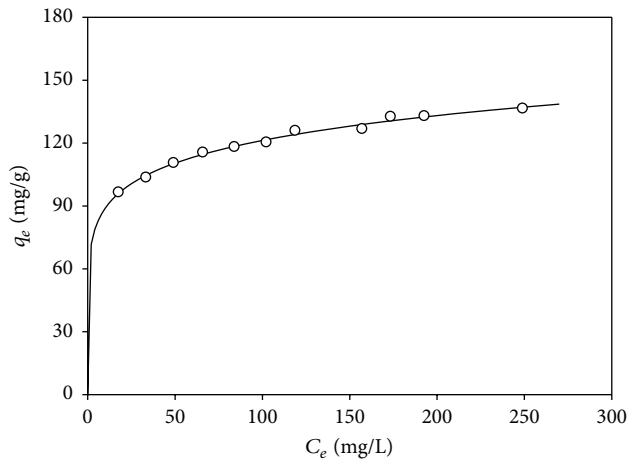

Figure 7: Biosorption equilibrium data and Freundlich isotherm for *Klebsiella* sp. 3S1.

Table 9: Maximum lead biosorption capacity of different microorganisms.

Biosorbent	q_m (mg/g)	Reference
Penicillium sp.	60.77	[21]
R. arrhizus	48.79	[22]
Ceratophyllum demersum	44.80	[23]
Bacillus cereus $M_{16}{}^1$	70.42	[24]
Aspergillus niger	34.92	[25]
Dried activated sludge	131.60	[26]
Caulerpa lentillifera	28.99	[27]
Cladophora fascicularis	227.70	[28]
Immobilised *Saccharomyces cerevisiae*	30.04	[29]
Recombinant *Escherichia coli*	108.99	[30]
Klebsiella sp. 3S1	140.19	In this study

the varying experimental conditions employed. However, it can be seen as *Klebsiella* sp. 3S1 exhibits good biosorption efficiency, among the highest that have been reported for lead ions.

4. Conclusions

This work concluded that the isolate *Klebsiella* sp. 3S1 may be employed to be used as an inexpensive biosorbent, highly efficient for Pb(II) uptake. Maximum biosorption capacity (140.19 mg/g dry cell) was obtained at 25°C and an initial pH of 5. As a result of TEM-EDX analysis, both cell-surface binding and bioaccumulation could be involved in Pb removal. The biosorption process was found to be dependent on experimental factors such as the biosorbent dosage, initial metal ion concentration, pH, temperature, and contact time. Biosorption equilibrium data fit better to the Freundlich model, which implies heterogeneous surface conditions. This result is in accordance with the kinetic studies, which show that the sorption process is slow and that biosorption is performed in two phases: a very fast initial rate within the first 5 min, followed by slow attainment of equilibrium within 1 to 2 days, both of which contribute to the total metal biosorption. FTIR and SEM-EDX techniques confirmed the interactions between lead ions and functional groups on the wall surface of *Klebsiella* sp. 3S1. Moreover, TEM-EDX analysis showed the presence of metal in the cytoplasm.

Future research should be carried out to develop a robust immobilisation method for wastewater treatment, including continuous biosorption with reuse and recycling.

Conflict of Interests

The authors declare that there is no conflict of interests regarding the publication of this paper.

Acknowledgment

The support of the Spanish Agency for International Development Cooperation (Project Reference A/018600/08) is greatly acknowledged.

References

[1] S. O. Lesmana, N. Febriana, F. E. Soetaredjo, J. Sunarso, and S. Ismadji, "Studies on potential applications of biomass for the separation of heavy metals from water and wastewater," *Biochemical Engineering Journal*, vol. 44, no. 1, pp. 19–41, 2009.

[2] B. Volesky, "Biosorption and me," *Water Research*, vol. 41, no. 18, pp. 4017–4029, 2007.

[3] B. Volesky and Z. R. Holan, "Biosorption of heavy-metals," *Biotechnology Progress*, vol. 11, no. 3, pp. 235–250, 1995.

[4] S. A. Kumar, M. K. Abyaneh, S. W. Gosavi et al., "Nitrate reductase-mediated synthesis of silver nanoparticles from $AgNO_3$," *Biotechnology Letters*, vol. 29, no. 3, pp. 439–445, 2007.

[5] C. Cervantes, A. E. Espino-Saldaña, F. Acevedo-Aguilar et al., "Interacciones microbianas con metales pesados," *Revista Latinoamericana de Microbiología*, vol. 48, pp. 203–210, 2006.

[6] R. A. Amer, F. Mapelli, H. M. El Gendi et al., "Bacterial diversity and bioremediation potential of the highly contaminated marine sediments at el max district (Egypt, mediterranean sea)," *BioMed Research International*, vol. 2015, 17 pages, 2015.

[7] M. L. Merroun, M. Nedelkova, J. J. Ojeda et al., "Bio-precipitation of uranium by two bacterial isolates recovered from extreme environments as estimated by potentiometric titration, TEM and X-ray absorption spectroscopic analyses," *Journal of Hazardous Materials*, vol. 197, pp. 1–10, 2011.

[8] M. A. Kumar, A. Vijayalakshmi, E. A. R. Lincy et al., "Biotransformation of reactive black HEBL into 3 nitroso-3-azabicyclo (3.2.2) nonane by an acclimated mixed culture," *International Journal of ChemTech Research*, vol. 6, no. 9, pp. 4172–4179, 2014.

[9] L. H. Mason, J. P. Harp, and D. Y. Han, "Pb neurotoxicity: neuropsychological effects of lead toxicity," *BioMed Research International*, vol. 2014, Article ID 840547, 8 pages, 2014.

[10] A. J. Muñoz, E. Ruiz, H. Abriouel et al., "Heavy metal tolerance of microorganisms isolated from wastewaters. Identification and evaluation of its potential for biosorption," *Chemical Engineering Journal*, vol. 210, pp. 325–332, 2012.

[11] Y. G. Bermúdez, I. L. R. Rico, E. Guibal, M. C. de Hoces, and M. Á. Martín-Lara, "Biosorption of hexavalent chromium from aqueous solution by *Sargassum muticum* brown alga. Application of statistical design for process optimization," *Chemical Engineering Journal*, vol. 183, pp. 68–76, 2012.

[12] M. Seenuvasan, K. S. Kumar, S. Abinandan et al., "Statistical analysis on stress induced lipid accumulation along with the major cell components of *Chlorella* sp," *International Journal of ChemTech Research*, vol. 6, no. 9, pp. 4186–4192, 2014.

[13] T. Vidhyadevi, A. Murugesan, S. S. Kalaivani et al., "Optimization of the process parameters for the removal of reactive yellow dye by the low cost *Setaria verticillata* carbon using response surface methodology: thermodynamic, kinetic, and equilibrium studies," *Environmental Progress & Sustainable Energy*, vol. 33, no. 3, pp. 855–865, 2014.

[14] J. Febrianto, A. N. Kosasih, J. Sunarso, Y.-H. Ju, N. Indraswati, and S. Ismadji, "Equilibrium and kinetic studies in adsorption of heavy metals using biosorbent: a summary of recent studies," *Journal of Hazardous Materials*, vol. 162, no. 2-3, pp. 616–645, 2009.

[15] Y. S. Ho, D. A. J. Wase, and C. F. Forster, "Kinetic studies of competitive heavy metal adsorption by sphagnum moss peat," *Environmental Technology*, vol. 17, no. 1, pp. 71–77, 1996.

[16] C. W. Cheung, J. F. Porter, and G. Mckay, "Sorption kinetic analysis for the removal of cadmium ions from effluents using bone char," *Water Research*, vol. 35, no. 3, pp. 605–612, 2001.

[17] I. Langmuir, "The adsorption of gases on plane surfaces of glass, mica and platinum," *The Journal of the American Chemical Society*, vol. 40, no. 9, pp. 1361–1403, 1918.

[18] H. Freundlich, "Adsorption in solutions," *Physical Chemistry*, vol. 57, pp. 384–410, 1906.

[19] R. Sips, "Combined form of Langmuir and Freundlich equations," *The Journal of Chemical Physics*, vol. 16, pp. 490–495, 1948.

[20] O. Redlich and D. L. Peterson, "A useful adsorption isotherm," *The Journal of Physical Chemistry*, vol. 63, no. 6, pp. 1024–1039, 1959.

[21] L. Ezzouhri, E. Ruiz, E. Castro et al., "Mechanisms of lead uptake by fungal biomass isolated from heavy metals habitats," *Afinidad*, vol. 67, no. 545, pp. 39–44, 2010.

[22] Y. Sag, A. Yalçuk, and T. Kutsal, "Mono and multi-component biosorption of heavy metal ions on *Rhizopus arrhizus* in a CFST," *Process Biochemistry*, vol. 35, no. 8, pp. 787–799, 2000.

[23] O. Keskinkan, M. Z. L. Goksu, M. Basibuyuk, and C. F. Forster, "Heavy metal adsorption properties of a submerged aquatic plant (*Ceratophyllum demersum*)," *Bioresource Technology*, vol. 92, no. 2, pp. 197–200, 2004.

[24] L. Ray, S. Paul, D. Bera, and P. Chattopadhyay, "Bioaccumulation of Pb (II) from aqueous solutions by *Bacillus cereus* M_{16}^{1}," *Journal for Hazardous Substance Research*, vol. 5, pp. 1–21, 2006.

[25] A. Y. Dursun, "A comparative study on determination of the equilibrium, kinetic and thermodynamic parameters of biosorption of copper(II) and lead(II) ions onto pretreated *Aspergillus niger*," *Biochemical Engineering Journal*, vol. 28, no. 2, pp. 187–195, 2006.

[26] X.-J. Wang, S.-Q. Xia, L. Cwen, J.-F. Zhao, J.-M. Chovelon, and J.-R. Nicole, "Biosorption of cadmium(II) and lead(II) ions from aqueous solutions onto dried activated sludge," *Journal of Environmental Sciences*, vol. 18, no. 5, pp. 840–844, 2006.

[27] P. Pavasant, R. Apiratikul, V. Sungkhum, P. Suthiparinyanont, S. Wattanachira, and T. F. Marhaba, "Biosorption of Cu^{2+}, Cd^{2+}, Pb^{2+}, and Zn^{2+} using dried marine green macroalga *Caulerpa lentillifera*," *Bioresource Technology*, vol. 97, no. 18, pp. 2321–2329, 2006.

[28] L. Deng, Y. Su, H. Su, X. Wang, and X. Zhu, "Sorption and desorption of lead (II) from wastewater by green algae *Cladophora fascicularis*," *Journal of Hazardous Materials*, vol. 143, no. 1-2, pp. 220–225, 2007.

[29] A. Çabuk, T. Akar, S. Tunali, and S. Gedikli, "Biosorption of Pb(II) by industrial strain of *Saccharomyces cerevisiae* immobilized on the biomatrix of cone biomass of *Pinus nigra*: equilibrium and mechanism analysis," *Chemical Engineering Journal*, vol. 131, no. 1–3, pp. 293–300, 2007.

[30] T. T. L. Nguyen, H. R. Lee, S. H. Hong, J.-R. Jang, W.-S. Choe, and I.-K. Yoo, "Selective lead adsorption by recombinant *Escherichia coli* Displaying a Lead-Binding Peptide," *Applied Biochemistry and Biotechnology*, vol. 169, no. 4, pp. 1188–1196, 2013.

[31] N. K. Srivastava and C. B. Majumder, "Novel biofiltration methods for the treatment of heavy metals from industrial wastewater," *Journal of Hazardous Materials*, vol. 151, no. 1, pp. 1–8, 2008.

[32] K. Aftab, K. Akhtar, A. Jabbar, I. H. Bukhari, and R. Noreen, "Physico-chemical study for zinc removal and recovery onto native/chemically modified *Aspergillus flavus* NA9 from industrial effluent," *Water Research*, vol. 47, no. 13, pp. 4238–4246, 2013.

[33] M. Kiliç, M. E. Keskin, S. Mazlum, and N. Mazlum, "Hg(II) and Pb(II) adsorption on activated sludge biomass: effective biosorption mechanism," *International Journal of Mineral Processing*, vol. 87, no. 1-2, pp. 1–8, 2008.

[34] X. Wei, L. Fang, P. Cai et al., "Influence of extracellular polymeric substances (EPS) on Cd adsorption by bacteria," *Environmental Pollution*, vol. 159, no. 5, pp. 1369–1374, 2011.

[35] Y. Wang, Q. Zhou, B. Li et al., "Differentiation in MALDI-TOF MS and FTIR spectra between two closely related species *Acidovorax oryzae* and *Acidovorax citrulli*," *BMC Microbiology*, vol. 12, article 182, 2012.

[36] G. Blázquez, M. A. Martín-Lara, G. Tenorio, and M. Calero, "Batch biosorption of lead(II) from aqueous solutions by olive tree pruning waste, equilibrium, kinetics and thermodynamic study," *Chemical Engineering Journal*, vol. 168, no. 1, pp. 170–177, 2011.

[37] R. Aravindhan, B. Madhan, J. R. Rao, and B. U. Nair, "Recovery and reuse of chromium from tannery wastewaters using *Turbinaria ornata* seaweed," *Journal of Chemical Technology and Biotechnology*, vol. 79, no. 11, pp. 1251–1258, 2004.

[38] R. Nadeem, T. M. Ansari, and A. M. Khalid, "Fourier transform infrared spectroscopic characterization and optimization of Pb(II) biosorption by fish (*Labeo rohita*) scales," *Journal of Hazardous Materials*, vol. 156, no. 1–3, pp. 64–73, 2008.

[39] T. Akar, S. Tunali, and I. Kiran, "*Botrytis cinerea* as a new fungal biosorbent for removal of Pb(II) from aqueous solutions," *Biochemical Engineering Journal*, vol. 25, no. 3, pp. 227–235, 2005.

[40] S. T. Akar, A. Gorgulu, B. Anilan, Z. Kaynak, and T. Akar, "Investigation of the biosorption characteristics of lead(II) ions onto *Symphoricarpus albus*: batch and dynamic flow studies," *Journal of Hazardous Materials*, vol. 165, no. 1–3, pp. 126–133, 2009.

[41] W.-B. Lu, J.-J. Shi, C.-H. Wang, and J.-S. Chang, "Biosorption of lead, copper and cadmium by an indigenous isolate *Enterobacter* sp. J1 possessing high heavy-metal resistance," *Journal of Hazardous Materials*, vol. 134, no. 1–3, pp. 80–86, 2006.

[42] J. Maldonado, A. Solé, Z. M. Puyen, and I. Esteve, "Selection of bioindicators to detect lead pollution in Ebro delta microbial mats, using high-resolution microscopic techniques," *Aquatic Toxicology*, vol. 104, no. 1-2, pp. 135–144, 2011.

[43] N. Perdrial, N. Liewig, J.-E. Delphin, and F. Elsass, "TEM evidence for intracellular accumulation of lead by bacteria in subsurface environments," *Chemical Geology*, vol. 253, no. 3-4, pp. 196–204, 2008.

[44] Y. S. Ho, J. C. Y. Ng, and G. McKay, "Removal of lead(II) from effluents by sorption on peat using second-order kinetics," *Separation Science and Technology*, vol. 36, no. 2, pp. 241–261, 2001.

[45] K. Vijayaraghavan and Y.-S. Yun, "Bacterial biosorbents and biosorption," *Biotechnology Advances*, vol. 26, no. 3, pp. 266–291, 2008.